

THERMAL CONVERSION OF BIOMASS AND BIOMASS COMPONENTS TO BIOFUELS AND BIO-CHEMICALS

A Dissertation
Presented to
The Academic Faculty

by

Haoxi Ben

In Partial Fulfillment
of the Requirements for the Degree
Doctor of Philosophy in the
School of Chemistry and Biochemistry

Georgia Institute of Technology
May, 2013

THERMAL CONVERSION OF BIOMASS AND BIOMASS COMPONENTS TO BIOFUELS AND BIO-CHEMICALS

Approved by:

Dr. Arthur J. Ragauskas, Advisor
School of Chemistry and Biochemistry
Georgia Institute of Technology

Dr. Stefan France
School of Chemistry and Biochemistry
Georgia Institute of Technology

Dr. Charles L. Liotta
School of Chemistry and Biochemistry
Georgia Institute of Technology

Dr. Yunlin Deng
Chemical and Biomolecular Engineering
Georgia Institute of Technology

Dr. Preet Singh
School of Materials Science and Engineering
Georgia Institute of Technology

Date Approved: [Dec 12, 2012]

ACKNOWLEDGEMENTS

It has been a long way full of happiness to go from the starting of graduate study at Georgia Institute of Technology in January 2009 to the accomplishment of the Ph. D. dissertation. This would not be possible without the love, care, support, and advice from many individuals. I would like to sincerely say ‘thank you’ to all of them.

First and foremost, I would like to express my sincere gratitude to my advisor, Dr. Arthur J. Ragauskas, for his support, patience, added considerably and encouragement throughout my graduate studies. I appreciate his vast knowledge and skill in many areas. The knowledge I gained from him will greatly help me in my future endeavors. I would also like to thank my committee members, Dr. Charles L. Liotta, Dr. Stefan France, Dr. Yulin Deng, and Dr. Preet Singh, for their insightful comments and supports from the initial to the final level of this project.

I am grateful to my co-workers at Georgia Tech, especially Dr. Lenong Allison, Dr. Shaobo Pan, Dr. Fang Huang, and Dr. Yunqiao Pu for their support in many aspects during the completion of this project.

I owe my deepest gratitude to my wife, Yu Wu, for her understanding and love during the past few years. Her support and encouragement was in the end what made this dissertation possible.

I also would like to thank my parents for their strong support and complete understanding all the way, and all my good friends in the United States for the wonderful times and lasting memories we shared together.

I would especially like to appreciate my former advisor, Dr. Meifang Wu. Thank

you for starting my scientific life and for training me the fundamental experiment skills, which are the groundwork of my Ph.D. project.

Finally, I would like to acknowledge the financial support from the Paper Science and Engineering Fellowship program at the Institute of Paper Science and Technology.

TABLE OF CONTENTS

ACKNOWLEDGEMENTS	III
LIST OF TABLES	XII
SUMMARY	XXXII
CHAPTER 1: INTRODUCTION	1
CHAPTER 2: LITERATURE REVIEW	4
2.1 PROBLEM STATEMENT	4
2.2 LIGNOCELLULOSE	6
2.2.1 Cellulose	7
2.2.2 Hemicelluloses	9
2.2.3 Lignin	12
2.3 PYROLYSIS OF BIOMASS COMPONENTS	15
2.3.1 Lignin pyrolysis products	15
2.3.1.1 Gas products of pyrolysis of lignin	15
2.3.1.2 Liquid products of pyrolysis of lignin	16
2.3.2 PYROLYSIS OF CELLULOSE	24
2.3.3 PYROLYSIS OF HEMICELLULOSE	31
2.4 CHARACTERIZATION METHODS OF PYROLYSIS OIL	35
2.4.1 FT-IR analysis of lignin pyrolysis oil	35
2.4.2 NMR analysis of pyrolysis oil	37
2.4.3 Elemental analysis, viscosity, acidity, heating value and solid residue	40

of pyrolysis oil	40
CHAPTER 3: EXPERIMENTAL MATERIALS AND PROCEDURES	45
3.1 MATERIALS.....	45
3.1.1 Chemicals.....	45
3.1.2 Biomass.....	45
3.2 EXPERIMENTAL PROCEDURE	45
3.2.1 Lignin preparation.....	45
3.2.1.1 Kraft lignin.....	45
3.2.1.2 Ethanol Organosolv Lignin (EOL)	46
3.2.2 Preparation of pyrolysis sample.....	47
3.2.3 Equipment and process of pyrolysis	47
3.2.3.1 Pyrolysis process and system.....	47
3.2.3.2 Torrefaction process.....	48
3.2.4 Hydrogenation process.....	49
3.3 ANALYSIS PROCEDURE.....	50
3.3.1 Characterization of pyrolysis oils by GPC.....	50
3.3.2 Elemental analysis of lignin and heavy oil and carbon content of	50
hydrogenation products.....	50
3.3.3 SEM characterization of catalyst	51
3.3.4 GC-MS analysis of hydrogenation products.....	51
3.3.5 Higher heating value (HHV) measurement	51
3.3.6 Monosaccharide and Klason lignin content analysis	51
3.3.7 Characterization of pyrolysis oil by NMR.....	52

3.3.7.1 Quantitative ^1H -NMR	52
3.3.7.2 DEPT-135 ^{13}C -NMR.....	52
3.3.7.3 Quantitative ^{13}C -NMR.....	53
3.3.7.4 Quantitative ^{31}P -NMR	53
3.3.7.5 Characterization of pyrolysis oil by HSQC-NMR.....	53
3.3.7.6 Solid-state CP/MAS ^{13}C -NMR	54
CHAPTER 4: PYROLYSIS OF SW KRAFT LIGNIN, CELLULOSE AND PINE	
WOOD	55
4.1 INTRODUCTION	55
4.2 EXPERIMENTAL SECTION.....	59
4.2.1 Materials and Methods.....	59
4.2.2 Lignin separation and purification	60
4.2.3 Equipment and process of pyrolysis	60
4.2.4 Characterization of pyrolysis oils by GPC.....	60
4.3 RESULTS AND DISCUSSION.....	60
4.3.1 Yields of pyrolysis products.....	60
4.3.2 GPC analysis of SW kraft lignin pyrolysis oils	63
4.3.3 Heating values of SW kraft lignin pyrolysis oils	64
CHAPTER 5: NMR CHARACTERIZATION OF PYROLYSIS OILS PRODUCED	
FROM SW KRAFT LIGNIN, CELLULOSE AND PINE WOOD	66
5.1 INTRODUCTION	66
5.2 EXPERIMENTAL SECTION.....	67
5.3 RESULTS AND DISCUSSION.....	67

5.3.1 ^{31}P -NMR analysis of pyrolysis oils	67
5.3.2 ^{13}C -NMR analysis of pyrolysis oils	74
5.3.3 HSQC-NMR analysis of pyrolysis oils.....	83
5.3.3.1 HSQC-NMR analysis of pyrolysis oils produced from softwood kraft lignin	84
5.3.3.2 HSQC-NMR analysis of pyrolysis oils produced from cellulose.....	89
5.3.3.3 HSQC-NMR analysis of pyrolysis oils produced from pine wood.	93
5.4. CONCLUSION	95
CHAPTER 6: IN SITU NMR CHARACTERIZATION OF PYROLYSIS OIL DURING THE ACCELERATED AGING PROCESS.....	97
6.1 INTRODUCTION	97
6.2 EXPERIMENTAL SECTION	99
6.2.1 Chemicals and biomass.....	99
6.2.2 Pyrolysis process and system.....	99
6.2.3 In situ NMR characterization of pyrolysis oils during the accelerated aging process.....	99
6.2.3.1 ^1H -NMR.....	100
6.2.3.2 ^{13}C -NMR.....	100
6.2.3.3 HSQC-NMR	100
6.3 RESULTS AND DISCUSSIONS.....	101
6.4 CONCLUSION	113
CHAPTER 7: PYROLYSIS OF KRAFT LIGNIN WITH ADDITIVES	115
7.1 INTRODUCTION	115

7.2 EXPERIMENTAL SECTION.....	118
7.3 RESULTS AND DISCUSSION.....	118
7.3.1 Yields of pyrolysis products.....	118
7.3.2 Quantitative ³¹ P-NMR analysis of pyrolysis oils.....	119
7.3.3 Quantitative ¹³ C-NMR analysis of pyrolysis oils	125
7.3.4 GPC analysis of pyrolysis oils	128
7.4 CONCLUSION	129
CHAPTER 8: THE INFLUENCE OF SI/AL RATIO OF ZSM-5 ZEOLITE ON THE	
PROPERTIES OF LIGNIN PYROLYSIS PRODUCTS	131
8.1 INTRODUCTION	131
8.2 MATERIALS AND METHODS	133
8.2.1 Lignin separation and purification	134
8.2.2 Preparation of pyrolysis sample.....	134
8.2.3 Equipment and process of pyrolysis	134
8.2.4 Characterization of pyrolysis oils	134
8.3 RESULTS AND DISCUSSION.....	135
8.3.1 Yields of pyrolysis products.....	135
8.3.2 Quantitative ³¹ P-NMR analysis of pyrolysis oils.....	136
8.3.3 Quantitative ¹³ C-NMR analysis of pyrolysis oils	141
8.3.4 HSQC-NMR analysis of pyrolysis oils.....	144
8.3.5 GPC and elemental analysis of pyrolysis oils.....	147
8.4 CONCLUSION	149
CHAPTER 9: ONE STEP THERMAL CONVERSION OF LIGNIN TO THE	

GASOLINE RANGE LIQUID PRODUCTS BY USING ZEOLITES AS ADDITIVES	151
9.1 INTRODUCTION	151
9.2 MATERIALS AND METHODS	154
9.2.1 Lignin separation and purification	154
9.2.2 Preparation of pyrolysis sample	154
9.2.3 Equipment and process of pyrolysis	155
9.2.4 Characterization of pyrolysis oils	156
9.3. RESULTS AND DISCUSSION	156
9.3.1 Yields of pyrolysis products	156
9.3.2 Quantitative ³¹ P-NMR analysis of pyrolysis oils	157
9.3.3 Quantitative ¹³ C-NMR analysis of pyrolysis oils	160
9.3.4 HSQC-NMR analysis of pyrolysis oils	163
9.3.5 GPC analysis of pyrolysis oils	166
9.4 CONCLUSION	167
CHAPTER 10: PRODUCTION OF RENEWABLE GASOLINE FROM AQUEOUS PHASE HYDROGENATION OF LIGNIN PYROLYSIS OIL	170
10.1 INTRODUCTION	170
10.2 EXPERIMENTAL SECTION	173
10.3 RESULTS AND DISCUSSION	173
10.4 CONCLUSIONS	181
CHAPTER 11: OVERALL CONCLUSIONS	183
CHAPTER 12: RECOMMENDATIONS FOR FUTURE WORK	188

APPENDIX A: TORREFACTION OF LOBLOLLY PINE	189
A.1 INTRODUCTION	189
A.2 EXPERIMENTAL SECTION.....	191
A.3 RESULTS AND DISCUSSION.....	192
A.4 CONCLUSIONS.....	201
APPENDIX B: COPYRIGHT PERMISSIONS	202
REFERENCES	225

LIST OF TABLES

Table 1. Major biomass components indifferent softwoods, hardwoods and residue species. ^{11, 12}	6
Table 2. DP of native wood and non-woody celluloses after nitration using the viscometric method. ¹⁵⁻¹⁷	8
Table 3. Cellulose crystallinity from several biomasses. ^{14, 15, 18}	9
Table 4. Amount and composition of sugar units (wt%) of different hardwood and softwood species. ^{19, 20}	11
Table 5. DP of hemicelluloses in several biomasses. ²¹	12
Table 6. Reported abundance of major linkages in softwood and hardwood lignins. ^{22, 23}	14
Table 7. Weight-average molecular weight (M_w), number-average molecular weight (M_n), polydispersity (D) and approximate DP of various lignins isolated from different wood species.	15
Table 8. Reported major gas products of pyrolysis of lignin.....	16
Table 9. Summary of lignin pyrolysis conditions and the yield of pyrolysis products	18
Table 10. GC-MS detected components in the lignin pyrolysis oils. ^{35, 41-46}	19

Table 11. GC-MS detected components in the cellulose pyrolysis oils ^a . 58, 59, 61-64	28
Table 12. FT-IR assignments of biomass pyrolysis oil.....	36
Table 13. NMR detectable functional groups in pyrolysis oils. ^{9, 10, 48, 71, 81-90}	39
Table 14. Elemental analysis of pyrolysis oils. ^a	41
Table 15. Viscosity, acidity, higher heating value (HHV) and solid residue in the pyrolysis oils ^a	43
Table 16. Major components reported to present in lignin pyrolysis oil.	57
Table 17. Yields of light oil, heavy oil, char and gas for the pyrolysis of SW kraft lignin at 400, 500, 600 and 700 °C.	61
Table 18. Yields of light oil, heavy oil, char and gas for the pyrolysis of cellulose at 400, 500 and 600 °C.	63
Table 19. Yields of light oil, heavy oil, char and gas for the pyrolysis of pine at 400, 500 and 600 °C.	63
Table 20. Molecular weight distribution and polydispersity (D) of heavy oils produced by pyrolysis of SW kraft lignin at 400, 500, 600 and 700 °C.	64
Table 21. Higher heating value of heavy oils produced by pyrolysis of SW kraft lignin at 400, 500, 600 and 700 °C.	65

Table 22. Chemical shifts and integration regions for pyrolysis oil and lignin after derivative with TMDP by a quantitative ^{31}P -NMR. ¹⁰⁸	68
Table 23. Hydroxyl group contents of SW kraft lignin and different heavy oils produced by pyrolysis of SW kraft lignin at 400, 500, 600 and 700 °C determined by quantitative ^{31}P -NMR after derivatization with TMDP.....	72
Table 24. Weight percentage of four major components in light oils produced by pyrolysis of SW kraft lignin at 400, 500, 600 and 700 °C, determined by quantitative ^{31}P -NMR after derivatization with TMDP.	74
Table 25. ^{13}C -NMR chemical shift assignment range of lignin pyrolysis oil based on literature compounds. ^{15, 21-26}	77
Table 26. Integration results for SW kraft lignin and heavy oils produced by pyrolysis of SW kraft lignin at 400, 500, 600 and 700 °C, detected by quantitative ^{13}C -NMR with using the assignment range showed in Table 25. The results were shown as the percentage of carbon.....	80
Table 27. Detailed structures of assignments for HSQC-NMR analysis of pyrolysis oil produced from softwood kraft lignin.	86
Table 28. Detailed structures of assignments for HSQC-NMR analysis of pyrolysis oil produced from cellulose.....	90

Table 29. ^1H -NMR chemical shift assignment ranges and functional group contributions for the pyrolysis oils produced from pine residue during the accelerated aging process at 80°C and aged at room temperature for one year.	103
Table 30. Functional group contributions for the fresh and one year room temperature aged lignin and cellulose pyrolysis oils, and poplar pyrolysis oil after accelerated aging process at 80 °C for 60 h, detected by ^1H -NMR. ^[a]	103
Table 31. ^{13}C -NMR chemical shift assignment ranges and functional group contributions for the pyrolysis oils produced from pine residue during the accelerated aging process at 80 °C and aged at room temperature for one year. The results are shown as percentage of carbon.....	107
Table 32. Functional group contributions for the fresh and one year room temperature aged lignin and cellulose pyrolysis oils and poplar pyrolysis oil after accelerated aging process at 80 °C for 60 h. Detected by ^{13}C -NMR and the results are shown as percentage of carbon. ^[a]	108
Table 33. Chemical shifts and integration regions for pyrolysis oil and lignin derivatized with TMDP in a quantitative ^{31}P -NMR.	120
Table 34. ^{13}C -NMR chemical shift assignment range of lignin pyrolysis oil based on the chemical shift database created in our previous work. ⁹	125
Table 35. $\text{SiO}_2/\text{Al}_2\text{O}_3$ mole ratio and code name used in this work of each zeolite.	134

Table 36. HHV, energy yield (%) and carbon yield (%) of heavy oil, and mass yields (%) of light oil, heavy oil, char and gas for the pyrolysis of pure SW kraft lignin and pyrolysis of SW kraft lignin with 1.0/1.0 ($W_{\text{additive}}/W_{\text{lignin}}$) of H-ZSM-5 zeolites as additives at 600 °C for 10 min.....	136
Table 37. Chemical shifts and integration regions for lignin pyrolysis oils in a quantitative ^{31}P -NMR, after derivatized with TMDP. ^{9, 90}	138
Table 38. ^{13}C -NMR chemical shift assignment range of lignin pyrolysis oil based on the chemical shift database created in our previous work. ⁹	143
Table 39. Elemental analysis for the pyrolysis of pure SW kraft lignin and pyrolysis of SW kraft lignin with 1.0/1.0 ($W_{\text{additive}}/W_{\text{lignin}}$) of H-ZSM-5 zeolites as additives at 600 °C for 10 min. The results are shown in weight percentage.	149
Table 40. $\text{SiO}_2/\text{Al}_2\text{O}_3$ mole ratio, framework, code name used in this work and channel structure ^{136, 139, 184, 185, 188, 191, 194, 196} of each zeolite.	155
Table 41. Chemical shifts and integration regions for lignin pyrolysis oil derivatized with TMDP in a quantitative ^{31}P -NMR. ^{9, 71, 87, 90}	158
Table 42. ^{13}C -NMR chemical shift assignment range of lignin pyrolysis oil based on the chemical shift database created in our previous work. ⁹	162
Table 43. ^1H -NMR chemical shift assignment ranges and functional group contributions for the EOL heavy oil and first and second step hydrogenation products.	176

Table 44. ^{13}C -NMR chemical shift assignment ranges and functional group contributions for the EOL heavy oil and first and second step hydrogenation products.	177
Table 45. Influence of the temperatures and residence times on the mass yield, HHV, energy densification ratio and energy yield of the torrefied Loblolly pine wood.	194
Table 46. Influence of the temperatures and residence times on the carbohydrates contents of the torrefied Loblolly pine wood. ^a	195
Table 47. NMR chemical shifts assignments of wood. ^{150, 218-221}	198

LIST OF FIGURES

Figure 1. Three major projects in this dissertation.	3
Figure 2. Cellulose molecular structure.	8
Figure 3. Major types of hemicelluloses in softwoods and hardwoods.	10
Figure 4. Three phenyl propane precursors of lignin and the enzymatic synthesis pathway from coniferyl unit to one of the most abundant linkages in lignin structure— β -O-4 linkage.	13
Figure 5. The possible decomposition pathways of lignin during the pyrolysis. ⁴⁹⁻⁵⁵	24
Figure 6. Conversion of biomass-derived carbohydrates to the liquid alkanes by acid-catalyzed dehydration which was followed by aldol condensation. ⁵⁶	25
Figure 7. One step conversion of cellobiose to C ₆ -alcohols with Pt, Pd, Rh or Ru nanocluster catalyst. ⁵⁷	25
Figure 8. Proposed primary decomposition of cellulose and secondary decomposition of the anhydrosugars such as levoglucosan. ⁵⁸	26
Figure 9. Tentative thermal decomposition pathways of hemicellulose. ⁶⁵	32
Figure 10. Slow pyrolysis system used in this work.	48

Figure 11. Two immiscible liquid products and solid product for pyrolysis of biomass.	48
Figure 12. Two competitive reactions during the pyrolysis of SW kraft lignin.	61
Figure 13. Reactions of the phosphorous reagent (TMDP) with various hydroxyl functional groups and the ^{31}P -NMR assignment of phosphitylated compounds. ¹⁰⁸	68
Figure 14. ^{31}P -NMR spectra for the heavy oil produced by pyrolysis of SW kraft lignin at 600 °C derivatized with TMDP.	71
Figure 15. The possible decomposition pathways of ether bond in lignin during the pyrolysis. ⁴⁹⁻⁵⁵	72
Figure 16. ^{13}C -NMR chemical shifts distribution of aromatic C-H, C-C and C-O for compounds reported present in pyrolysis oils.....	75
Figure 17. ^{13}C -NMR chemical shifts distribution of various functional groups (from 0-215 ppm) for compounds reported present in pyrolysis oils.	76
Figure 18. ^{13}C -NMR chemical shifts distribution of methyl-aromatic carbons for compounds, reported present in pyrolysis oils.....	76
Figure 19. Quantitative ^{13}C -NMR spectra for the heavy oil produced by pyrolysis of SW kraft lignin at 600 °C.....	79
Figure 20. The possible pathway to form aromatic C-O bond and C-C bond in pyrolysis oil. ⁴⁹⁻⁵⁵	81

Figure 21. The possible pyrolysis pathway of primary decomposed functional groups in lignin during the pyrolysis.	82
Figure 22. ^1H -NMR and ^{13}C -NMR chemical shifts distribution of various functional groups for compounds reported present in lignin pyrolysis oils. The assignments range for each functional groups are circled in the specific area. (The assignments range may vary due to the limitations of chemical shift database)	86
Figure 23. Aromatic C-H bonds in the HSQC-NMR spectra for the pyrolysis oils produced by pyrolysis of SW kraft lignin from 400 to 600 °C (from left to right).	87
Figure 24. Methoxyl groups in the HSQC-NMR spectra for the pyrolysis oils produced by pyrolysis of SW kraft lignin from 400 to 600 °C (from left to right).	87
Figure 25. Aliphatic C-H bonds in the HSQC-NMR spectra for the pyrolysis oils produced by pyrolysis of SW kraft lignin from 400 to 600 °C (from left to right).	87
Figure 26. Reported bond energy (kcal/mol) for various C-H and C-O bonds in lignin model compound. ^{115, 116}	88
Figure 27. The summary of tentative decomposition and rearrangement pathways of methoxyl groups in lignin during the pyrolysis. ^{49, 51, 115}	88
Figure 28. ^1H -NMR and ^{13}C -NMR chemical shifts distribution of various functional groups for compounds reported present in pyrolysis oils produced from cellulose. ^{58, 64, 61-63} The assignments range for each functional groups are circled in the specific area.	90

Figure 29. HSQC-NMR spectra and the assignments of each carbon in the levoglucosan presented in pyrolysis oils produced by pyrolysis of cellulose from 400 to 600 °C (from left to right).	91
Figure 30. The summary of tentative mechanism in the literatures for the formation of levoglucosan, HMF and aromatic rings during the pyrolysis of cellulose. ^{58, 88, 117, 118}	91
Figure 31. Aromatic C-H bonds in the HSQC-NMR spectra for the pyrolysis oils produced by pyrolysis of cellulose from 400 to 600 °C (from left to right).	92
Figure 32. Aliphatic C-H bonds in the HSQC-NMR spectra for the pyrolysis oils produced by pyrolysis of cellulose from 400 to 600 °C (from left to right).	92
Figure 33. HSQC-NMR spectra and the assignment of 5-hydroxymethyl-furfural (HMF, compound H in Table 28) presented in pyrolysis oils produced by pyrolysis of cellulose from 400 to 600 °C (from left to right).	92
Figure 34. HSQC-NMR spectra and the assignments of each carbon in the levoglucosan presented in pyrolysis oils produced by pyrolysis of pine wood from 400 to 600 °C (from left to right).	94
Figure 35. Aromatic C-H bonds in the HSQC-NMR spectra for the pyrolysis oils produced by pyrolysis of pine wood from 400 to 600 °C (from left to right).	94
Figure 36. Methoxyl groups in the HSQC-NMR spectra for the pyrolysis oils produced by pyrolysis of pine wood from 400 to 600 °C (from left to right).	94

Figure 37. Aliphatic C-H bonds in the HSQC-NMR spectra for the pyrolysis oils produced by pyrolysis of pine wood from 400 to 600 °C (from left to right).	95
Figure 38. The ¹ H-NMR integration results for each functional group in the pyrolysis oils produced from pine residue during the accelerated aging process at 80 °C.	104
Figure 39. The ¹³ C-NMR integration results for each functional group in the pyrolysis oils produced from pine residue during the accelerated aging process at 80 °C.	109
Figure 40. Tentative chemical pathways for the reactions occurred during the accelerated aging process of pine residue pyrolysis oil at 80 °C. ^{9, 132-134}	110
Figure 41. Aromatic C-H bonds in the HSQC spectra for the pyrolysis oils produced by pyrolysis of pine residue at 600 °C and aged at 80 °C for 0 h and 60 h (from left to right).	111
Figure 42. HSQC spectra and the assignments of each carbon in the levoglucosan presented in the pyrolysis oils produced by pyrolysis of pine residue at 600 °C and aged at 80 °C for 0 h and 60 h (from left to right).	112
Figure 43. Methoxyl groups in the HSQC spectra for the pyrolysis oils produced by pyrolysis of pine residue at 600 °C and aged at 80 °C for 0 h and 60 h (from left to right).	112

Figure 44. Aliphatic C-C bonds in the HSQC spectra for the pyrolysis oils produced by pyrolysis of pine residue at 600 °C and aged at 80 °C for 0 h and 60 h (from left to right).

..... 112

Figure 45. Yields of light oil, heavy oil, char and gas for the pyrolysis of pure SW kraft lignin and pyrolysis of SW kraft lignin with 0.1/1.0 ($W_{\text{additive}}/W_{\text{lignin}}$) of NiCl_2 , 0.5/1.0 ($W_{\text{additive}}/W_{\text{lignin}}$) of H-ZSM-5 zeolite, 1.0/1.0 ($W_{\text{additive}}/W_{\text{lignin}}$) of H-ZSM-5 zeolite and 1.0/1.0 ($W_{\text{additive}}/W_{\text{lignin}}$) of Ni-ZSM-5 zeolite as additives at 700 °C for 10 min. 119

Figure 46. ^{31}P -NMR spectra for the heavy oils produced by pyrolysis of SW kraft lignin (top) and pyrolysis of SW kraft lignin with Ni-ZSM-5 as the additive (bottom) at 700 °C for 10 min, derivatized with TMDP..... 121

Figure 47. Hydroxyl group contents of different heavy oils produced by pyrolysis of pure SW kraft lignin and pyrolysis of SW kraft lignin with 0.1/1.0 ($W_{\text{additive}}/W_{\text{lignin}}$) of NiCl_2 , 0.5/1.0 ($W_{\text{additive}}/W_{\text{lignin}}$) of H-ZSM-5 zeolite, 1.0/1.0 ($W_{\text{additive}}/W_{\text{lignin}}$) of H-ZSM-5 zeolite and 1.0/1.0 ($W_{\text{additive}}/W_{\text{lignin}}$) of Ni-ZSM-5 zeolite as additives at 700 °C for 10 min, determined by quantitative ^{31}P -NMR after derivatization with TMDP..... 122

Figure 48. The possible decomposition pathways of ether bond in lignin during the pyrolysis.⁹ 123

Figure 49. Weight percentage of four major components in light oils produced by pyrolysis of pure SW kraft lignin and pyrolysis of SW kraft lignin with 0.1/1.0 ($W_{\text{additive}}/W_{\text{lignin}}$) of NiCl_2 , 0.5/1.0 ($W_{\text{additive}}/W_{\text{lignin}}$) of H-ZSM-5 zeolite, 1.0/1.0 ($W_{\text{additive}}/W_{\text{lignin}}$) of H-ZSM-5

zeolite and 1.0/1.0 ($W_{\text{additive}}/W_{\text{lignin}}$) of Ni-ZSM-5 zeolite as additives at 700 °C for 10 min, determined by quantitative ^{31}P -NMR after derivatization with TMDP..... 124

Figure 50. Quantitative ^{13}C -NMR spectra for the heavy oil produced by pyrolysis of SW kraft lignin (top) and pyrolysis of SW kraft lignin with Ni-ZSM-5 as the additive (bottom) at 700 °C for 10 min. 127

Figure 51. Integration results for the SW kraft lignin and the heavy oils produced by pyrolysis of pure SW kraft lignin and pyrolysis of SW kraft lignin with 0.1/1.0 ($W_{\text{additive}}/W_{\text{lignin}}$) of NiCl_2 , 1.0/1.0 ($W_{\text{additive}}/W_{\text{lignin}}$) of H-ZSM-5 zeolite and 1.0/1.0 ($W_{\text{additive}}/W_{\text{lignin}}$) of Ni-ZSM-5 zeolite as additives at 700 °C for 10min, detected by quantitative ^{13}C -NMR with using the assignment range showed in Table 34. The results were shown as the percentage of carbon. 127

Figure 52. The primary decomposed functional groups in lignin during the pyrolysis. ⁹ 128

Figure 53. Molecular weight distribution and polydispersity of heavy oils produced by pyrolysis of pure SW kraft lignin and pyrolysis of SW kraft lignin with 0.1/1.0 ($W_{\text{additive}}/W_{\text{lignin}}$) of NiCl_2 , 0.5/1.0 ($W_{\text{additive}}/W_{\text{lignin}}$) of H-ZSM-5 zeolite, 1.0/1.0 ($W_{\text{additive}}/W_{\text{lignin}}$) of H-ZSM-5 zeolite and 1.0/1.0 ($W_{\text{additive}}/W_{\text{lignin}}$) of Ni-ZSM-5 zeolite as additives at 700 °C for 10 min. 129

Figure 54. Hydroxyl group contents of different heavy oils produced by pyrolysis of pure SW kraft lignin and pyrolysis of SW kraft lignin with 1.0/1.0 ($W_{\text{additive}}/W_{\text{lignin}}$) of H-ZSM-5

zeolites as additives at 600 °C for 10 min, determined by quantitative ^{31}P -NMR after derivatization with TMDP. 139

Figure 55. The primary decomposed functional groups in lignin during the pyrolysis (circled by dash line in lignin model structure) and the possible cracking pathways on zeolite. ¹⁶⁸⁻¹⁷⁸ 140

Figure 56. Weight percentage of four major components in light oils produced by pyrolysis of pure SW kraft lignin and pyrolysis of SW kraft lignin with 1.0/1.0 ($W_{\text{additive}}/W_{\text{lignin}}$) of H-ZSM-5 zeolites as additives at 600 °C for 10 min, determined by quantitative ^{31}P -NMR after derivatization with TMDP. 141

Figure 57. Integration results for the SW kraft lignin and the heavy oils produced by pyrolysis of pure SW kraft lignin and pyrolysis of SW kraft lignin with 1.0/1.0 ($W_{\text{additive}}/W_{\text{lignin}}$) of H-ZSM-5 zeolites as additives at 600 °C for 10 min, detected by quantitative ^{13}C -NMR. 144

Figure 58. Aromatic C-H bonds in the HSQC-NMR spectra for the pyrolysis oils produced by pyrolysis of SW kraft lignin with H-ZSM-5 zeolites, from left top to right bottom is L, Z23, Z30, Z50, Z80 and Z280 upgraded pyrolysis oil. 146

Figure 59. Methoxyl groups in the HSQC-NMR spectra for the pyrolysis oils produced by pyrolysis of SW kraft lignin with H-ZSM-5 zeolites, from left top to right bottom is L, Z23, Z30, Z50, Z80 and Z280 upgraded pyrolysis oil. 146

Figure 60. Aliphatic C-H bonds in the HSQC-NMR spectra for the pyrolysis oils produced by pyrolysis of SW kraft lignin with H-ZSM-5 zeolites, from left top to right bottom is L, Z23, Z30, Z50, Z80 and Z280 upgraded pyrolysis oil.....	147
Figure 61. Molecular weight distribution and polydispersity of heavy oils produced by pyrolysis of pure SW kraft lignin and pyrolysis of SW kraft lignin with 1.0/1.0 ($W_{\text{additive}}/W_{\text{lignin}}$) of H-ZSM-5 zeolites as additives at 600 °C for 10 min.	148
Figure 62. Summary of experimental procedure.	155
Figure 63. Yields (wt%) of light oil, heavy oil, char (excludes the weight of zeolite) and gas for the pyrolysis of pure SW kraft lignin and pyrolysis of SW kraft lignin with 1.0/1.0 ($W_{\text{additive}}/W_{\text{lignin}}$) of Z, Y, B, F and M zeolites as additives at 600 °C for 10 min.	156
Figure 64. Hydroxyl group contents (mmol/g of heavy oil) of different heavy oils produced by pyrolysis of pure SW kraft lignin and pyrolysis of SW kraft lignin with 1.0/1.0 ($W_{\text{additive}}/W_{\text{lignin}}$) of Z, Y, B, F and M zeolites as additives at 600 °C for 10 min, determined by quantitative ^{31}P -NMR after derivatization with TMDP.....	159
Figure 65. Weight percentage of four major components in light oils produced by pyrolysis of pure SW kraft lignin and pyrolysis of SW kraft lignin with 1.0/1.0 ($W_{\text{additive}}/W_{\text{lignin}}$) of Z, Y, B, F and M zeolites as additives at 600 °C for 10 min, determined by quantitative ^{31}P -NMR after derivatization with TMDP.....	160
Figure 66. Integration results for the SW kraft lignin and the heavy oils produced by pyrolysis of pure SW kraft lignin and pyrolysis of SW kraft lignin with 1.0/1.0	

($W_{\text{additive}}/W_{\text{lignin}}$) of Z, Y, B, F and M zeolites as additives at 600 °C for 10 min, detected by quantitative ^{13}C -NMR with using the assignment range showed in Table 42. The results were shown as the percentage of carbon.	163
Figure 67. Aromatic C-H bonds in the HSQC-NMR spectra for the pyrolysis oils produced by pyrolysis of SW kraft lignin with various zeolites, from left top to right bottom is L, Z, Y, B, F and M upgraded pyrolysis oil.....	165
Figure 68. Methoxyl groups in the HSQC-NMR spectra for the pyrolysis oils produced by pyrolysis of SW kraft lignin with various zeolites, from left top to right bottom is L, Z, Y, B, F and M upgraded pyrolysis oil.	165
Figure 69. Aliphatic C-H bonds in the HSQC-NMR spectra for the pyrolysis oils produced by pyrolysis of SW kraft lignin with various zeolites, from left top to right bottom is L, Z, Y, B, F and M upgraded pyrolysis oil.....	166
Figure 70. The reported possible degradation pathway of methoxyl groups on the surface of zeolite. ¹⁶⁸⁻¹⁷⁰	166
Figure 71. Molecular weight distribution and polydispersity of heavy oils produced by pyrolysis of pure SW kraft lignin and pyrolysis of SW kraft lignin with 1.0/1.0 ($W_{\text{additive}}/W_{\text{lignin}}$) of Z, Y, B, F and M zeolites as additives at 600 °C for 10 min.	167
Figure 72. Summary of experimental procedure.	175

Figure 73. ^1H -NMR spectra for the EOL heavy oil, first and second step hydrogenation products. (from top to bottom).....	176
Figure 74. Quantitative ^{13}C -NMR, DEPT-135 and HSQC-NMR spectra for the EOL heavy oil and first step hydrogenation product. (from top to bottom)	179
Figure 75. DEPT-135 and HSQC-NMR spectra for the second step hydrogenation product.	179
Figure 76. Tentative reaction pathways of HYD and HDO process of EOL heavy oil. ²⁰³⁻²⁰⁷	180
Figure 77. Quantitative ^{13}C -NMR for EOL heavy oil and tar from first step HYD catalyst (from top to bottom), and SEM for the original catalyst, catalyst after first and second step HYD process (from left to right).	181
Figure 78. CP/MAS ^{13}C -NMR spectra (from bottom to top) of original Loblolly pine wood, torrefied wood samples produced by torrefaction of Loblolly pine wood at 250 °C for 0.25, 0.50, 1.00, 2.00, 4.00, 6.00 and 8.00 hours.....	197
Figure 79. CP/MAS ^{13}C -NMR spectra (from bottom to top) of torrefied Loblolly pine wood samples produced by torrefaction of Loblolly pine wood at 300 °C for 4.00 hours, 250°C for 4.00 hours, 300 °C for 0.50 hours and 250 °C for 0.50 hours.	200

Figure 80. Hypothesized pathways of decomposition of major wood components and the formation of new functional groups and condensed aromatic units during the torrefaction. ^{58, 117, 118, 134, 222, 224-228}	200
--	-----

LIST OF ABBREVIATIONS

Ar	Aromatic
CDCl ₃	Deuterated chloroform
CP/MAS	Cross polarization/magnetic angle spinning
D	Polydispersity
DEPT	Distortionless Enhancement by Polarization Transfer
DMSO	Dimethyl sulfoxide
DP	Degree of polymerization
DSC	Differential scanning calorimetry
EDTA	Ethylenedinitrilotetraacetic acid
EOL	Ethanol organosolv lignin
FT-IR	Fourier transform infrared
GC	Gas chromatography
GPC	Gel permeation chromatography
h	Hour
HDO	Hydrodeoxygenation
HMF	5-Hydroxymethyl furfural
HPLC	High pressure liquid chromatography
HSQC	Heteronuclear Single-Quantum Correlation
HW	Hardwood
HYD	Hydrogenation
min	Minute

MBMS	Molecular-beam mass spectrometry
M _n	Number average molecular weight
MS	Mass spectroscopy
M _w	Weight average molecular weight
NHND	endo-N-hydroxy-5-norbornene-2,3-dicarboximide
NMR	Nuclear magnetic resonance
ppm	Part-per-million
PAH	polyaromatic hydrocarbon
RT	Room temperature
s	Second
SEM	Scanning electron microscopy
SW	Softwood
T	Temperature
T ₁	Spin-lattice relaxation time
TGA	Thermogravimetric analysis
THF	Tetrahydrofuran
TMDP	2-chloro-4,4,5,5-tetramethyl-1,3,2-dioxaphospholane
UV	Ultraviolet
XRD	X-ray diffraction
1 D	1 dimensional
2 D	2 dimensional

SUMMARY

With declining petroleum resources, increasing fuel demands and growing concerns about the effects of carbon dioxide emissions from fossil fuels, it is imperative to find sustainable resource for energy and chemicals. Biomass is a renewable resource for sustainable production of fuels and chemicals that, to date, have been made primarily from fossil resources. Lignin is a major natural aromatic polymer and a main constituent of lignocellulosics biomass; however, it has received less biorefining efforts than plant polysaccharides. For example, the US paper industry produces over 50 million tons of extracted lignin per year but only 2% is used commercially in products. The remainder is burned as a low value fuel to recover energy. Therefore, one step thermal conversion of lignin and biomass to gasoline range (molecular weight is ~ 105 g/mol) of simple petrochemicals such as benzene, toluene, xylene, phenol and catechol appears to be very pragmatic. Further upgrading process including hydrogenation of pyrolysis oils to produce total aliphatic products also provides insight into the conversion from biomass to fuels.

This thesis examined the conversions of biomass and biomass components to petrochemicals and total aliphatic gasoline like products. There are three major projects of the thesis. Since biomass is very complicated, to understand the thermal decomposition pathways of biomass, the pyrolytic behaviors of various biomass components including lignin and cellulose under different reaction were investigated in the first phase. Due to complexity and limited volatility, the thermal decomposition products from biomass bring insurmountable obstacles to the traditional analysis methods such as GC-MS, UV

and FT-IR. Therefore, precise characterization of the whole portion of thermal decomposition products has significant impacts on providing insight into the pyrolysis pathways and evaluating the upgrading processes. Various NMR methods to characterize different functional groups presented in liquid and solid pyrolysis products by ^1H , ^{13}C , ^{31}P , 2D-HSQC and solid state ^{13}C -NMR were introduced in the second phase. Nevertheless, the major drawback towards commercialization of pyrolysis oils are their challenging properties including poor volatility, high oxygen content, molecular weight, acidity and viscosity, corrosiveness and cold flow problems. In situ upgrading the properties of pyrolysis oils during thermal conversion process by employing zeolites has been discussed in the third phase. The further hydrogenation of pyrolysis oils to total aliphatic gasoline like products by heterogeneous catalysis in “green medium” – water has also been examined in the third project.

CHAPTER 1: INTRODUCTION

The U.S. Department of Agriculture and U.S. Department of Energy established a vision to derive 25% of chemicals and materials and 20% of transportation fuels from biomass by 2030.¹ Among the various conversion technologies being investigated, pyrolysis has been reported as one of the economic ways (i.e., low capital and operating costs) to utilize biomass for bio-fuels and bio-chemicals.²

The products from whole biomass pyrolysis are complicated. Understanding the whole biomass pyrolysis pathways calls for fundamental analysis of pyrolysis of major biomass components—cellulose and lignin. Chapter 4 investigated pyrolytic behaviors of these two major biomass components as well as the whole biomass. In addition, the complexity nature of pyrolysis oils brings a huge barrier to the traditional analysis methods such as GC-MS, GPC and FT-IR. GC-MS analysis has always been used to analyze individual components in pyrolysis oil, however, only a small portion could be detected by GC due to poor volatility. Although spectroscopic technique such as FT-IR provides insights into the whole portion of pyrolysis oil, the ability of such method to deal with complex mixture like pyrolysis oil is very limited. Owing to the complicated components, characterization of the whole portion of pyrolysis oil will provide insight into the following chemical upgrading process, which is a challenging but crucial undertaking. NMR has the ability to analyze the whole portion of pyrolysis oil and has some advantages over traditional methods. It could also characterize more than thirty different functional groups in the pyrolysis oil and provide quantitative results. (Chapter 5)

Nevertheless, the major drawback towards commercialization of pyrolysis oils are several challenging properties including poor volatility, high oxygen content, acidity and viscosity, corrosiveness and cold flow problems.³ Hence, Chapter 6 examined the chemical changes of pyrolysis oils during the aging process, which is another huge barrier to the usage of pyrolysis oil. Therefore, how to upgrade the properties of pyrolysis oil is a very challenging topic. Chapters 7-9 addressed such issues and accomplished the one step thermal conversion of lignin to the gasoline range (molecular weight is ~105 g/mol) simple petrochemicals such as catechol, toluene, xylene and phenol by employing zeolites. Further upgrading process including hydrogenation of pyrolysis oil to produce total aliphatic gasoline like products has also been investigated in Chapter 10. Figure 1 shows three main projects of this dissertation.

The major objectives of this dissertation are summarized as follows:

- ❖ Investigated pyrolytic behaviors of various biomasses and biomass components at different temperatures. (Chapter 4)
- ❖ Accomplished the process of producing bio-coal—torrefaction, which could provide bio-coal to reduce the CO₂ emissions. (Appendix A)
- ❖ Provided various innovations of characterization of pyrolysis/torrefaction products including the first reported efforts to analyze whole portion of pyrolysis oils by HSQC-NMR. (Chapter 5)
- ❖ Created several chemical shifts databases for the components presented in the pyrolysis oils to facilitate the characterizations by NMR. (Chapter 5)

- ❖ Examined the accelerated aging process of pyrolysis oils by in situ NMR characterization. (Chapter 6)
- ❖ Converted lignin to the gasoline range (molecular weight is ~ 105 g/mol) simple petrochemicals by employing zeolites. (Chapter 7-9)
- ❖ Explored the influence from Si/Al ratio and framework of zeolites on the properties of upgraded pyrolysis oil. (Chapter 8, 9)
- ❖ Produced renewable gasoline from hydrogenation of lignin pyrolysis oil in “Green solvent”—water. (Chapter 10)

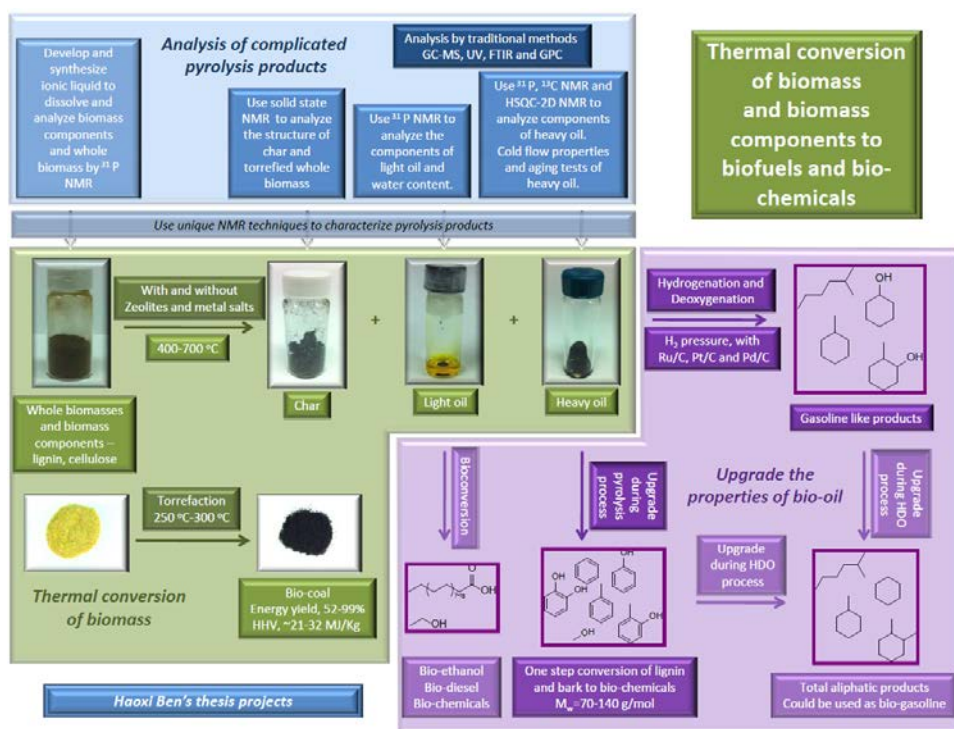


Figure 1. Three major projects in this dissertation.

Chapter 2: LITERATURE REVIEW*

2.1 Problem Statement

Over the last century, worldwide energy consumption has increased by 17 fold⁴ and this demand is predicted to grow by more than 50% by 2025.⁵ Known viable petroleum reserves are predicted to be consumed in less than fifty years at present rates of consumption. In addition, the carbon dioxide emissions from the consumption of fossil fuels have been growing at an average rate of ~2% per year; and the rate continues to increase. Growing concerns about the effects of carbon dioxide emissions from fossil fuels call for sustainable energy sources, such as biomass. Biomass is a renewable resource for the sustainable production of fuels and chemicals that, to date, have been made primarily from fossil resources. Because of its carbon neutrality, relative abundance and non-food competition,⁶ the use of biofuels and biochemicals could increase economic growth and provide environmental benefits. The U.S. Department of Agriculture and U.S. Department of Energy both strongly propose to expand the usage of biomass as a resource of energy and chemical, and they also established a vision to derive 25% of chemicals and materials and 20% of transportation fuels from biomass by 2030.⁷

* The part of this literature review was submitted to BioEnergy Research, 2012. It is entitled as “Lignin Pyrolysis Components and Upgrading – Technology Review”. The other authors are Arthur J. Ragauskas from the Institute of Paper Science and Technology and School of Chemistry and Biochemistry at Georgia Institute of Technology; Wei Mu from the Institute of Paper Science and Technology and School of Chemical and Biomolecular Engineering at Georgia Institute of Technology; Yulin Deng from the Institute of Paper Science and Technology and School of Chemical and Biomolecular Engineering at Georgia Institute of Technology. Approximately 80% of this literature review has been written as a book chapter and will be published by World Scientific Publishing Co. It is entitled as “Pyrolysis of Biomass to Bio-oils”. The other author is Arthur J. Ragauskas from the Institute of Paper Science and Technology and School of Chemistry and Biochemistry at Georgia Institute of Technology. The copyright permissions will be submitted to the thesis office of Gatech.

Among the various conversion technologies that has been investigated, pyrolysis has been reported as one of the economic ways (i.e., low capital and operating costs) to utilize biomass for bio-fuels and bio-chemicals.² The whole biomass pyrolysis products are complicated. To fully understand the pyrolytic behavior of the whole biomass, the fundamental analysis of pyrolysis of major biomass components—cellulose, hemicellulose, lignin and for barks—tannin appears to be very pragmatic. In addition, owing to the complicated components, characterization of the properties of pyrolysis oil will provide insight into the following upgrading process. The complexity nature of pyrolysis oils brings a huge barrier to the traditional analysis methods such as GC-MS, GPC and FT-IR. GC-MS analysis has always been used to analyze individual components in pyrolysis oil, however, only a small portion could be detected by GC due to the poor volatility.⁸ The spectroscopic technique such as FT-IR could give insights into the whole portions of pyrolysis oil. Unfortunately, the ability of such method to deal with complex mixture like pyrolysis oil is very limited. NMR has the ability to analyze the whole portion of pyrolysis oil and has some advantages compare to the traditional methods. It could characterize more than thirty different functional groups present in the pyrolysis oil and provide quantitative results.^{9, 10} Nevertheless, the major drawback towards commercialization of pyrolysis oils are several challenging properties including poor volatility, high oxygen content, acidity and viscosity, corrosiveness, cold flow and aging problems.³ Therefore, upgrading technologies that convert bio-oils to a potential substitution of diesel and gasoline fuels are necessary.

2.2 Lignocellulose

Lignocellulosic biomass provides an abundant sustainable feedstock for biofuel and it contains three major constituents: cellulose, hemicelluloses and lignin. Table 1 summarizes the distribution of the three major biopolymers in several hardwoods, softwoods and agricultural residue species.^{11, 12}

Table 1. Major biomass components indifferent softwoods, hardwoods and residue species.^{11, 12}

Wood Species		Wood components ^a		
		Cellulose (%)	Lignin (%)	Hemicelluloses (%)
Softwoods	<i>Piceaglauca</i>	41	27	31
	<i>Abiesbalsamea</i>	42	29	27
	<i>Pinus strobes</i>	41	29	27
	<i>Tsugacanadensis</i>	41	33	23
	<i>Norway spruce</i>	46	28	25
	<i>Loblolly pine</i>	39	31	25
	<i>Thujaoccidentalis</i>	41	31	26
Hardwoods	<i>Eucalyptus globulus</i>	45	19	35
	<i>Acer rubrum</i>	45	24	29
	<i>Ulmusamericana</i>	51	24	23
	<i>Populus tremuloides</i>	48	21	27
	<i>Betulapapyrifera</i>	42	19	38
	<i>Fagusgrandifolia</i>	45	22	29

Table 2 continued				
Residues	Pine residues ^b	45	27	20
	Pine bark	32	34	19

^a all samples were analyzed extractives free

^b Pine residues are mixtures of stumps, limbs, tops, and dead trees

2.2.1 Cellulose

Cellulose is the most abundant biopolymer and has an approximately 100×10^9 metric tons annual biosynthesis rate.⁵ Generally, biomasses contain around 35-50% of cellulose, which is a linear polymer built up of β -D glucopyranose units covalently linked with 1→4 glycosidic bonds, with a degree of polymerization (DP) of ~300-15000. Table 2 summarizes the DP in different cellulose containing materials. Figure 2 shows the molecular structure of cellulose. In the native form of cellulose, the glucopyranose units in the cellulose chain are in the most thermodynamically stable conformation—chair conformation, which with the -CH₂OH and -OH groups in equatorial position.¹³ Due to the highly organized structure and the inter- and intra-molecular hydrogen bonds, in the native form, cellulose has a relatively high-degree of crystallinity averaging 50-70%.^{5, 6, 14} Table 3 summarizes the cellulose crystallinity from several biomasses.

Table 2. DP of native wood and non-woody celluloses after nitration using the viscometric method.¹⁵⁻¹⁷

Species	DP
Bagasse	925
Wheat straw	1045
E.regnans	1510
P. radiata	3063
Cotton linters	3170
Cotton stalks	1820
Aspen	4581
Nalita wood (12-30 months)	3181-3611
Jack pine	10300

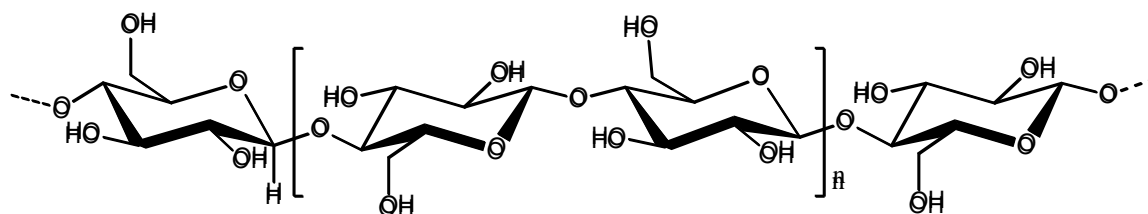


Figure 2. Cellulose molecular structure.

Table 3. Cellulose crystallinity from several biomasses.^{14, 15, 18}

Origin	Crystallinity (%)
Hybrid poplar	63 ^a
Loblolly pine	63 ^a
Alamo switchgrass	44 ^a
Bagasse	37 ^b
Wheat straw	35 ^b
E.regnans	37 ^b
P. radiata	34 ^b
Cotton linters	80 ^b
Norway spruce	67 ^b

^a Determined by CP/MAS ¹³C-NMR spectroscopy.

^b Determined by x-ray diffraction.

2.2.2 Hemicelluloses

Hemicelluloses are low DP (50-300) polysaccharides and contain arabinose, xylose, galactose, mannose, and glucose, along with side chains groups, such as acetyl, galacturonic acid, glucuronic acid, and 4-O-methylglucuronic acid. The major hemicelluloses in softwoods (SW) are galactoglucomannans and arabinoglucuronoxylan, and a small amount of arabinogalactan, xyloglucan, and other glucans. For hardwood, the predominant hemicellulose is glucuronoxylan and glucomannan with limited amount of galactans and glucans.⁵ Figure 3 shows the major types of hemicelluloses in softwoods and hardwoods.

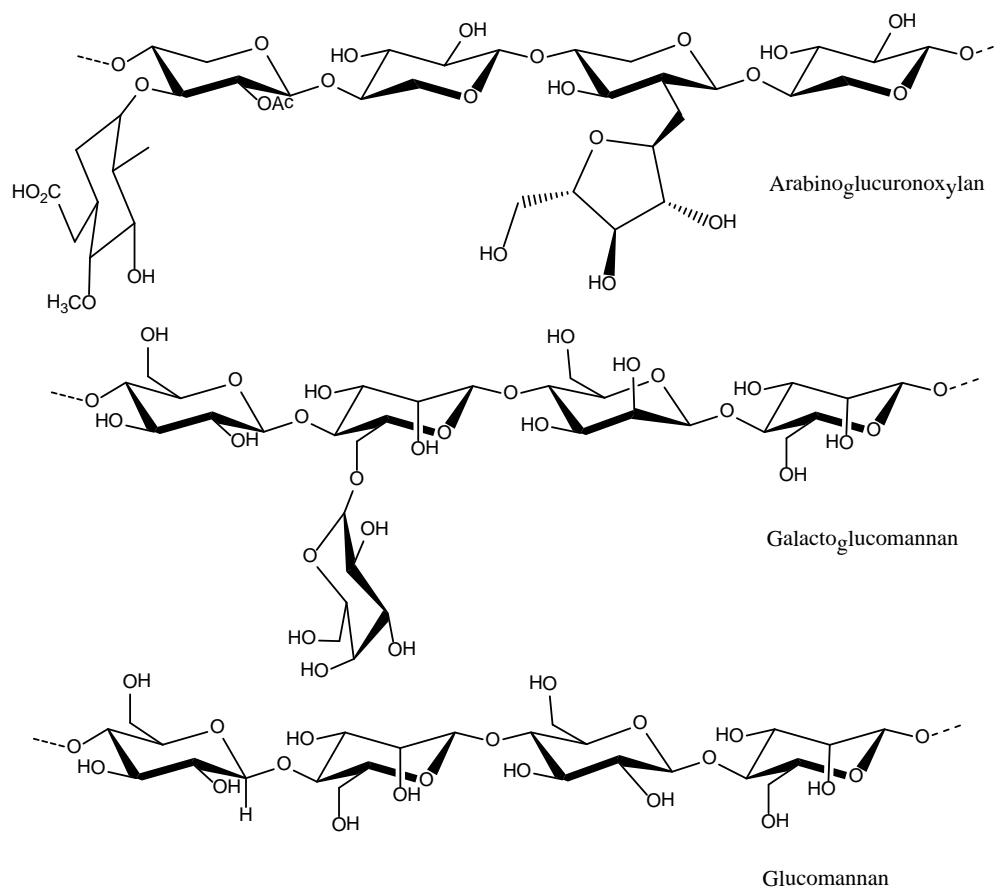


Figure 3. Major types of hemicelluloses in softwoods and hardwoods.

Willfor et al.^{19, 20} have examined the polysaccharides in 11 industrially important hardwood and 12 softwood species. They found that the most abundant sugar in the softwood hemicellulose is mannose; correspondingly, the most abundant sugar in hardwood hemicellulose is xylose. Representative data from this study is summarized in Table 4. The DP of some hemicelluloses in several hardwood and softwood species is summarized in Table 5.

Table 4. Amount and composition of sugar units (wt%) of different hardwood and softwood species.^{19, 20}

Wood Species	Ara	Xyl	Gal	Glc	Man	Rha	GlcA	GalA	4- <i>O</i> - MeGlcA
Hardwood									
<i>Acacia crassicarpa</i>	0.3	11.7	11.4	2.2	0.2	0.30	0.2	1.8	2.6
<i>Betula pendula</i>	0.5	23.6	1.3	1.8	0.9	0.5	0.3	2.2	3.7
<i>Eucalyptus globulus</i>	0.6	14.0	2.3	5.6	0.3	0.5	0.2	2.0	2.5
<i>Populus deltoides</i>	0.5	17.2	0.8	2.5	2.7	0.5	0.2	2.5	2.5
<i>Populus tremula</i>	0.5	19.6	1.1	4.2	1.3	0.5	0.1	2.4	2.5
Softwood									
<i>Picea abies</i>	1.4	5.8	2.0	3.3	9.0	0.2	0.3	1.6	9.8
<i>Picea mariana</i>	1.5	5.0	2.8	3.8	9.6	0.2	0.4	1.6	0.9
<i>Abies lasiocarpa</i>	1.6	5.0	4.0	4.0	10.0	0.3	0.4	1.5	0.9
<i>Larix laricina</i>	2.7	5.1	8.6	4.0	10.5	0.2	0.6	1.4	1.1
<i>Pinus resinosa</i>	2.3	6.8	4.0	3.7	8.5	0.3	0.5	1.6	1.3

Table 5. DP of hemicelluloses in several biomasses. ²¹

Origin	Hemicellulose	DP
Birch	Glucuronoxylan	~112
Aspen	Glucuronoxylan	~112
Spruce	Arabinoglucuronoxylan	~126
	Galactoglucomannan	~125
Pine	Arabinoglucuronoxylan	~126
	Galactoglucomannan	~125
Larch	Arabinoglucuronoxylan	~126
	Galactoglucomannan	~125

2.2.3 Lignin

As the second most abundant biomass component and the primary renewable aromatic resource in nature, lignin is distinctly different from cellulose and hemicelluloses. Lignin is one of the most complex natural polymers in regards of its chemical structure and composition. It is synthesized by enzymatic dehydrogenative polymerization of 4-hydroxyphenyl propanoid units. Figure 4 indicates the three phenyl propane precursors of lignin and the enzymatic synthesis pathway from coniferyl unit to one of the most abundant linkages in lignin structure— β -O-4 linkage. Some other major types of linkages and the reported abundance in softwood and hardwood lignins have been shown in Table 6.^{22, 23} Guerra et al. examined the molecular weights of various lignins isolated from different wood species and the results are summarized in Table 7.

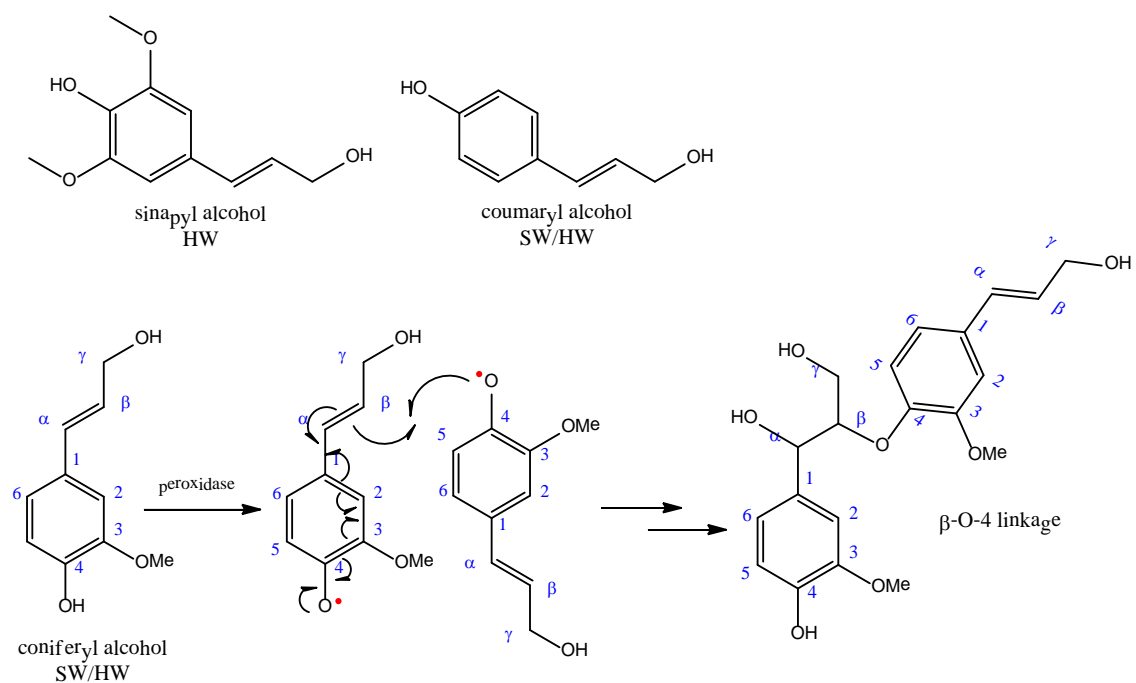
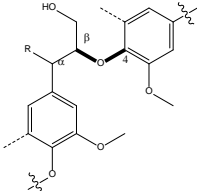
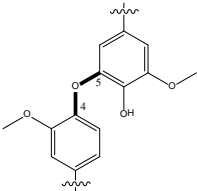
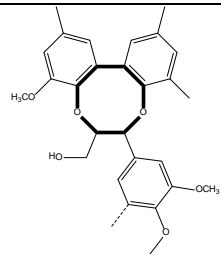


Figure 4. Three phenyl propane precursors of lignin and the enzymatic synthesis pathway from coniferyl unit to one of the most abundant linkages in lignin structure— β -O-4 linkage.

Table 6. Reported abundance of major linkages in softwood and hardwood lignins.^{22, 23}

Linkage	β -O-4	4-O-5	Dibenzodioxocin	
C-O linkage				
Abundance				
Per 100				
C ₉ -units				
Softwood	45-50	4-7	5-7	
Hardwood	60-62	7-9	0-2	

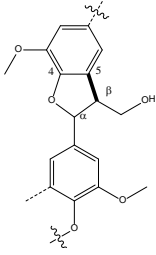
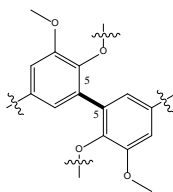
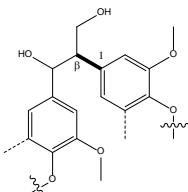
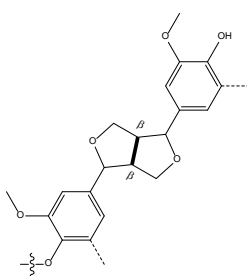
Linkage	β -5	5-5	β -1	β - β
C-C linkage				
Abundance				
Per 100				
C ₉ -units				
Softwood	9-12	19-22	7-9	2-4
Hardwood	3-11	3-9	1-7	3-12

Table 7. Weight-average molecular weight (M_w), number-average molecular weight (M_n), polydispersity (D) and approximate DP of various lignins isolated from different wood species.

Origin	M_w	M_n	D	DP ^a
Douglas Fir	38000	7600	5.0	42-211
White Fir	52000	6300	8.2	35-289
Redwood	30100	4700	6.4	26-167
<i>E. globules</i>	32000	8700	3.7	48-178
Southern Pine	57600	9700	5.9	54-320

^a DP is calculated on the basis of phenyl propanoid units.

2.3 Pyrolysis of biomass components

2.3.1 Lignin pyrolysis products

2.3.1.1 Gas products of pyrolysis of lignin

From the 1980's to the early 2000's, many lignin pyrolysis researches focused on the gas products.²⁴⁻³⁰ Some major gas components reported in the literatures have been summarized in Table 8. Carbon monoxide and carbon dioxides are the top two most abundant components in the gas phase of pyrolysis of lignin. Normally, more than half percentages of gas products are these two components.²⁴⁻²⁹ Methane has also been reported as another major gas component and the yield could be up to ~5 wt% of dry lignin.^{24,25} Methane, carbon monoxide and carbon dioxides were found to increase in yield as the reactor temperature increased from 500 to 900 °C,^{25,26,29,30} nevertheless the content of methane decrease at a higher heating rate.²⁷ Most interestingly, Ferdous et al.^{27,28} indi-

cated that pyrolysis of lignin also produces ~25 mol% of H₂ in the gas phase and the content significantly increased with increasing thermal conversion temperature. It is well known that H₂ and CO are the major components of syngas, which are used to produce synthetic petroleum, whereas the gas products of pyrolysis of lignin could also be used as syngas.

Table 8. Reported major gas products of pyrolysis of lignin.

Major gas components of pyrolysis of lignin ^a				
CH ₄ ²⁴⁻³⁰	C ₂ H ₄ ^{24-26, 29, 30}	C ₂ H ₆ ^{24-26, 29, 30}	C ₃ H ₆ ^{24-26, 29, 30}	C ₄ H ₈ ^{24-26, 29, 30}
CO ²⁴⁻³⁰	CO ₂ ²⁴⁻²⁹	H ₂ ^{27, 28}	HCHO ^{24, 26, 30}	CH ₃ CHO ^{24-26, 30}

^a The pyrolysis temperatures are from 300-1000 °C and lignins are isolated from both softwood and hardwood by kraft and ethanol-based pulping process.

2.3.1.2 Liquid products of pyrolysis of lignin

Most of the pyrolysis works used GC-MS to analyze the liquid pyrolysis products.³¹⁻⁴⁷ By using pyrolysis (Py)-GC-MS, Jimenez et al.⁴⁷ indicated that softwood lignins yielded guaiacyl derivatives, coniferaldehyde and coniferyl alcohol as the major products; hardwood lignins produced guaiacyl and syringyl derivatives, syringaldehyde, coniferyl alcohol and sinapyl alcohol. Pyrolysis of bamboo lignin produced p-vinylphenol as the major compound. Similarly, Jiang et al.³⁵ also used Py-GC-MS to analyze pyrolysis products of lignin over a temperature range of 400-800 °C and indicated that the maximum yield of phenolic compounds was obtained at 600 °C. Most of the phenolic compounds had an individual yield of less than 1 wt% of lignin on a dry ash free basis.

Greenwood et al.⁴² pyrolyzed *Douglas* fir and *Q. nigra* water oak lignin in a laser micro-pyrolysis-GC-MS system. They found that guaiacol, 4-methyl-guaiacol, vinylguaiacol, eugenol, vanillin and coniferylaldehyde are the major components in the pyrolysis oil produced from *Douglas* fir lignin. For the *Q. nigra* water oak lignin pyrolysis oil, guaiacol, 4-methyl-guaiacol, vinylguaiacol, syringol, eugenol, 3, 5-dimethoxyacetophenone, 4-methyl 2, 5-dimethoxy benzaldehyde, 4-allyl-dimethoxylphenol, syringaldehyde, 2, 6-dimethoxyl-2-propylphenol and sinapaldehyde are found as the major components. Jegers et al.⁴⁴ also indicated that guaiacol, 4-methylguaiacol, 4-ethylguaiacol, catechol, 4-methylcatechol, 4-ethylcatechol, phenol, cresol and 4-ethylphenol are the major products of pyrolysis of lignin. As the most abundant products, the content of guaiacol and 4-methylguaiacol are ~5.3 wt% of dry lignin. Lou et al.³⁷ examined the effect of temperature on the composition of pyrolysis products and indicated that the contents of methoxyl contained components, such as guaiacol, 4-methylguaiacol, 4-vinylguaiacol and syringol decreased at higher pyrolysis temperature. In contrast, the contents of non-methoxyl contained compounds, like cresols, ethyl-phenol, and 2, 6-dimethyl-phenol increased with increasing treatment temperature. A summary of lignin pyrolysis conditions and the yield of pyrolysis products are shown in Table 9.

Table 9. Summary of lignin pyrolysis conditions and the yield of pyrolysis products

Lignin	Reactor	Temperature (°C)	Tar (wt %)	Char (wt %)	Gas (wt %)
Kraft lignin (wheat straw and sarkanda grass) ⁴⁵	Fluidized bed	500	31	49	6
	Fluidized bed	410-560	31	34	12
	Fluidized bed	475-525	50	42	8
	Entrained flow	700	37	35	28
	Batch	480	22	48	30
Kraft lignin (pine)			23	41	39
Lignoboost TM (pine)	Fluidized bed ⁴⁸	550	22	29	49
EOL (<i>pinus radiata</i>)			16	63	21
Kraft lignin	Fixed bed ²⁷	800	3-5	43-48	49-52
EOL			14-21	35-44	41-44
Kraft lignin	Fix bed ²⁸	650	13	47	40
EOL			19	39	42
Klason lignin (almond shells) ²⁶	Micro pyroprobe reactor	500	53	34	7
		600	64	20	9
		700	55	17	17
		800	50	15	22
		900	43	14	29

To understand the possible decomposition pathways of lignin during the pyrolysis process and to find an effective upgrading method, many researchers choose to use pyro-

lysis oil model compounds to simplify the simulation model. Therefore, how to choose appropriate pyrolysis oil model compounds, which represent real pyrolysis oils, exhibits its significance. To facilitate this part of work, a summary of GC-MS detected components in the lignin pyrolysis oils reported from seven literatures^{35, 41-46} is shown in Table 10.

Table 10. GC-MS detected components in the lignin pyrolysis oils.^{35, 41-46}

GC-MS detected components in lignin pyrolysis oils ^a		
Phenol ^{35, 41-46}	4'-Hydroxy-3'-methoxy acetophenone ^{35, 41-43, 45, 46}	4-Allyl-dimethoxyphenol ⁴²
	Acetovanillone	
	Acetoguaiacone	
2-Methylphenol ^{35, 41-46}	5-Tert-butylpyrogallol ³⁵	Dimethoxypropyl phenol ⁴²
o-Cresol		
4-Methylphenol ^{35, 41, 42, 44, 45}	1-(4-Hydroxy-3-methoxyphenyl)-2-propanone ^{35, 45, 46}	Coniferylaldehyde ^{42, 46}
p-Cresol	Guaiacyl acetone	
2-Methoxyphenol ^{35, 41-46}	2-(3,4-Dimethoxyphenyl)-6-methyl-3,4-chromanediol ³⁵	Sinapaldehyde ^{42, 46}
Guaiacol		
2,6-Dimethylphenol ^{35, 43, 45}	3,4-Dimethylbenzoic acid ^{35, 43}	2,6-Dimethoxy-4-methyl-phenol ^{41, 46}
2,6-Xylenol		4-Methylsyringol

Table 10 continued		
4-Ethylphenol ^{35, 41, 44, 45} p-Ethylphenol	3-Methoxy-4-hydroxybenzoic acid ³⁵	1-(4-Hydroxy-3-methoxy phenyl) propyne ⁴¹
3-Methylbenzaldehyde ³⁵ m-Tolualdehyde	4-Ethyl-1,2-dimethoxy-benze ne ³⁵	4-Ethyl-2,6- dimethoxy phenol ^{41, 46} 4-Ethylsyringol
2-Hydroxy-6-methylbenzal dehyde ³⁵	4-Propenylsyringol ^{35, 41, 46} 4-Propenyl-2,6-dimethoxyphe nol	4-Vinyl-2,6-dimethoxy-ph enol ^{41, 46} Vinylsyringol
2-Ethylphenol ^{35, 44, 45}	Ferulic acid ³⁵ 3-Hydroxy-4- methoxycinnamic acid	4-Propyl-2,6-dimethoxyph enol ⁴¹
4-Methoxy-3- methylphenol ³⁵	4-Hydroxy-3,5-dimethoxyben zaldehyde ^{35, 41, 42, 45, 46} Syringaldehyde	Syringylacetone ^{41, 46}
2-Methoxy-4- methylphenol ^{35, 41-46} 4-Methylguaiacol	Acetosyringone ^{35, 41, 42, 45} 4'-Hydroxy-3',5'- dimethoxyacetophenone	m-Cresol ^{43, 44}
Catechol ^{35, 42-45} 1,2-Benzenediol	1-(2,6-Dihydroxy-4-methoxy phenyl)-1-butanone ³⁵ Desaspidinol	p-Propylphenol ⁴⁴
Benzofuran ³⁵	Syringic acid ³⁵	6-Ethylguaiacol ⁴⁴

Table 10 continued		
p-Isopropylphenol ³⁵	2,3,5-Trimethyl phenol ⁴⁵	2-Methoxy-4-propylpheno
p-Cumenol		1 ^{43, 44, 46}
		4-Propylguaiacol
		4-Methyl-1,2-benzenediol
2-Ethyl-4-methylphenol ³⁵	3-Ethyl phenol ⁴³⁻⁴⁵	43, 44
		4-Methylcatechol
3-Methoxy-1,2-		
benzenediol ^{35, 44, 45}	1,2,3-Trimethoxybenzene ⁴⁵	6-Ethylcatechol ⁴⁴
3-Methoxycatechol		
3-Methyl-1,2-benzenediol		
35, 42-45		
3-Methylpyrocatechol	Coniferyl alcohol ⁴³⁻⁴⁵	3-Methylguaiacol ⁴⁶
3-Methylcatechol		
2-Methoxy-4-ethylphenol	Methoxyeugenol ^{41, 45}	
35, 41-46	4-Hydroxy-3,5-	
	dimethoxyallylbenzene	3-Ethylguaiacol ⁴⁶
	4-Allyl-2,6-dimethoxyphenol	
		Propioguaiacone ⁴⁶
4-(2-Propenyl)phenol ³⁵	1-Methoxy-3-methylbenzene	1-(4-Hydroxy-3-methoxy-
	42	phenyl)-propan-1-one
p-Isopropenylphenol ³⁵	Indene ⁴²	6-Hydroxy-5,7-dimethoxy
		-indene ⁴⁶

Table 10 continued

2-Methoxy-4-vinylphenol		
35, 41, 42, 45, 46	1,2,3-Trimethylbenzene ⁴²	Dihydroconiferyl alcohol ⁴⁶
4-Vinylguaiacol		
3-Methyl-5-methoxyphenol ³⁵	1,2,4-Trimethylbenzene ⁴²	Propiosyringone ⁴⁶
4-Ethyl-1,3-benzenediol ⁴³	Mesitylene ⁴²	Dihydrosinapyl alcohol ⁴⁶
4-Ethylresorcinol		
2,6-Dimethoxyphenol ^{35, 41, 42, 45, 46}	4-Ethenylphenol ^{41, 42}	Sinapyl alcohol ⁴⁶
Syringol	Vinylphenol	
2,5-Dimethyl-1,4-benzenediol ³⁵	m-Dimethoxybenzene ⁴²	2,3-dimethylphenol ⁴³
		2,3-xilenol
2,4-Dimethoxyphenol ³⁵	Veratrole ⁴²	Naphthalene ^{42, 43}
2',4'-Dimethylacetophenone ³⁵	p-Dimethoxybenzene ⁴²	Benzene ⁴⁵
4-Ethyl-1,2-benzenediol ^{35, 44}	Dimethyl catechol ⁴²	Styrene ⁴⁵
4-Ethylpyrocatechol		
Eugenol ^{35, 41-43, 45, 46}	Vinylcatechol ⁴²	p-Xylene ⁴⁵
3-Hydroxy-4-methoxybenzaldehyde ^{35, 42, 45}	Vanillin ^{41-43, 46}	Ethylbenzene ⁴⁵
Isovanillin		

Table 10 continued		
2,5-Dimethoxy- benzylalcohol ³⁵	3',5'-Dimethoxyacetophenone ⁴²	Toluene ⁴⁵
2-Methoxy-4-(1-propenyl) phenol ^{35, 41-43, 45, 46}	4-Methyl 2,5-dimethoxy benzaldehyde ⁴²	
Isoeugenol		
4'-Hydroxy-3'-methoxyacet ophenone ^{35, 41-43, 45, 46}	Fluorene ⁴²	
Acetovanillone		
Acetoguaiacone		
^a The pyrolysis temperatures are from 400-800 °C		

There are approximately one hundred compounds in Table 10 and almost all of them contain a phenol structure. Furthermore, phenol, acetovanillone, cresols, guaiacol, 4-ethylphenol, syringaldehyde, acetosyringone, 4-methylguaiacol, catechol, 3-methylcatechol, 4-methylguaiacol, 4-vinylguaiacol, vanillin, syringol, eugenol, isoeugenol and acetovanillone have been reported in more than four references and many of them could also be found in other references.^{33, 36-38, 40} Therefore, these components could be used as potential candidates for the model compounds study on pyrolysis of lignin. Figure 5 summarizes the reported possible decomposition pathways of lignin during the pyrolysis.

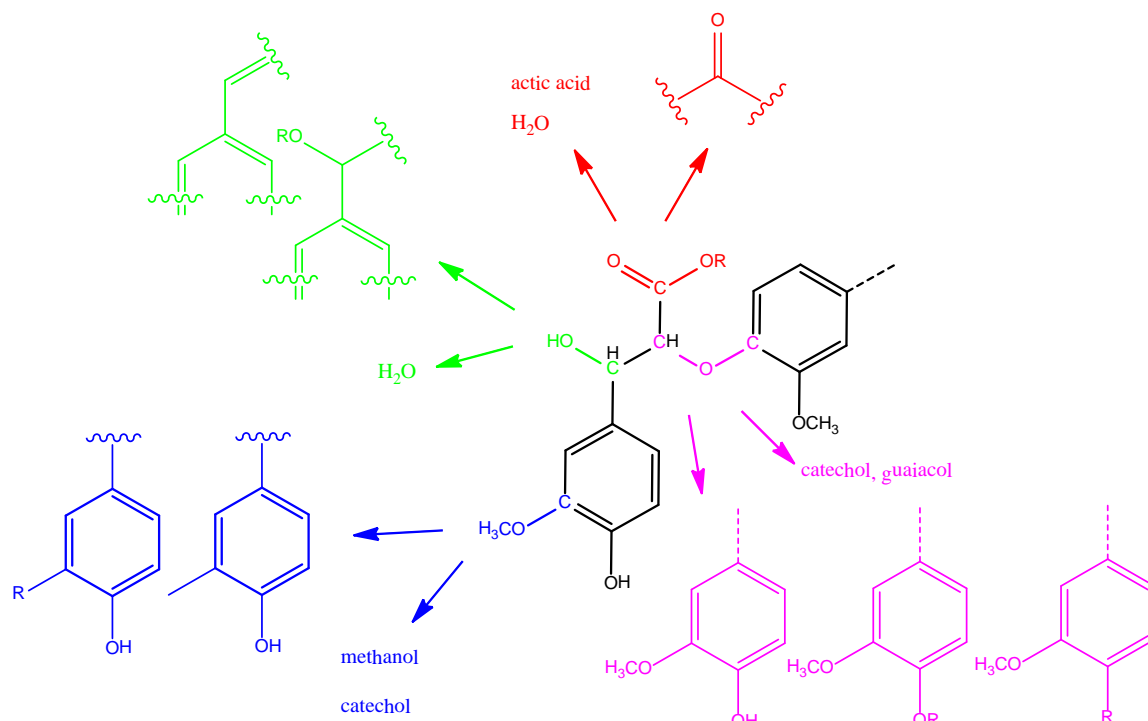


Figure 5. The possible decomposition pathways of lignin during the pyrolysis.⁴⁹⁻⁵⁵

2.3.2 Pyrolysis of cellulose

Cellulose is the most abundant biopolymer. Generally, biomasses contain around 35-50% of cellulose, which is a polymer of β -(1, 4)-glucan with a degree of polymerization of ~300-15000. Figure 2 shows the model structure of cellulose. Other than the biochemical conversion of cellulose to ethanol—a second generation bio-ethanol, some researchers also reported to convert this biopolymer and its model compound such as glucose to liquid fuels and chemicals. For example Huber et al.⁵⁶ examined the conversion of biomass-derived carbohydrates to the liquid alkanes by acid-catalyzed dehydration, which was followed by aldol condensation. The productions of liquid alkanes have the molecular weight in the transportation fuel range and contain 90% of energy of the car-

bohydrate and H_2 feeds. Figure 6 shows this conversion process. One step conversion of cellobiose to C_6 -alcohols with Pt, Pd, Rh or Ru nanocluster catalyst at $120\text{ }^\circ\text{C}$, 4 MPa and different pHs has also been investigated in the literature and is illustrated in Figure 7.⁵⁷ By using a Ru nanocluster catalyst at pH 2, cellobiose could completely be converted to sorbitol.

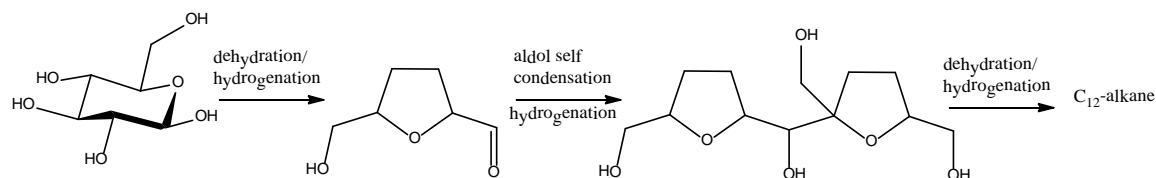


Figure 6. Conversion of biomass-derived carbohydrates to the liquid alkanes by acid-catalyzed dehydration which was followed by aldol condensation.⁵⁶

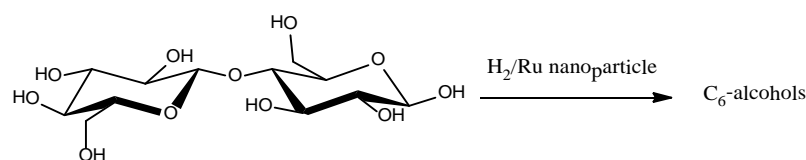


Figure 7. One step conversion of cellobiose to C_6 -alcohols with Pt, Pd, Rh or Ru nanocluster catalyst.⁵⁷

As the major component in the biomass, cellulose plays an important role in understanding pyrolysis pathways of the whole biomass. Shen et al.⁵⁸ employed pyrolysis-GC-MS to investigate the mechanism of cellulose pyrolysis and effects of temperature and residence time. The main products in the cellulose pyrolysis oil include levoglucosan, hydroxyacetaldehyde, hydroxyactone, pyruvic aldehyde, glyceraldehyde, 5-hydroxymethyl-furfural and furfural. The contents of most of these main products increased when the temperature or residence time was elevated, nevertheless the yield of pyrolysis oil decreased when temperature exceeded $570\text{ }^\circ\text{C}$. The content of the major

components in cellulose pyrolysis oil—levoglucosan was more than 50% molar fraction of pyrolysis oil and decreased with the elevated temperature. In the meanwhile, the yield of char reached the minimum and remained consistent when temperature exceeded 550 °C. The authors also indicated that the formation of CO is improved with increased temperature and residence time, whereas slight change was observed for the yield of CO₂. The content of CO was up to 20.2 wt % of cellulose, while the yield of H₂ was ~0.9 wt% of cellulose. This result indicated that the gas products of pyrolysis of cellulose could also be used as the syngas to produce synthetic petroleum.

On the basis of the study on mechanism, most of hydroxyactone was found to be produce from the direct conversion of cellulose molecules, while the formation of pyruvic aldehyde is mainly from the secondary decomposition of levoglucosan. The authors⁵⁸ have proposed the primary decomposition of cellulose and secondary decomposition of the anhydrosugars such as levoglucosan, which have been summarized in Figure 8.

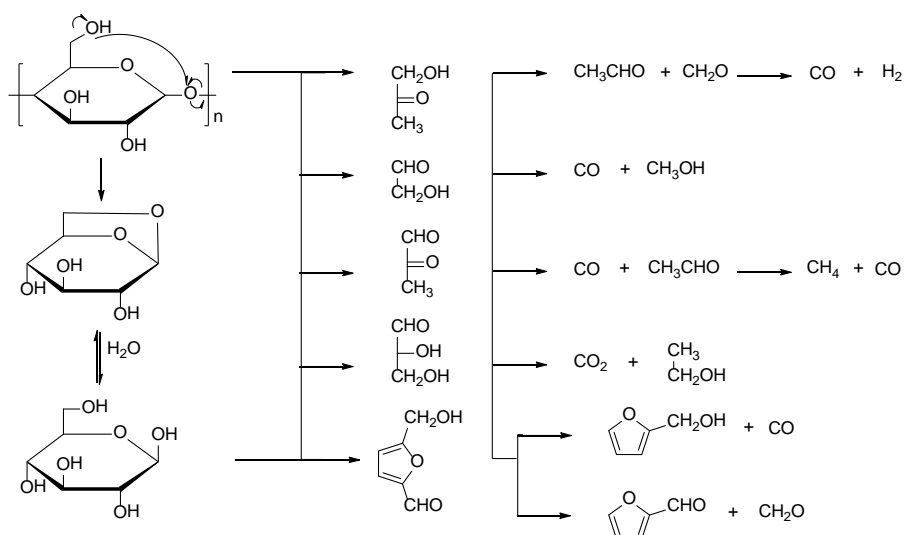


Figure 8. Proposed primary decomposition of cellulose and secondary decomposition of the anhydrosugars such as levoglucosan.⁵⁸

Wang et al.⁵⁹ investigated the interaction of biomass components including cellulose, hemicellulose and lignin during the pyrolysis process. By the use of GC-MS, levoglucosan, 2, 5-diethoxytetrahydrofuran, 1-hydroxy-2-propanone, altrose and 2-hydroxy-2-cyclopenten-1-one have been detected as major components in the cellulose pyrolysis oil. In addition, the authors indicated that the interaction of cellulose and hemicellulose significantly improved the formation of 2, 5-diethoxytetrahydrofuran but inhibited the formation of altrose and levoglucosan. Similarly, Alen et al.⁶⁰ indicated that the cellulose pyrolysis oil could be summarized as several compound groups including the volatiles, which mainly contains carbon monoxide, carbon dioxide, methanol, acetaldehyde, acetic acid, hydroxyacetaldehyde (glycolaldehyde), 1-hydroxy-2-propanone (acetol), and some C_5 -hydrocarbons; the anhydroglucopyranose (levoglucosan); the anhydroglucofuranose (1,6-anhydro- β -D-glucofuranose); the dianhydroglucopyranose (1,4;3,6-dianhydro- α -D-glucopyranose) and the furans which include (2H)-furan-3-one, 5-methyl-(3H)-furan-2-one (α -angelicalactone), 2-furaldehyde (furfural), 5-methyl-2-furaldehyde, and 5-hydroxymethyl-3-furaldehyde. They also concluded that at lower temperatures (400-600 °C), the main products of pyrolysis of cellulose are anhydrosugars; however, at higher pyrolysis temperatures (800-1000 °C), these anhydrosugars will be secondarily decomposed to volatiles.

To facilitate the analysis of pyrolysis of cellulose and further upgrading process, a summary of the GC-MS detected components in the cellulose pyrolysis oils reported from six references is shown in Table 11.^{58, 59, 61-64} Levoglucosan has been reported as the

most abundant component in the cellulose pyrolysis oil, the content is more than 50 wt% of pyrolysis oil. Furfural and 5-hydroxymethylfurfural are also the major components in the cellulose pyrolysis oil.

Table 11. GC-MS detected components in the cellulose pyrolysis oils ^a. ^{58, 59, 61-64}

Acetone	resorcinol	2-butanone
Phenol	4-methyl-5h-furan-2-one	propenic acid
		acrylic acid
propanal	1,2,4-cyclopentantrione	ethylene glycol
2-propenal	2-hydroxy-3-methyl-2-	2,3-pentandione
	cyclopenten-1-one	2,3-pentanedione
Furan	1,4-benzenediol	acetyl methyl carbi-
	hydroquinone	nol
		acetoin
formic acid	2-hydroxybenzaldehyde	2-cyclopentenone
	salicylaldehyde	2-cyclopenten-1-one
3-buten-2-one	4-methylphenol	2-furanemethanol
	p-cresol	furfuryl alcohol
acetic acid	3-furancarboxylic acid methyl es- ter	2-furanone
2-butenal	(2-methoxyethyl) cyclohexane	2-hydroxy-2-cyclope
Crotonaldehyde		ntene-1-one
Table 11 continued		

1-hydroxy-2-propanone	methyl 2-furoate	3-methyl-2,5-furanedione
hydroxyacetone	methyl-2-furancarboxylate	citraconic anhydride
2,5-dimethylfuran	3-methylphenol	5-methylfurfural
	m-cresol	5-methyl-2-furaldehyde
2-methylfuran	3,5-dihydroxytoluene	o-cresol
	5-methylresorcinol	
acetic acid methyl ester	1-(2-furanyl)-2-hydroxy-ethanone	2-hydroxy-3-methyl-4-pyranone
methyl acetate		
2-oxopropanoic acid methyl ester	4-hydroxy-2,5-dimethyl-3(2H)-furanone	dihydro-4-hydroxy-2-furanone
	dihydro-3-methylene-2(3H)-furanone	
3-furaldehyde	alpha-methylene-gamma-butyrolactone	benzoic acid
furfural	maltol	catechol
2-furaldehyde	3-hydroxy-2-methyl-4-pyrone	1,2-benzenediol
4-cyclopentene-1,3-dione	3-ethyl-2-hydroxy-2-cyclopenten-1-one	1,2-dihydroxy-3-methylbenzene
cyclopenten-1,3-dione		3-methylcatechol

Table 11 continued

2-propylfuran	5,6-dihydro-6-methyl-2H-pyran-3(4H)-one	hexane
2(3H)-furanone,5-methyl-3-penten-4-olide	5-hydroxy-2-methyl-4H-pyran-4-one	hydroxyacetaldehyde
2-propanone,1-(acetyloxy)-acetonyl acetate	2,3-dihydro-3,5-dihydroxy-6-methyl-4H-pyran-4-one	2-hydroxy-2-cyclopenten-1-one
Furfuryl formate	3,5-dihydroxy-2-methyl-4H-pyran-4-one	1,3-butadiene-1-carboxylic acid
2-acetylfuran	1,2,3-benzotriol pyrogallol	ethylbenzene
2,3,5-trimethylfuran	Hydroxyquinol	5-methyl-2(5H)-furanone 2-penten-4-olide
2(3H)-furanone	5-hydroxymethyl-2-furancarboxaldehyde 5-(hydroxymethyl)furfural	2-methyl-pentanone
1,2-cyclohexanediol	2,3-dihydro-1h-inden-1-one 1-indanone	3-methyl-1,2-cyclopentadion
2H-pyran-2-one 2-pyrone	levoglucosan	2,4-dimethylphenol 2,4-xilenol
4H-pyran-4-one	2,3-butandione	stilbene

^a The pyrolysis temperatures are from 350-730 °C.

2.3.3 Pyrolysis of hemicellulose

Hemicellulose is a short-chain branched and substituted polymer of sugars with a degree of polymerization of ~70-200; and typically biomass contains 25-30 wt% of hemicellulose. In contrast to cellulose, hemicellulose is a polymer of several different sugar monomers. It contains five-carbon sugars including xylose and arabinose as well as six-carbon sugars including galactose, glucose and mannose. All of these sugar monomers are highly substituted with acetic acid. The most abundant sugar in the softwood hemicellulose is mannose; correspondingly, xylose is most abundant in the hardwood hemicellulose.⁵

Surprisingly, limited information on pyrolysis of hemicellulose was mentioned in literatures although hemicellulose is one of the major components in biomass, there are only very limited information about pyrolysis of hemicellulose in the literature. Patwardhan et al.⁶⁵ examined the pyrolytic behaviors of switchgrass hemicellulose and a total of 16 different products were quantitatively identified. The authors indicated that the pyrolysis products of pure hemicellulose can be classified into three categories a) low-molecular-weight compounds including CO (2.8 wt%), CO₂ (18.8 wt%), formic acid (11.0 wt%), acetaldehyde (0.7 wt%), acetic acid (1.1 wt%), and acetol (3.0 wt%); b) furan/pyran ring derivatives including 2-methyl furan (1.5 wt%), 2-furaldehyde (2.2 wt%) and dianhydro xyloses (9.2 wt%) and c) anhydro sugars—anhydro xylopyranoses (3.4 wt%). In the meanwhile, there are 10.7 wt% of char, 15.1 wt% of water and 4.9 wt % of xylose. The authors also investigated the influence of temperatures on products from hemicellulose pyrolysis. The results showed that when the pyrolysis temperatures increased

from 250-600 °C, the content of CO and CO₂ almost linearly increased from 0.5-4.7 wt% and from 2.7-24 wt%, respectively. Similarly, the yield of formic acid linearly increased from 5.4-15.6 wt% when the thermal treatment temperature increased from 350-600 °C. In contrast with the increasing gas yield at higher pyrolysis temperatures, the yield of char decreased from 24 wt% at 300 °C to 6.3 wt% at 600 °C. Based on the literature reports, the authors also proposed tentative thermal decomposition pathways of hemicellulose, which have been summarized in Figure 9.

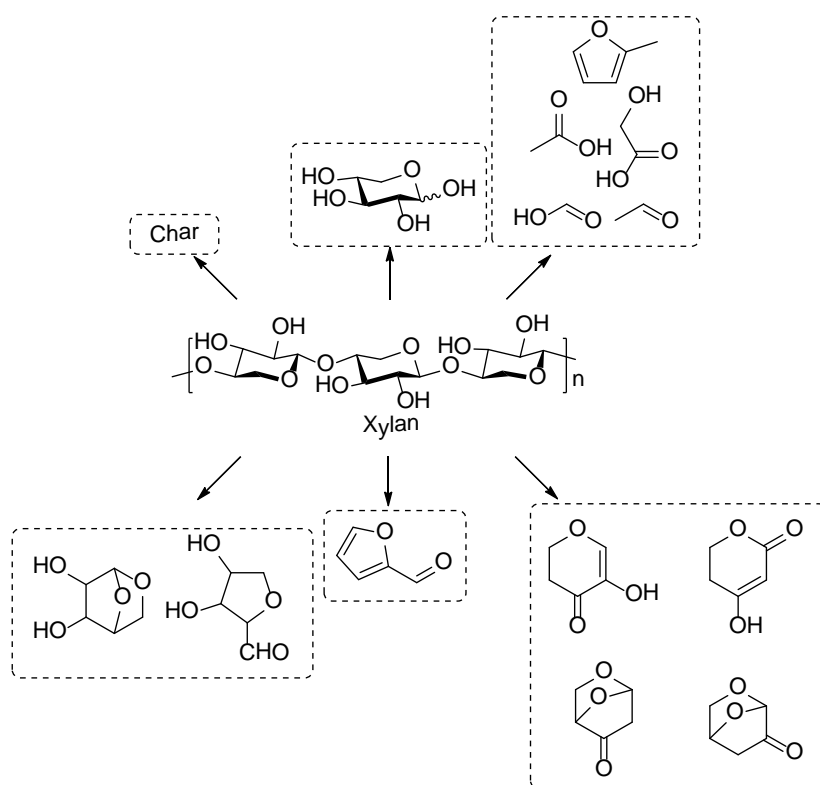


Figure 9. Tentative thermal decomposition pathways of hemicellulose.⁶⁵

Lv et al.⁶⁶ investigated the effects of pyrolysis temperatures (400-900 °C) on the pyrolysis products from corn stalk hemicellulose. They indicated that the yield of char linearly decreased but the yield of gas products increased when the pyrolysis temperature

elevated. The maximum yield of liquid products (48.2 wt%) occurred at 450 °C. The pyrolysis oils were composed of ketones, furans, carboxylic acids, and alcohols. Ketones have been reported as the most abundant type of liquid products, which was up to 71 area% of pyrolysis oil detected by GC-MS. The 1-hydroxy-2-propanone (19 area% at 450 °C – 26 area% at 900 °C), 1-hydroxy-2-butanone (12 area% at 450 °C – 11 area% at 900 °C), 2-cyclopenten-1-one (5 area% at 450 °C – 7 area% at 900 °C), 2-methyl-2-cyclopenten-1-one (4 area% at 450 °C – 6 area% at 900 °C), 3-methyl-1,2-cyclopentanedione (4 area% at 450 °C – 7 area% at 900 °C) and 4-hydroxy-3-hexanone (3 area% at 450 °C – ~0 area% at 900 °C) are the major components as the ketones type pyrolysis products. Furfural (15 area% at 450 °C – 14 area% at 900 °C), dihydro-2(3H)-furanone (~3 area% from 450 °C – 900 °C) and 2,5-dihydro-3,5-dimethyl-2-furanone (~2 area% from 450 °C – 900 °C) are the major type of furans in hemicellulose pyrolysis products. Acetic acid (16 area% at 450 °C – 11 area% at 900 °C) and propanoic acid (3 area% at 450 °C – ~0 area% at 900 °C) are the main acid products from pyrolysis of hemicellulose. Cyclobutanol (2 area% at 450 °C – ~0 area% at 900 °C) has been listed as the major alcohol type product. The top four gas products were CO₂, CO, H₂, and CH₄ (sorted by content), and there are also small amount of C₂H₄ and C₂H₆ produced from hemicellulose. Similarly to Patwardhan,⁶⁵ Lv also indicated that the formation of CO₂ is due to the cleavage of acetyl and carboxyl groups in hemicellulose and a higher pyrolysis temperature favored such cracking, and thus increased CO₂ formation. The authors also indicated that the formations of CO, H₂, and CH₄ and other gas products such as C₂H₄ and C₂H₆ are related to the secondary decomposition of liquid products, which will also be improved at higher reactor temperature and

lead to an increasing yield of such gas products. The authors examined the char by SEM and found that the surface of the higher temperature produced char was more smooth and porous.

Peng et al.⁶⁷ characterized pyrolysis of wheat straw hemicellulose by TG, DTG and pyrolysis-GC-MS. They indicated that the major weight loss of hemicellulose occurred between 190-315 °C and the main components in the hemicellulose pyrolysis oil were acetic acid, 2-furaldehyde, cyclopenten-1-one and small amounts of aromatic compounds including 2-ethyl-5-methyl-phenol and 2,5-dimethyl-phenol. In the meanwhile, Shen et al.⁶⁸ also investigated the pyrolytic behaviors of beech wood hemicellulose by TG-FTIR and pyrolysis-GC-FTIR. They found that methanol (0.81 wt% at 425 °C – 1.14 wt% at 690 °C), acetic acid (4.44 wt% at 425 °C – 2.45 wt% at 690 °C), acetone (0.69 wt% at 425 °C – 1.06 wt% at 690 °C), furfural (1.94 wt% at 425 °C – 3.16 wt% at 690 °C) and 1,4-Anhydro-D-xylopyranose (3.84 wt% at 425 °C – 0.69 wt% at 690 °C) were the major components in the pyrolysis oil produced from beech wood hemicellulose. In addition, the authors discussed the formation pathways of some major pyrolysis products. For instance, the authors indicated that the decomposition of xylan units produced furfural and 1,4-anhydro-D-xylopyranose, and the formation of acetic acid and CO₂ is due to the primary cleavage of O-acetylxylan unit. The xylan unit was also proposed as the main precursor for the formation of <C3 fragments and gas products including CO, H₂ and CH₄. The primary decomposition of 4-O-methylglucuronic acid unit produces methanol and the decomposition of the ring-opened intermediate products or secondary decomposition of the fragments forms acetone and CO.

2.4 characterization methods of pyrolysis oil

2.4.1 FT-IR analysis of lignin pyrolysis oil

Most compounds in Table 10 and 11 have a molecular weight below 220 g/mol. However, some researchers have detected the average molecular weight of pyrolysis oil by GPC and reported that the molecular weights were from 210-1700 g/mol.⁶⁹⁻⁷² Due to the limitation of volatility of high molecular weight components in the pyrolysis oil, it has been indicated that only about 40% of pyrolysis oil could be detected by GC.⁸ Therefore, many researchers also tried to find alternative characterization method, which could analyze the whole portion of pyrolysis oil, such as FT-IR.^{46, 73-78} Liu et al.⁷⁵ did a mechanistic study of hardwood and softwood lignin pyrolysis using a thermogravimetric analyzer coupled with a Fourier transform infrared spectrometry (TG-FTIR). They indicated that lignin undergoes three consecutive sets of reactions during pyrolysis including the evaporation of water, the formation of primary volatiles and the release of small molecular gases. At first, the absorbed water is released by evaporation, and then at a higher temperature (above 100 °C) water is generated by the dehydration of lignin aliphatic hydroxyl groups. The authors also indicated that phenols, in addition to alcohols, aldehydes, acids and CO, CO₂ CH₄ were the major gaseous products. Scholze et al.⁴⁶ also characterized pyrolysis oil by FT-IR and indicated a correlation between carbonyl absorption bands and oxygen content as well as carbon content. Lievens et al.⁷⁹ demonstrated the deconvolution of the region of 1490–1850 cm⁻¹ in the FT-IR spectra could provide detailed information about various carbonyl groups in various pyrolysis oils. To facilitate this promising fast analysis method of pyrolysis oils, a summary of the assignment ranges from seven references^{46, 73-75, 77, 78, 80} are shown in Table 12.

Table 12. FT-IR assignments of biomass pyrolysis oil.

Wave number (cm ⁻¹)	Assignments ^{46, 73-75, 77, 78, 80}
3429	O-H stretching vibration, H ₂ O
3000-3040	Aromatic ring C-H stretching
2930-2980	Asymmetrical C-H stretching, vibration of aliphatic CH ₃ and CH ₂
2850-2870	Symmetrical C-H stretching, vibration of aliphatic CH ₃ and CH ₂
1701-1734	C=O stretch in unconjugated ketones, carbonyl and ester groups
1652-1666	C=O stretch in conjugated aryl ketones
1593-1609	Aromatic ring vibrations and C=O stretch
1504-1515	Aromatic ring vibrations
1462-1464	Asymmetric C-H bending (in CH ₃ and -CH ₂ -)
1420-1424	Aromatic ring vibrations
1365	Symmetric deformation of C-H in methyl groups
1360	Phenolic hydroxyl vibrations
1270	Vibrations of guaiacyl rings and stretching vibrations of C-O bonds
1214-1233	C-C, C-O and C=O stretching
1190	Vibrations of methoxyl group
1160	Deformation vibrations of C-H bonds in benzene rings
1140	Deformation vibration of C-H bonds in guaiacyl rings
1115	Vibrations of ester linkage
1114-1125	Aromatic in-plane C-H bending

Table 12 continued

1075-1090	Deformation vibrations of C-O bonds in secondary alcohols and aliphatic ethers
1030-1033	Deformation vibrations of C-H bonds in aromatic rings
914-919	Aromatic out-of-plane C-H bending
852-859	Aromatic out-of-plane C-H bending in positions 2, 5 and 6 of guaiacyl units
833	Vibrations of C-H bonds in syringyl units
720-740	Bending out of the plane C-H
730-675	Bending out of the plane =CH

2.4.2 NMR analysis of pyrolysis oil

It is well known that pyrolysis oil is a very complex mixture, whereas the ability of FT-IR to comprehend the details of pyrolysis oil is limited. Most recently, some research work^{48, 71, 81-88} introduce NMR, including quantitative ^1H , ^{31}P and ^{13}C -NMR, and semi-quantitative HSQC-NMR to characterize pyrolysis oils. Mullen et al.⁸¹ analyzed various pyrolysis oils produced from switchgrass, alfalfa stems, corn stover, guayule (whole plant and latex-extracted bagasse), and chicken litter by ^1H , ^{13}C , and ^{13}C -DEPT (Distortionless Enhancement Polarization Transfer)-NMR. They found that pyrolysis oil from chicken litter had the lowest overall amount of methyl groups and had the highest ketone content of the pyrolysis oils studied. The ^{13}C and DEPT-NMR analysis indicated that the pyrolysis oils from corn stover and switchgrass had the fewest aliphatic carbons. The large amount of methine (CH_1) groups in the corn stover pyrolysis oil suggested that

its aliphatic groups were highly branched. However, there were almost the same amounts of methyl ($-\text{CH}_3$) groups as its methine groups, while the percentage of $-\text{CH}_2-$ was low, it indicated that these branches were very short and could mostly be methyl groups. Conversely, pyrolysis oil from switchgrass appeared to have more straight-chain aliphatics. The authors also indicated that the aromatic region of these pyrolysis oils had $\text{CH}_0:\text{CH}_1$ ratios of $>2:1$, which represents highly complex substituted (at least four substituents) benzene rings. On the basis of 50 pyrolysis oil model compounds, Joseph et al.⁸³ have measured the T1 and proposed assignments range for both ^{13}C -NMR and ^1H -NMR.

To solve spectral overlapping problems when using ^{13}C -NMR to analyze the pyrolysis oils, HSQC-NMR¹⁰ was used to analyze various C-H bonds present in the pyrolysis oils. The fingerprint analysis of HSQC-NMR spectral data provided chemical shift assignment of twenty-seven (fourteen from lignin pyrolysis oil) different types of C-H bonds present in pyrolysis oils produced from cellulose, lignin and pine wood. The HSQC-NMR for the lignin pyrolysis oils showed that there were two different types of methoxyl group in the pyrolysis oils, which indicated that the native methoxyl group in the kraft lignin will rearrange to another type during the thermal treatment. As the main products of pyrolysis cellulose—levoglucosan^{10, 89} was shown to be increased with the increasing pyrolysis temperature from 400 to 600 °C, furfurals and phenols were also found as the major components in the cellulose pyrolysis oils. The content of 5-hydroxymethyl-furfural (HMF) in the cellulose pyrolysis oil decreased at higher thermal treatment temperature, which indicated that HMF could be further decomposed at higher temperature. The content of aromatic C-H and aliphatic C-H bonds in the lignin

pyrolysis oils increased with increasing pyrolysis temperature, which was attributed to the rearrangement and the cleavage of ether bonds or methoxyl groups in the lignin structure. The analysis of HSQC-NMR for the pine wood pyrolysis oils indicated that levoglucosan was also one of the major components presented in the pyrolysis oils and most of aromatic C-H and aliphatic C-H bonds in the pine wood pyrolysis oils produced from lignin component. Table 13 summarized the functional groups presented in pyrolysis oils, which could be analyzed by NMR.

Table 13. NMR detectable functional groups in pyrolysis oils.^{9, 10, 48, 71, 81-90}

¹ H-NMR ^{48, 71, 81, 82, 85}	³¹ P-NMR ^{9, 84, 86, 87, 90}	¹³ C-NMR ^{a, 48, 81, 83-88}	HSQC ^{a, 10}	
- <u>CH</u> O,				
-COO <u>H</u>				
Ar <u>H</u> , <u>HC</u> =C-				
- <u>CH</u> _n -O-, <u>CH</u> _n -O-				
- <u>CH</u> ₃ , - <u>CH</u> _n -				

Table 13 continued

^aThe HSQC-NMR and ¹³C-NMR detectable functional groups are based on our previous work which are the first reported efforts in the literature to fully characterize pyrolysis oil by NMR.

2.4.3 Elemental analysis, viscosity, acidity, heating value and solid residue of pyrolysis oil

The major drawback towards commercialization of pyrolysis oils are several challenging properties including poor volatility, high oxygen content, acidity and viscosity, corrosiveness, cold flow and aging problems.³ The reported results of elemental analysis, viscosity, acidity, heating value and solid residue for various pyrolysis oils have

been summarized in Tables 14 and 15. The elemental analysis results show that the oxygen contents in the whole biomass pyrolysis oils are much higher than the lignin pyrolysis oils, which may due to the higher oxygen contents in the carbohydrates in the whole biomass. Limited amount of sulfur has been found in some whole biomass pyrolysis oils, especially in the barks pyrolysis oils. Due to the kraft pulping process, the kraft lignins always contain a small amount of sulfur, which explains the relatively higher sulfur contents in the kraft lignins pyrolysis oils. Table 15 exhibits the relatively high viscosity and acidity of various pyrolysis oils, which bring huge barriers to the usage as the precursor of biofuels. The relatively lower heating values for some biomass pyrolysis oils may be due to the production of water and mixed in the pyrolysis oils. The solid residue in pyrolysis oils could also be a problem during the storage and transportation.

Table 14. Elemental analysis of pyrolysis oils. ^a

Biomass	C	H	O	S	N
Switchgrass ⁸¹	52.97	6.43	39.13	-	0.38
Corn stover ⁸¹	53.97	6.92	37.94	<0.05	1.18
Alfalfa stems ⁸¹	57.00	7.89	31.30	0.07	3.75
Guayule (whole) ⁸¹	69.93	8.54	19.31	0.20	2.92
Guayule bagasse ⁸¹	69.97	7.96	21.38	0.07	0.82
Pine (pinusstrobes) ⁸⁵	59.2	6.6	34.2	-	<0.5
Pistachio shell ⁸⁰	67.35	8.36	23.70	-	<0.59
Indulin AT lignin ⁴⁸	69.79	3.39	15.02	2.17	0.57
Acetocell lignin ⁴⁸	71.42	4.38	21.43	<0.05	<0.5

Table 14 continued

Pine wood ⁴³	52.64	7.53	39.52	0.019	0.09
Oak wood ⁴³	47.19	4.51	47.97	0.022	0.12
Pine bark ⁴³	53.99	6.97	38.21	0.035	0.37
Oak bark ⁴³	45.57	6.05	47.75	0.28	0.32
Forestry residue ⁹¹	38-44	7-8	48-53	-	0.1-0.3
Pine ⁹¹	44-47	~7	46-49	-	<0.1
Pine bark (pinusbrutia Ten.) ⁹²	63.93	7.61	28.36	-	0.10
Pine ⁹³	40.6	7.6	51.7	0.01	<0.1
Forestry residue brown ⁹³	41.4	7.4	50.9	0.03	0.3
Forestry residue green ⁹³	41.2	8.0	50.5	0.02	0.3
Eucalyptus Crandis ⁹³	42.3	7.5	50.1	0.02	0.1
Barley straw ⁹³	26.5	9.0	62.7	-	0.9
Timothy hay ⁹³	32.1	8.5	58.7	-	0.6
Reed canary grass ⁹³	39.3	7.7	51.8	-	0.6
Hybrid poplar ⁹⁴	57.3	6.3	36.2	0.02	0.18
Willow ⁹⁵	43.17	7.15	49.49	0.10	0.10
Switch grass ⁹⁵	38.30	7.42	54.08	0.10	0.10
Reed canary grass ⁹⁵	38.42	7.89	53.49	0.10	0.10
Straw ⁹⁵	28.2	8.78	62.83	0.10	0.10
<i>Dactylisglomerata</i> ⁹⁵	36.75	8.82	52.46	0.10	1.88
<i>Festucaarundinace</i> ⁹⁵	32.05	9.76	56.69	0.10	1.41
<i>Loliumperenne</i> ⁹⁵	30.64	9.63	58.86	0.10	0.77

Table 14 continued						
Soft wood kraft Lignin ⁷¹		66.4	6.5	22.0	4.7	-
Lignoboost lignin ⁷¹		69.0	6.6	22.8	1.2	-
Common fuels ^b	Gasoline	85-88	12-15	0	0	0
	Diesel	87	13	0	0	0

^a The pyrolysis temperatures are from 400-800 °C

^b Data is based on <http://www.afdc.energy.gov/pdfs/fueltable.pdf>

Table 15. Viscosity, acidity, higher heating value (HHV) and solid residue in the pyrolysis oils^a.

Biomass	Viscosity (cSt)	Acidity (pH)	HHV (MJ/kg)	Solid residue (wt%)
Pine ⁹³	50 °C 27.5	2.4	18.7	-
Forestry residue brown ⁹³	40 °C 17	3.2	16.9	-
Forestry residue green ⁹³	40 °C 24	-	16.7	-
Eucalyptus crandis ⁹³	40 °C 23	2.2	17.3	-
Barley straw ⁹³	-	3.7	11.1	-
Timothy hay ⁹³	40 °C 5	3.4	13.3	-
Reed canary grass ⁹³	-	3.6	16.0	-
Pine ⁸⁵	20 °C, 22.60 Pa S	2.66	24.73	0.11

Table 15 continued

Pine wood ⁴³	50 °C, 154 cP under 0.05 shear rate in s ⁻¹	3.1	21.9	0.197
Oak wood ⁴³	50 °C, 171 cP under 0.05 shear rate in s ⁻¹	3.1	18.7	0.184
Pine bark ⁴³	50 °C, 2529 cP under 0.05 shear rate in s ⁻¹	3.2	18.3	0.428
Oak bark ⁴³	50 °C, 5047 cP under 0.05 shear rate in s ⁻¹	3.2	19.0	0.080
Forestry residue ⁹¹	-	2.9-3.3	15.7-17.4	0.02-0.11
Pine ⁹¹	-	2.4-2.6	17.8-19.0	0.03-0.29
Pine bark (pinu- sbrutia Ten.) ⁹²	-	-	31.03	-
Gasoline ^b	20 °C, 0.5-0.6 mm ² /s	-	46.52	-
Diesel ^b	20 °C, 2.8-5.0 mm ² /s	-	45.76	-

^a The pyrolysis temperatures are from 400-800 °C.

^b Data is based on <http://www.afdc.energy.gov/pdfs/fueltable.pdf>

CHAPTER 3: EXPERIMENTAL MATERIALS AND PROCEDURES

3.1 Materials

3.1.1 Chemicals

All reagents used in this study were purchased from VWR International or Sigma-Aldrich (St. Louis, MO) and used as received. All gases were purchased from Airgas. (South region, Atlanta, GA). Zeolites (CBV 2314, CBV 3020E, CBV 5524G, CBV 8014, CBV 28014, CP 814, CBV 710, CP 914C and CBV 21A) were purchased from Zeolyst, Inc.

3.1.2 Biomass

Wood chips used in this study were acquired from a 15-year old Loblolly pine tree from the southeastern US. Detailed information about this material has been reported by Huang et al.¹² The wood chips were refined with a Wiley mill through a 0.13 cm screen and dried under high vacuum at 50 °C for 48 h. Pine wood samples were stored at ~ 0 °C prior to use.

3.2 Experimental procedure

3.2.1 Lignin preparation

3.2.1.1 Kraft lignin

Kraft lignin was isolated from a commercial softwood kraft pulping liquor following published methods.⁹ In brief, the cooking liquor was filtered through filter paper and the filtrate was treated with EDTA-2Na⁺ (0.50 g/100.0 mL liquor) and stirred for 1 h.

The liquor was adjusted to a pH value of 6.0 with 2.00 M H₂SO₄ and stirred vigorously for 1 h. The liquors were then further acidified to a pH of 3.0 and frozen at -20 °C. After thawing, the precipitates were collected on a medium sintered glass funnel and washed three times with cold water by suspending the precipitates in the water and stirring vigorously at 0 °C for 1 h. The precipitates were collected, air dried, and soxhlet extracted with pentane for 24 h. The solid product was air dried and further dried under high vacuum at 45 °C for 48 h. The resulting purified kraft lignin sample (ash wt% is ~0.5 wt%) was stored at -5 °C.

3.2.1.2 Ethanol Organosolv Lignin (EOL)

The milled pine wood was ethanol-organosolv-pretreated as previously described in the literatures.⁹⁶⁻⁹⁹ Briefly, a 100.0 g (dry weight) sample of the milled pine wood was treated with 65% ethanol/water solution with 1.2 w/w% sulfuric acid as a catalyst at 170 °C for 60 min. The solid to liquid ratio used was 1:8. The pre-treatments were carried out in a Parr reactor (one liter) equipped with a temperature controller (Parr Instrument Company, Moline, IL). The pre-treated pine wood was washed with warm (60 °C) ethanol/water (8:1, 3×50.0 mL). The washes were combined and 3 volumes of water were added to precipitate the Ethanol Organosolv Lignin (EOL), which was collected by centrifugation and air dried. The EOL was purified by Soxhlet extraction with pentane and stored at ~ 0 °C prior to use. The yields were from 5-15 wt % of biomass.

3.2.2 Preparation of pyrolysis sample

Different types (MFI, FAU, BEA, FER and MOR) of zeolite and metal salt (NiCl_2) were used as the additives in this work. The pyrolysis samples were mechanical stirred lignin with 1:1 or 2:1 weight ratio of zeolites and metal salt. All the zeolites were activated in the pyrolysis tube at $500\text{ }^\circ\text{C}$ under nitrogen for 6 h.

3.2.3 Equipment and process of pyrolysis

3.2.3.1 Pyrolysis process and system

The pyrolysis system is shown in Figure 10. Pyrolysis experiments were conducted in a quartz pyrolysis tube heated with a split-tube furnace. Typically, the pyrolysis sample (4.00 g) was placed in a quartz sample boat that was then positioned in the center of a pyrolysis tube. A K-type thermal couple was immersed in the sample powder during the pyrolysis to measure the heating rate ($\sim 2.7^\circ\text{C/s}$). The pyrolysis tube was flushed with nitrogen gas and the flow rate was adjusted to a value of 500 mL/min and then inserted in the pre-heated furnace. The outflow from pyrolysis was passed through two condensers, which were immersed in liquid N_2 . (Note: liquid N_2 was used for experimental convenience) Upon completion of pyrolysis, the reaction tube was removed from the furnace and allowed to cool to room temperature under constant N_2 flow. The condensers were then removed from liquid nitrogen. The pyrolysis char and oil were collected for subsequent chemical analysis. In general, the liquid products contained two immiscible phases referred to as heavy and light oil. (Figure 11) The light oil was acquired by decantation and the heavy oil was recovered by washing the reactor with acetone followed by evaporation

under reduced pressure. Char yields were determined gravimetrically and gas formation was calculated by mass difference. The errors of the yields are $\sim \pm 2\%$.

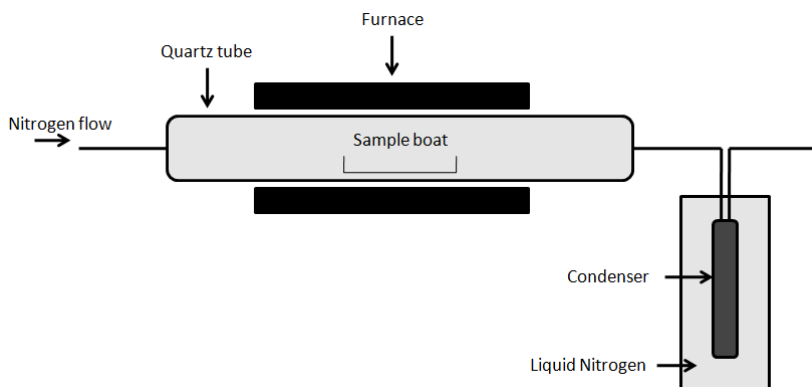


Figure 10. Slow pyrolysis system used in this work.

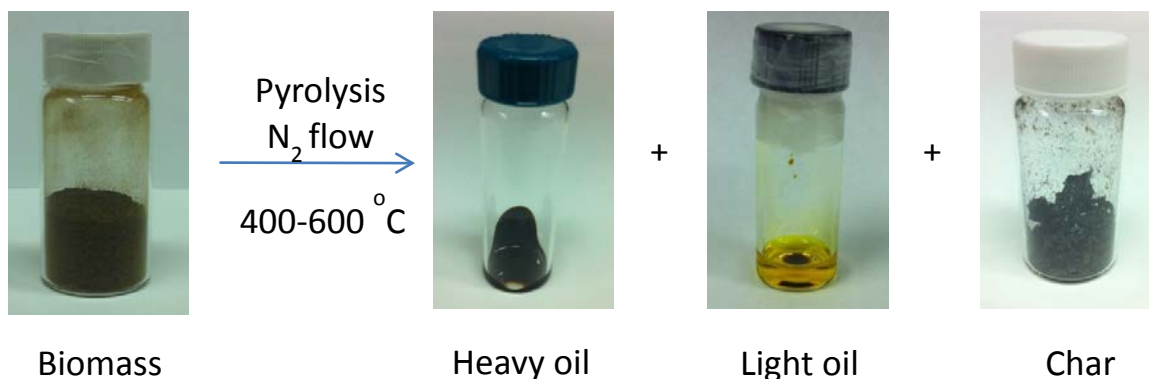


Figure 11. Two immiscible liquid products and solid product for pyrolysis of biomass.

3.2.3.2 Torrefaction process

Torrefaction experiments were conducted in the same system shown in Figure 10. Typically, the torrefaction sample (~ 5.00 g) was placed in a quartz sample boat that was then positioned in the center of torrefaction tube. The torrefaction tube was flushed with nitrogen gas and the flow rate was adjusted to a value of 500 mL/min and then inserted in the pre-heated furnace. Upon completion of torrefaction, the reaction tube was removed

from the furnace and cooled to room temperature under constant N₂ flow. The torrefied wood was collected for subsequent chemical analysis and the yield was determined gravimetrically.

3.2.4 Hydrogenation process

Hydrogenation of EOL heavy oil was examined in two steps. Both experiments were carried out in a 75 mL Parr 4590 Micro Stirred Reactor. In the first step, 150.0 mg heavy oil and 20.00 mL DI water were loaded in a glass liner with 15.0 mg 5 wt% Ru/activated carbon catalyst (Alfa Aesar, Product No. 7440-18-8). The reactor was then purged 5 times with nitrogen gas to remove the air present in the reaction vessel. Then the reactor was purged 5 times with hydrogen to replace nitrogen. The initial hydrogen pressure was set to 10 Mpa and the stirring rate was 200 rpm. The reactor temperature stay at 300 °C for 4 hours and the reactor pressure was stable at ~14 Mpa. After hydrogenation process, the reactor was quenched by ice water. After the first step hydrogenation, the EOL heavy oil has been upgraded to water soluble components and the water solution of the products was filtered through a 0.45 µm syringe filter. The filtrate was further upgraded by the second step hydrogenation, which was conducted at 250 °C for 2 hours with the initial hydrogen pressure of 10 Mpa and 10.0 mg 5 wt% Ru/activated carbon as the catalyst. The carbon yield of first and second step HYD process of overall molar% of carbon content in the heavy oil = Carbon amount from TOC test of products/ Carbon amount calculated from elemental analysis of heavy oil. The carbon yield from first to second step HYD = Carbon amount from TOC test of first step HYD product/ Carbon amount from TOC test of second step HYD product.

3.3 Analysis procedure

3.3.1 Characterization of pyrolysis oils by GPC

The weight average molecular weight (M_w), number average molecular weight (M_n) and molecular weight polydispersity of the heavy oils were determined by Gel Permeation Chromatography (GPC) analysis following literature methods.⁹ Prior to GPC analysis, the heavy oil samples were dissolved in THF (1 mg/mL) and filtered through a 0.45 μ m syringe filter. The samples were injected into a Polymer Standards Service (PSS) Security 1200 system featuring Agilent High-Performance Liquid Chromatography (HPLC) vacuum degasser, isocratic pump, refractive index (RI) detector and UV detector (270 nm). Separation was achieved with four Waters Styragel columns (HR0.5, HR2, HR4, HR6) using tetrahydrofuran (THF) as the mobile phase (1.0 mL/min) with injection volumes of 30 μ L. Data collection and processing were performed using PSS WinGPC Unity software. Molecular weights (M_n and M_w) were calibrated against a calibration curve. The calibration curve was created by fitting a third order polynomial equation to the retention volumes obtained from a series of narrow molecular weight distribution polystyrene standards (i.e., 7.21×10^3 , 4.43×10^3 , 1.39×10^3 , 5.80×10^2 Da), Dioctyl phthalate ($M_w=390$ g/mol), 2, 2'-Dihydroxy-4, 4'-dimethoxyl-benzophenone ($M_w=274$ g/mol), 2-phenylhydroquinone ($M_w=186$ g/mol), phenol ($M_w=94$ g/mol) and acetone ($M_w=58$ g/mol). The curve fit had an R^2 value of 0.998. The errors of M_w are $\sim \pm 3\%$.

3.3.2 Elemental analysis of lignin and heavy oil and carbon content of

hydrogenation products

Elemental analysis data of lignin and heavy oil was obtained by Atlantic Micro

lab. Inc. (Norcross, GA) utilizing combustion to determine carbon, hydrogen and sulfur contents and the oxygen content was calculated by mass difference. The error is 0.3%.

The carbon contents of the 1st and 2nd step hydrogenation products were determined by Total Organic Carbon (TOC) analyzer. (Ionics Inc 1555B)

3.3.3 SEM characterization of catalyst

The catalyst samples were imaged with a scanning electron microscope (Hitachi S-800) with 12 kV acceleration voltages.

3.3.4 GC-MS analysis of hydrogenation products

The GC-MS analysis of hydrogenation products was conducted by Agilent 5975C MSD and 7890A GC with a 7693 auto sampler. The Agilent HP-5MS, 19091S-433 column was used. The GC oven was programmed with the following temperature regime: hold at 50 °C for 5 min, ramp to 200 °C at 5 °C/min and hold at 200 °C for 5 min.

3.3.5 Higher heating value (HHV) measurement

The higher heating values of lignin and heavy oils were measured in a Parr 1261 isoperibol bomb calorimeter according to the literature report.^{88, 100}

3.3.6 Monosaccharide and Klason lignin content analysis

Monosaccharide and Klason lignin content of the native wood and torrefied wood samples were analyzed by Dionex chromatography, high performance anion exchange chromatography with pulsed amperometric detection (HPAEC–PAD) for monosaccharide

analysis on the basis of reported methods.¹⁰⁰ In brief, the extractive free and tannin-free samples were treated with 72 wt % sulfuric acid for 4 h at 30 °C and then diluted to 3 wt% sulfuric acid using deionized water and subsequently autoclaved at 121 °C for 1 h. The resulting solution was cooled to room temperature and was used for the detection of sugar composition by HPAEC–PAD. The acid insoluble residue was reported as the Klason lignin and char content of the native wood and torrefied wood samples.

3.3.7 Characterization of pyrolysis oil by NMR

All liquid NMR spectral data reported in this study were recorded with a Bruker Avance/DMX 400 MHz NMR spectrometer. All the NMR data processing and plots were carried out using MestReNova v7.1.0 software's default processing template (zero-filling is 32 K) and automatic phase and baseline correction.

3.3.7.1 Quantitative ¹H-NMR

Quantitative ¹H-NMR was acquired with 16 transients and 1s pulse delay by employing a standard Bruker pulse sequence “zg” at room temperature. (Note: the longest T1 was determined to be 0.16 s).

3.3.7.2 DEPT-135 ¹³C-NMR

DEPT-135 ¹³C-NMR was employing a standard Bruker pulse sequence “dept135” with a 135° pulse angle, 2 s pulse delay, and 5000 scans at room temperature.

3.3.7.3 Quantitative ^{13}C -NMR

Quantitative ^{13}C -NMR were acquired using 100.0 mg heavy oil dissolved in 450 μL DMSO- d_6 employing an inverse gated decoupling pulse sequence, 90° pulse angle, a pulse delay of 5 s and 6000 scans at room temperature with a line-broadening (LB) of 5.0 Hz. The standard error is $\sim \pm 3\%$.

3.3.7.4 Quantitative ^{31}P -NMR

Quantitative ^{31}P -NMR were acquired after in situ derivatization of the samples using 10.0 mg of heavy oil or 4.0 mg for the light oil with 2-chloro-4,4,5,5-tetramethyl-1,3,2-dioxaphospholane (TMDP) in a solution of (1.6:1 v/v) pyridine/ CDCl_3 , chromium acetylacetonate (relaxation agent) and endo-N-hydroxy-5-norbornene-2,3-dicarboximide (NHND, internal standard which is used to evaluate the hydroxyl group contents of pyrolysis samples). ^{31}P -NMR spectra data was acquired using an inverse gated decoupling pulse sequence, 90° pulse angle, 25 s pulse delay, and 128 scans at room temperature with a LB of 4.0 Hz. The standard error is $\sim \pm 1.2\%$.

3.3.7.5 Characterization of pyrolysis oil by HSQC-NMR

HSQC-NMR were acquired using 100.0 mg pyrolysis oil dissolved in 450 μL methyl sulfoxide- d_6 (DMSO- d_6) employing a standard Bruker pulse sequence “hsqcetgpsi.2” with a 90° pulse, 0.11 s acquisition time, a 1.5 s pulse delay, a $^1\text{J}_{\text{C-H}}$ of 145 Hz, 48 scans and acquisition of 1024 data points (for ^1H) and 256 increments (for ^{13}C). The ^1H and ^{13}C pulse widths are $p1=11.30\ \mu\text{s}$ and $p3=10.00\ \mu\text{s}$, respectively. The ^1H and

^{13}C spectral widths are 13.02 ppm and 220.00 ppm, respectively. The central solvent peak was used for chemical shift calibration.

3.3.7.6 Solid-state CP/MAS ^{13}C -NMR

Solid-state CP/MAS ^{13}C -NMR was carried out using a Bruker DSX 300 NMR spectrometer operating at 75.48 MHz. The experiments were performed at ambient temperature using a Bruker 7 mm MAS probe. The samples were ground and packed into 7 mm ZrO rotors, which were spun at 4 kHz.

CHAPTER 4: PYROLYSIS OF SW KRAFT LIGNIN, CELLULOSE AND PINE WOOD*

4.1 Introduction

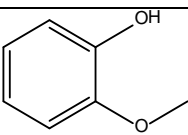
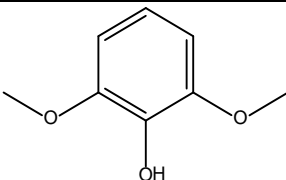
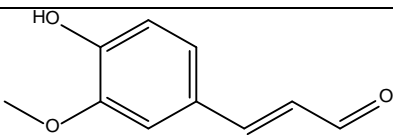

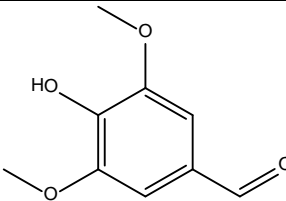
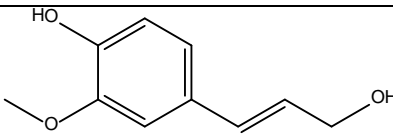
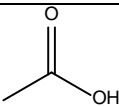
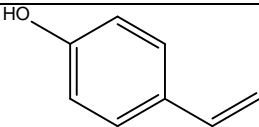
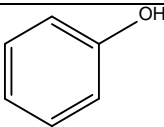
Over the last century, worldwide energy consumption has increased 17 fold⁴ and this demand is predicted to grow by more than 50% by 2025.⁵ Known petroleum reserves are predicted to be consumed in less than fifty years at present rates of consumption. Cellulose from wood and other biomass is now generally recognized as a major renewable resource for fuels and chemicals. As the second most abundant biomass component and the primary renewable aromatic resource in nature, lignin, however, has received much less attention than plant polysaccharides as a resource for biofuels. For example, the US paper industry produces over 50 million tons of extracted lignin per year and yet only 2% of this material is used commercially in products. The remainder is burned as a low value fuel to recover energy. Recently, new lignin separation technology has been developed to recover and utilize lignin as a resource for biofuels and chemicals.¹⁰¹ The pyrolysis of biomass, including biomass components, such as lignin and cellulose, is a promising approach to utilize this resource for fuels and chemicals. The product of pyrolysis of biomass, known as bio-oil, has been identified as inexpensive renewable liquid fuel which can be further upgraded to green gasoline/diesel.¹⁰²

* The full data of this research were accepted for publication in *Energy and Fuels*, 2011. They are entitled as “NMR characterization of pyrolysis oils from kraft lignin” and “Heteronuclear Single-Quantum Correlation–Nuclear Magnetic Resonance (HSQC–NMR) fingerprint analysis of pyrolysis oils”. The other author is Arthur J. Ragauskas from the Institute of Paper Science and Technology and School of Chemistry and Biochemistry at Georgia Institute of Technology. Reprinted with permission from “Ben, H.; Ragauskas, A. J., NMR Characterization of Pyrolysis Oils from Kraft Lignin. *Energy Fuels* 2011, 25, (5), 2322-2332.” Copyright 2011 American Chemical Society. Reprinted with permission from “Ben, H.; Ragauskas, A. J., Heteronuclear Single-Quantum Correlation–Nuclear Magnetic Resonance (HSQC–NMR) Fingerprint Analysis of Pyrolysis Oils. *Energy Fuels* 2011, 25, (12), 5791-5801.” Copyright 2011 American Chemical Society.

The pyrolysis of lignin yielding low-molecular weight compounds has been examined for the past fifty years. In the 1980's and 1990's, Iatridis et al.²⁹ pyrolyzed softwood kraft lignin at 400 - 700 °C and they quantitatively measured some of the products by GC. Carbon monoxide, carbon dioxide, C₁-C₄ hydrocarbons, methanol and phenols were shown to increase by 1-6 wt% with pyrolysis temperature. Jimenez et al.⁴⁷ used pyrolysis-GC-MS to characterize the vapors produced by pyrolysis of softwood, hardwood and grass lignins at 510 °C. Softwood lignins yielded guaiacyl derivatives, coniferaldehyde and coniferyl alcohol as the major products; hardwood lignins gave guaiacyl and syringyl derivatives, syringaldehyde, coniferyl alcohol and sinapyl alcohol. Pyrolysis of bamboo lignin produced p-vinylphenol as the major compound. Nunn et al.³⁰ studied fast pyrolysis of milled hardwood lignin in the range of 327-1127 °C. They found that the total weight loss of the lignin sample increased with pyrolysis temperature up to 86 w/w % at 777 °C, above this temperature the yield varied slightly. Pyrolysis oil generation was reported to yield a maximum of 53 w/w % at 627 °C and then declined to 47 w/w % at 877 °C. Gas generation increased significantly (up to 20 wt %) with temperature up to 877 °C; whereas the char yields reached an asymptote yield of 15 w/w % at 677 °C. These results suggested a secondary cracking of the pyrolysis oil to the gas occurs above 677 °C. J. Caballero et al.²⁴⁻²⁶ also indicated that at a temperature range of 650-700 °C secondary reactions of bio-oil began. They analyzed yields from thirteen pyrolysis experiments products as a function of temperature by GC. Methane, CO and CO₂ were found to increase by 10 wt % in yield as the reactor temperature increased from 500 to 900 °C. Whereas some products, such as methanol, formaldehyde, acetaldehyde and acetic acid were found to decrease when the pyrolysis temperature was increased by ~1 wt%. Finally,

other products were found to have a maximum yield with a pyrolysis temperature of ~700 °C, such as ethylene, benzene and other aromatics. Table 16 shows the structures of some compounds reported to present in pyrolysis oil.

Table 16. Major components reported to present in lignin pyrolysis oil.

Name	guaiacol	syringol	coniferaldehyde
Structure			
Name	methanol	syringaldehyde	coniferyl alcohol
Structure			
Name	acetic acid	p-vinylphenol	phenol
Structure			

More recently, Scholze et al.^{46, 69} used pyrolysis-GC-MS, FT-IR, GPC, and qualitative ¹³C-NMR to characterize the water-insoluble fraction (pyrolytic lignin) from pyrolysis oil, which was produced from pyrolysis of milled wood (hardwood and softwood) lignin samples. Using GPC, they determined the average molecular weight of pyrolytic lignin was between 650 and 1300 g/mol. From the assignments of qualitative ¹³C-NMR data, they suggested that some lignin subunits were still intact after pyrolysis. On the

other hand, the authors also indicated the formation of new aromatic C-C bonds at the former syringyl C-5 position. Ferdous et al.^{27, 28} studied the effects of the flow rate of the carrier gas, heating rate and temperature on the pyrolysis of Alcell and Kraft lignin and the corresponding bio-oil composition and gas yield. They concluded that the flow rate of carrier gas did not have any significant effect on the conversion, whereas with an increase in the heating rate both lignin conversion and hydrogen production increased. Consistent with the results of Nunn and Caballero, Ferdous also indicated that around 700 °C the pyrolysis oil will begin to go through a secondary pyrolysis reaction which will convert pyrolysis oil to gas products. Liu et al.⁷⁵ did a mechanistic study of hardwood and softwood lignin pyrolysis using a thermogravimetric analyzer coupled with a Fourier transform infrared spectrometry (TG-FTIR). They indicated that lignin undergoes three consecutive sets of reactions during pyrolysis including the evaporation of water, the formation of primary volatiles and the release of small molecular gases. At first, the absorbed water is released by evaporation, and then at a higher temperature (above 100 °C) water is generated by the dehydration of lignin aliphatic hydroxyl groups. The authors also indicated that phenols, in addition to alcohols, aldehydes, acids and CO, CO₂ CH₄ were the major gaseous products. Wang et al.⁷⁸ compared the pyrolysis behavior of lignins, which were isolated from Manchurian and Mongolian Scots pine. Using TG-FTIR to monitor pyrolysis products, they reported that the highest degradation rates of lignin was at ≈380 °C and the highest release rate of CO, CO₂, methanol, formaldehyde and phenols was below 400 °C. A recent report by Nowakowski et al.⁴⁵ summarized an international collaboration of fourteen laboratories that examined the fast pyrolysis of lignin isolated from non-woody plants. They concluded that the decomposition of lignin starts at 120 °C and

extends over a wider temperature range than the thermal decomposition of the whole biomass. Lignin was also reported to produce a pyrolysis oil in 25-50% yield which is less than what is produced from whole biomass.

Shen et al.⁵⁸ pyrolyzed cellulose at 430-730 °C and analyzed pyrolysis products by GC-MS and FT-IR. They found that levoglucosan (1, 6-anhydro- β -D-glucopyranose) is the main component in the bio-oil (more than 50 molar fraction %). Furfural (~1 molar fraction %) and 5-hydroxymethyl-furfural (~2 molar fraction %) were also found as major thermal decomposition products of cellulose. Wild et al.¹⁰³ did a review about biomass pyrolysis for chemicals, they summarized that the major chemicals from the pyrolysis of lignocellulosic biomass are acetic acid, furfural, furans, methanol, levoglucosan, hydroxyacetaldehyde, guaiacol, syringol, catechols, phenols and other oxygenated aromatics. The yields for the pyrolysis oils are from 30-75 wt%.

In this chapter, pyrolytic behaviors of lignin, cellulose and whole biomass—pine wood will be discussed. The influence of pyrolysis temperatures on the yields of pyrolysis products will also be investigated.

4.2 Experimental section

4.2.1 Materials and Methods

Chemicals and biomass used in this study was shown in 3.1 section of this dissertation.

4.2.2 Lignin separation and purification

Lignin separation and purification procedure was shown in 3.2.1.1 section of this dissertation.

4.2.3 Equipment and process of pyrolysis

Pyrolysis system and process was shown in 3.2.3.1 section of this dissertation.

4.2.4 Characterization of pyrolysis oils by GPC

Characterization procedure was shown in 3.3.1 section of this dissertation.

4.3 Results and Discussion

4.3.1 Yields of pyrolysis products

The yields from pyrolyzing a softwood kraft lignin at temperatures of 400 – 700 °C with a heating rate of ~ 2.7 °C/s are summarized in Table 17 and these results indicate that the yields of char, gas and total pyrolysis oil were correlated with the reaction temperature. The char content decreased linearly from 57% to 38% with an increase in pyrolysis temperature. In contrast, the yield of total pyrolysis oil, heavy oil and gas increased with an increased reactor temperature. There are two competitive reactions, which are shown in Figure 12, during the pyrolysis — the primary pyrolysis of lignin and the secondary decomposition of pyrolysis oil. At 700 °C, the increased gas yield was almost the same as the decreased char yield and the yield of total pyrolysis oil was comparable to that acquired at 600 °C. These results indicate that the formation of pyrolysis oil from lignin is almost the same as its decomposition at this temperature, which is comparable to

recent literature reports.^{29, 30}

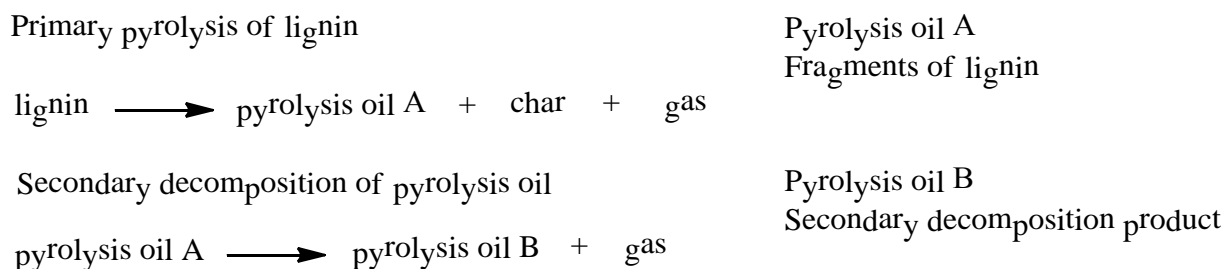


Figure 12. Two competitive reactions during the pyrolysis of SW kraft lignin.

Table 17. Yields of light oil, heavy oil, char and gas for the pyrolysis of SW kraft lignin at 400, 500, 600 and 700 °C.

Pyrolysis Temperature ¹ /°C	Pyrolysis Mass % Yield				
	Light oil	Heavy oil	Total pyrolysis oil	Char	Gas
400	12.09	22.45	34.54	57.21	8.25
500	13.21	27.82	41.03	46.67	12.30
600	14.20	30.01	44.21	40.48	15.31
700	10.44	33.83	44.27	38.14	17.59

¹ All reactions were preformed for 30 min

The yields of the light oil, heavy oil, char and gas for the pyrolysis of cellulose and pine wood are summarized in Tables 18 and 19. The results show that lignin yields mostly a heavy oil and char, in contrast, cellulose produced the least amount of heavy oil and char but the most light oil for the three biomass samples examined in this study. The results also show that the yield of char decreased and the yield of gas increased at higher

reactor temperatures, which indicate the higher pyrolysis temperature prefer to produce more gas products. Table 17 indicated that the formation of pyrolysis oil from lignin (primary pyrolysis) is almost the same as its decomposition (secondary decomposition) near 700 °C, which imply that 700 °C should be the highest temperature to produce pyrolysis oil. For the pyrolysis of cellulose, Table 18 shows the yields of pyrolysis oil and char decreased but the yield of gas increased with increasing reactor temperatures (400-600 °C) which indicates that the point of primary pyrolysis of cellulose and the secondary decomposition of pyrolysis oil is lower than 400 °C. A recent report by Chen et al.¹⁰⁴ gave a similar result employing TGA (thermo gravimetric analysis) to analyze the thermal treatment of cellulose which indicated that cellulose was almost completely decomposed below 400 °C. For the pyrolysis of pine wood, Table 19 shows that the yield of pyrolysis oil only slightly increased (0.85%) when the thermal treatment increased from 500 to 600 °C, in contrast, the yield of gas increased by 2.55%, which indicates that 500 °C is close to the point of primary pyrolysis of pine wood and secondary decomposition of pyrolysis oil. Chen et al.¹⁰⁵ have noted a similar result when they examined bamboo, willow, coconut shell and wood (*Ficusbenjamina L.*) by TGA and found that once the temperature is above 500 °C, the weight loss is not significant, a consequence of thermal decomposition of other heavy components occurring.

Table 18. Yields of light oil, heavy oil, char and gas for the pyrolysis of cellulose at 400, 500 and 600 °C.

Pyrolysis Temperature/ °C	Pyrolysis Mass % Yield				
	Light oil	Heavy oil	Total pyrolysis oil	Char	Gas
400	61.31	11.11	72.42	17.34	10.24
500	61.26	10.81	72.07	13.52	14.41
600	58.83	10.47	69.30	11.17	19.53

Table 19. Yields of light oil, heavy oil, char and gas for the pyrolysis of pine at 400, 500 and 600 °C.

Pyrolysis Temperature °C	Pyrolysis Mass % Yield				
	Light oil	Heavy oil	Total pyrolysis oil	Char	Gas
400	39.78	19.78	59.56	29.11	11.33
500	44.08	20.65	64.73	23.66	11.61
600	43.79	21.79	65.58	20.26	14.16

4.3.2 GPC analysis of SW kraft lignin pyrolysis oils

Along with characterizing the functional groups present in pyrolysis oil, another key biofuel parameter is the molecular weight profiles. The number average and weight average molecular weights (M_n and M_w) and polydispersity values for the four heavy oils produced by pyrolysis of softwood kraft lignin between 400-700 °C are presented in Table 20. This analysis indicates an increase in molecular weight of the heavy pyrolysis oil with an increased reactor temperature. Westerhof et al.⁵³ has reported a similar result of bio-oil produced from pine at different temperatures. The polydispersity values of the heavy oils increase with an increased pyrolysis temperature, which could be attributed to

several factors, including greater release of more condensed fragments with high molecular weights and more secondary decomposed pyrolysis oils with low molecular weights at higher reactor temperatures.

Table 20. Molecular weight distribution and polydispersity (D) of heavy oils produced by pyrolysis of SW kraft lignin at 400, 500, 600 and 700 °C.

Pyrolysis Temperature	M _n (g/mol)	M _w (g/mol)	D(M _w /M _n)
400 °C	133.75	209.54	1.57
500 °C	155.80	260.64	1.67
600 °C	169.72	304.95	1.80
700 °C	181.65	363.78	2.00

4.3.3 Heating values of SW kraft lignin pyrolysis oils

Heating value is another key biofuel parameter profile. The higher heating values (HHV) for the four heavy oils produced by pyrolysis of softwood kraft lignin between 400-700 °C are presented in Table 21. This analysis indicates an increase in HHV of the heavy pyrolysis oil with an increased pyrolysis temperature. The HHVs of those pyrolysis oils are comparable with ethanol (29.8 MJ/Kg) ⁵⁶ and coal (~31.0 MJ/Kg), and higher than methanol (22.7 MJ/Kg) and wood (~20.0 MJ/Kg) but lower than gasoline (47.3 MJ/Kg) and diesel oil (45.7 MJ/Kg). ⁵⁷

Table 21. Higher heating value of heavy oils produced by pyrolysis of SW kraft lignin at 400, 500, 600 and 700 °C.

Pyrolysis Temperature	Higher heating value	
	BTU/LB	MJ/Kg
400 °C	12783	29.73
500 °C	12720	29.83
600 °C	12960	30.10
700 °C	13083	30.48

Since biomass is very complicated, to understand the thermal decomposition pathways of biomass, the pyrolytic behaviors of various biomass components including lignin and cellulose as well as whole biomass under different temperatures have been investigated in this Chapter. For the SW kraft lignin studied, 600 °C was the optimized pyrolysis temperature. For the pyrolysis of cellulose, the yields of pyrolysis oil and char decreased but the yield of gas increased with increasing reactor temperatures (400-600 °C) which indicates that the point of primary pyrolysis of cellulose and the secondary decomposition of pyrolysis oil is lower than 400 °C. For the pyrolysis of pine wood, the yield of pyrolysis oil only slightly increased (0.85%) when the thermal treatment increased from 500 to 600 °C, in contrast, the yield of gas increased by 2.55%, which indicates that 500 °C is close to the point of primary pyrolysis of pine wood and secondary decomposition of pyrolysis oil. In the next Chapter, the characterizations of various pyrolysis oils by NMR methods including ^{13}C , ^{31}P and HSQC-NMR will be discussed. The possible decomposition pathways of lignin and cellulose to the major pyrolysis products will also be investigated.

CHAPTER 5: NMR CHARACTERIZATION OF PYROLYSIS OILS PRODUCED FROM SW KRAFT LIGNIN, CELLULOSE AND PINE WOOD^{*}

5.1 Introduction

Due to the complexity nature of pyrolysis oils brings a huge barrier for the traditional analysis methods such as GC-MS, GPC and FT-IR. GC-MS analysis has always been used to analyze individual components in pyrolysis oil, however, only a small portion could be detected by GC due to the poor volatility. The spectroscopic technique such as FT-IR could give insights into the whole portions of pyrolysis oil. Unfortunately, the ability of such method to deal with complex mixture like pyrolysis oil is very limited. Therefore, precise characterization of the whole portion of thermal decomposition products has significant impacts on providing insight into the thermal decomposition pathways and evaluating the upgrading processes. This chapter will introduce various NMR methods to characterize different functional groups presented in liquid products by ^1H , ^{13}C , ^{31}P and 2D-HSQC, which is the first report effort to be used to analyze pyrolysis oil. Several chemical shifts databases for the components presented in the pyrolysis oils were created to facilitate the characterizations by NMR. Four different types of protons, eight types of hydroxyl groups, fifteen different carbons and thirty different C-H bonds in the

^{*} The full data of this research were accepted for publication in *Energy and Fuels*, 2011. They are entitled as "NMR characterization of pyrolysis oils from kraft lignin" and "Heteronuclear Single-Quantum Correlation–Nuclear Magnetic Resonance (HSQC–NMR) fingerprint analysis of pyrolysis oils". The other author is Arthur J. Ragauskas from the Institute of Paper Science and Technology and School of Chemistry and Biochemistry at Georgia Institute of Technology. Reprinted with permission from "Ben, H.; Ragauskas, A. J., NMR Characterization of Pyrolysis Oils from Kraft Lignin. *Energy Fuels* 2011, 25, (5), 2322-2332." Copyright 2011 American Chemical Society. Reprinted with permission from "Ben, H.; Ragauskas, A. J., Heteronuclear Single-Quantum Correlation–Nuclear Magnetic Resonance (HSQC–NMR) Fingerprint Analysis of Pyrolysis Oils. *Energy Fuels* 2011, 25, (12), 5791-5801." Copyright 2011 American Chemical Society.

whole portion of pyrolysis oil could be analyzed by NMR. The possible thermal decomposition pathways for the lignin and cellulose have also been discussed in this chapter.

5.2 Experimental section

Please see the sections 3.1; 3.2.1; 3.2.1.1; 3.2.3; 3.2.3.1; 3.3.7.2-5 of this dissertation for the details.

5.3 Results and Discussion

5.3.1 ^{31}P -NMR analysis of pyrolysis oils

Phosphitylation of hydroxyl groups using 2-chloro-4,4,5,5-tetramethyl-1,3,2-dioxaphospholane has been developed to quantitatively determine hydroxyl functional groups in various substrates including coal pyrolysis condensates,¹⁰⁶ coal extracts,¹⁰⁷ lignin and biofuel precursors.¹⁰⁸ The overall chemistry of phosphorous derivatization is summarized in Figure 13 and the ^{31}P -NMR chemical shifts and integration regions of the phosphitylated aryl/alkyl hydroxyl groups and water with TMDP are summarized in Table 22.

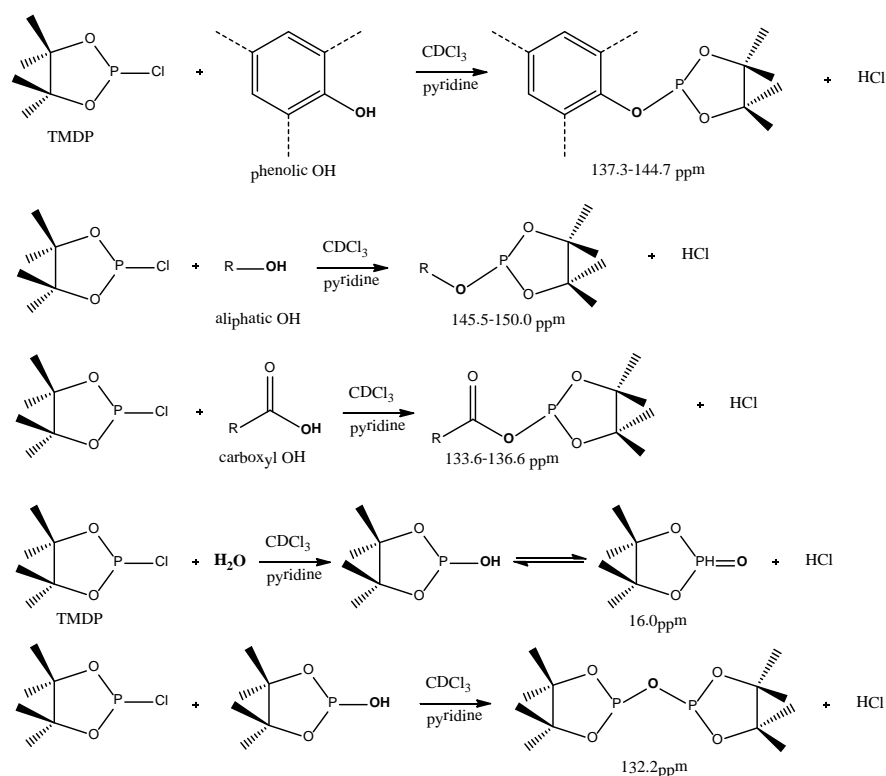
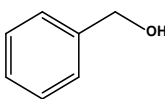
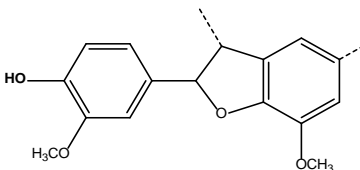
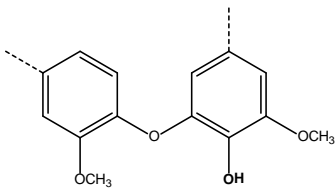
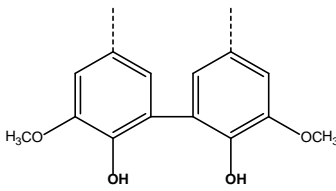
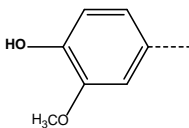
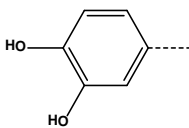
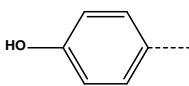
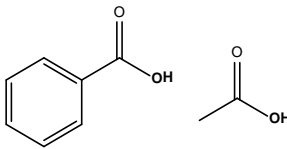


Figure 13. Reactions of the phosphorous reagent (TMDP) with various hydroxyl functional groups and the ^{31}P -NMR assignment of phosphitylated compounds.¹⁰⁸

Table 22. Chemical shifts and integration regions for pyrolysis oil and lignin after derivative with TMDP by a quantitative ^{31}P -NMR.¹⁰⁸

Functional group	Integration region (ppm)	Examples
endo-N-hydroxy-5-norbornene-2,3-dicarboximide (NHND, internal standard)	151.0 - 152.8	

Table 22 continued

				—OH
Aliphatic OH			150.0 - 145.5	
C ₅ substituted Condensed phenolic OH	β-5		144.7 - 142.8	
	4-O-5		142.8 - 141.7	
	5-5		141.7 - 140.2	
Guaiacyl phenolic OH			140.2 - 139.0	
Catechol type OH			139.0 - 138.2	
<i>p</i> -hydroxy-phenyl OH			138.2 - 137.3	
Acid-OH			136.6 - 133.6	
Water peak			133.1-131.3, 16.9-15.1	

Note: chemical shift provided is for the hydroxyl group in bold and with underline after treated with TMDP.

A typical ^{31}P -NMR spectrum for a heavy oil is shown in Figure 14 and the integration for all the heavy oils and the starting lignin are summarized in Table 23. Compared to lignin, the heavy oils contained less aliphatic hydroxyl group, C_5 substituted/condensed phenolic hydroxyl group and carboxyl acid group. The decreased concentration of aliphatic hydroxyl and acid groups is significant as it indicates that the lignin side chain hydroxyl groups were readily eliminated during the thermal treatment. The cleavage of side chain hydroxyl groups was attributed to the dehydration aliphatic hydroxyl groups to form water and sites of unsaturation. The mechanism of decomposition of carboxyl group was attributed to the loss of carbon dioxide during pyrolysis. In contrast, the content of guaiacyl, p-hydroxy phenyl and catechol type hydroxyl groups increased after pyrolysis. This was attributed to the cleavage of ether bonds during the pyrolysis. Prior pyrolysis studies with lignin model compounds have indicated that thermal cleavage of $\beta\text{-O-4}$ ether bond will form guaiacyl, p-hydroxy-phenyl hydroxyl group and catechols, which supports our studies.⁴⁹⁻⁵⁵ Possible reaction pathways for thermal cleavage are illustrated in Figure 15.

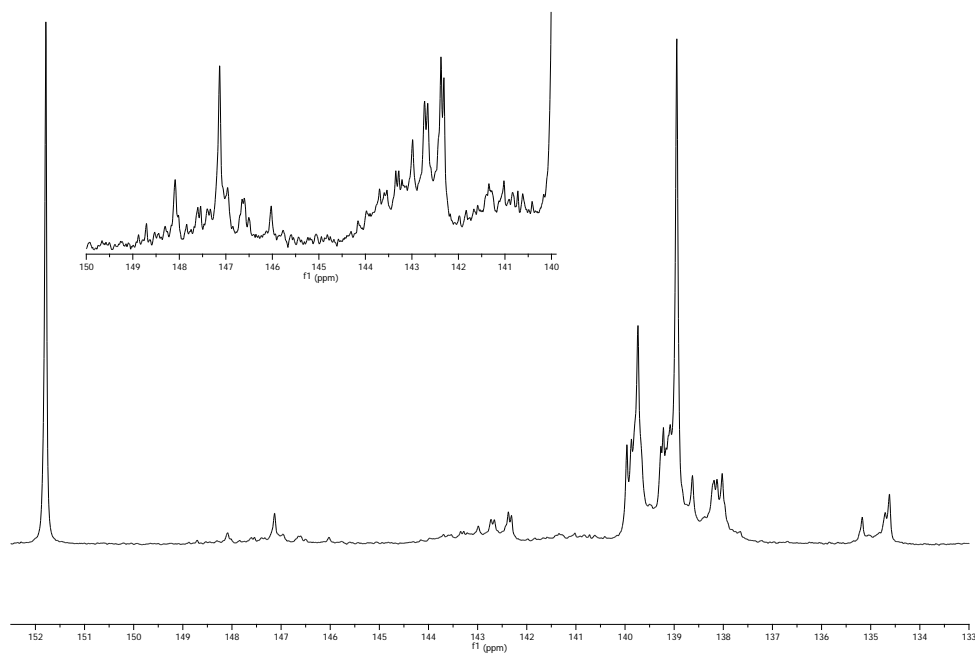


Figure 14. ^{31}P -NMR spectra for the heavy oil produced by pyrolysis of SW kraft lignin at 600 °C derivatized with TMDP.

Table 23. Hydroxyl group contents of SW kraft lignin and different heavy oils produced by pyrolysis of SW kraft lignin at 400, 500, 600 and 700 °C determined by quantitative ³¹P-NMR after derivatization with TMDP.

Functional group		Hydroxyl Group Contents /(mmol/g heavy oil)				
		400 °C	500 °C	600 °C	700 °C	Lignin
Aliphatic OH		0.28	0.36	0.36	0.35	1.73
C ₅ substituted	β-5	0.47	0.47	0.40	0.41	0.59
Condensed	4-O-5	0.26	0.31	0.31	0.34	0.42
Phenolic OH	5-5	0.35	0.35	0.31	0.30	0.76
Guaiacyl phenolic OH		3.05	2.93	2.33	2.28	1.53
Catechol type OH		1.34	1.49	2.02	2.22	0.17
<i>p</i> -hydroxy-phenyl OH		0.33	0.46	0.49	0.55	0.14
Acid-OH		0.26	0.33	0.37	0.37	1.05

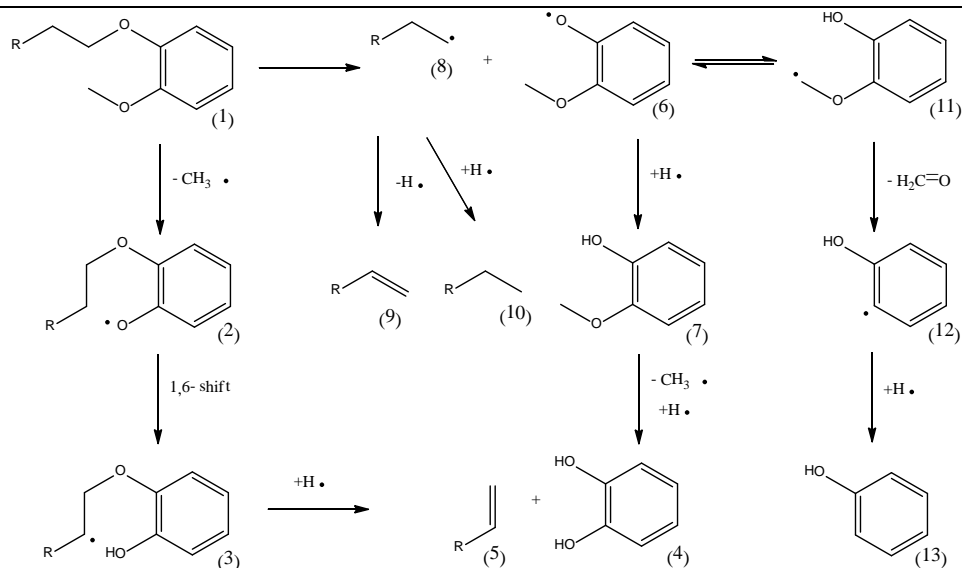


Figure 15. The possible decomposition pathways of ether bond in lignin during the pyrolysis.⁴⁹⁻⁵⁵

The results in Table 23 indicate that the concentration of guaiacyl hydroxyl groups decreased with increasing pyrolysis temperature from 400 - 700 °C. In contrast, the yield of catechol type and *p*-hydroxy-phenyl hydroxyl group increased with this increase in pyrolysis temperature. This result, combined with the possible decomposition pathways suggests that guaiacol (7) could be further converted to catechol (4) or phenol (13) at higher pyrolysis temperatures.

Because the methoxy phenoxy radical (6) is more favored than the *o*-hydroxy phenoxy methyl radical (11),⁴⁹ the content of *p*-hydroxy-phenyl hydroxyl groups in the pyrolysis oil should be lower than the catechol type and guaiacyl hydroxyl groups, which is consisted with the results shown in Table 23. In addition, based on ³¹P-NMR results, there are nonlinearly changes of the contents of guaiacyl and catechol type hydroxyl groups between 500 °C and 600 °C which could be attributed to several factors including greater release of more condensed structures and improved cleavage of methoxyl groups at higher reactor temperatures.

In contrast with the heavy oils, the ³¹P-NMR data from the light oils exhibited fewer signals that were relatively easy to identify. These samples contained approximately 80 w/w% of water and 10 w/w% of three other components as summarized in Table 24. Base on the chemical shift data in the literature^{106, 109} three peaks were assigned to methanol (147.9 ppm), catechol (138.9 ppm) and acetic acid (134.6 ppm) which were also detected as the major components in the light oil by GC-MS. The yield of catechol in the light oil increased as the pyrolysis temperature was increased from 400 °C to 700 °C,

which is similar to the results observed in the heavy oil analysis. In contrast, the concentration of methanol and acetic acid in light oil decreased as the reactor temperature was increased.

Table 24. Weight percentage of four major components in light oils produced by pyrolysis of SW kraft lignin at 400, 500, 600 and 700 °C, determined by quantitative ^{31}P -NMR after derivatization with TMDP.

Major components in light oil	w/w% in light oil			
	400 °C	500 °C	600 °C	700 °C
Methanol	8.10	6.24	6.24	5.02
Catechol	0.44	0.66	1.32	1.98
Acetic acid	1.62	1.26	1.20	0.90
Water	78.50	79.39	79.85	80.01

5.3.2 ^{13}C -NMR analysis of pyrolysis oils

To fully characterize the functional groups in the pyrolysis oils, a detailed analysis of these products was accomplished using ^{13}C -NMR. To help facilitate this analysis, the chemical shifts of 97 compounds^{15, 21-26} reported present in pyrolysis oils were summarized in a map of chemical shifts. Figure 16 shows the results of this analysis. Although each chemical moiety is a unique data entry, some compounds had multiply signals in the assigned spectral regions which resulted in overlapping chemical shifts. For this analysis, it is apparent that 80% of the aromatic C-O bonds have a chemical shift range of 142.0 –

166.5 ppm, 79% of aromatic C-C bonds have a chemical shift between 142.0 - 125.0 ppm and 81% of aromatic C-H bonds have a chemical shift between 125.0-95.8 ppm. Figure 17 shows the distribution of over 1000 chemical shifts data and the assignment range results. With the exception of olefinic carbons, the other six carbon bond ranges were reasonably well separated. In addition, two kinds of methyl-aromatic carbons in the aliphatic C-C range are also analyzed and shown in Figure 18. Based on those results, a structural assignment range was developed and this analysis is summarized in Table 25. The whole database can be found as the supplementary data of this paper.

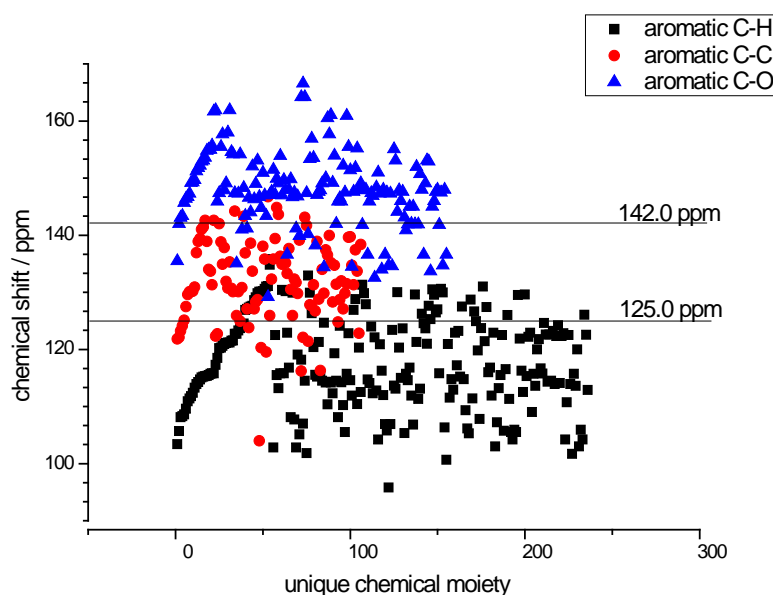


Figure 16. ¹³C-NMR chemical shifts distribution of aromatic C-H, C-C and C-O for compounds reported present in pyrolysis oils.

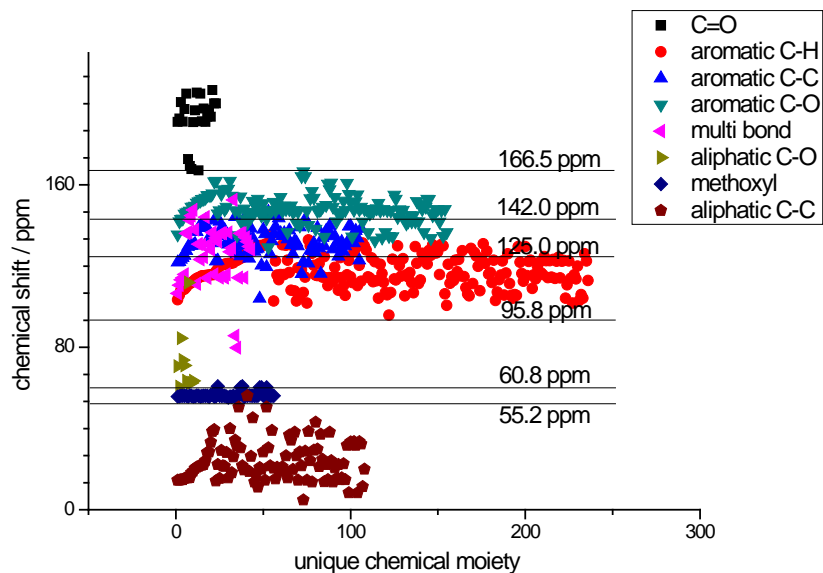


Figure 17. ^{13}C -NMR chemical shifts distribution of various functional groups (from 0-215 ppm) for compounds reported present in pyrolysis oils.

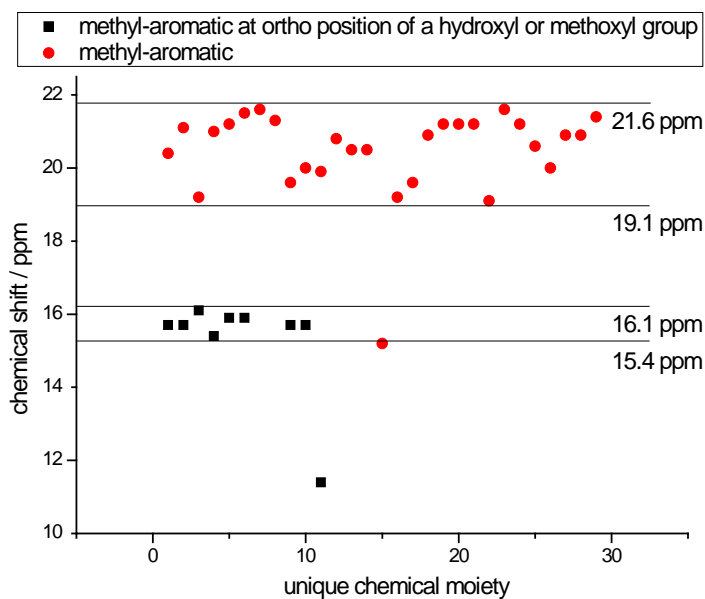
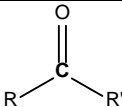
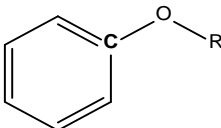
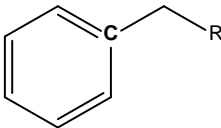
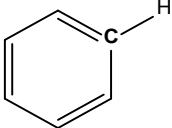
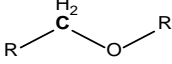
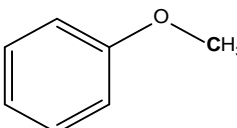
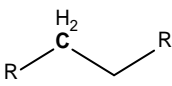
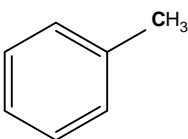
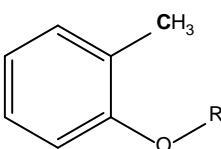


Figure 18. ^{13}C -NMR chemical shifts distribution of methyl-aromatic carbons for compounds, reported present in pyrolysis oils.

Table 25. ^{13}C -NMR chemical shift assignment range of lignin pyrolysis oil based on literature compounds.^{15, 21-26}

Functional group	Integration region (ppm)	Examples
Carbonyl or Carboxyl bond	215.0 – 166.5	
Aromatic C-O bond	166.5 – 142.0	
Aromatic C-C bond	142.0 – 125.0	
Aromatic C-H bond	125.0 – 95.8	
Aliphatic C-O bond	95.8 – 60.8	
Methoxyl-Aromatic bond	60.8 – 55.2	
General	55.2 – 0.0	
Methyl – Aromatic	21.6 – 19.1	
Methyl – Aromatic at ortho position of a hydroxyl or methoxyl group	16.1 – 15.4	

A typical ^{13}C -NMR spectrum for a heavy oil is shown in Figure 19 and the results of this analysis are summarized in Table 26. This data shows that the carbonyl group content was reduced after pyrolysis, and methoxyl group was significantly eliminated after pyrolysis, especially at higher pyrolysis temperatures. Based on the ^{13}C -NMR results, nearly 70%-80% of the carbons from heavy oil are aromatic carbon. The number of aromatic C-O and C-C bonds in heavy oil increased with increasing pyrolysis temperatures from 400 - 700 °C. In contrast, the number of aromatic C-H bond decreased with an increasing reactor temperature. Considering the number of aliphatic C-O bonds removed during pyrolysis and the possible reaction pathways presented in the literature⁴⁹⁻⁵⁵ the formation of aromatic C-O bond may due to radical reactions between aromatic and aliphatic hydroxyl groups. In addition, there are much more aliphatic C-C bonds in the heavy oils than lignin. Two kinds of methyl-aromatic carbons in the aliphatic C-C range have also been analyzed. Those methyl-aromatic C-C bonds have been formed during the pyrolysis and the content increased with a reactor temperature increase from 400 - 600 °C. It seems that those methyl-aromatic bonds could also be decomposed at 700 °C. A possible pathway of formation of aromatic C-O bond and C-C bonds are provided in Figure 20.

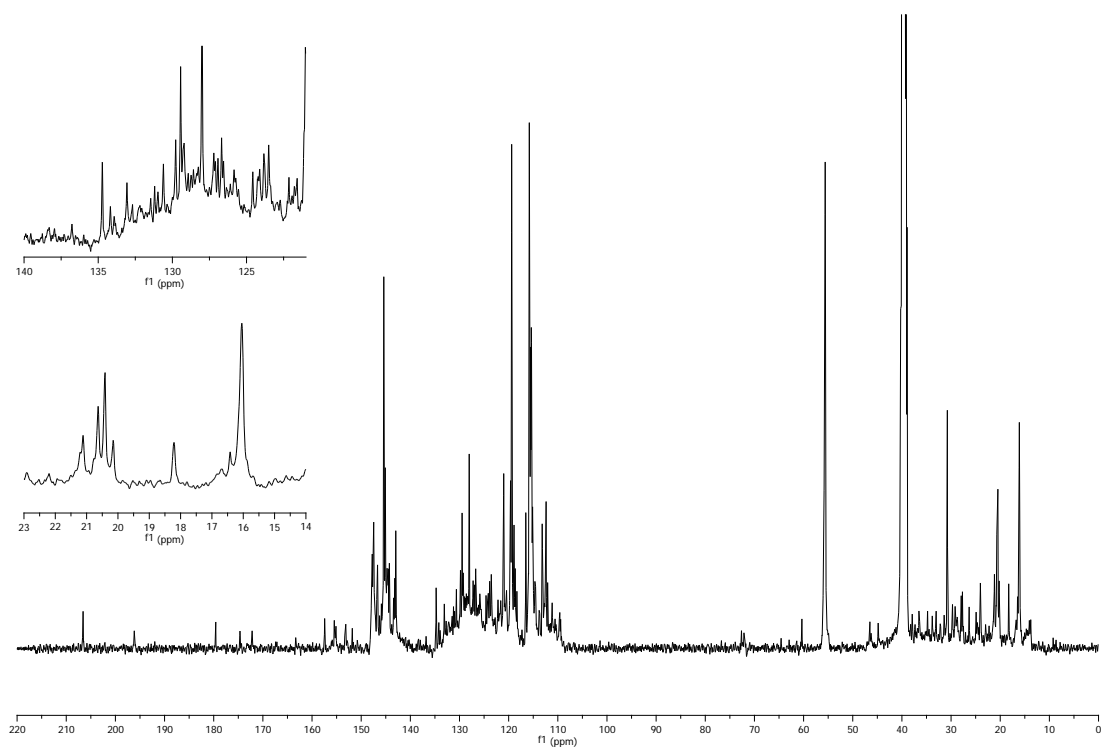


Figure 19. Quantitative ^{13}C -NMR spectra for the heavy oil produced by pyrolysis of SW kraft lignin at 600 °C.

Table 26. Integration results for SW kraft lignin and heavy oils produced by pyrolysis of SW kraft lignin at 400, 500, 600 and 700 °C, detected by quantitative ^{13}C -NMR with using the assignment range showed in Table 25. The results were shown as the percentage of carbon.

Functional groups	400 °C	500 °C	600 °C	700 °C	lignin
C=O	0.5	0.6	0.9	0.3	1.6
Aromatic C-O	15.7	16.3	16.7	20.6	27.3
Aromatic C-C	14.0	15.9	22.7	26.9	25.8
Aromatic C-H	36.5	33.2	29.7	29.4	26.4
Aliphatic C-O	0.6	0.5	0.1	0.5	5.8
Methoxyl	9.6	8.5	5.4	4.5	12.9
Aliphatic C-C general	23.1	25.0	24.4	17.8	0.3
Methyl – Aromatic	3.9	4.3	4.5	3.2	0.0
Methyl – Aromatic at ortho position of a hydroxyl or methoxyl group	2.4	2.7	3.3	2.2	0.0

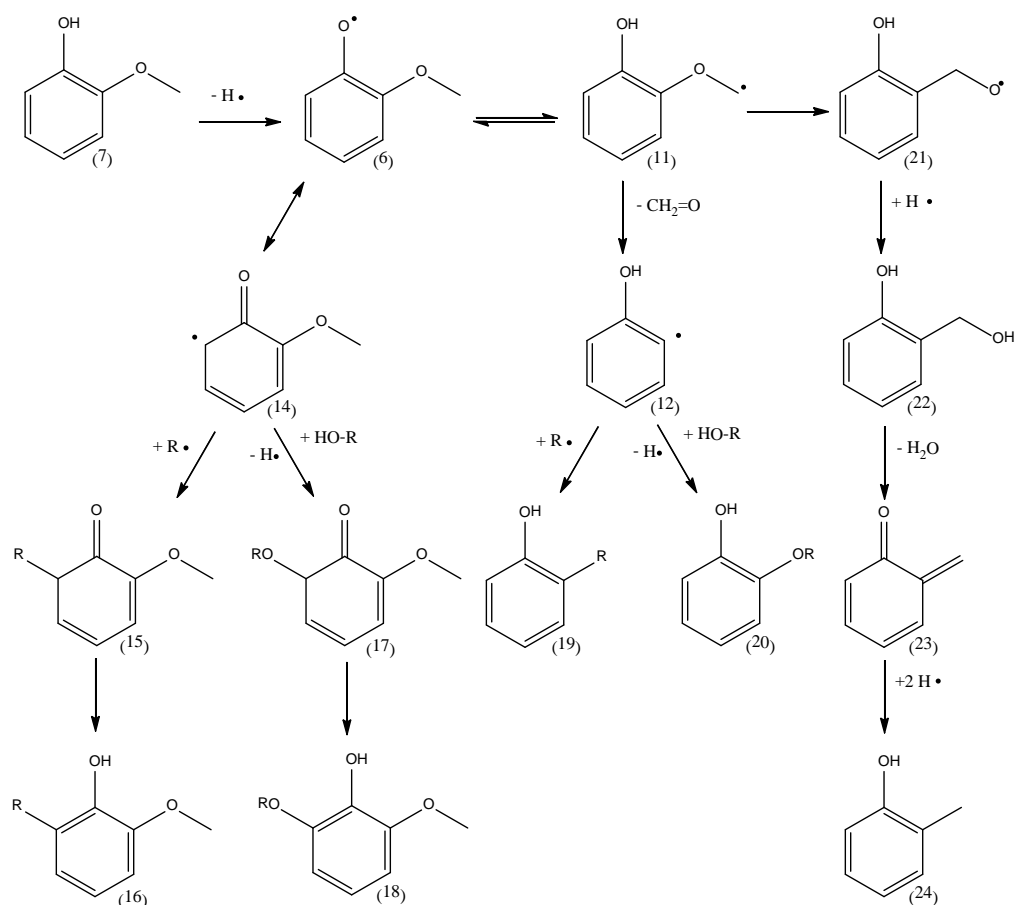


Figure 20. The possible pathway to form aromatic C-O bond and C-C bond in pyrolysis oil.⁴⁹⁻⁵⁵

The radical reactions shown in Figure 20 have been proposed by some researchers^{50, 85} to be favored at higher pyrolysis temperatures, which mean the number of aromatic C-O and C-C bond, will increase with increasing reactor temperatures. The change in the aromatic C-H bonds is interrelated with C-O and C-C bond, if the number of aromatic C-O and C-C bond is increased, the number of aromatic C-H bond will be decreased. Therefore, the proposed pathways shown in the Figure 20 are supported by the results in Table 26. Similarly, with the ³¹P-NMR results for the heavy oils, nonlinearly changes occurred between 500 and 600 °C as was found in ¹³C-NMR results. Based on

the possible pathways to form aromatic C-C bond during pyrolysis the cleavage of methoxyl groups and aromatic C-H bonds could produce aromatic radicals and subsequently form aromatic C-C bonds. In addition, at 600 °C the reactor temperature may provide enough energy to release more condensed lignin fragments, which contain more aromatic C-C bonds. The possible pyrolysis pathways of primary decomposed functional groups in lignin during the pyrolysis have been summarized in Figure 21.

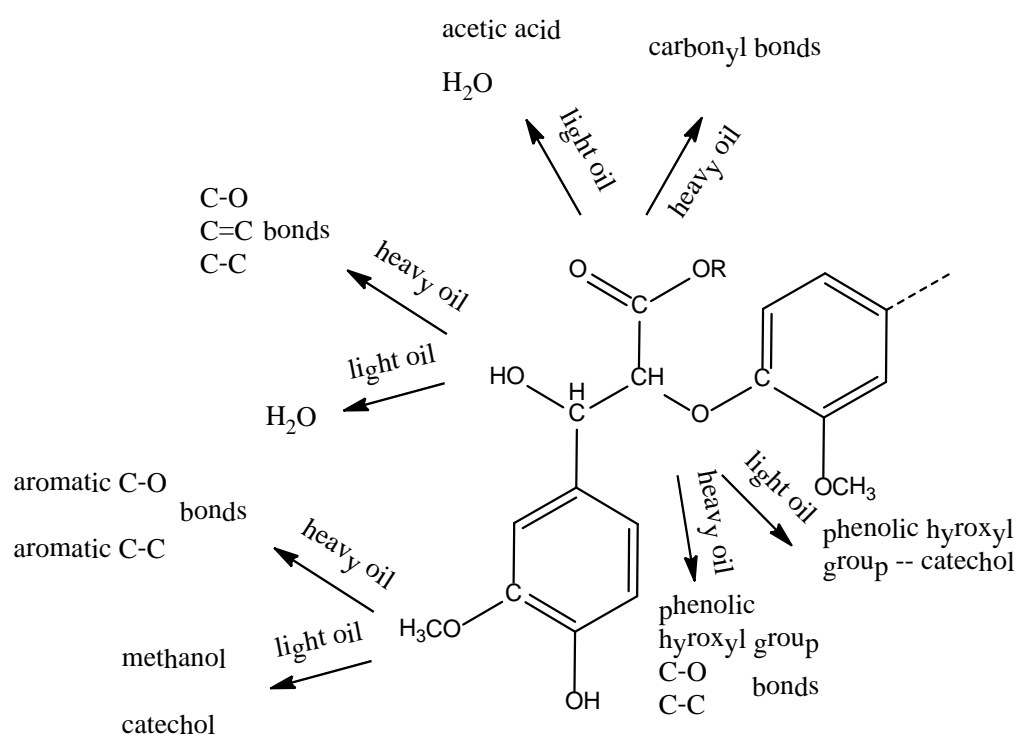


Figure 21. The possible pyrolysis pathway of primary decomposed functional groups in lignin during the pyrolysis.

The pyrolysis of softwood kraft lignin was accomplished at 400, 500, 600 and 700 °C. The yields of pyrolysis oil, char and gas indicated that 700 °C was the point of primary decomposition of lignin and the secondary decomposition of pyrolysis oil. For the SW

kraft lignin studied, 600 °C was the optimized pyrolysis temperature. The ^{31}P -NMR results for the light oil showed that it contained nearly 80 w/w% water and another 10 w/w% was methanol, catechol and acetic acid. The large amount of water was attributed to dehydration reactions of lignin during pyrolysis. Based on the results of ^{13}C and ^{31}P -NMR for the heavy oil and lignin, the aliphatic OH, carboxyl and methoxyl group in the lignin are the primary target functional groups to decompose during the pyrolysis, the cleavage of ether bond in the lignin is another primary decomposition during the thermal treatment. Further, the results of ^{13}C -NMR and GPC indicated that at higher temperature, there would be more aromatic C-O and C-C bond in the heavy oil, and the heavy oil would have a larger molecular weight and polydispersity value.

In summary, the detailed characterization of this pyrolysis oil provides insight into the mechanisms of pyrolysis of lignin and its products. These results will be of value in the development of tailored catalysts to upgrade these bio-oils to green fuels.

5.3.3 HSQC-NMR analysis of pyrolysis oils

Our previous study found that the light oils produced from pyrolysis of lignin contain ~80 w/w% of water whereas the light oil from cellulose and pine wood contained ~40-60 w/w% of water. The heavy oils were further analyzed by quantitative 1-D NMR and a series of functional groups were determined including carbonyl groups, aromatic C-H, C-O and C-C bonds, aliphatic C-C and C-O bonds and methoxyl groups. This analysis was complicated by the spectral overlap of some signals. It is well appreciated that the limitations of 1-D NMR can be addressed using modern 2-D NMR techniques, which

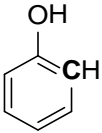
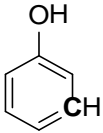
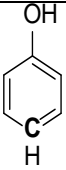
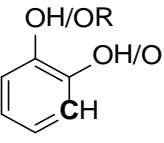
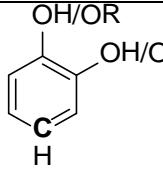
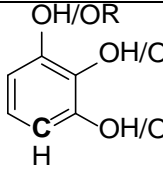
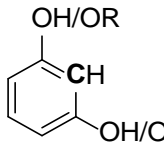
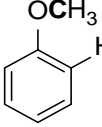
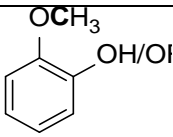
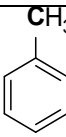
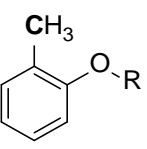
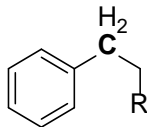
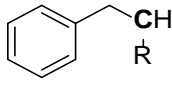
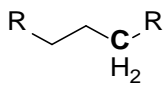
has been used to analysis lignin,¹¹⁰⁻¹¹² cellulose,¹¹³ and whole biomass.^{103, 112, 114} To fully characterize the functional groups in the pyrolysis oils, HSQC-NMR was used to analyze the total pyrolysis oils from kraft lignin, cellulose and pine wood by dissolving the light and heavy oil in deuterated DMSO. To help facilitate this analysis, three chemical shift databases of compounds reported to be presented in pyrolysis oils were employed for data analysis. The detailed information of those three chemical shift databases can be found in the supporting material.

5.3.3.1 HSQC-NMR analysis of pyrolysis oils produced from softwood kraft lignin

The ^1H and ^{13}C -NMR chemical shifts of 97 compounds reported^{15, 21-26} present in pyrolysis oils are summarized in a 2-D map of chemical shifts. Figure 22 shows the results of this analysis; the detailed structures of the assignments are shown in Table 27. The aromatic C-H bonds, methoxyl groups and aliphatic C-H bonds in the HSQC-NMR spectra for the heavy oils produced by pyrolysis of SW kraft lignin from 400 to 600 °C are shown in Figures 23-25, separately. Figure 23 shows that the content of A2 kind of aromatic C-H bond (aromatic C-H bond in the meta-position of phenol) increases with the increasing pyrolysis temperature, which is consistent with the results in our previous work. The content of phenol was also found to increase with the reactor temperature. There are no peaks belong to the B3 and B4 types of aromatic C-H bonds which indicate that SW kraft lignin will not produces any syringyl type of aromatic products during the pyrolysis process. The contents of all the aromatic C-H bonds shown in Figure 23 slightly increased with the increasing thermal treatment temperature, these aromatic C-H bonds could be formed by the cleavage of ether bonds and methoxyl groups. Figure 24 shows

two different kinds of methoxyl groups presented in pyrolysis oils, because there is no C1 (no hydroxyl or ether bond in the ortho position of methoxyl group) type of methoxyl group in the native kraft lignin, which suggest that this kind of methoxyl group was created by the pyrolysis process. On the basis of reported ^{115, 116} bond energies for various C-H and C-O bonds in lignin model compound (Figure 26), the aliphatic C-O bond in the methoxyl groups will be the first point to decompose during the thermal treatment, Figure 27 shows the possible decomposition and rearrangement pathways of methoxyl groups in lignin during the pyrolysis,^{49, 51} which indicates that the native methoxyl group (C2) will rearrange to another type (C1). Figure 25 shows that the content of methyl-aromatic carbon (D1 and D2) increased with increasing pyrolysis temperatures from 400-600 °C, our previous work also indicated the same result by quantitative ¹³C-NMR. The possible formation pathways of methyl-aromatic carbons were proposed in Figure 27. Similarly, the contents of all the other types of aliphatic C-H bonds also slightly increased with the increasing reactor temperature. The formation of those aliphatic carbons may due to the rearrangement of ether bonds or the cleavage of side chains in lignin.

Table 27. Detailed structures of assignments for HSQC-NMR analysis of pyrolysis oil produced from softwood kraft lignin.

						
A1	A2	A3	B1	B2	B3	B4
						
C1	C2	D1	D2	D3	D4	D5

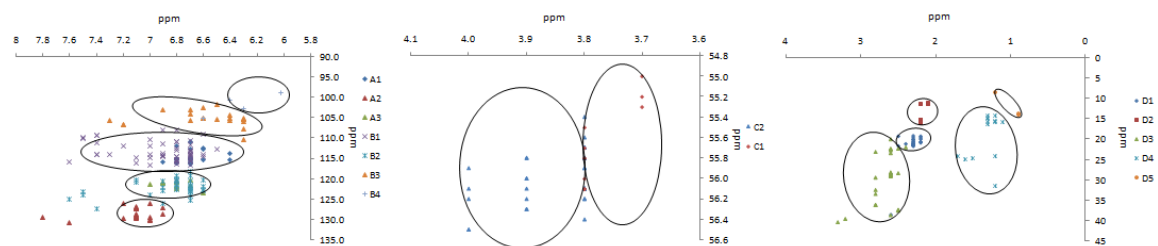


Figure 22. ^1H -NMR and ^{13}C -NMR chemical shifts distribution of various functional groups for compounds reported present in lignin pyrolysis oils. The assignments range for each functional groups are circled in the specific area. (The assignments range may vary due to the limitations of chemical shift database)

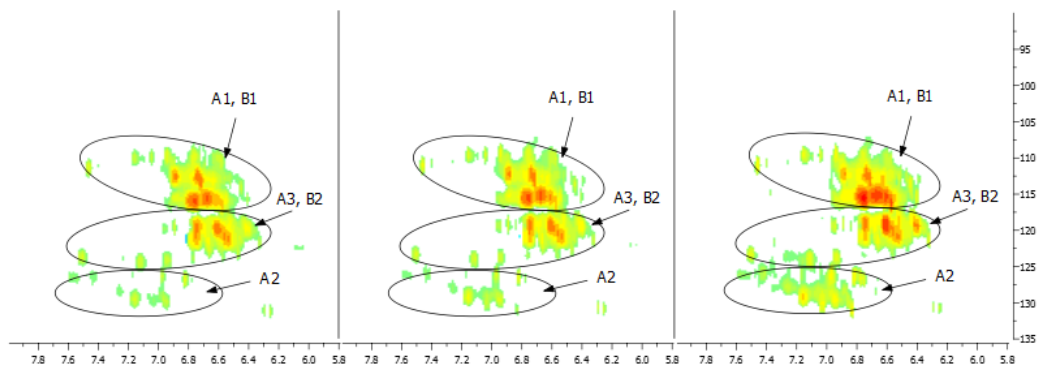


Figure 23. Aromatic C-H bonds in the HSQC-NMR spectra for the pyrolysis oils produced by pyrolysis of SW kraft lignin from 400 to 600 °C (from left to right).

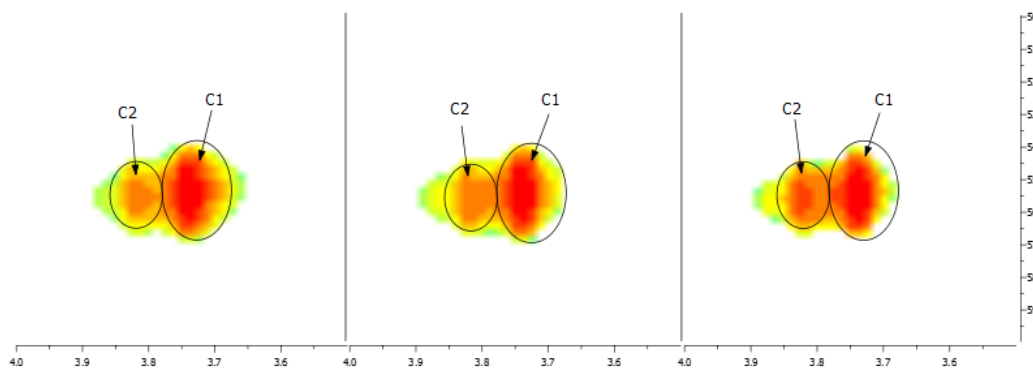


Figure 24. Methoxyl groups in the HSQC-NMR spectra for the pyrolysis oils produced by pyrolysis of SW kraft lignin from 400 to 600 °C (from left to right).

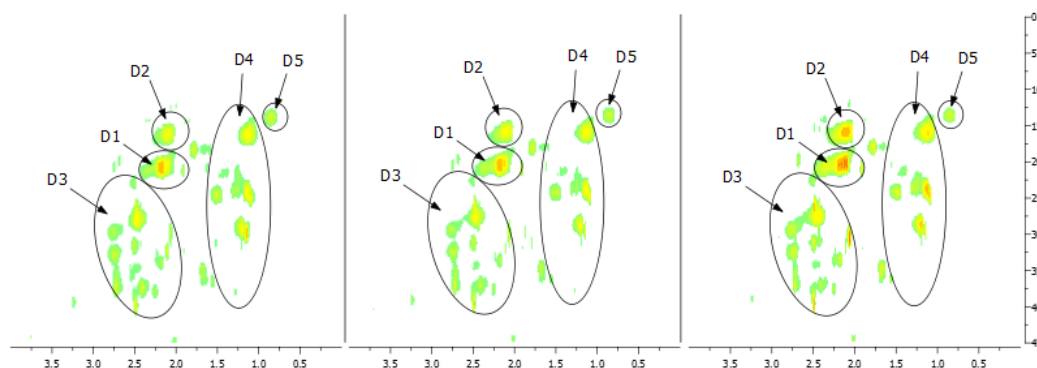
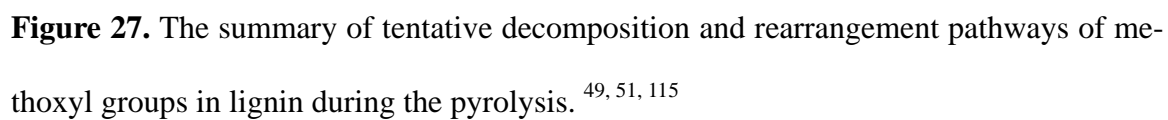
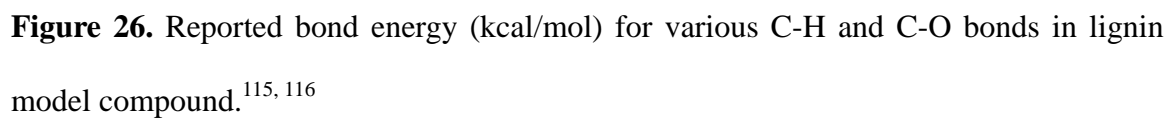


Figure 25. Aliphatic C-H bonds in the HSQC-NMR spectra for the pyrolysis oils produced by pyrolysis of SW kraft lignin from 400 to 600 °C (from left to right).



5.3.3.2 HSQC-NMR analysis of pyrolysis oils produced from cellulose

Figure 28 shows 2-D maps of ^1H and ^{13}C -NMR chemical shifts of the compounds reported^{58, 64, 61-63} present in pyrolysis oils produced from cellulose, the detailed structural assignments are shown in Table 28. Figure 29 shows HSQC-NMR spectra and the assignments of each carbon in the levoglucosan (I) presented in the cellulose pyrolysis oils, the intensity of those peaks indicates that levoglucosan is one of the major products in the cellulose pyrolysis oil. Shen et al.⁵⁸ and Moldoveanu⁶⁴ also found the similar result by analysis of cellulose pyrolysis oils with GC-MS. The content of levoglucosan only slightly increased with increasing pyrolysis temperature, which is consistent with prior results. Figure 31 shows the aromatic C-H bonds in the HSQC-NMR spectra for the cellulose pyrolysis oils. It indicates that the furans (compounds E1 and E2 in Table 28) and phenols are the major aromatic products in the cellulose pyrolysis oils and the pyrolysis temperature only has limited effect on the contents of those products. Figure 32 shows that the methyl-furfural (or other compounds containing furan ring, compound F in Table 28) and the α -carbon nearby the carbonyl group (G) are the major type of aliphatic C-H bonds presented in the bio-oils produced from cellulose. Another major compound present in the cellulose pyrolysis oil is 5-hydroxymethyl-furfural (HMF, compound H in Table 28) and its assignment in the HSQC-NMR spectra is shown in Figure 33. The content of HMF decreased with the increasing pyrolysis temperature, which indicates that HMF undergoes further decomposition at higher pyrolysis temperature. The summary of tentative mechanism in the literatures^{58, 88, 117, 118} for the formation of levoglucosan, HMF and aromatic rings during the pyrolysis of cellulose are shown in Figure 30.

Table 28. Detailed structures of assignments for HSQC-NMR analysis of pyrolysis oil produced from cellulose.

E1	E2	F	G	H	I

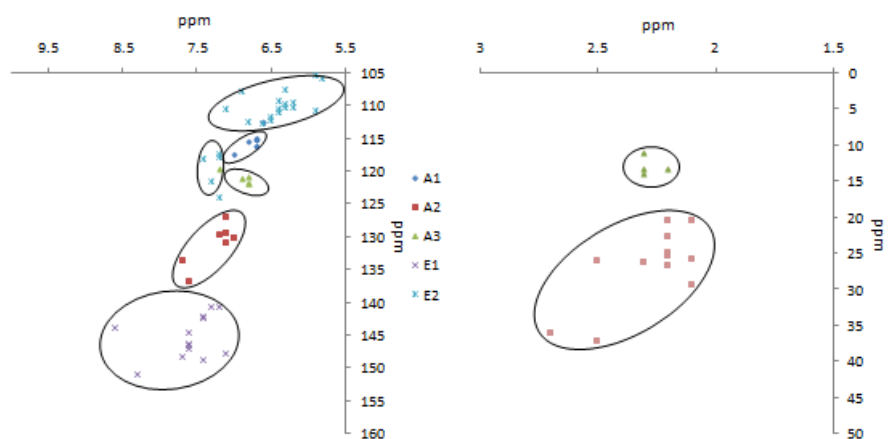


Figure 28. ¹H-NMR and ¹³C-NMR chemical shifts distribution of various functional groups for compounds reported present in pyrolysis oils produced from cellulose.^{58, 64,61-63}

The assignments range for each functional groups are circled in the specific area.

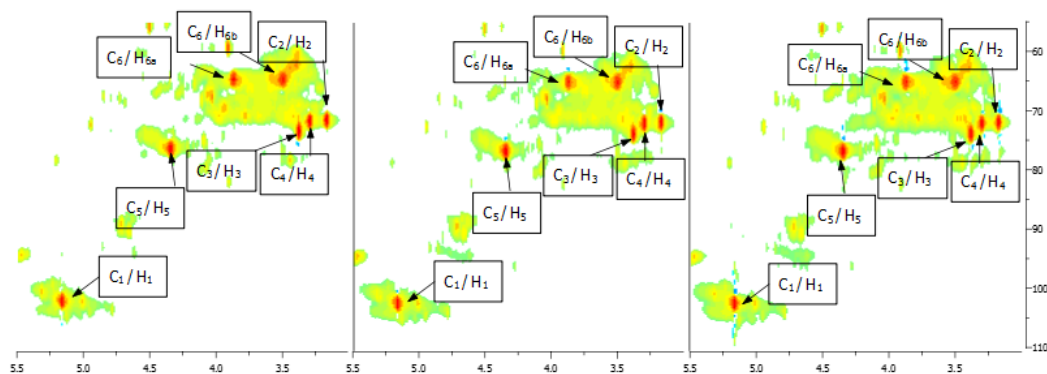


Figure 29. HSQC-NMR spectra and the assignments of each carbon in the levoglucosan presented in pyrolysis oils produced by pyrolysis of cellulose from 400 to 600 °C (from left to right).

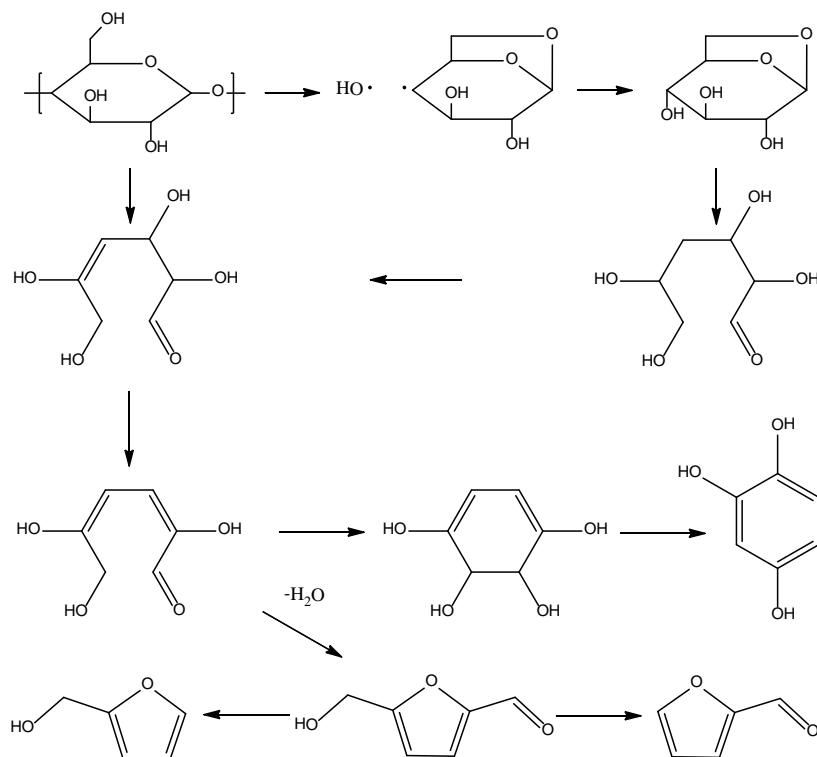


Figure 30. The summary of tentative mechanism in the literatures for the formation of levoglucosan, HMF and aromatic rings during the pyrolysis of cellulose.^{58, 88, 117, 118}

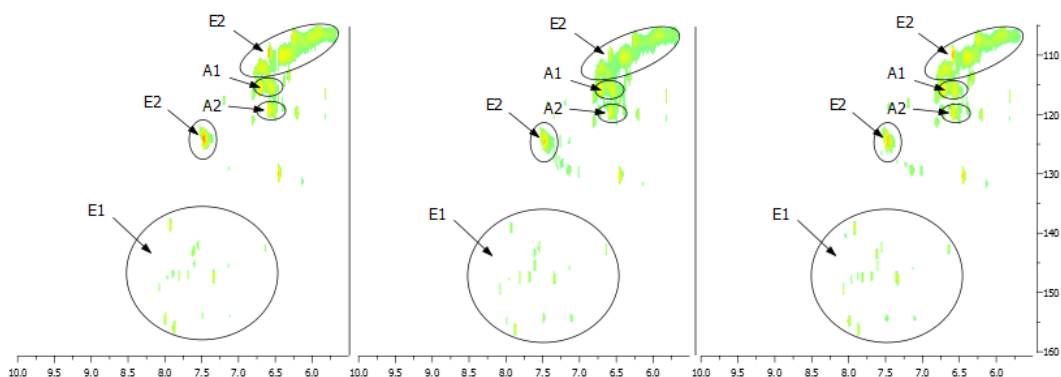


Figure 31. Aromatic C-H bonds in the HSQC-NMR spectra for the pyrolysis oils produced by pyrolysis of cellulose from 400 to 600 °C (from left to right).

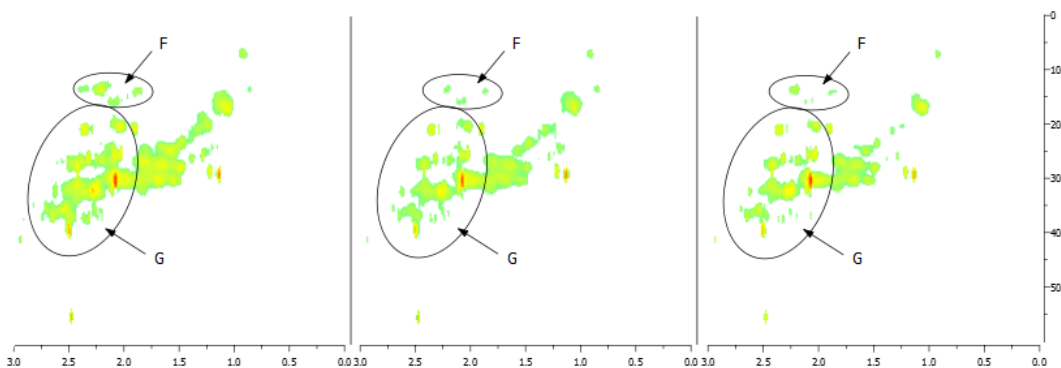


Figure 32. Aliphatic C-H bonds in the HSQC-NMR spectra for the pyrolysis oils produced by pyrolysis of cellulose from 400 to 600 °C (from left to right).

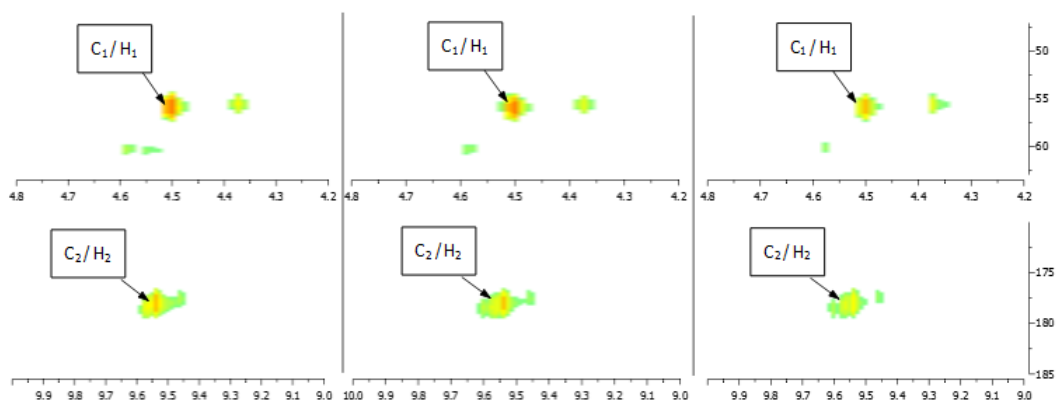


Figure 33. HSQC-NMR spectra and the assignment of 5-hydroxymethyl-furfural (HMF,

compound H in Table 28) presented in pyrolysis oils produced by pyrolysis of cellulose from 400 to 600 °C (from left to right).

5.3.3.3 HSQC-NMR analysis of pyrolysis oils produced from pine wood.

Similarly to the pyrolysis of cellulose, levoglucosan is also one of the major components presented in pine wood pyrolysis oil. Figure 34 shows HSQC-NMR spectra and the assignments of each carbon in the levoglucosan (I) presented in the pine wood pyrolysis oils, and the content of levoglucosan slightly increased from 9%-11% with the increasing pyrolysis temperatures. (detected by quantitative ^{13}C -NMR, the results are shown in percentages of total carbon.) Figure 35 shows the aromatic C-H bonds in the HSQC-NMR spectra for the pine wood pyrolysis oils. It indicates that the major aromatic components in the pine wood pyrolysis oils contain A1, A2, A3, B1 and B2 types of aromatic C-H bonds, which is comparable with lignin pyrolysis oils; in addition, the contents of those aromatic C-H bonds increase with increasing pyrolysis temperature, which is also consisted with pyrolysis oils produced from SW kraft lignin. Figure 36 indicates that there are more rearranged methoxyl groups (C1) than the native type (C2) in the pyrolysis oils produced from pine wood, which is also similar with lignin pyrolysis oils. Figure 37 shows that the contents of aliphatic C-H bonds slightly increased (from 24-26%, detected by quantitative ^{13}C -NMR, the results are shown in percentages of total carbon) with the increasing reactor temperature and most of those aliphatic C-H bonds result from the pyrolysis of the lignin component.

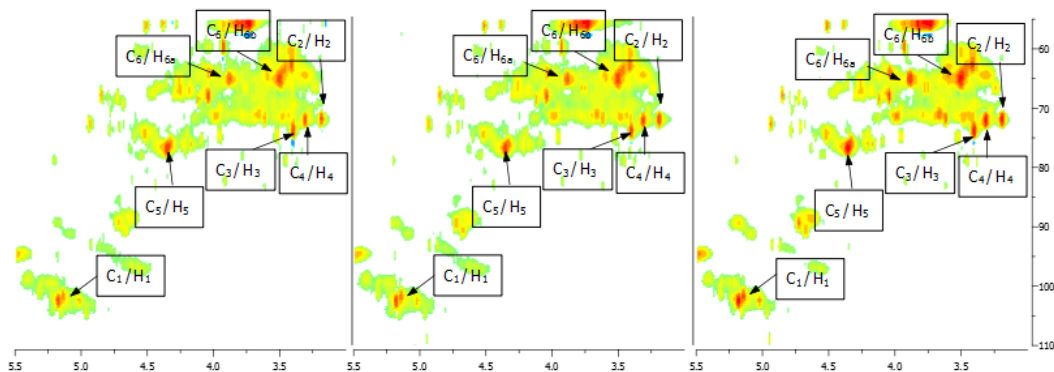


Figure 34. HSQC-NMR spectra and the assignments of each carbon in the levoglucosan presented in pyrolysis oils produced by pyrolysis of pine wood from 400 to 600 °C (from left to right).

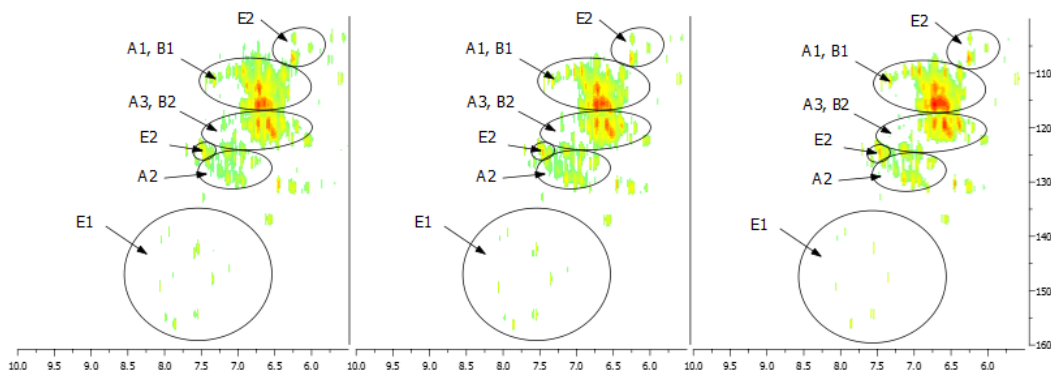


Figure 35. Aromatic C-H bonds in the HSQC-NMR spectra for the pyrolysis oils produced by pyrolysis of pine wood from 400 to 600 °C (from left to right).

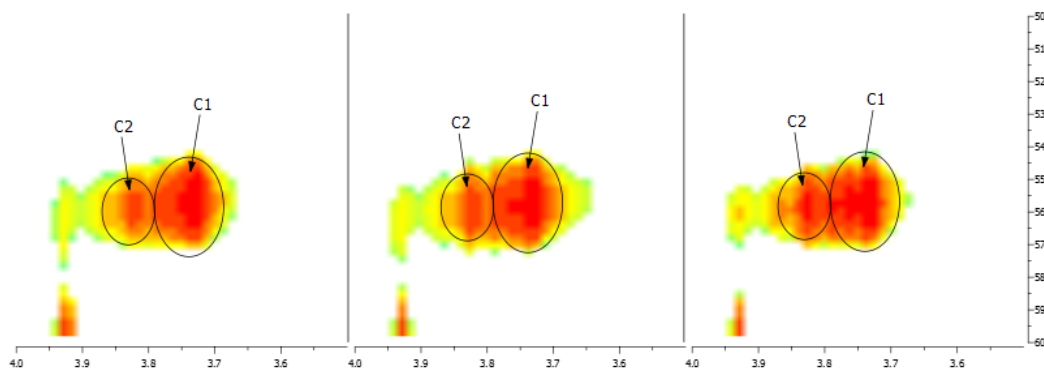


Figure 36. Methoxyl groups in the HSQC-NMR spectra for the pyrolysis oils produced by pyrolysis of pine wood from 400 to 600 °C (from left to right).

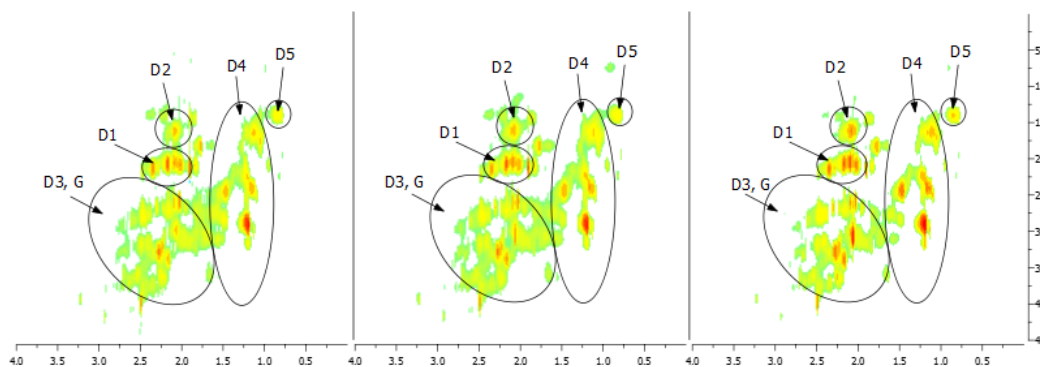


Figure 37. Aliphatic C-H bonds in the HSQC-NMR spectra for the pyrolysis oils produced by pyrolysis of pine wood from 400 to 600 °C (from left to right).

5.4. Conclusion

The HSQC-NMR analysis of pyrolysis oils produced from softwood kraft lignin, cellulose and Loblolly pine wood at 400, 500 and 600 °C was examined. The fingerprint analysis of HSQC-NMR spectral data provides chemical shift assignment of twenty-seven different types of C-H bonds present in pyrolysis oils. The HSQC-NMR for the lignin pyrolysis oils showed that there are two different types of methoxyl group present in the pyrolysis oils, which indicated that the native methoxyl group in the kraft lignin will rearrange to another type during the thermal treatment. The content of aromatic C-H and aliphatic C-H bonds in the lignin pyrolysis oils increased with increasing pyrolysis temperature, which was attributed to the rearrangement and the cleavage of ether bonds or methoxyl groups in the lignin structure. On the basis of HSQC-NMR analysis for the pyrolysis oils produced from cellulose, levoglucosan was found as the major component and the content increased from 46 to 53% (detected by quantitative ^{13}C -NMR, the results are shown in percentages of total carbon) with the pyrolysis temperature increased from 400 to 600 °C. Furfural (or other compounds containing furan ring) and phenol were also

found as the major components in the cellulose pyrolysis oils. The content of 5-hydroxymethyl-furfural (HMF) decreased at higher thermal treatment temperature, which indicated that HMF could be further decomposed at higher temperature. The analysis of HSQC-NMR for the pine wood pyrolysis oils indicated that levoglucosan is also one of the major components presented in the pyrolysis oils and most of aromatic C-H and aliphatic C-H bonds in the pine wood pyrolysis oils produced from lignin component.

Chapter 6: IN SITU NMR CHARACTERIZATION OF PYROLYSIS OIL DURING THE ACCELERATED AGING PROCESS*

6.1 INTRODUCTION

Biofuels are increasingly being viewed as a promising alternative fuel resource due to the growing concerns about increasing global energy consumption and the effects of growing carbon dioxide emissions from fossil fuels.⁵ Loblolly pine (*Pinustaeda*) is one of the abundant softwood species in the southeastern United States and widely used in various industries.¹² Harvesting operations leave large amount of residues (e.g., stumps, limbs, tops and dead trees), which represent an important source of energy and chemicals.¹¹⁹ Pyrolysis has been reported as one of the economic ways (i.e., low capital and operating costs) to utilize biomass for bio-fuels and bio-chemicals.² The liquid products of pyrolysis of biomass known as pyrolysis oil however have several challenging properties including high oxygen and water content, high viscosity and acidity, poor volatility, corrosiveness, and aging problem.^{3, 13} Many researchers have investigated the aging process of pyrolysis oils. Some chemical and physical properties of pyrolysis oils have been examined during the aging process. It is well known that the viscosity of pyrolysis oils increases with storage of time, especially when the oils are stored or handled at high temperature.^{72, 95, 120-126} The average molecular weight of pyrolysis oils also increases

* The full data of this research was accepted for publication in ChemSusChem, 2012. It is entitled as “In situ NMR characterization of pyrolysis oil during accelerated aging”. The other author is Arthur J. Ragauskas from the Institute of Paper Science and Technology and School of Chemistry and Biochemistry at Georgia Institute of Technology. Reproduced by permission of John Wiley and Sons.

during the storage^{72, 95, 121, 123} and it has been indicated that the formation of larger molecules is one of the reason for the increasing viscosity of pyrolysis oils during the storage. Since the water content of the pyrolysis oils has been found to increase during the aging, it has been considered as one of the by-products of the aging process.^{72, 121, 122, 124-126} By using small-angle neutron scattering (SANS), pyrolysis oils have been shown to be nanostructured fluids, constituting a complex continuous phase and nanoparticles mainly formed by the association of units of pyrolytic lignin components from biomass. The aggregation of these units produces branched structures is reported to be responsible for the aging.¹²⁷ Compared to the well known properties include viscosity, water content and molecular weight of aged pyrolysis oils, only a few of researchers have characterized aged pyrolysis oils primarily by FT-IR and GC/MS to identify changes in chemical structures. By the use of FT-IR, esterification of pyrolysis oils has been proposed as one of the major reactions during the aging.¹²² Compare to freshly generated pyrolysis oil, the contents of hydroxyacetaldehyde,^{95, 124} furfurals¹²⁴ and guaiacols¹²⁴ in the aged pyrolysis oils have been detected to decrease by GC/MS.

To fully understand the fundamental chemistry of the aging process of pyrolysis oils, we investigated chemical structural changes by NMR. For the aged pyrolysis oils which have very high molecular weights (~500-1710 g/mol), the traditional analysis methods, such as FT-IR and GC/MS, could not provide the insight into the chemical structures.¹²⁸ In contrast, NMR has a much higher resolution and provides detailed structural information of pyrolysis products.^{9, 71, 90, 129} In addition, the heating function of the NMR equipment provides an opportunity for in situ characterization of pyrolysis oil dur-

ing the accelerated aging process. The general goal of this work was to examine the relationship between the structures of pyrolysis oil at various time points during the accelerated aging process (at 80 °C) by ^1H -NMR, ^{13}C -NMR and Heteronuclear Single-Quantum Correlation (HSQC) NMR.

6.2 Experimental Section

6.2.1 Chemicals and biomass

All reagents used in this study were purchased from VWR International or Sigma-Aldrich (St. Louis, MO) and used as received. Loblolly pine (*Pinustaeda*) residue was collected from a University of Georgia research plot in Macon, GA. Hybrid poplar (*populustrichocarpa x deltoides*) was obtained from Oak Ridge National Laboratory, Oak Ridge, TN.^{130, 131} The wood samples were refined with a Wiley mill through a 0.13 cm screen and dried under high vacuum at 50 °C for 48 h and stored at ~ 0 °C prior to use. Lignin was isolated from a commercial U.S.A. softwood kraft pulping liquor, following published method.^{9, 90}

6.2.2 Pyrolysis process and system

Please see section 3.2.3 of this dissertation for details.

6.2.3 In situ NMR characterization of pyrolysis oils during the accelerated aging process

All NMR spectral data reported in this study were recorded with a Bruker Avance/DMX 400 MHz NMR spectrometer. The pyrolysis oil produced from pine resi-

due at 600 °C was added into a 5 mm NMR tube with a 3 mm DMSO- d_6 insert tube for locking.

6.2.3.1 ^1H -NMR

Quantitative ^1H -NMR was acquired with 8 transients and 5 s pulse delay at 80 °C. The spectrum was recorded every 3 h. The data was carried out using MestReNova v7.1.0 software's default processing template with a line-broadening (LB) of 1.0 Hz and zero filling of 64 K. The phase and baseline are automatic corrected by MestReNova v7.1.0.

6.2.3.2 ^{13}C -NMR

Quantitative ^{13}C -NMR employing an inverse gated decoupling pulse sequence, 90° pulse angle, a pulse delay of 5 s at 80 °C and 632 scans.^{9,90} The spectrum was recorded every 3 h. The data was processed out using MestReNova v7.1.0 software's default processing template with a LB of 5.0 Hz and zero filling of 64 K. The phase and baseline are automatic corrected by MestReNova v7.1.0.

6.2.3.3 HSQC-NMR

HSQC-NMR were accomplished employing a standard Bruker pulse sequence “hsqcetgpsi.2” with a 90° pulse, 0.11 s acquisition time, a 1.5 s pulse delay, a $^1\text{J}_{\text{C-H}}$ of 145 Hz, 16 scans at 80 °C and acquisition of 1024 data points (for ^1H) and 256 increments (for ^{13}C). The ^1H and ^{13}C pulse widths are p1=11.30 μs and p3=10.00 μs , respectively. The ^1H and ^{13}C spectral widths are 13.02 ppm and 220.00 ppm, respectively. The spec-

trum was recorded every 3 h. HSQC data processing and plots were carried out using MestReNova v7.1.0 software's default processing template and automatic phase and baseline correction.

6.3 Results and discussions

^1H -NMR and ^{13}C -NMR assignment ranges and integration results for the pyrolysis oils produced from pine residue during the accelerated aging process at 80 °C are summarized in Tables 29 and 31. To facilitate the analysis, the integration results for each functional group versus time are summarized in Figures 38 and 39. To compare with the accelerated aging process, a one year room temperature (RT) aged pine residue pyrolysis oil also has been investigated and the NMR results shown in Tables 30 and 32. The ^1H -NMR integration results line plots show that the content of carbonyl and carboxyl protons slightly increases during accelerated aging process. Ortega et al.¹²⁵ indicated that the pH value of mixed hardwood pyrolysis oils decrease during the aging, which supports our results. The protons in the aliphatic groups also increase during the aging process, which indicates the formation of aliphatic functional groups. In contrast, the content of protons of aliphatic groups containing C-O bonds decrease during aging, which is evidence of the decomposition of ether and methoxyl groups. The content of aromatic protons also slightly decrease, which suggests that the aryl condensation reactions are also occurring during aging. For the RT aged pyrolysis oil, the same chemical trends have been found. Compare to the 60 h accelerated aged pyrolysis oil, the one year RT aged oil has a more serious aging phenomena.

To verify if these chemical trends during the aging process work for the other types of pyrolysis oil, the fresh and aged pyrolysis oils produced from two major biomass components—lignin and cellulose and a hardwood—poplar wood have also been investigated. The ^1H and ^{13}C -NMR results are shown in Tables 30 and 32. Compare to the cellulose and whole biomass pyrolysis oil, lignin pyrolysis oil has much more aromatic, carbonyl and carboxyl protons but relatively lower amount of protons in aliphatic groups containing C-O bonds. For the two types of aliphatic protons, lignin pyrolysis oil has a much higher aging rate than the cellulose pyrolysis oil. Therefore, for the whole biomass pyrolysis oils such as pine and poplar wood pyrolysis oils, the pyrolysis components may result from lignin in the whole biomass may have more responsibilities for the aging. Compare to the second 30 h accelerated aging process, there are relatively more differences between each types of protons at the first 30 h treatment which indicates the aging rate is not constant. Nolte et al.¹²³ found a similar phenomena of the viscosity changes of an oak pyrolysis oil during the accelerated aging process. For all the tested pyrolysis oils, the chemical trends in the aging process are the same which indicates similar aging mechanisms may be involved in all aging processes.

Table 29. ^1H -NMR chemical shift assignment ranges and functional group contributions for the pyrolysis oils produced from pine residue during the accelerated aging process at 80°C and aged at room temperature for one year.

Type of protons	Range ^[a] (ppm)	0 h	60 h	One year
$-\underline{\text{C}}\underline{\text{H}}\text{O}, -\text{COO}\underline{\text{H}}$	10-9.6	0.2	0.4	0.8
$\text{Ar}\underline{\text{H}}, \underline{\text{H}}\text{C}=\text{C}-$	8.2-6.0	12.0	11.2	10.8
$-\underline{\text{C}}\underline{\text{H}}_n\text{-O-}, \underline{\text{C}}\underline{\text{H}}_3\text{-O-}$	6.0-3.0	45.7	43.2	39.2
$-\underline{\text{C}}\underline{\text{H}}_3, -\underline{\text{C}}\underline{\text{H}}_n-$	0.5-3.0	42.1	45.2	49.2

[a] The assignment ranges are on the basis of literature reports.^{71, 81}

Table 30. Functional group contributions for the fresh and one year room temperature aged lignin and cellulose pyrolysis oils, and poplar pyrolysis oil after accelerated aging process at 80°C for 60 h, detected by ^1H -NMR.^[a]

Type of protons	Lignin		Cellulose		Poplar wood		
	Fresh	Aged	Fresh	Aged	0 h	30 h	60 h
$-\underline{\text{C}}\underline{\text{H}}\text{O}, -\text{COO}\underline{\text{H}}$	5.0	5.2	0.3	0.7	0.4	0.6	0.6
$\text{Ar}\underline{\text{H}}, \underline{\text{H}}\text{C}=\text{C}-$	29.2	27.1	2.3	1.5	11.2	10.5	10.0
$-\underline{\text{C}}\underline{\text{H}}_n\text{-O-}, \underline{\text{C}}\underline{\text{H}}_3\text{-O-}$	34.3	22.8	66.1	63.0	43.4	36.6	35.9
$-\underline{\text{C}}\underline{\text{H}}_3, -\underline{\text{C}}\underline{\text{H}}_n-$	31.5	44.9	31.3	34.8	45.0	52.3	53.5

[a] The assignment ranges are on the basis of literature reports.^{71, 81}

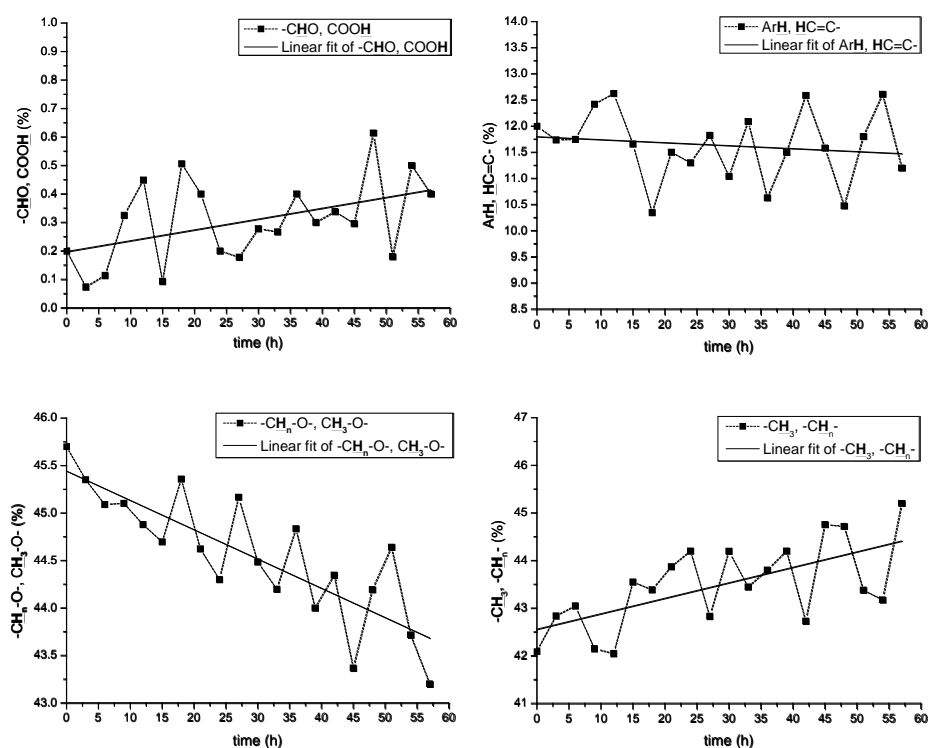


Figure 38. The ^1H -NMR integration results for each functional group in the pyrolysis oils produced from pine residue during the accelerated aging process at 80 °C.

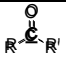
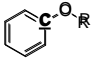
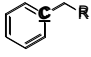
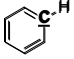
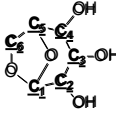
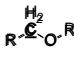
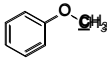
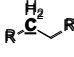
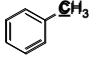
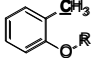
To fully characterize the changes of functional groups in the pyrolysis oils during accelerated aging at 80 °C, a detailed analysis of ten different types of carbons presented in the pyrolysis oils was accomplished using ^{13}C -NMR. Similarly with ^1H -NMR results, the contents of aromatic C-H bonds and aliphatic C-O bonds (including levoglucosan and methoxyl groups) decrease during the aging. Shen et al.⁵⁸ studied the mechanism for the thermal decomposition of cellulose and indicated that the anhydrosugars such as levoglucosan could further decompose to small molecule or furfural. Figure 40 shows the tentative chemical pathways for the decomposition. The condensation reactions between two aliphatic C-O bonds could also be completed by release of water,^{121, 122, 126} which will

produce an ether bond and lead to reduce the content of aliphatic C-O bonds. In contrast, the contents of aliphatic C-C bonds, aromatic C-O and C-C bonds increased during the aging process. The condensation reactions to form aromatic C-O and C-C bonds during the thermal treatment of lignin and lignin model compounds have been reported in the literature.^{51, 132} During the aging, such polymerization reactions could be initiated by organic peroxides presented in pyrolysis oils, which can spontaneously decompose, generating radicals.¹²¹ The possible reaction pathways are shown in Figure 40 and such type of condensation leads to reduce the contents of aromatic C-H bonds, which is supported by the ¹H and ¹³C-NMR. Other than radical initiated condensation, Binder et al.¹³³ reported an acid-catalyzed self-condensation of organosolv lignin and lignin model compounds in ionic liquid. The α -ethers in lignin could undergo acid-catalyzed elimination to form electrophilic methide intermediates. These can react with lignin nucleophiles to form condensed structures linked by carbon-carbon bonds. Brosse et al.¹³⁴ also proposed a cross linking reaction (see the Figure 40 for the detail) between formaldehyde which is the decomposed products of carbohydrates and aromatic C-H bonds during the thermal treatment of beech wood. Such cross linking reaction will form new aromatic C-C bonds and consume aromatic C-H bond and carbonyl groups. All the condensation reactions summarized in Figure 40 consume aliphatic C-O bonds, including levoglucosan and methoxyl groups, and form new aromatic C-C and C-O bonds, which is consistent with our NMR results. In addition, such condensation reactions also increase the molecular weight of the pyrolysis components, which could explain the well known aging phenomena – increasing average molecular weight of pyrolysis oil with the storage of time. For in-

stance, the molecular weight of poplar pyrolysis oil increased from 260 to 928 g/mol after 60 h accelerated aging at 80 °C.

Similarly with ^1H -NMR result, the one year RT aged pine wood pyrolysis oil shows more serious aging properties. Cellulose pyrolysis oil is relatively more stable than the lignin pyrolysis oil under the same aging condition, which may due to the less complexity, since about 50% of carbon signals came from levoglucosan. Compare to the pine, there are more methoxyl groups in the poplar pyrolysis oil which can be readily attributed to the fact that because the hardwood contains syringyl type lignin^{87, 135} which contains two methoxyl groups per benzene ring. For this pyrolysis oil, the differences between the fresh and aged oil are more significant than the one from pine wood. It has been reported^{115, 116} that methoxyl-aromatic bonds are one of the first groups to decompose during thermal treatment. Hence, the greater content of methoxyl groups in the poplar pyrolysis oil may initiate further aging reactions and cause more serious aging issues than pine wood pyrolysis oil. Consistent with ^1H -NMR results, the chemical trends in the aging process detected by ^{13}C -NMR are the same for all the tested pyrolysis oils.

Table 31. ^{13}C -NMR chemical shift assignment ranges and functional group contributions for the pyrolysis oils produced from pine residue during the accelerated aging process at 80 °C and aged at room temperature for one year. The results are shown as percentage of carbon.

Type of carbons	Range ^[a] (ppm)	Structure	0 h	60 h	One year
Carbonyl	215.0 – 166.5		7.1	6.8	6.0
Aromatic C-O	166.5 – 142.0		9.8	12.3	12.1
Aromatic C-C	142.0 – 125.0		12.0	12.3	12.9
Aromatic C-H	125.0 – 95.8		21.9	20.2	18.6
Levoglucozan	C1 102.3, C2 72.0		5.2	4.6	4.3
	C3 73.7, C4 71.7				
	C5 76.5, C6 64.9				
Aliphatic C-O	95.8 – 60.8		22.1	19.2	18.7
Methoxyl	60.8 – 55.2		3.1	2.7	2.2
Aliphatic C-C	55.2 – 0.0		24.0	26.5	29.5
Methyl – Aromatic	21.6 – 19.1		2.0	1.9	1.7
Methyl – Aromatic'	16.1 – 15.4		0.2	0.4	0.9

[a] The assignment ranges are on the basis of literature reports.^{71, 81}

Table 32. Functional group contributions for the fresh and one year room temperature aged lignin and cellulose pyrolysis oils and poplar pyrolysis oil after accelerated aging process at 80 °C for 60 h. Detected by ^{13}C -NMR and the results are shown as percentage of carbon.

[a]

Type of carbons	Lignin		Cellulose		Poplar wood		
	Fresh	Aged	Fresh	Aged	0 h	30 h	60 h
Carbonyl	2.6	1.0	3.0	2.4	7.3	6.9	6.9
Aromatic C-O	16.6	18.7	6.7	9.8	11.5	13.3	14.3
Aromatic C-C	17.2	21.5	0.3	0.5	12.6	13.5	14.3
Aromatic C-H	34.5	30.8	16.1	14.4	22.2	21.3	20.4
Levoglucozan	0.00	0.00	53.0	50.1	4.3	3.8	3.5
Aliphatic C-O	4.5	1.5	66.3	66.1	16.7	13.8	12.9
Methoxyl	6.4	5.3	1.9	1.1	6.3	5.4	4.6
Aliphatic C-C	18.2	21.2	5.7	5.7	23.4	25.8	26.6
Methyl – Aromatic	3.3	3.2	2.0	1.5	5.3	4.6	4.2
Methyl – Aromatic'	2.5	2.9	0.0	0.0	0.7	0.8	0.9

[a] The assignment ranges are on the basis of literature reports.^{71, 81}

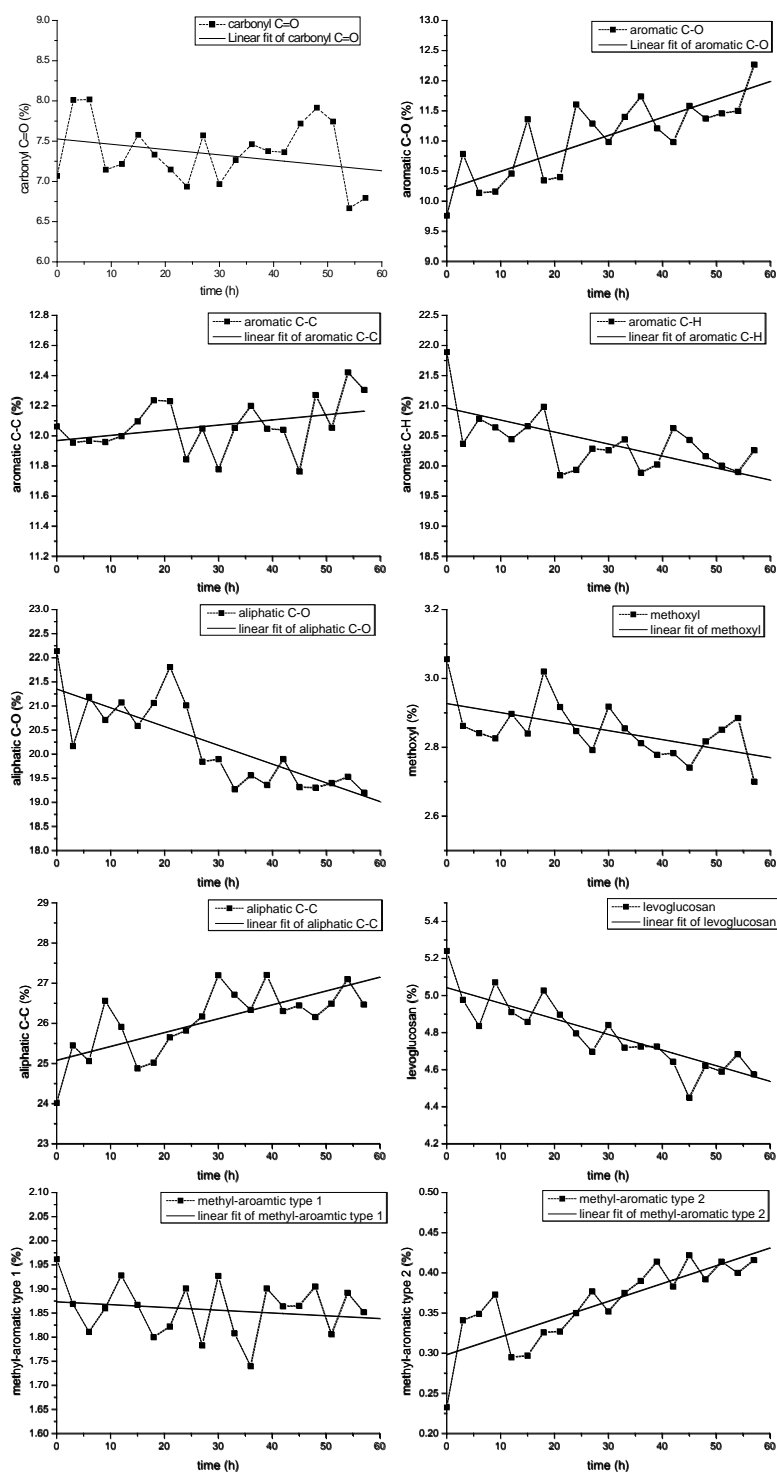


Figure 39. The ^{13}C -NMR integration results for each functional group in the pyrolysis oils produced from pine residue during the accelerated aging process at 80 °C.

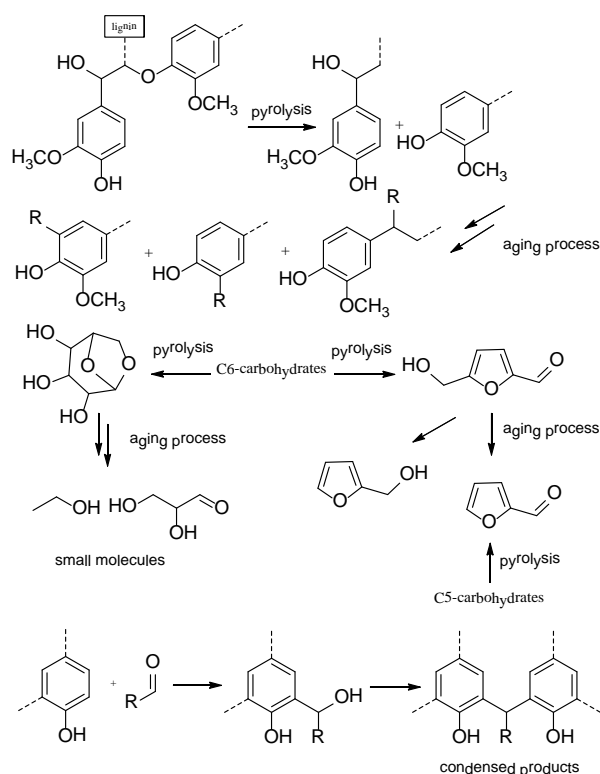


Figure 40. Tentative chemical pathways for the reactions occurred during the accelerated aging process of pine residue pyrolysis oil at 80 °C.^{9, 132-134}

Our previous research using HSQC-NMR to analyze the pyrolysis oil provided chemical-shift assignments of more than 20 different types of C-H bonds presented in the pyrolysis oils. Figures 41 to 44 show the HSQC analysis results for the native and the pyrolysis oil after 60 h accelerated aging process at 80 °C. Consistent with ¹H-NMR and ¹³C-NMR results, the contents of all types of aromatic C-H bonds and aliphatic C-O bonds decreased after 60 h accelerated aging process. Figure 41 shows the contents of the aromatic C-H bonds in the ortho and para position of a hydroxyl groups decreased more quickly than the aromatic C-H bonds in the meta position of a hydroxyl groups which indicates that the former two types of aromatic C-H bonds are more favored for the con-

condensation reactions and the possible reaction pathway shown in Figure 40 also supports this result. The native type of methoxyl groups (with a hydroxyl or methoxyl in the ortho position) also decomposes after aging process. Oasmaa et al.¹²⁴ reported that the guaiacol content in the forestry residue pyrolysis oil decrease during storage, which is consistent with our results.

Compared to the pine pyrolysis oil, there are significant amount of syringyl type products in the poplar pyrolysis oil which decrease during the aging process. The content of levoglucosan in the poplar pyrolysis oil decreases more dramatically than the pine wood pyrolysis oil, which indicates the pyrolysis oil produced from hardwood has a higher aging rate than the one from softwood.

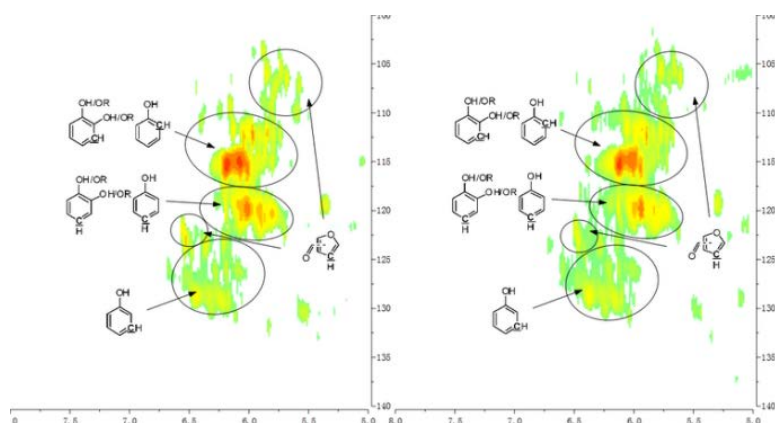


Figure 41. Aromatic C-H bonds in the HSQC spectra for the pyrolysis oils produced by pyrolysis of pine residue at 600 °C and aged at 80 °C for 0 h and 60 h (from left to right).

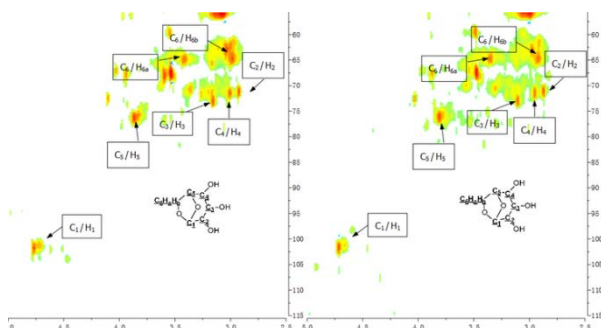


Figure 42. HSQC spectra and the assignments of each carbon in the levoglucosan presented in the pyrolysis oils produced by pyrolysis of pine residue at 600 °C and aged at 80 °C for 0 h and 60 h (from left to right).

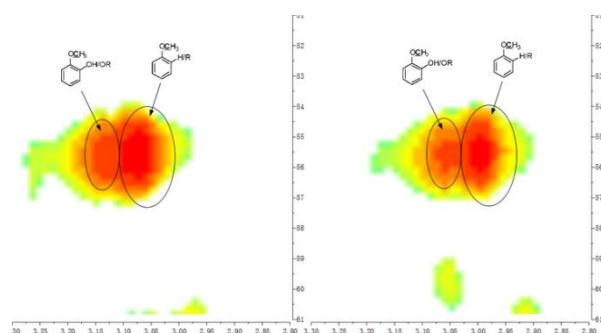


Figure 43. Methoxyl groups in the HSQC spectra for the pyrolysis oils produced by pyrolysis of pine residue at 600 °C and aged at 80 °C for 0 h and 60 h (from left to right).

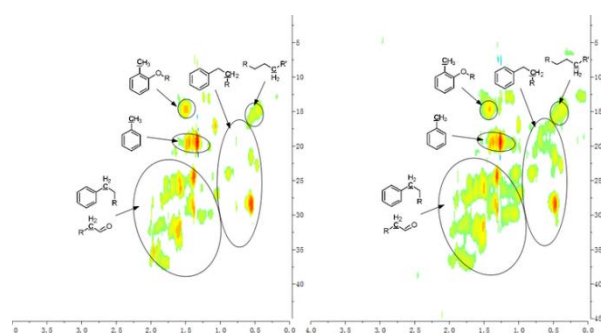


Figure 44. Aliphatic C-C bonds in the HSQC spectra for the pyrolysis oils produced by pyrolysis of pine residue at 600 °C and aged at 80 °C for 0 h and 60 h (from left to right).

6.4 Conclusion

In summary, in situ NMR characterization of pine residue pyrolysis oil using quantitative ^1H -NMR, ^{13}C -NMR and HSQC-NMR during the accelerated aging process (at 80°C) was examined. As far as we are aware, this is the first reported effort to investigate the chemical structural changes of pyrolysis oil components during the accelerated aging process by NMR analysis. The ^1H -NMR, ^{13}C -NMR and HSQC-NMR results indicate that the content of aliphatic C-O bonds, aromatic C-H bonds decrease during the aging process. In contrast, the contents of aliphatic C-C bonds, aromatic C-C and C-O bonds increase. The condensation reactions between two aliphatic C-O bonds could be completed by release of water, which will produce an ether bond and lead to reduce the content of aliphatic C-O bonds. The condensation reaction to form aromatic C-O and C-C bonds could be initiated by instable organic peroxides presented in pyrolysis oils, which can spontaneously decompose, generating radicals. The cross linking reaction between formaldehyde which is the decomposed products of carbohydrates and aromatic C-H bonds could also form new aromatic C-C bonds and consume aromatic C-H bond and carbonyl groups. The HSQC-NMR also shows that the contents of the aromatic C-H bonds in the ortho and para position of a hydroxyl groups decreased more quickly than the aromatic C-H bonds in the meta position of a hydroxyl groups which indicates that the former two types of aromatic C-H bonds are more favored for the condensation reactions. All of condensation reactions mentioned above consume aliphatic C-O bonds, including levoglucosan and methoxyl groups, and form new aromatic C-C and C-O bonds. In addition, such condensation reactions also increase the molecular weight of the pyrolysis components. The content of levoglucosan decrease during the aging indicates the

anhydrosugars such as levoglucosan could be further decomposed. These chemical trends also work for the other types of pyrolysis oil, such as the pyrolysis oils produced from two major biomass components—lignin and cellulose and a hardwood—poplar wood. In addition, these results suggest that the pyrolysis components result from lignin in the whole biomass may have more responsibilities for the aging effects. The hardwood pyrolysis oil has a higher aging rate than the softwood pyrolysis oil, which may due to the syringyl type products in the hardwood pyrolysis oil. To Nevertheless, the concept established in this work opens up a new opportunity for the investigation of chemical structural changes of pyrolysis oil during the aging process, which will provide insight into the mechanism of aging process. These results will be of value in the development of tailored catalyst to upgrade pyrolysis oil to thermal stable green fuels.

Chapter 7: PYROLYSIS OF KRAFT LIGNIN WITH ADDITIVES*

7.1 Introduction

The pyrolysis of lignin, including kraft lignin, is a promising approach to utilize this resource for fuels and chemicals. The product of pyrolysis of lignin, known as bio-oil, however, has several challenging properties including a mixture of compounds with a high oxygen content, poor volatility, high acidity and viscosity,³ which significantly limits its usage as a fuel.

Many researchers have examined use additives including, zeolite and metal salts to upgrade the properties of bio-oil during the pyrolysis of lignin. For example, Mullen et al.³⁸ used analytical pyrolysis methods (Py-GC-MS) to pyrolyze four different lignins at 650 °C with 1/1 or 3/1 ($W_{\text{additive}}/W_{\text{lignin}}$) H-ZSM-5 zeolite and CoO/MoO₃. They suggested that H-ZSM-5 zeolite could improve the depolymerization of lignin and CoO/MoO₃ facilitated the production of aromatic hydrocarbons through a direct deoxygenation of methoxyphenol units. Zhao et al.¹³⁶ upgraded the water-insoluble fraction (pyrolytic lignin) from pyrolysis oil of rice husk, with several additives, including H-ZSM-5, MCM-41, SBA-15 and β -zeolite from 500 to 800 °C. They found that compared to the results of pyrolysis without catalyst, most of oxygenates are converted to arenes and polycyclic aromatic hydrocarbons over zeolites and indicated

* The full data of this research was accepted for publication in Energy and Fuels, 2011. It is entitled as "Pyrolysis of kraft lignin with additives". The other author is Arthur J. Ragauskas from the Institute of Paper Science and Technology and School of Chemistry and Biochemistry at Georgia Institute of Technology. Reprinted with permission from "Ben, H.; Ragauskas, A. J., Pyrolysis of Kraft Lignin with Additives. *Energy Fuels* **2011**, 25, (10), 4662-4668." Copyright 2011 American Chemical Society.

that this conversion was favored at higher temperatures. French et al.¹³⁷ used molecular-beam mass spectrometry (MBMS) to analyze the product vapor from pyrolysis of cellulose, straw lignin and ground aspen wood with forty different additives at 400, 500 and 600 °C. They found that the highest yield of hydrocarbons (~16 wt. %) was achieved using nickel, cobalt, iron, and gallium-substituted ZSM-5 zeolite during the pyrolysis. Consistent with the results of Zhao et al.¹³⁶, they also suggested that the zeolites could improve deoxygenation reactions during pyrolysis, in addition, they also indicated that the best-performing catalysts belonged to ZSM-5 zeolite while larger-pore zeolites showed less deoxygenation activity. Jackson et al.¹³⁸ used sand, H-ZSM-5 zeolite, K-ZSM-5 zeolite, Al-MCM-41, solid phosphoric acid and Co/Mo/Al₂O₃ as additives in the pyrolysis of lignin at 600 °C and analyzed the gas and liquid product by GC-MS. They found that H-ZSM-5 zeolite almost completely deoxygenated the liquid phase producing simple aromatics and naphthalenics.

In addition, many researchers have examined the use additives for the pyrolysis of biomass. Aho et al.¹³⁹ used H-Y, H-Beta, H-ZSM-5 and mordenite zeolites as additives to pyrolyze pine wood at 450 °C. They concluded that the yield of the pyrolysis product was only slightly influenced by the different structures of the zeolite. However, the chemical components of bio-oil were dependent on the structures of zeolite, such that, the content of ketones was higher and the amount of acids and alcohols was lower in the bio-oil when ZSM-5 was used as an additive during the pyrolysis. Zhang et al.¹⁴⁰ studied the effects of the flow rate of the carrier gas, temperature and the particle size for the pyrolysis of corncob with H-ZSM-5 zeolite monitoring bio-oil composition and gas yield.

They concluded that the optimal bio-oil yield was 56.8 wt. % and the use of H-ZSM-5 zeolite caused a marked decrease of the heavy oil fraction and an increase in water and gas yields. They also indicated that the use of H-ZSM-5 zeolite with pyrolysis of corncob the contents of aromatic hydrocarbons in the bio-oil increased eight-fold whereas the oxygen content of the bio-oil decrease by 25%. Pan et al.¹⁴¹ pyrolyzed *Nannochloropsis* *sp.* microalga residue with different amounts of H-ZSM-5 zeolites at 300, 350, 400, 450, and 500 °C. They found that the optimal conditions for pyrolysis oil yield (~45 wt. %) occurred with a pyrolysis temperature of 400 °C and an additive-to-material ratio of 1:1. They also indicated that the use of zeolite during pyrolysis yielded a bio-oil that had a lower oxygen content, higher heating value and a higher content of aromatic hydrocarbons. The pyrolysis of several biomasses such as, corn stalks,¹⁴² cassava rhizome,^{143, 144} hybrid poplar wood,¹⁴⁵ rice husks,¹⁴⁶ and pine^{147, 148} with ZSM-5 zeolites have also been studied in recent years. All of these studies reported that zeolites when mixed with biomass during pyrolysis resulted in a pyrolysis oil with less oxygen content.

Most of the reported additives studies have focused on the pyrolysis of biomass¹³⁹⁻¹⁴⁸ while only a few have examined the behavior of lignin in the presence of additives during pyrolysis.^{38, 137, 138} Compare to the limited ability of GC-MS¹²⁸ to analyze the chemical complexity of bio-oil, NMR analysis provides detailed structural information of the total pyrolysis oil^{9, 81, 83-85, 149-151} and the starting lignin.^{152, 153}

Our previous work⁹ focused on the relationship between the structure of pyrolysis oil and the temperature of pyrolysis. The general goal of this work is to examine the

efforts of zeolites and nickel salts as pyrolysis additives for kraft softwood lignin by determining the chemical structural features of the resulting bio-oils by NMR and GPC analysis.

7.2 Experimental section

Please see the sections 3.1; 3.2.1; 3.2.2; 3.2.3; 3.2.3.1; 3.3.3-4 of this dissertation for the details.

7.3 Results and Discussion

To reduce the variation in the procedure and from the analysis, all the data shown in this study are the average of duplicated experiments.

7.3.1 Yields of pyrolysis products

Our previous pyrolysis studies of softwood kraft lignin in the temperature range of 400 - 700 °C indicated that 700 °C was the point of primary decomposition of lignin and the secondary decomposition of pyrolysis oil.⁹ In this study, 700 °C was used as the pyrolysis temperature to avoid the bulk secondary pyrolysis reactions. The yields from pyrolyzing a softwood kraft lignin with different additives at 700 °C with a heating rate of ~2.7 °C /s are summarized in Figure 45 and these results indicate that the yields of gas and total pyrolysis oil were influenced by the additives. The char content was comparable for the control and additive studies, which suggests that the additives have very limited effects on the primary decomposition of lignin. In contrast, the yield of total pyrolysis oil and heavy oil decreased after the use of NiCl₂ and H-ZSM-5 as the additives. Correspon-

dingly, the yield of light oil and gas increased with used those additives. These results suggest that NiCl_2 and H-ZSM-5 enhances the secondary reactions of pyrolysis heavy oil to the light oil or gas.

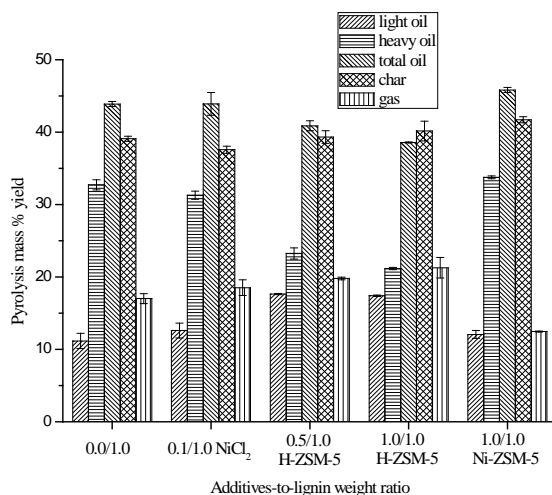


Figure 45. Yields of light oil, heavy oil, char and gas for the pyrolysis of pure SW kraft lignin and pyrolysis of SW kraft lignin with 0.1/1.0 ($W_{\text{additive}}/W_{\text{lignin}}$) of NiCl_2 , 0.5/1.0 ($W_{\text{additive}}/W_{\text{lignin}}$) of H-ZSM-5 zeolite, 1.0/1.0 ($W_{\text{additive}}/W_{\text{lignin}}$) of H-ZSM-5 zeolite and 1.0/1.0 ($W_{\text{additive}}/W_{\text{lignin}}$) of Ni-ZSM-5 zeolite as additives at 700 °C for 10 min.

7.3.2 Quantitative ^{31}P -NMR analysis of pyrolysis oils

Phosphitylation of hydroxyl groups using 2-chloro-4, 4, 5, 5-tetramethyl-1, 3, 2-dioxaphospholane (TMDP) has been developed to quantitatively determine hydroxyl functional groups in various substrates including coal pyrolysis condensates,¹⁰⁶ lignin,¹⁵²⁻¹⁵⁴ bio-oil from pyrolysis of biomass^{9, 155} and coal extracts.¹⁰⁶ The ^{31}P -NMR chemical shifts and integration regions of the phosphitylated aryl/alkyl hydroxyl groups and water with TMDP are summarized in Table 33 following literature methods.⁹

Table 33. Chemical shifts and integration regions for pyrolysis oil and lignin derivatized with TMDP in a quantitative ^{31}P -NMR.

Functional group		Integration region (ppm)
endo-N-hydroxy-5-norbornene-2,3-dicarboximide (NHND, internal standard)		151.0 - 152.8
Aliphatic OH		150.0 - 145.5
C ₅ Substituted guaiacyl phenolic OH	β -5	144.7 - 142.8
	4-O-5	142.8 - 141.7
	5-5	141.7 - 140.2
Guaiacyl phenolic OH		140.2 - 139.0
Catechol type OH		139.0 - 138.2
<i>p</i> -hydroxy-phenyl OH		138.2 - 137.3
Carboxylic acid-OH		136.6 - 133.6
Water		133.1-131.3,16.9-15.1

Typical ^{31}P -NMR spectra data for the heavy oils produced by the pyrolysis of SW kraft lignin and pyrolysis with Ni-ZSM-5 are shown in Figure 46 and the integration results for the heavy oils are summarized in Figure 47. The use of H-ZSM-5 zeolite as an additive for pyrolysis yielded heavy oils with less aliphatic hydroxyl groups and carboxyl acid groups than the control. The elimination of aliphatic hydroxyl and acid groups is almost complete indicating the loss of these groups was enhanced in the presence of H-ZSM-5 zeolite during the thermal treatment. Figure 48 highlights potential decomposition pathways of ether bonds in lignin during the pyrolysis. The heavy oil generated from

lignin in the presence of zeolite contained less guaiacyl, catechol type hydroxyl groups and more p-hydroxy-phenyl hydroxyl groups. Based on the proposed pathways, those changes of phenolic hydroxyl groups indicate that the conversion of ether bonds to the p-hydroxy-phenyl hydroxyl groups was enhanced in the presence of H-ZSM-5 zeolite during the thermal treatment. For the three pyrolysis samples with zeolite as the additive, the pyrolysis trial with 1.0/1.0 ($W_{\text{H-ZSM-5}}/W_{\text{lignin}}$) zeolite performed better upgrading effects than the other two.

The use of NiCl_2 as an additive for pyrolysis yielded heavy oils with less, guaiacyl, catechol type and p-hydroxy-phenyl hydroxyl groups. Zou et al.¹⁵⁶ has reported a similar results that after the use of NiCl_2 as additive during the pyrolysis of coal the pyrolysis oil contains less phenols.

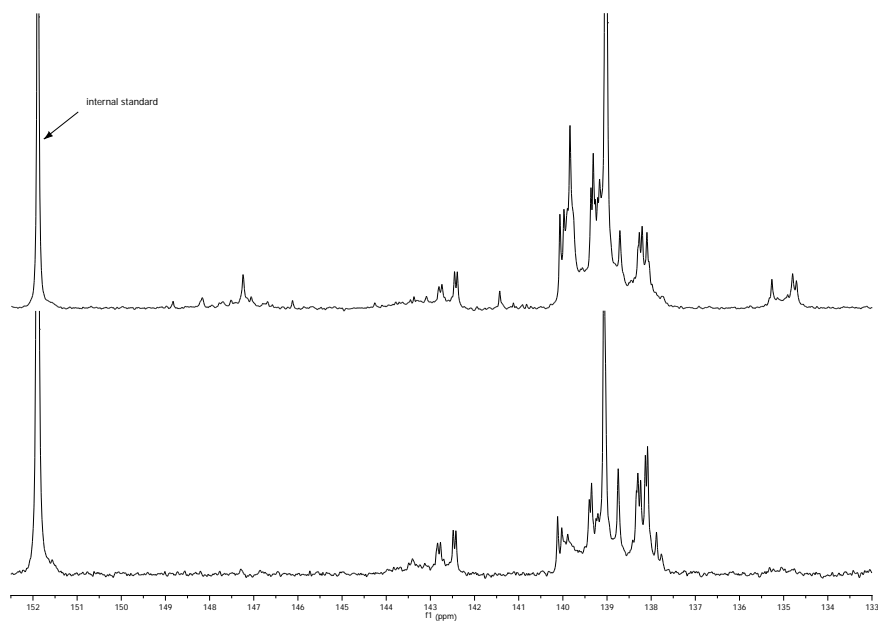


Figure 46. ^{31}P -NMR spectra for the heavy oils produced by pyrolysis of SW kraft lignin (top) and pyrolysis of SW kraft lignin with Ni-ZSM-5 as the additive (bottom) at 700 °C for 10 min, derivatized with TMDP.

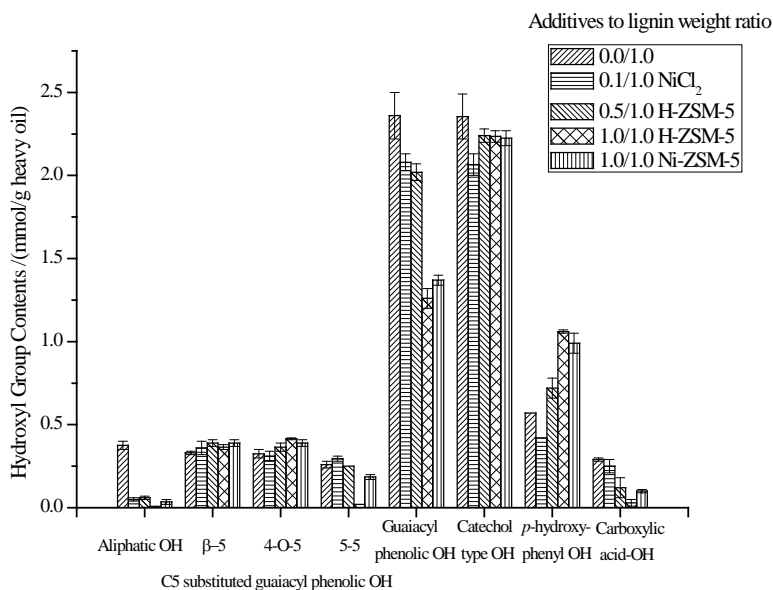


Figure 47. Hydroxyl group contents of different heavy oils produced by pyrolysis of pure SW kraft lignin and pyrolysis of SW kraft lignin with 0.1/1.0 ($W_{\text{additive}}/W_{\text{lignin}}$) of NiCl_2 , 0.5/1.0 ($W_{\text{additive}}/W_{\text{lignin}}$) of H-ZSM-5 zeolite, 1.0/1.0 ($W_{\text{additive}}/W_{\text{lignin}}$) of H-ZSM-5 zeolite and 1.0/1.0 ($W_{\text{additive}}/W_{\text{lignin}}$) of Ni-ZSM-5 zeolite as additives at 700 °C for 10 min, determined by quantitative ^{31}P -NMR after derivatization with TMDP.

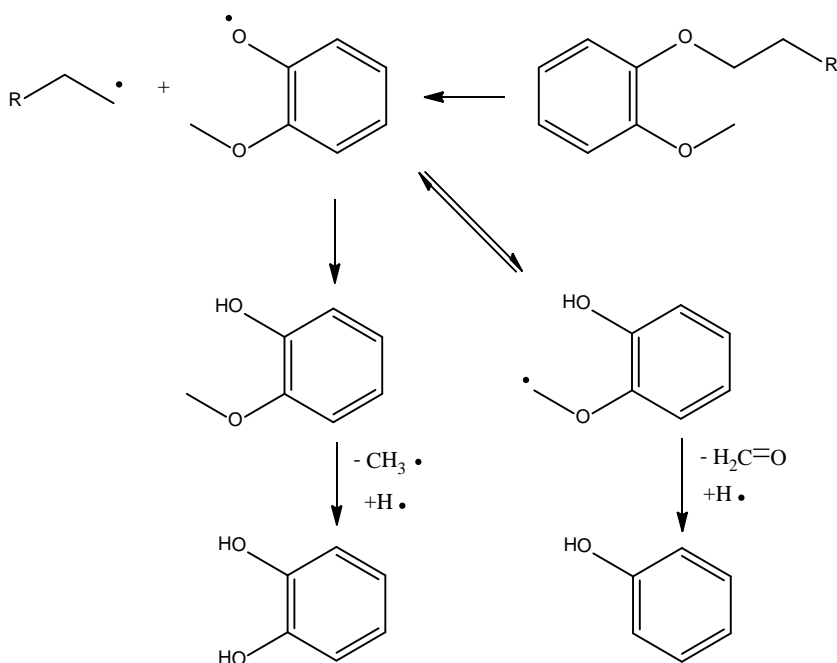


Figure 48. The possible decomposition pathways of ether bond in lignin during the pyrolysis.⁹

In contrast with the heavy oils, the ^{31}P -NMR data from the light oils exhibited fewer signals that were readily identified. These samples contained more than 80 w/w% of water and less than 10 w/w% of three other components as summarized in Figure 49. Based on the chemical shift data in the literature^{106, 109} and our previous work⁹ the three peaks were assigned to methanol (δ 147.9 ppm), catechol (δ 138.9 ppm) and acetic acid (δ 134.6 ppm). The yield of methanol, acetic acid and catechol in the light oil significantly decreased when zeolite was used as an additive during pyrolysis which is similar to the results observed in the heavy oil analysis. In contrast, the concentration of water in light oil increased, which is further evidence for the improved dehydration by the zeolite during the pyrolysis. For the three pyrolysis samples with zeolite as the additive, the light oil produced with 1.0/1.0 ($W_{\text{Ni-ZSM-5}}/W_{\text{lignin}}$) zeolite contains less catechol and acetic acid

but more water than the other two.

The concentration of water in light oil increased when NiCl_2 was used as an additive, which indicates that NiCl_2 could improve the dehydration reaction during the pyrolysis. Bru et al.¹⁵⁷ used $\text{Ni}(\text{NO}_3)_2$ as an additive during the pyrolysis of oak sawdust, and they indicated that the use of the nickel salt increased the water content of pyrolysis oil which is consistent with results in this study.

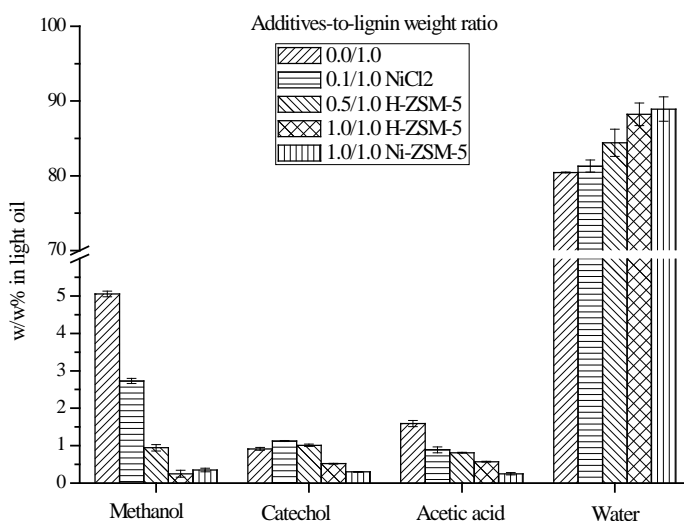


Figure 49. Weight percentage of four major components in light oils produced by pyrolysis of pure SW kraft lignin and pyrolysis of SW kraft lignin with 0.1/1.0 ($W_{\text{additive}}/W_{\text{lignin}}$) of NiCl_2 , 0.5/1.0 ($W_{\text{additive}}/W_{\text{lignin}}$) of H-ZSM-5 zeolite, 1.0/1.0 ($W_{\text{additive}}/W_{\text{lignin}}$) of H-ZSM-5 zeolite and 1.0/1.0 ($W_{\text{additive}}/W_{\text{lignin}}$) of Ni-ZSM-5 zeolite as additives at 700 °C for 10 min, determined by quantitative ^{31}P -NMR after derivatization with TMDP.

7.3.3 Quantitative ^{13}C -NMR analysis of pyrolysis oils

To fully characterize the functional groups in the heavy oils, a detailed analysis of these products was accomplished using ^{13}C -NMR. To help facilitate this analysis, a chemical shift database of compounds reported to be present in pyrolysis oils was employed for data analysis⁹ and this analysis is summarized in Table 34.

Table 34. ^{13}C -NMR chemical shift assignment range of lignin pyrolysis oil based on the chemical shift database created in our previous work.⁹

Functional group	Integration region (ppm)
Carbonyl or Carboxyl bond	215.0 – 166.5
Aromatic C-O bond	166.5 – 142.0
Aromatic C-C bond	142.0 – 125.0
Aromatic C-H bond	125.0 – 95.8
Aliphatic C-O bond	95.8 – 60.8
Methoxyl-Aromatic bond	60.8 – 55.2
General	55.2 – 0.0
Methyl – Aromatic ($\text{CH}_3\text{-Ar}$)	21.6 – 19.1
Aliphatic C-C bond	Methyl – Aromatic at ortho position of a hydroxyl or methoxyl group ($\text{CH}_3\text{-Ar'}$)
	16.1 – 15.4

Typical ^{13}C -NMR spectra for the heavy oils produced by pyrolysis of SW kraft lignin and pyrolysis of SW kraft lignin with Ni-ZSM-5 are shown in Figure 50. The integration results of this analysis for the heavy oils are summarized in Figure 51. This data shows that the carbonyl groups and the aliphatic C-O bonds are completely decomposed in the heavy oil and compared to the lignin ~80% of methoxyl groups are eliminated after pyrolysis with zeolite as an additive. The percentage of aromatic ether substituted carbons in the heavy oil decreased and aromatic C-C bonds increased upon the use of a zeolite, which indicates that the zeolite improves the cleavage of ether bonds in lignin. Therefore, it was concluded that ZSM-5 zeolite could improve the decomposition of most oxygen substituents including aliphatic hydroxyl groups, carboxyl groups, aromatic-methoxyl bonds and the ether bonds in the lignin (see Figure 52) during the pyrolysis, which indicates that the heavy oil contains relatively less oxygen after the use of zeolite. In addition, there were less aliphatic C-C bonds in the heavy oils generated from lignin in the presence of zeolite. In contrast, methyl-aromatic C-C bonds have been formed during the pyrolysis and the content increased after pyrolysis with zeolite as an additive. For two zeolite assisted pyrolysis experiments reported in this study, H-ZSM-5 performed better than the Ni-ZSM-5 zeolite at deoxygenation.

The use of NiCl_2 as an additive for pyrolysis yielded heavy oils with more aromatic carbons and less aliphatic carbons, including methyl-aromatic C-C bonds. Zou et al.¹⁵⁶ has reported a similar result with the use of NiCl_2 as additive during the pyrolysis of coal yielding an oil that contained less aliphatic hydrocarbons.

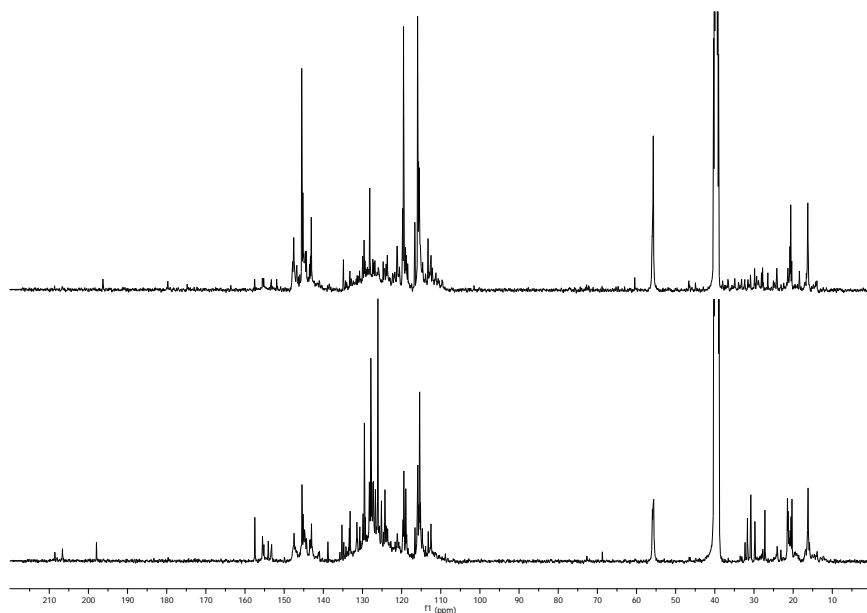


Figure 50. Quantitative ^{13}C -NMR spectra for the heavy oil produced by pyrolysis of SW kraft lignin (top) and pyrolysis of SW kraft lignin with Ni-ZSM-5 as the additive (bottom) at 700 °C for 10 min.

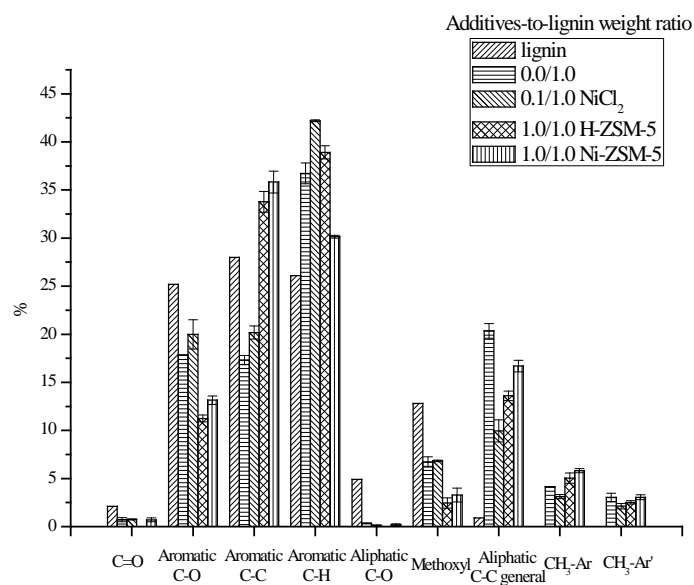


Figure 51. Integration results for the SW kraft lignin and the heavy oils produced by pyrolysis of pure SW kraft lignin and pyrolysis of SW kraft lignin with 0.1/1.0 ($W_{\text{addi-}}$

tive/ W_{lignin}) of NiCl_2 , 1.0/1.0 ($W_{\text{additive}}/W_{\text{lignin}}$) of H-ZSM-5 zeolite and 1.0/1.0 ($W_{\text{additive}}/W_{\text{lignin}}$) of Ni-ZSM-5 zeolite as additives at 700 °C for 10min, detected by quantitative ^{13}C -NMR with using the assignment range showed in Table 34. The results were shown as the percentage of carbon.

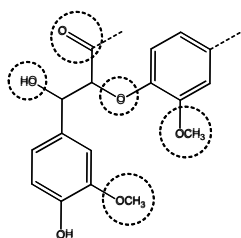


Figure 52. The primary decomposed functional groups in lignin during the pyrolysis.⁹

7.3.4 GPC analysis of pyrolysis oils

Along with characterizing the functional groups present in pyrolysis oil, another key biofuel parameter is the molecular weight profiles. The number average and weight average molecular weights (M_n and M_w) and polydispersity values for the heavy oils produced by pyrolysis of softwood kraft lignin produced with and without different additives at 700 °C are summarized in Figure 53. This analysis indicates a slight decrease in the molecular weight of the heavy oil after the use of H-ZSM-5 zeolite. Williams et al.¹⁴⁶ has reported a similar result of the bio-oil produced from pyrolysis of rice husks with H-ZSM-5 zeolite. In contrast, the molecular weight of heavy oil increased after the use of NiCl_2 as an additive. The polydispersity values of the heavy oils increase after pyrolysis

of lignin with additives, which is another evidence for the enhanced secondary decomposition of pyrolysis oils.

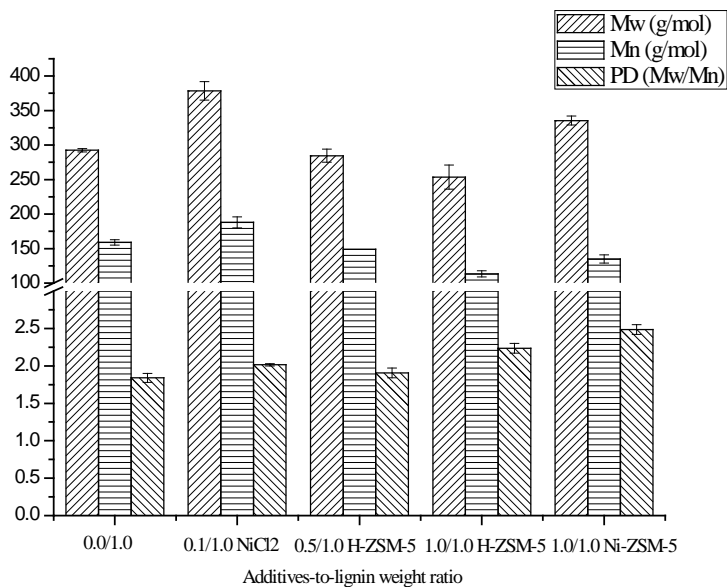


Figure 53. Molecular weight distribution and polydispersity of heavy oils produced by pyrolysis of pure SW kraft lignin and pyrolysis of SW kraft lignin with 0.1/1.0 ($W_{\text{additive}}/W_{\text{lignin}}$) of NiCl₂, 0.5/1.0 ($W_{\text{additive}}/W_{\text{lignin}}$) of H-ZSM-5 zeolite, 1.0/1.0 ($W_{\text{additive}}/W_{\text{lignin}}$) of H-ZSM-5 zeolite and 1.0/1.0 ($W_{\text{additive}}/W_{\text{lignin}}$) of Ni-ZSM-5 zeolite as additives at 700 °C for 10 min.

7.4 Conclusion

The pyrolysis of softwood kraft lignin with NiCl₂, H-ZSM-5 and Ni-ZSM-5 zeolite as the additives was accomplished at 700 °C. The yields of pyrolysis products indicated that the use of NiCl₂ and H-ZSM-5 reduced the mass yield of pyrolysis oil and increased the yield of gas. In contrast, the char content was almost the same after the use of the additives, which suggests that those two additives have very limited effects on the

primary decomposition of lignin, but could improve the secondary reactions of pyrolysis oil. The ^{31}P -NMR results for the light oil showed that after the use of zeolite, the concentration of water in light oil increased, which is the evidence for the improved dehydration by the zeolite during the pyrolysis. In contrast, the yields of methanol and acetic acid in the light oil decreased, which indicate that zeolite could improve the decomposition of the aliphatic OH and carboxyl group in the lignin during the pyrolysis. The results of ^{13}C and ^{31}P -NMR for the heavy oils indicated that the carbonyl groups and the aliphatic C-O bonds are almost completely decomposed, and compare to the lignin, about 80% of methoxyl groups are eliminated after pyrolysis with H-ZSM-5 zeolite as the additive. Therefore, it could be concluded that zeolite could improve the decomposition of all the primary decomposed functional groups during the pyrolysis. Further, the results of ^{13}C -NMR indicated that after the use of H-ZSM-5 zeolite, the heavy oil has a relatively lower oxygen content, which indicates that H-ZSM-5 could also improve the deoxygenation during the pyrolysis of lignin. The results of GPC analysis of the pyrolysis oil from SW kraft lignin accomplished in the presence of H-ZSM-5 zeolite had a lower molecular weight than the control pyrolysis experiment accomplished with no zeolite.

In summary, the detailed characterization of this pyrolysis oil indicates the use of zeolite as the additive during the pyrolysis of lignin could provide a bio-oil has less acidity, relatively lower oxygen content and lower molecular weight, which makes bio-oil more suitable for the green fuel.

Chapter 8: THE INFLUENCE OF SI/AL RATIO OF ZSM-5 ZEOLITE ON THE PROPERTIES OF LIGNIN PYROLYSIS PRODUCTS*

8.1 Introduction

The use of biomass for renewable energy production is increasingly being viewed as a promising alternative method to reduce net carbon dioxide emissions and gain long term energy security.⁵ Among the various conversion technologies being investigated, pyrolysis has been reported as one of the economic ways (i.e., low capital and operating costs) to utilize biomass for bio-fuels and bio-chemicals.² Lignin is the second most abundant biomass component and the primary renewable aromatic resource in nature, lignin, however, it has received much less attention than plant polysaccharides as a resource for biofuels. Kraft lignin obtained by precipitation from the cooking liquor of the kraft pulping process is abundant and has been used as a low-value material.^{101, 158} The major drawback towards commercialization of pyrolysis oils are several challenging properties including poor volatility, high oxygen content, acidity and viscosity, corrosiveness and cold flow problems.³ Therefore, upgrading technologies that convert bio-oils to a potential substitution of diesel and gasoline fuels are necessary. Among these technologies, in situ upgrading pyrolysis oil during the pyrolysis process appears to be pragmatic.¹³

* The full data of this research was accepted for publication in ACS Sustainable Chemistry & Engineering, 2012. It is entitled as “The influence of Si/Al ratio of ZSM-5 zeolite on the properties of lignin pyrolysis products”. The other author is Arthur J. Ragauskas from the Institute of Paper Science and Technology and School of Chemistry and Biochemistry at Georgia Institute of Technology. The copyright permissions will be submitted to the thesis office of Gatech.

Many researchers have used zeolites to upgrade the properties of pyrolysis oil during the pyrolysis process. For example, Mullen et al.³⁸ used analytical pyrolysis methods (Py-GC-MS) to pyrolyze four different lignins at 650 °C and they indicated that H-ZSM-5 zeolite could improve the depolymerization of lignins. French et al.¹³⁷ used molecular-beam mass spectrometry (MBMS) to analyze the product vapors from pyrolysis of cellulose, straw lignin and ground aspen wood with forty different additives at 400, 500 and 600 °C. They found that the highest yield of hydrocarbons (~16 wt. %) was achieved using nickel, cobalt, iron, and gallium-substituted ZSM-5 zeolite during the pyrolysis. Consistent with the results of Mullen et al.³⁸ and Zhao et al.,¹³⁶ they suggested that the zeolites could improve deoxygenation reactions during pyrolysis, in addition, they also indicated that the best-performing catalysts belonged to ZSM-5 zeolites. Jackson et al.¹³⁸ used sand, H-ZSM-5 and K-ZSM-5 zeolite as additives during the pyrolysis of lignin at 600 °C and analyzed the gas and liquid products by GC-MS. They found that H-ZSM-5 zeolite almost completely deoxygenated the liquid phase producing simple aromatics and naphthalenics. The pyrolysis of several biomasses such as, corn stalks,^{140, 142} cassava rhizome,^{143, 144} hybrid poplar wood,¹⁴⁵ rice husks,¹⁴⁶ and pine wood^{139, 147, 148} with ZSM-5 zeolites have also been studied in recent years. All of these studies indicated that the use of zeolite during pyrolysis yielded a bio-oil that had lower oxygen content. Most of the researchers have focused on the pyrolysis of biomass¹³⁹⁻¹⁴⁸ while only a few have examined the behavior of lignin in the presence of additives during pyrolysis.^{38, 137} Different Si/Al ratios of zeolite have been shown to affect the cracking reactions of model compounds during thermal treatment.¹⁵⁹⁻¹⁶⁵ However, only a few researchers have investigated the influence of different Si/Al ratios of zeolite on the

properties of pyrolysis products. For example, Aho et al.¹⁶⁶ pyrolyzed pine wood with various H-Beta zeolites and they indicated that zeolites with lower Si/Al ratios formed less organic oil, more water and polyaromatic hydrocarbons.

Our previous work⁹⁰ investigated the efforts of zeolites and nickel salt as pyrolysis additives for softwood kraft lignin and found that H-ZSM-5 zeolite was shown to improve the decomposition of aliphatic hydroxyl, carboxyl and methoxyl groups and ether bonds in the lignin during the pyrolysis. To avoid the limitation of several analysis methods such as GC-MS and FT-IR for pyrolysis oils, we introduced the use of Nuclear Magnetic Resonance (NMR) including ¹H, ¹³C, ³¹P and Heteronuclear Single-Quantum Correlation (HSQC)-NMR to characterize various pyrolysis oils.^{9, 10, 71} The general goal of this work was to examine the influence of Si/Al ratio of zeolite on the properties of pyrolysis products. This was accomplished by using NMR and GPC to analyze the liquid products of pyrolysis of a softwood kraft lignin with different ZSM-5 zeolite as the additives. One of our related works about investigating the influence of different frameworks of zeolites with similar Si/Al ratio has been accepted by RSC Advances.¹⁶⁷

8.2 Materials and Methods

All reagents used in this study were purchased from VWR International or Sigma-Aldrich (St. Louis, MO) and used as received. Lignin was isolated from a commercial U.S.A. softwood kraft pulping liquor. ZSM-5 (CBV 2314, CBV 3020E, CBV 5524G, CBV 8014 and CBV 28014) zeolites were purchased from Zeolyst, Inc.

8.2.1 Lignin separation and purification

Please see section 3.2.1.1 of this dissertation for the details.

8.2.2 Preparation of pyrolysis sample

Different ZSM-5 (CBV 2314, CBV 3020E, CBV 5524G, CBV 8014 and CBV 28014) zeolites were used as additives in this work. The pyrolysis samples were mechanical stirred with a 1:1 mass ratio of lignin to zeolite. All the zeolites were pre-activated in a pyrolysis tube at 500 °C under nitrogen for 6 h. The detailed information of each zeolite can be found in Table 35.

Table 35. SiO₂/Al₂O₃ mole ratio and code name used in this work of each zeolite.

	CBV	CBV	CBV	CBV	CBV
	2314	3020E	5524G	8014	28014
SiO ₂ /Al ₂ O ₃ mole ratio	23	30	50	80	280
Code name	Z23	Z30	Z50	Z80	Z280

8.2.3 Equipment and process of pyrolysis

Please see section 3.2.3.1 of this dissertation for the details.

8.2.4 Characterization of pyrolysis oils

Please see sections 3.3.1-2; 3.3.4-7 for the details.

8.3 Results and Discussion

8.3.1 Yields of pyrolysis products

The HHV, and energy, carbon and mass yields from pyrolyzing a softwood kraft lignin with different ZSM-5 zeolites at 600 °C are summarized in Table 36. These results indicate that the yields of char slightly increased after the use of additives and the char yield is almost constant for all zeolites which suggest that the additives have very limited effects on the primary decomposition of lignin. In contrast, the yield of heavy oil decreased after the use zeolite. Correspondingly, the yield of light oil and gas increased with used zeolites. In addition, pyrolysis samples with lower Si/Al ratio zeolites formed relatively less heavy oil but more light oil. Our previous work indicated that light oil contains ~70-90 wt% of water and another 10 wt% of methanol, catechol and acetic acid.^{9, 90} Aho et al.¹⁶⁶ pyrolyzed pine wood with various H-Beta zeolites and they indicated that zeolites with lower Si/Al ratios formed less organic oil, but more water, which supported our results. HHV for the heavy oil upgraded by Z280 are similar with the control pyrolysis oil, which indicates that the H-ZSM-5 zeolite with a very large SiO₂/Al₂O₃ mole ratio only limited affects the properties of pyrolysis oil. Nevertheless, both energy and carbon yields show that Z50 upgraded pyrolysis oil remained most energy and carbon from the SW kraft lignin, which indicates this type of zeolite is a promising candidate to upgrade the properties of pyrolysis oil.

Table 36. HHV, energy yield (%) and carbon yield (%) of heavy oil, and mass yields (%) of light oil, heavy oil, char and gas for the pyrolysis of pure SW kraft lignin and pyrolysis of SW kraft lignin with 1.0/1.0 ($W_{\text{additive}}/W_{\text{lignin}}$) of H-ZSM-5 zeolites as additives at 600 °C for 10 min.

Pyrolysis Samples ^a	Mass yield (%)				HHV (MJ/kg)	Energy yield ^b (%)	Carbon yield ^c (%)
	light oil	heavy oil	char	gas			
Lignin (L)	14.47	28.97	44.21	12.35	30.78	33.11	27.52
L+Z23	17.21	23.81	44.50	14.48	31.24	27.63	23.55
L+Z30	17.60	24.47	47.02	10.91	31.55	28.68	24.33
L+Z50	15.18	27.17	46.68	10.97	31.38	31.67	26.90
L+Z80	14.74	26.53	46.57	12.16	31.27	30.81	25.96
L+Z280	17.49	25.05	48.33	9.13	30.21	28.10	24.14

^a All the yields are on the basis of duplicated tests.

^b Energy yield=mass yield* (HHV of heavy oil/HHV of dried SW kraft lignin)

HHV of dried SW kraft lignin is 26.92 MJ/kg

^c Carbon yield=mass yield*(carbon% of heavy oil/carbon% of dried SW kraft lignin)

8.3.2 Quantitative ³¹P-NMR analysis of pyrolysis oils

Our previous work^{9, 71, 87, 90} introduced quantitative ³¹P-NMR to quantitatively determine hydroxyl functional groups in pyrolysis oils. The ³¹P-NMR chemical shifts and integration regions of the phosphitylated aryl/alkyl hydroxyl groups and water with 2-chloro-4, 4, 5, 5-tetramethyl-1, 3, 2-dioxaphospholane (TMDP) are summarized in

Table 37. The integration results for the heavy oils shown in Figure 54. For all the heavy oils, the integration results show that there are significant amount (from 2 to 3 mmol/g of heavy oil) of guaiacyl and catechol types of hydroxyl groups. If there is only one of these two types of functional groups in each pyrolysis oil components, there should be >11-17 wt% of catechol and its derivatives and >24-37 wt% of guaiacol and its derivatives in the heavy oils. After the use of H-ZSM-5 zeolite as an additive the aliphatic hydroxyl groups and carboxylic acid in the heavy oils are nearly completely decomposed. With the exception of those two hydroxyl groups, the heavy oil produced from pyrolysis of lignin with Z280 are similar with the control pyrolysis oil, which indicate that the H-ZSM-5 zeolite with very large SiO₂/Al₂O₃ mole ratio has limited effects on the phenolic hydroxyl groups of pyrolysis oil during the pyrolysis process. Other than Z280, after the use of H-ZSM-5 zeolites, the contents of C₅ substituted and normal guaiacyl phenolic hydroxyl groups decreased with the increasing SiO₂/Al₂O₃ mole ratio of zeolites. In contrast, the contents of catechol type and *p*-hydroxy-phenyl hydroxyl groups increased when a high SiO₂/Al₂O₃ mole ratio zeolite was used. Since those two types of hydroxyl groups are the decomposition products of methoxyl-aromatic bonds and ether bonds in the lignin structure^{9, 90} this indicates that a zeolite with a relatively higher SiO₂/Al₂O₃ mole ratio could improve the cleavage of aromatic C-O bonds including methoxy groups and ether bonds more efficiently. Some possible degradation pathways of ether bonds and methoxyl groups on the surface of zeolite have been proposed in literatures¹⁶⁸⁻¹⁷⁰ and these are summarized in Figure 55. The limited amount of aliphatic OH also decreased after the use of a high SiO₂/Al₂O₃ mole ratio zeolite, which indicates an enhanced dehydration of aliphatic C-O bonds. In contrast, the content of carboxylic acid-OH increased with the

increasing SiO₂/Al₂O₃ mole ratio, which suggest that zeolite with lower SiO₂/Al₂O₃ mole ratio is more effective for the decomposition of carboxylic acid. Several researchers have examined the effects of zeolite on the dehydration and decarboxylation of model compounds.^{168, 171-175} The tentative mechanisms in the literatures have been shown in Figure 55.

Table 37. Chemical shifts and integration regions for lignin pyrolysis oils in a quantitative ³¹P-NMR, after derivatized with TMDP.^{9, 90}

Functional group		Integration region (ppm)
endo-N-hydroxy-5-norbornene-2,3-dicarboximide (NHND, internal standard)		151.0 - 152.8
Aliphatic OH		150.0 - 145.5
C ₅ Substituted guaiacyl phenolic OH	β-5	144.7 - 142.8
	4-O-5	142.8 - 141.7
	5-5	141.7 - 140.2
Guaiacyl phenolic OH		140.2 - 139.0
Catechol type OH		139.0 - 138.2
<i>p</i> -hydroxy-phenyl OH		138.2 - 137.3
Carboxylic acid-OH		136.6 - 133.6
Water		133.1-131.3,16.9-15.1

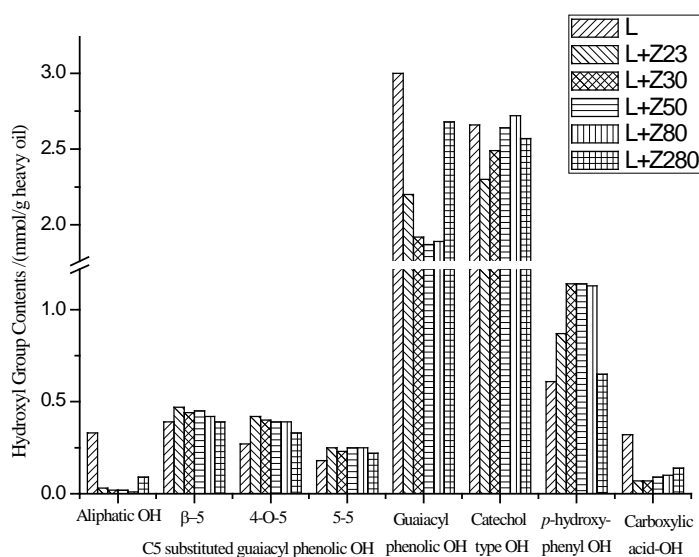


Figure 54. Hydroxyl group contents of different heavy oils produced by pyrolysis of pure SW kraft lignin and pyrolysis of SW kraft lignin with 1.0/1.0 ($W_{\text{additive}}/W_{\text{lignin}}$) of H-ZSM-5 zeolites as additives at 600 °C for 10 min, determined by quantitative ^{31}P -NMR after derivatization with TMDP.

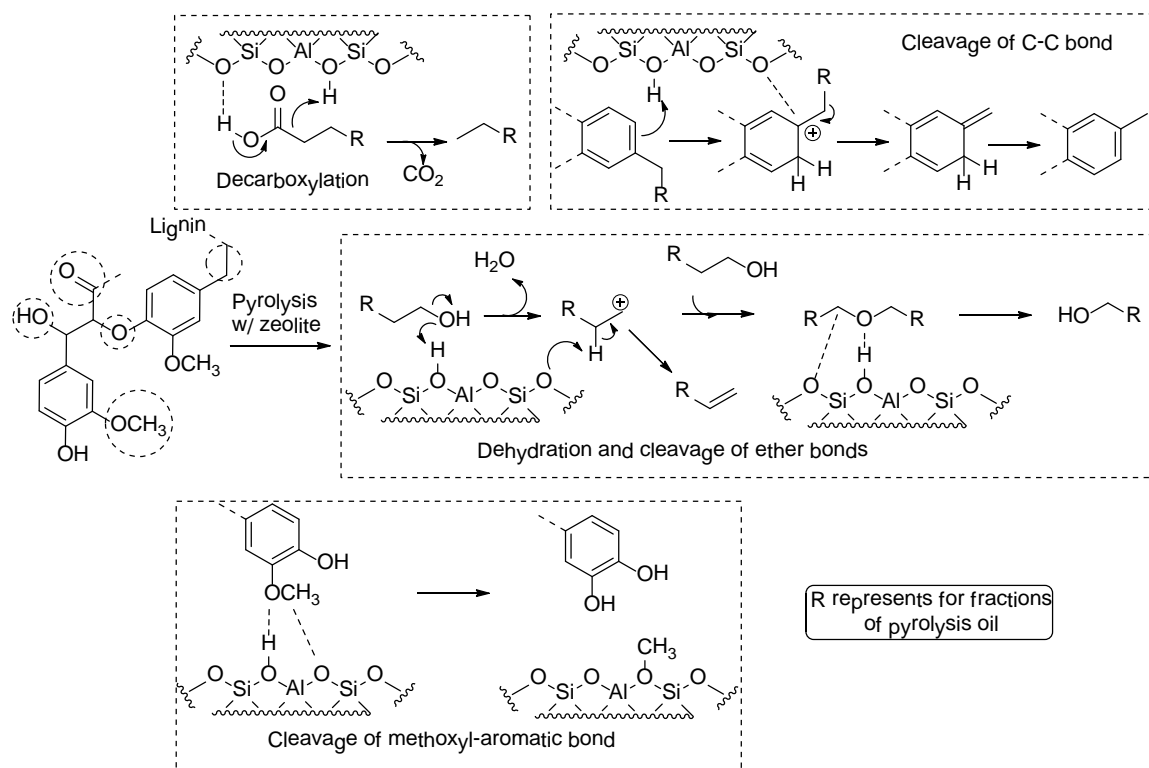


Figure 55. The primary decomposed functional groups in lignin during the pyrolysis (circled by dash line in lignin model structure) and the possible cracking pathways on zeolite.¹⁶⁸⁻¹⁷⁸

Our previous works indicated that the light oils contain more than 80 wt% of water and another 10 wt% of methanol, catechol and acetic acid.^{9, 71, 90} The integration results of those four major components in the light oils are summarized in Figure 56. The yields of methanol, catechol and acetic acid in the light oil significantly decreased when H-ZSM-5 zeolite was used as an additive. Methanol is the major product of cleavage of methoxyl groups in lignin structure and catechols are the further decomposition products of guaiacols.⁹ The yields of those two components increased with the increasing SiO₂/Al₂O₃ mole ratio of zeolite, which indicate an improved decomposition of methoxyl

group and consist with ^{31}P -NMR results for the heavy oils. Similar with heavy oils, the content of carboxylic acid-OH in light oil also increased after used a higher $\text{SiO}_2/\text{Al}_2\text{O}_3$ mole ratio zeolite. The concentration of water in light oil also increased after the use of zeolite. With the exception of Z280, the water contents increased after the use of a higher $\text{SiO}_2/\text{Al}_2\text{O}_3$ mole ratio zeolite. Water is the dehydration product of aliphatic C-O bonds,⁹ the higher water content indicates an enhanced decomposition of aliphatic hydroxyl groups, which is also supported by the ^{31}P -NMR results for the heavy oils.

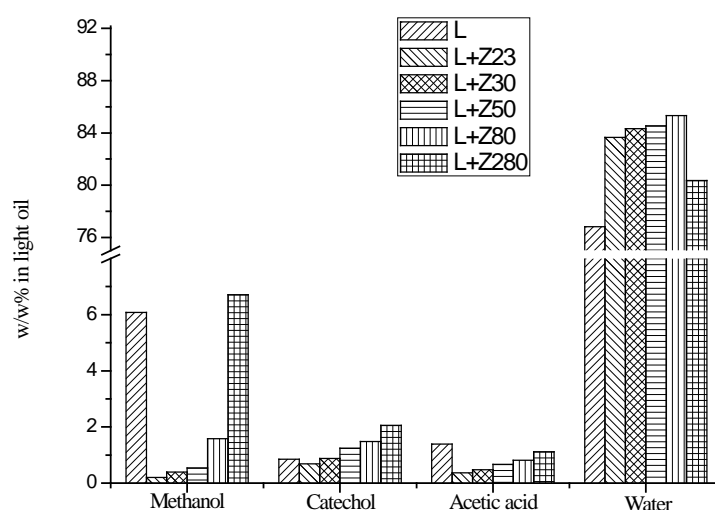


Figure 56. Weight percentage of four major components in light oils produced by pyrolysis of pure SW kraft lignin and pyrolysis of SW kraft lignin with 1.0/1.0 ($W_{\text{additive}}/W_{\text{lignin}}$) of H-ZSM-5 zeolites as additives at 600 °C for 10 min, determined by quantitative ^{31}P -NMR after derivatization with TMDP.

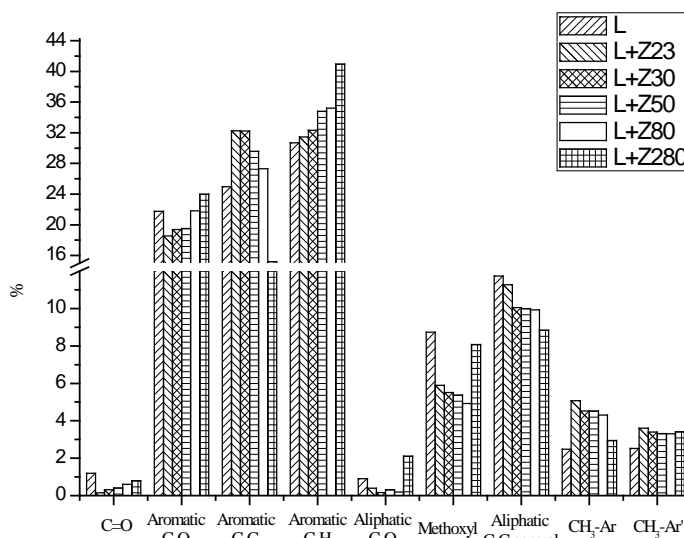
8.3.3 Quantitative ^{13}C -NMR analysis of pyrolysis oils

To fully characterize the functional groups in the heavy oils, a detailed analysis of

heavy oils was accomplished using ^{13}C -NMR. The ^{13}C -NMR chemical shift assignment ranges are based on our previous work⁹ and shown in the Table 38. The integration results of this analysis for the heavy oils are summarized in Figure 57. This data show that compared to the use of other zeolites, the effects of Z280 on the heavy oil are very limited and the product is more similar with the control heavy oil, which is consistent with ^{31}P -NMR results. The carbonyl groups are nearly completely eliminated and the content increased with the increasing $\text{SiO}_2/\text{Al}_2\text{O}_3$ mole ratio of H-ZSM-5 zeolite, which is additional evidence that the upgraded pyrolysis oil has lower acidity. After the use of zeolite, the content of methoxyl groups in the heavy oil decreased by ~45% and the decomposition of this functional group is improved when a higher $\text{SiO}_2/\text{Al}_2\text{O}_3$ mole ratio of H-ZSM-5 zeolite is used. This effect could explain the increasing contents of catechol type hydroxyl groups in the heavy and light oils detected by ^{31}P -NMR. The percentage of aromatic C-C bonds decreased upon the use of a higher $\text{SiO}_2/\text{Al}_2\text{O}_3$ mole ratio zeolite, which suggests that the zeolite with a higher $\text{SiO}_2/\text{Al}_2\text{O}_3$ mole ratio favors to cleave aromatic C-C bonds or prevent the formation of such bonds. There are also less aliphatic C-C bonds after the use of zeolite. Zeolite has been reported¹⁷⁶⁻¹⁷⁸ to improve the cleavage of aliphatic C-C bonds, which could explain the reduced content of such bonds in the upgraded pyrolysis oil. The possible pathways reported in the literatures have been summarized in Figure 55. The two types of methyl aromatic bonds in the heavy oils are the rearrangement products of methoxyl groups.⁹ Since the cleavage of methoxyl groups have been enhanced, the content of those two methyl aromatic bonds also increased after the use of zeolite. The increased aromatic C-O bonds in the upgraded heavy oils indicate a higher phenol hydroxyl groups, which is supported by ^{31}P -NMR results.

Table 38. ^{13}C -NMR chemical shift assignment range of lignin pyrolysis oil based on the chemical shift database created in our previous work.⁹

Functional group		Integration region (ppm)
Carbonyl or Carboxyl bond		215.0 – 166.5
Aromatic C-O bond		166.5 – 142.0
Aromatic C-C bond		142.0 – 125.0
Aromatic C-H bond		125.0 – 95.8
Aliphatic C-O bond		95.8 – 60.8
Methoxyl-Aromatic bond		60.8 – 55.2
Aliphatic C-C bond	General	55.2 – 0.0
	Methyl – Aromatic ($\text{CH}_3\text{-Ar}$)	21.6 – 19.1
	Methyl – Aromatic at ortho position	
	of a hydroxyl or methoxyl group ($\text{CH}_3\text{-Ar}'$)	16.1 – 15.4



Note: results are shown as percentage of total carbon.

Figure 57. Integration results for the SW kraft lignin and the heavy oils produced by pyrolysis of pure SW kraft lignin and pyrolysis of SW kraft lignin with 1.0/1.0 ($W_{\text{additive}}/W_{\text{lignin}}$) of H-ZSM-5 zeolites as additives at 600 °C for 10 min, detected by quantitative ^{13}C -NMR.

8.3.4 HSQC-NMR analysis of pyrolysis oils

To solve the overlaps problem when using ^{13}C -NMR to analyze the pyrolysis oils, our previous work demonstrated the value of HSQC-NMR to analyze various C-H bonds presented in the pyrolysis oils.¹⁰ The HSQC-NMR spectrum for the pyrolysis oils after the use of various H-ZSM-5 zeolites are shown in Figures 58-60. HSQC-NMR results show that after the use of zeolite as additive, the pyrolysis oils contain some polyaromatic hydrocarbons (PAH) and the content decreased with the increasing $\text{SiO}_2/\text{Al}_2\text{O}_3$ mole ratio of zeolite, which are supported by the GC-MS analysis. The formation of PAH on the

surface of zeolites was also observed by several model compounds studies.¹⁷⁹⁻¹⁸² It has been reported that the Brønsted acid sites of H-ZSM-5 zeolites could be calculated by the unit cell formula of the zeolite ($H_nAl_nSi_{96-n}O_{192}$ for H-ZSM-5 zeolite).¹⁶¹ Therefore, the Brønsted acid sites for H-ZSM-5 zeolites used in this work linearly decreased from 0.35 mmol/g (Z23) to 0.03mmol/g (Z280). Figure 55 shows that the improved cracking pathways of pyrolysis oil on the zeolites always involve protons from Brønsted acid sites, which indicate the more acidic zeolites should perform better upgrading results. However, both ³¹P and ¹³C-NMR results show that the H-ZSM-5 zeolite with a relatively higher SiO₂/Al₂O₃ (~50-80) was more effective to upgrade the properties of pyrolysis oil. Since the PAH has been reported as the precursor of coke^{181, 182} which will deactivate the zeolite, the higher contents of PAH in more acidic zeolite upgraded pyrolysis oils provide insight into the reason why Z50 performs better upgrading results than Z23. The intensity of aromatic C-H bonds increased after using zeolite, which is consistent with our ¹³C-NMR result. The native methoxyl groups (with a hydroxyl group or ether bond in the ortho position) decreased after adding zeolite during the pyrolysis and the content decreased when a higher SiO₂/Al₂O₃ mole ratio zeolite was employed. After the use of zeolite, there are more methyl aromatic bonds in the pyrolysis oil, which is also supported by our ¹³C-NMR results.

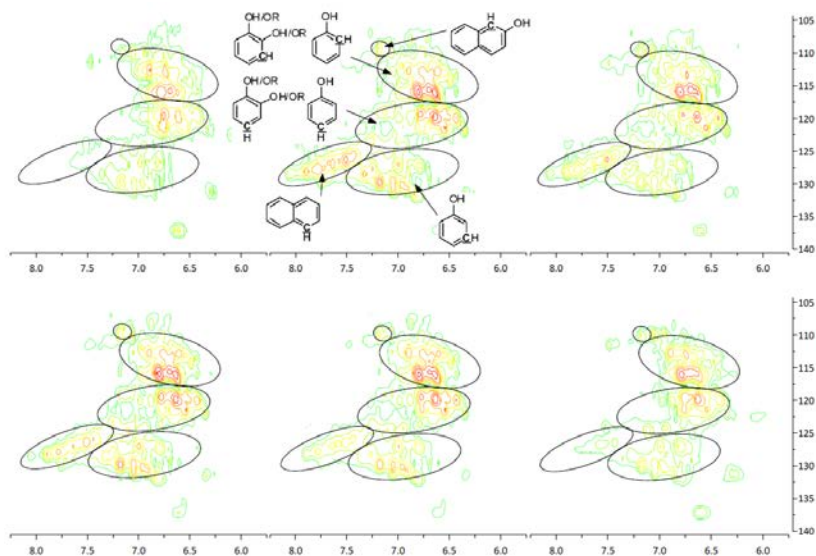


Figure 58. Aromatic C-H bonds in the HSQC-NMR spectra for the pyrolysis oils produced by pyrolysis of SW kraft lignin with H-ZSM-5 zeolites, from left top to right bottom is L, Z23, Z30, Z50, Z80 and Z280 upgraded pyrolysis oil.

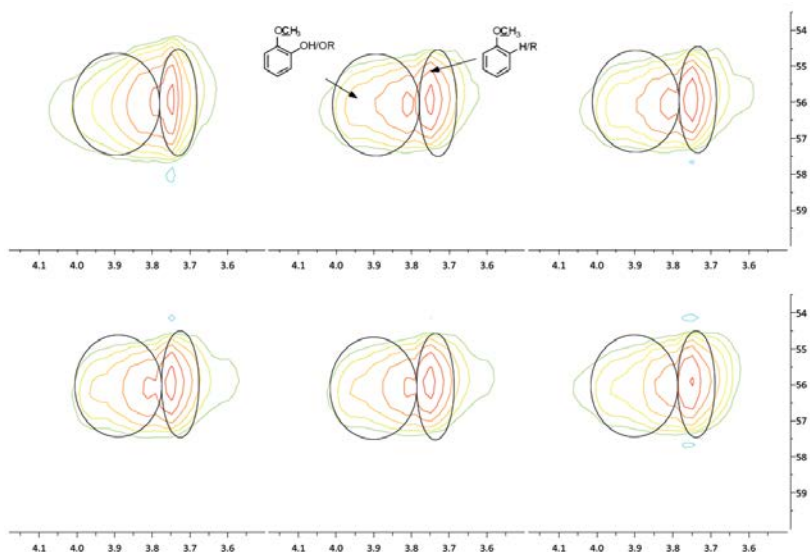


Figure 59. Methoxyl groups in the HSQC-NMR spectra for the pyrolysis oils produced by pyrolysis of SW kraft lignin with H-ZSM-5 zeolites, from left top to right bottom is L, Z23, Z30, Z50, Z80 and Z280 upgraded pyrolysis oil.

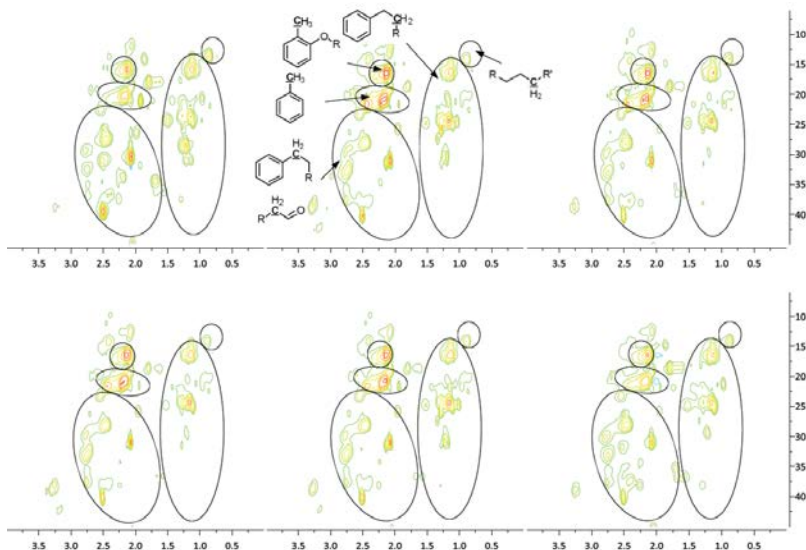


Figure 60. Aliphatic C-H bonds in the HSQC-NMR spectra for the pyrolysis oils produced by pyrolysis of SW kraft lignin with H-ZSM-5 zeolites, from left top to right bottom is L, Z23, Z30, Z50, Z80 and Z280 upgraded pyrolysis oil.

8.3.5 GPC and elemental analysis of pyrolysis oils

The number average, weight average molecular weights (M_n and M_w) and polydispersity values for the heavy oils produced by pyrolysis of softwood kraft lignin with zeolite at 600 °C are summarized in Figure 61. This analysis indicates the molecular weight decreased by 8-16% after the use of H-ZSM-5 zeolite. The lower molecular weight of upgraded pyrolysis oil is the evidence of enhanced decomposition of methoxyl group, carboxyl acid and dehydration of aliphatic hydroxyl groups. The results of elemental analysis for pyrolysis oils are shown in Table 39. After the use of zeolites, the carbon contents of heavy oils increased up to 5%. In contrast, there is up to 13% less oxygen in the upgraded pyrolysis oils, which indicates zeolite could improve the deoxygenation during the pyrolysis process. Most interestingly, the sulfur content also

decreased by 50% after using Z50 as the additive, which exhibits a potential method to decrease the sulfur content in the kraft lignin pyrolysis oils.

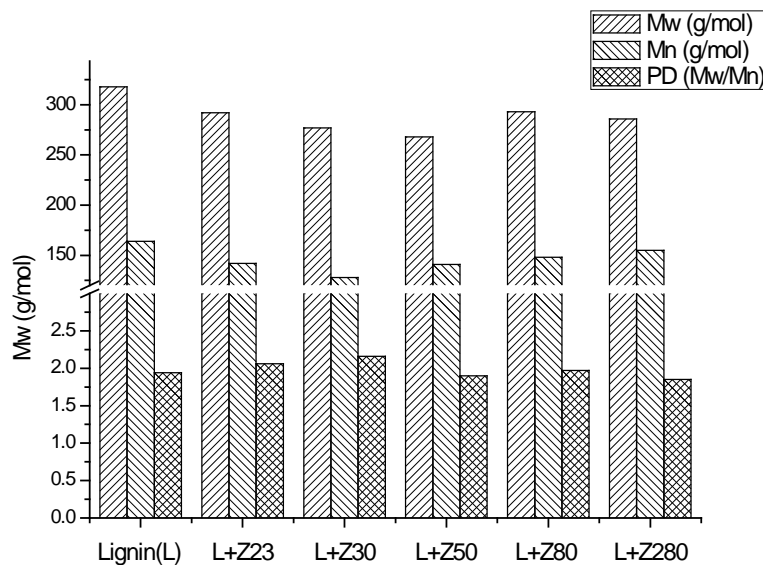


Figure 61. Molecular weight distribution and polydispersity of heavy oils produced by pyrolysis of pure SW kraft lignin and pyrolysis of SW kraft lignin with 1.0/1.0 ($W_{\text{additive}}/W_{\text{lignin}}$) of H-ZSM-5 zeolites as additives at 600 °C for 10 min.

Table 39. Elemental analysis for the pyrolysis of pure SW kraft lignin and pyrolysis of SW kraft lignin with 1.0/1.0 ($W_{\text{additive}}/W_{\text{lignin}}$) of H-ZSM-5 zeolites as additives at 600 °C for 10 min. The results are shown in weight percentage.

Pyrolysis samples ^a	C	H	O	S
Lignin (L)	70.64	6.80	21.31	1.25
L+Z23	73.53	6.68	18.90	0.89
L+Z30	73.93	6.67	18.49	0.91
L+Z50	73.61	6.71	19.05	0.63
L+Z80	72.75	6.79	19.59	0.87
L+Z280	71.65	6.78	20.74	0.83

^aDried SW kraft lignin contains 74.35 wt% of carbon, 6.60 wt% of hydrogen, 17.79 wt% of oxygen and 1.26 wt% of sulfur.

8.4 Conclusion

The pyrolysis of softwood kraft lignin with various H-ZSM-5 zeolites as the additives was accomplished at 600 °C. The yields of char slightly increased after the use of additives and the char yield is almost constant for all zeolites, which suggests that the additives have very limited effects on the primary decomposition of lignin. The yield of heavy oil decreased but the yield of light oil and gas increased after the use of zeolite. In addition, pyrolysis samples with lower Si/Al ratio zeolites formed relatively less heavy oil but more light oil. After the use of H-ZSM-5 zeolite, the aliphatic hydroxyl groups and carboxylic acid in the heavy oils are nearly completely decomposed, which represents a more suitable precursor for the biofuel. With the exception of those two

hydroxyl groups, the heavy oils produced from pyrolysis of lignin with Z280 are similar with the control pyrolysis oil, which indicate that the H-ZSM-5 zeolite with very large $\text{SiO}_2/\text{Al}_2\text{O}_3$ mole ratio has limited effects on the properties of pyrolysis oil. The results of ^{13}C and ^{31}P -NMR for the heavy oils indicate that the H-ZSM-5 zeolite with a relatively higher $\text{SiO}_2/\text{Al}_2\text{O}_3$ mole ratio is more effective to improve the cleavage of methoxyl groups, ether bonds and aliphatic C-C bonds, and dehydration of aliphatic hydroxyl groups. In contrast, the content of carboxylic acid-OH in both heavy and light oil increased with the increasing $\text{SiO}_2/\text{Al}_2\text{O}_3$ mole ratio, which suggest that zeolite with lower $\text{SiO}_2/\text{Al}_2\text{O}_3$ mole ratio is more effective for the decomposition of carboxylic acid. HSQC-NMR results show that after the use of additive, the pyrolysis oils contain some polyaromatic hydrocarbons (PAH) and the content decreased with the increasing $\text{SiO}_2/\text{Al}_2\text{O}_3$ mole ratio of zeolite. GPC results show that the molecular weight decreased by 8-16% after the use of various H-ZSM-5 zeolites.

Chapter 9: ONE STEP THERMAL CONVERSION OF LIGNIN TO THE GASOLINE RANGE LIQUID PRODUCTS BY USING ZEOLITES AS ADDITIVES*

9.1 Introduction

With declining petroleum resources, increasing fuel demands and growing concerns about the effects of carbon dioxide emissions from fossil fuels, it is imperative to develop sustainable production of fuels and chemicals. Biomass is a renewable resource for the sustainable production of fuels and chemicals that, to date, have been made primarily from fossil resources. The U.S. Department of Agriculture and U.S. Department of Energy established a vision to derive 25% of chemicals and materials and 20% of transportation fuels from biomass by 2030.⁷ Lignin is a natural aromatic polymer and a main constituent of lignocellulosics biomass; however, it has received much less biorefining efforts than plant polysaccharides^{5, 101, 158} due to its complexity, biological recalcitrance and its relative thermal stability, as its weight loss occurs in a very wide temperature range from 160-900 °C.¹⁸³ Furthermore, it is well known that the pyrolysis of lignin yields more char and the least amount of bio-oil when compared to cellulose or whole biomass.^{10,3} It has been reported that most of the water insoluble and the aromatic C-H groups from the pyrolysis of whole biomass pyrolysis oils can be attributed to the pyrolysis of lignin.¹⁰ Therefore, upgrading technologies that convert lignin to a potential

* The full data of this research was accepted for publication in RSC Advances, 2012. It is entitled as “One step thermal conversion of lignin to the gasoline range liquid products by using zeolites as additives”. The other author is Arthur J. Ragauskas from the Institute of Paper Science and Technology and School of Chemistry and Biochemistry at Georgia Institute of Technology. Reproduced by permission of The Royal Society of Chemistry. <http://pubs.rsc.org/en/content/articlelanding/2012/ra/c2ra22616b>

replacement for diesel and gasoline could provide an attractive biofuel technology and also provide insight into the conversion of whole biomass to green fuels. One step thermal conversion of lignin to gasoline range (molecular weight is ~105 g/mol) liquid products or simple petrochemicals such as benzene, toluene, xylene, phenol and catechol appears to be very pragmatic.

Zeolites are a promising class of additives to improve the properties of pyrolysis oils and it has been examined by several researchers. For example, Murzin's group investigated pyrolysis of pine wood with various zeolites, including Beta (BEA), Y (FAU), ZSM-5 (MFI), Mordenite (MOR) and Ferrierite (FER) zeolites.^{139, 166, 184-186} They concluded that the mass yield of pyrolysis product was only slightly influenced by the types of zeolite, whereas the chemical compositions of bio-oil were dependent on the structure of the zeolite employed. The content of ketones was higher and the amount of acids and alcohols was lower in the bio-oil when ZSM-5 was used as an additive during the pyrolysis. With using a Mordenite zeolite the content of polyaromatic hydrocarbons was relatively low. Beta, Y and Ferrierite zeolites were more effective at catalyzing dehydration and decarbonylation reactions. Huber's group¹⁸⁷⁻¹⁸⁹ also examined the influence of zeolite on the properties of pyrolysis products produced from pine wood, cellulose and glucose. They reported that the thermal conversion of glucose to aromatics was a function of the pore size of the zeolite catalyst. Small pore zeolites did not produce aromatics. In contrast, medium pore size (5.2-5.9 Å) zeolites produce mostly aromatic products. Higher coke, lower aromatics and reduced oxygenated species were observed with the use of large pore zeolites. Zhao et al.¹³⁶ upgraded the water-insoluble fraction

(pyrolytic lignin) from pyrolysis oil of rice husks with several additives, including ZSM-5 and Beta zeolites. They found that compared to the Beta zeolite, ZSM-5 produced more aromatics and less coke. Most of oxygenates were found to be converted to arenes and polycyclic aromatic hydrocarbons with zeolites and this conversion was favored at higher temperatures. French et al.¹³⁷ used molecular-beam mass spectrometry (MBMS) to analyze the product vapor from pyrolysis of cellulose, straw lignin and ground aspen wood with forty different additives at 400, 500 and 600 °C. They found that the highest yield of hydrocarbons (~16 wt. %) was achieved using metal-substituted ZSM-5 zeolite during pyrolysis and the best-performing catalyst belonged to ZSM-5 zeolite while larger-pore zeolites showed less deoxygenation activity.

The pyrolysis of several biomasses such as, corn stalks,^{140, 142} cassava rhizome,^{143, 144} maple,^{190, 191} poplar,^{145, 192} rice husks,^{136, 146} bamboos,¹⁹³ empty palm fruit bunch,¹⁹⁴ oak,¹⁹⁵ beech^{164, 196} and pine^{147, 148} with various zeolites have also been studied in recent years. Most of the reported additives studies have focused on the pyrolysis of biomass, while only a few have examined the behavior of lignin in the presence of additives during pyrolysis. The goal of this work is to convert lignin to low molecular weight aromatics (molecular weight is ~100 g/mol) in one step, which could then be used as a precursor for gasoline and/or the possible substitution of petrochemicals such as phenol and catechol. This was accomplished by using a series of zeolites as pyrolysis additives to influence the chemical components generated during the pyrolysis of lignin. To characterize the whole portions of various pyrolysis oils, we used Nuclear Magnetic Resonance (NMR) including ¹³C, ³¹P and Heteronuclear Single-Quantum Correlation (HSQC)-NMR^{9, 10, 71, 87,}

⁹⁰ as the analysis technique.

9.2 Materials and Methods

All reagents used in this study were purchased from VWR International or Sigma-Aldrich (St. Louis, MO) and used as received. Lignin was isolated from a commercial U.S.A. softwood kraft pulping liquor. Zeolites (CBV 3020E, CP 814, CBV 710, CP 914C and CBV 21A) were purchased from Zeolyst, Inc.

9.2.1 Lignin separation and purification

Please see section 3.2.1.1 of this dissertation for the details.

9.2.2 Preparation of pyrolysis sample

Different types (MFI, FAU, BEA, FER and MOR) of zeolite were used as the additives in this work. The pyrolysis samples were mechanical stirred lignin with 1:1 weight ratio of zeolites and all the zeolites were activated in the pyrolysis tube at 500 °C under nitrogen for 6 h. Detailed information of each zeolite used can be found in Table 40.

Table 40. SiO₂/Al₂O₃ mole ratio, framework, code name used in this work and channel structure^{136, 139, 184, 185, 188, 191, 194, 196} of each zeolite.

	CBV 3020E	CBV 720	CP814E	CP914C	CBV 21A
SiO ₂ /Al ₂ O ₃ mole ratio	30	30	25	20	20
Frame work	MFI	FAU	BEA	FER	MOR
Code name	Z	Y	B	F	M
Pore dimension	3	3	3	2	1
Pore size (Å)	5.1×5.5 5.3×5.6	7.4×7.4	6.6×6.7 5.6×5.6	3.5×4.8 4.2×5.4	6.5×7.0 2.6×5.7

9.2.3 Equipment and process of pyrolysis

Please see section 3.2.3.1 of this dissertation for the details. A summary of experimental procedure was shown in Figure 62.

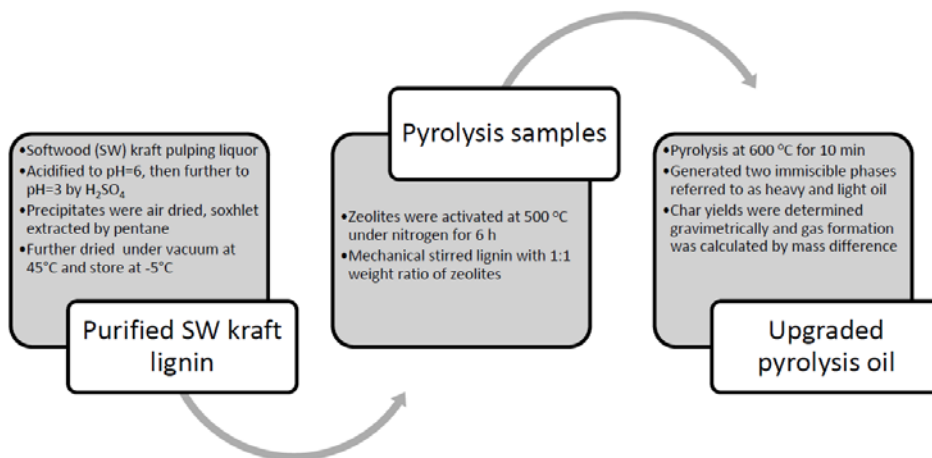


Figure 62. Summary of experimental procedure.

9.2.4 Characterization of pyrolysis oils

Please see sections 3.3.1-2; 3.3.7 for the details.

9.3. Results and Discussion

9.3.1 Yields of pyrolysis products

The yields from pyrolyzing a softwood kraft lignin with different zeolites at 600 °C are summarized in Figure 63. These results indicate that the yields of char increased after the use of additives and pyrolysis of lignin with Y and B zeolites yielded the most char. Pyrolysis with F and M zeolites increased the yield of heavy oil. In contrast, after the use of Z, Y and B zeolites, lignin produced less heavy oil but more light oil. The differences between the yields of pyrolysis products indicate the influence of zeolite on the pyrolysis process is related to the type of zeolite framework.

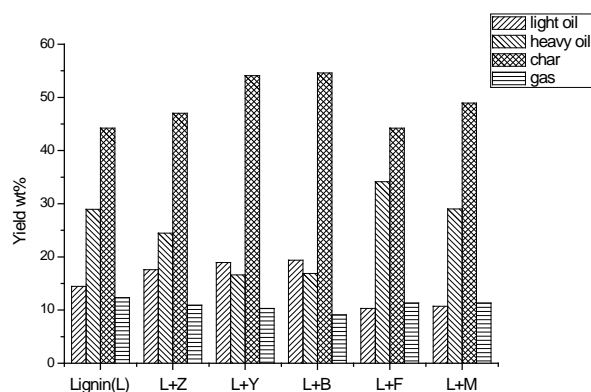


Figure 63. Yields (wt%) of light oil, heavy oil, char (excludes the weight of zeolite) and gas for the pyrolysis of pure SW kraft lignin and pyrolysis of SW kraft lignin with 1.0/1.0 ($W_{\text{additive}}/W_{\text{lignin}}$) of Z, Y, B, F and M zeolites as additives at 600 °C for 10 min.

9.3.2 Quantitative ^{31}P -NMR analysis of pyrolysis oils

Our previous work^{9, 71, 87, 90} introduced quantitative ^{31}P -NMR to determine hydroxyl functional groups in pyrolysis oils. The ^{31}P -NMR chemical shifts and integration regions of the phosphitylated aryl/alkyl hydroxyl groups and water with 2-chloro-4, 4, 5, 5-tetramethyl-1, 3, 2-dioxaphospholane (TMDP) are summarized in Table 41. The integration results for the heavy oils are summarized in Figure 64. After the use of Y and B zeolites as additives, the aliphatic hydroxyl groups in the heavy oils were completely decomposed. With the other three types of zeolite, the aliphatic hydroxyl groups also decreased by 70-95%. The results show that for the zeolites studied the resulting pyrolysis oils were significantly dehydrated. Compared to the Z, F and M zeolites, after the use of Y and B zeolites, the heavy oils contained more C_5 substituted guaiacyl phenolic, catechol and *p*-hydroxy-phenyl types of hydroxyl groups but less normal guaiacyl phenolic hydroxyl group. In contrast, with adding F and M zeolites, lignin pyrolysis yielded more normal guaiacyl phenolic but less *p*-hydroxy-phenyl and C_5 substituted guaiacyl phenolic types of hydroxyl groups. Since catechol and *p*-hydroxy-phenyl types of hydroxyl groups are the decomposition products of methoxyl-aromatic and ether bonds in the lignin structure,^{9, 90} this indicates that the Y and B zeolites could perform the cleavage of aromatic C-O bonds more effectively. After the use of zeolites, the content of carboxylic acid decreased by 44-85%, which is anticipated to be a much more suitable biofuel precursor. Compared to the other studied zeolites, Z and M zeolites could induce decarboxylation reactions more efficiently. Several researchers have reported similarly enhanced dehydration and decarboxylation of model compounds on the surface of zeolite.^{168, 171-175}

Table 41. Chemical shifts and integration regions for lignin pyrolysis oil derivatized with TMDP in a quantitative ^{31}P -NMR. ^{9, 71, 87, 90}

Functional group		Integration region (ppm)
endo-N-hydroxy-5-norbornene-2,3-dicarboximide (NHND, internal standard)		151.0 - 152.8
Aliphatic OH		150.0 - 145.5
C ₅ Substituted	β -5	144.7 - 142.8
	4-O-5	142.8 - 141.7
	5-5	141.7 - 140.2
Guaiacyl phenolic OH		140.2 - 139.0
Catechol type OH		139.0 - 138.2
<i>p</i> -hydroxy-phenyl OH		138.2 - 137.3
Carboxylic acid-OH		136.6 - 133.6
Water		133.1-131.3,
		16.9-15.1

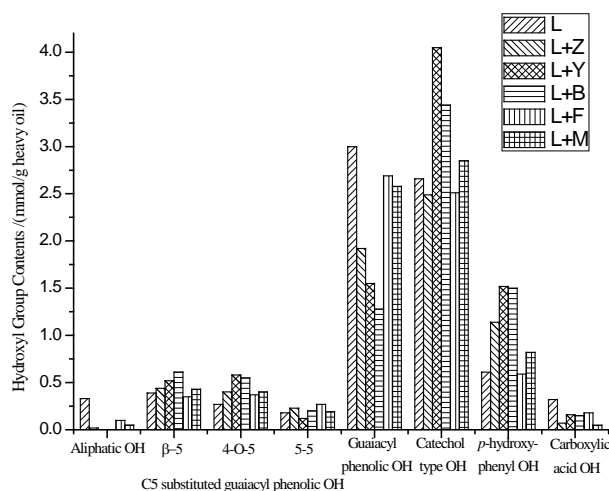


Figure 64. Hydroxyl group contents (mmol/g of heavy oil) of different heavy oils produced by pyrolysis of pure SW kraft lignin and pyrolysis of SW kraft lignin with 1.0/1.0 ($W_{\text{additive}}/W_{\text{lignin}}$) of Z, Y, B, F and M zeolites as additives at 600 °C for 10 min, determined by quantitative ^{31}P -NMR after derivatization with TMDP.

Our previous studies indicated that the light oils from pyrolysis of lignin contain more than 80 wt% of water and ~10 wt% of methanol, catechol and acidic acid.^{9, 71, 90} The integration results of those four major components in the light oils are summarized in Figure 65. For all the upgraded light oils, the yields of methanol and acetic acid significantly decreased. In contrast, the content of catechol increased after the use of zeolites. Compare to the Z, F and M zeolites, the use of Y and B zeolites yielded a light oil with increased catechol which indicates a more efficient decomposition of ether bond and methoxyl group. The content of catechol increased by 320% after the use of Y zeolite, this pure catechol in the light oil could be used as an alternative pathway for its synthesis. As anticipated, the content of the major dehydration product, water increased with the use

of zeolites.

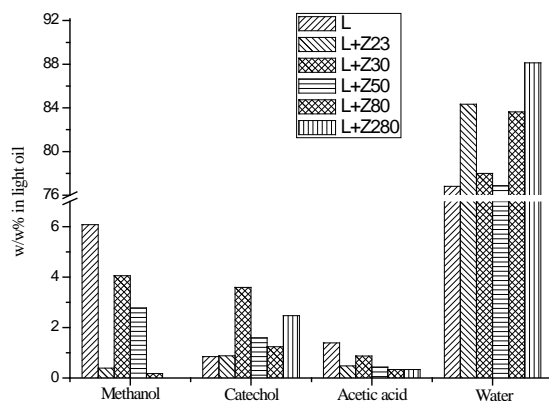


Figure 65. Weight percentage of four major components in light oils produced by pyrolysis of pure SW kraft lignin and pyrolysis of SW kraft lignin with 1.0/1.0 ($W_{\text{additive}}/W_{\text{lignin}}$) of Z, Y, B, F and M zeolites as additives at 600 °C for 10 min, determined by quantitative ^{31}P -NMR after derivatization with TMDP.

9.3.3 Quantitative ^{13}C -NMR analysis of pyrolysis oils

To fully characterize the functional groups in the heavy oils, a detailed analysis was accomplished by using ^{13}C -NMR. The ^{13}C -NMR chemical shift assignment ranges are based on our previous work⁹ and shown in the Table 42. The integration results of this analysis for the heavy oils are summarized in Figure 66. After the use of Y and B zeolites, the heavy oils contained ~80% less methoxy groups than the native pyrolysis oil, which indicates a very efficient decomposition of methoxyl groups and this result could explain the increasing contents of catechol type and *p*-hydroxy-phenyl hydroxyl groups detected by ^{31}P -NMR. The two types of methyl aromatic bonds in the heavy oils are reported to be the rearrangement products of methoxyl groups.⁹ After the use of these two zeolites, the

heavy oils contained relatively large amount of methyl aromatic bonds, which is evidence for the enhanced cleavage of methoxyl groups. The ^{13}C -NMR results also show that there were only 13-56% carbonyl groups remaining in the upgraded pyrolysis oils, which is consistent with ^{31}P -NMR results. It has been reported the acidity of pyrolysis oils is mainly (60-70%) derived from carboxylic acids and their content detrimentally impacts the stability of pyrolysis oils.¹⁹⁷ The significantly reduced amount of carboxylic acids in the zeolite upgraded pyrolysis oils represents a more stable pyrolysis oil which is expected to cause less corrosion problem.¹⁹⁷ With the use of F and M zeolites, the heavy oils contained relatively large amount of aromatic C-O bonds but the least amount of aromatic C-C bonds, which indicate that those two zeolites prefer to cleave aromatic C-C bonds or prevent the formation of such bonds. For the Y and B zeolites upgraded pyrolysis oils, the contents of oxygen substituents including aromatic C-O and aliphatic C-O bonds, carbonyl and methoxyl groups decreased by more than 40%. In addition, almost all the remaining oxygen functionality (up to ~87%) in these two upgraded pyrolysis oils belongs to the phenolic hydroxyl groups.

Table 42. ^{13}C -NMR chemical shift assignment range of lignin pyrolysis oil based on the chemical shift database created in our previous work.⁹

Functional group	Integration region (ppm)
Carbonyl or Carboxyl bond	215.0 – 166.5
Aromatic C-O bond	166.5 – 142.0
Aromatic C-C bond	142.0 – 125.0
Aromatic C-H bond	125.0 – 95.8
Aliphatic C-O bond	95.8 – 60.8
Methoxyl-Aromatic bond	60.8 – 55.2
General	55.2 – 0.0
Methyl – Aromatic	21.6 – 19.1
Aliphatic C-C bond (CH ₃ -Ar)	
Methyl – Aromatic at ortho position of a hydroxyl or methoxyl group (CH ₃ -Ar')	16.1 – 15.4

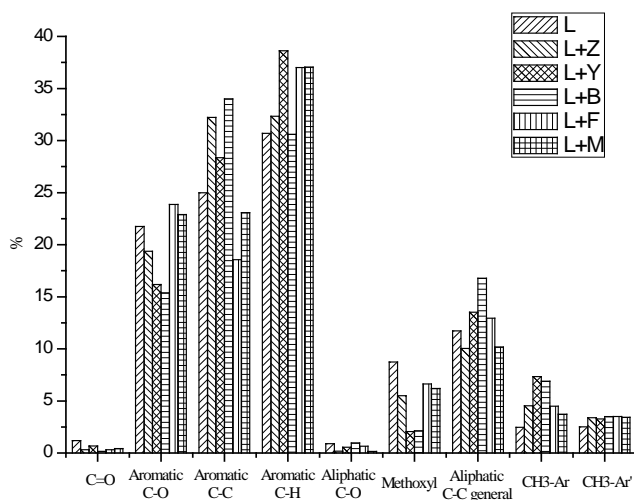


Figure 66. Integration results for the SW kraft lignin and the heavy oils produced by pyrolysis of pure SW kraft lignin and pyrolysis of SW kraft lignin with 1.0/1.0 ($W_{\text{additive}}/W_{\text{lignin}}$) of Z, Y, B, F and M zeolites as additives at 600 °C for 10 min, detected by quantitative ^{13}C -NMR with using the assignment range showed in Table 42. The results were shown as the percentage of carbon.

9.3.4 HSQC-NMR analysis of pyrolysis oils

To solve spectral overlapping problems when using ^{13}C -NMR to analyze the pyrolysis oils, our previous work demonstrated that HSQC-NMR was uniquely well suited to analyze various C-H bonds present in the pyrolysis oils.¹⁰ The HSQC-NMR spectra for the pyrolysis oils after the use of zeolites are shown in Figures 67-69. HSQC-NMR results show that after the use of Z, Y and B zeolites, the pyrolysis oils contained some polyaromatic hydrocarbons (PAH). In contrast, there were only very limited amount of PAH in the F and M zeolites upgraded pyrolysis oils and almost no PAH in the native pyrolysis oil. The native methoxyl groups (with a hydroxyl group or

ether bond in the ortho position) have been completely eliminated after adding Y zeolite during the pyrolysis. The improved degradation of methoxyl groups on the surface of zeolite have been reported in literatures.¹⁶⁸⁻¹⁷⁰ Since Y type zeolite has a relatively larger pore size and a three dimensional channel system^{136, 139, 184, 185, 188, 191, 194, 196} which could let small aromatics such as phenol, naphthalene, xylene^{169, 188} go through the channels and thereby improve the upgrading effect more efficiently. For the other pyrolysis samples, the decomposition of native type of methoxyl group also has been improved. The content of rearranged methoxyl groups (no hydroxyl group or ether bond in the ortho position) also decreased after the use of Y and B zeolites, which is consisted with the significant reduced amount of methoxyl groups detected by ¹³C-NMR. Compare to the rearranged methoxyl groups, the zeolites prefer to cleave the native methoxyl groups, which may due to the hydroxyl group in the ortho position facilitates the cleavage. The reported possible degradation pathway of methoxyl groups on the surface of zeolite have been summarized in Figure 70.¹⁶⁸⁻¹⁷⁰ After the use of zeolites, there were much more methyl aromatic bonds in the pyrolysis oil which is consistent with our ¹³C-NMR result. Compare to the native pyrolysis oil, the upgraded pyrolysis oils have relatively lower amount of long chain aliphatic C-C bonds. Zeolite has been reported¹⁷⁶⁻¹⁷⁸ to improve the cleavage of aliphatic C-C bonds in the model compounds, which could explain the reduced contents of such bonds in the upgraded pyrolysis oils.

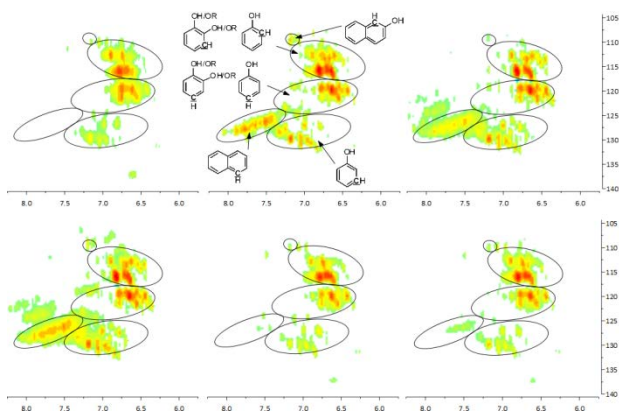


Figure 67. Aromatic C-H bonds in the HSQC-NMR spectra for the pyrolysis oils produced by pyrolysis of SW kraft lignin with various zeolites, from left top to right bottom is L, Z, Y, B, F and M upgraded pyrolysis oil.

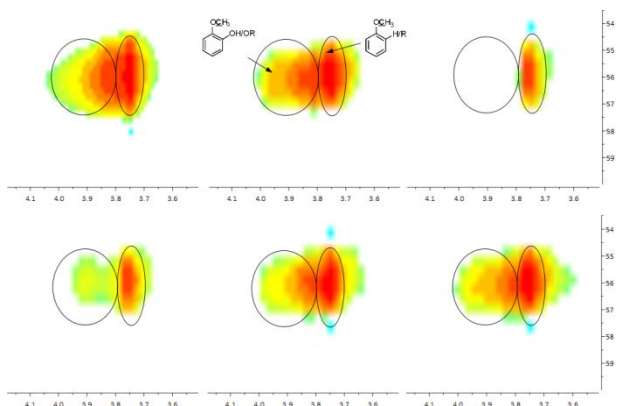


Figure 68. Methoxyl groups in the HSQC-NMR spectra for the pyrolysis oils produced by pyrolysis of SW kraft lignin with various zeolites, from left top to right bottom is L, Z, Y, B, F and M upgraded pyrolysis oil.

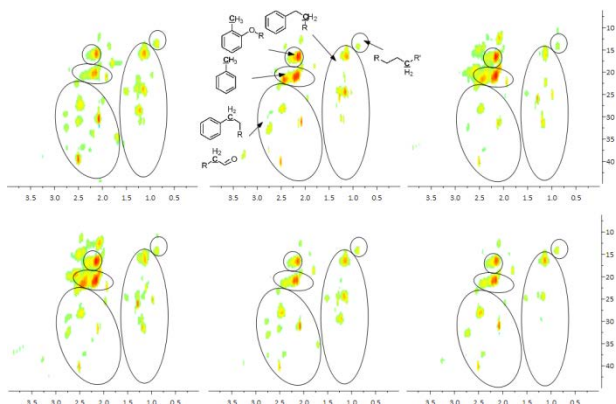


Figure 69. Aliphatic C-H bonds in the HSQC-NMR spectra for the pyrolysis oils produced by pyrolysis of SW kraft lignin with various zeolites, from left top to right bottom is L, Z, Y, B, F and M upgraded pyrolysis oil.

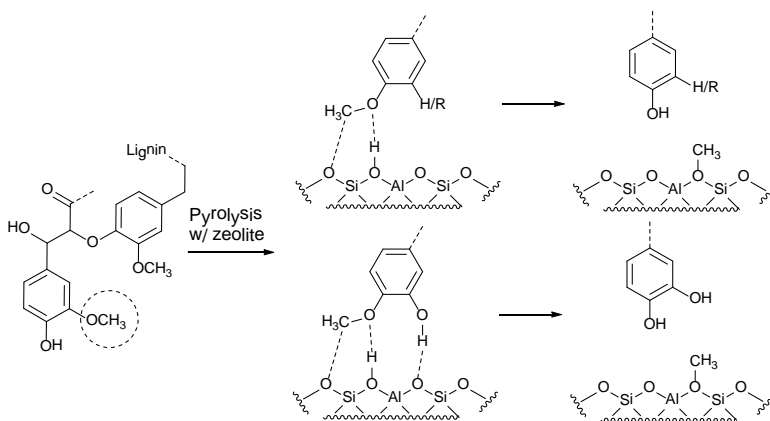


Figure 70. The reported possible degradation pathway of methoxyl groups on the surface of zeolite.¹⁶⁸⁻¹⁷⁰

9.3.5 GPC analysis of pyrolysis oils

The number average and weight average molecular weights (M_n and M_w) and polydispersity values for the heavy oils produced by pyrolysis of softwood kraft lignin with zeolites at 600 °C are summarized in Figure 71. This analysis indicates the molecular weight decreased to the gasoline range (80-120 g/mol) after the use of Y and B

zeolites, which represents simple aromatic molecules and could be used as the precursor of gasoline and possible substitution of petrochemicals. The GC-MS analysis of Y and B zeolites upgraded pyrolysis oils indicated that phenol, methyl phenols, dimethyl phenols, catechol, methyl catechols, naphthalene, methyl naphthalenes and guaiacol are the major components. In contrast, after adding F and M zeolites the molecular weights were almost intact.

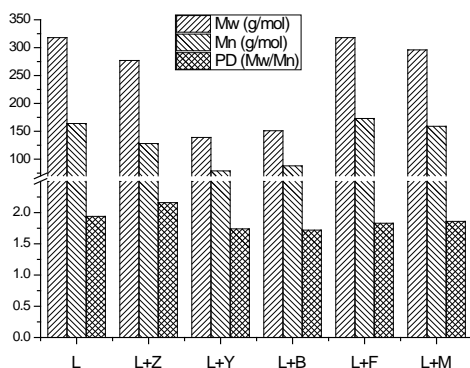


Figure 71. Molecular weight distribution and polydispersity of heavy oils produced by pyrolysis of pure SW kraft lignin and pyrolysis of SW kraft lignin with 1.0/1.0 ($W_{\text{additive}}/W_{\text{lignin}}$) of Z, Y, B, F and M zeolites as additives at 600 °C for 10 min.

9.4 Conclusion

The pyrolysis of softwood kraft lignin with five different zeolites, including MFI (Z), FAU (Y), BEA (B), FER (F) and MOR (M) as the additives was accomplished at 600 °C. Pyrolysis with F and M zeolites yielded more heavy oil but less light oil. In contrast, after the use of Z, Y and B zeolites, lignin produced less heavy oil but more light oil. The ^{31}P -NMR results show that by using Y and B zeolites, the aliphatic hydroxyl groups in

the heavy oils were completely decomposed. With using the other three types of zeolite, the aliphatic hydroxyl groups also decreased by 70-95%. These results indicate zeolites significantly improve the dehydration reactions, which will facilitate the deoxygenation of pyrolysis oil. Compare to the other types of zeolite, after the use of Y and B zeolites, both heavy and light oils contained more catechol type hydroxyl groups, which indicate the Y and B zeolites could perform the cleavage of aromatic C-O bonds more effectively. After using zeolites, the content of carboxylic acid decreased by 44-85%, which represents a much more suitable renewable fuel precursor. Compare to the other types of zeolite, Z and M zeolites prefer to improve the decarboxylation. After the use of Y and B zeolites, the heavy oils contained ~80% less methoxy groups than the native pyrolysis oil, and almost all the oxygen (up to ~87%) in these two upgraded pyrolysis oils belongs to the phenolic hydroxyl groups. The HSQC-NMR results show that with adding Z, Y and B zeolites, the pyrolysis oils contained some polyaromatic hydrocarbons (PAH). In contrast, there were very limited amount of PAH in F and M upgraded pyrolysis oils and almost no PAH in the native pyrolysis oil. Compare to rearranged methoxyl groups, all the tested zeolites prefer to cleave the native methoxyl groups, which may due to the hydroxyl groups in the ortho position facilitate the cleavage. The GPC results indicate that the pyrolysis oils upgraded by Y and B zeolites had a molecular weight profile in the gasoline range (80-120 g/mol).

In summary, the FAU (Y) and BEA (B) zeolites could significantly improve the cleavage of methoxyl-aromatic and ether bonds in the lignin and yield a pyrolysis oil that has a 'gasoline' range molecular weight. The upgraded pyrolysis oil could be used as the

precursor of gasoline and possible substitution of petrochemicals. The MFI (Z), FER (F) and MOR (M) zeolites could more efficiently decompose the carboxyl groups which will reduce the acidity of pyrolysis oils and make it more suitable for the usage as biofuel.

Chapter 10: PRODUCTION OF RENEWABLE GASOLINE FROM AQUEOUS PHASE HYDROGENATION OF LIGNIN PYROLYSIS OIL^{*}

10.1 Introduction

The hydrogenation of biomass pyrolysis oils to upgraded biofuels, especially the aliphatic compounds with a low boiling range has attracted significant research attention. However, compared with the water soluble phase of pyrolysis oils, the water insoluble parts are relatively difficult to upgrade due to the complex high molecular weight aromatic structures. To solve this problem, a two step hydrogenation of water insoluble pyrolysis oil (heavy oil) produced from pyrolysis of pine wood ethanol organosolv lignin (EOL) at 600 °C for 30 min was examined. Ru/C was used as the catalyst and water was used as the dispersant for the heavy oil and hydrogenation products. The carbon conversion yields for the first and second step hydrogenation are 35% and 33% (overall molar% of carbon content in the heavy oil), respectively. The products of first step of hydrogenation are primarily aromatic molecules which are produced from the hydrolytic cleavage of ether bond and methoxy groups in the heavy oils. Further hydrogenation was shown to convert the insoluble heavy oils (weight average molecular weight is 265 g/mol) to the aliphatic alcohols and other aliphatic components which could be used as renewable gasoline. As far as we know, this is the first reported effort to upgrade water

^{*} The full data of this research was accepted for publication in Fuel, 2012. It is entitled as “Production of renewable gasoline from aqueous phase hydrogenation of lignin pyrolysis oil”. The other authors are Arthur J. Ragauskas from the Institute of Paper Science and Technology and School of Chemistry and Biochemistry at Georgia Institute of Technology; Wei Mu from the Institute of Paper Science and Technology and School of Chemical and Biomolecular Engineering at Georgia Institute of Technology; Yulin Deng from the Institute of Paper Science and Technology and School of Chemical and Biomolecular Engineering at Georgia Institute of Technology. The permission was shown in appendix B.5.

insoluble parts of lignin pyrolysis oil to the total aliphatic components by aqueous phase by hydrogenation.

Increasing worldwide energy consumption and limited petroleum resources combined with economic, environmental and political concerns have boosted research on the development of new processes for the production of renewable fuels and chemicals.⁵ Due to its carbon neutrality, relative abundance, renewability and nonfood competition,^{6, 14} lignocellulosics are increasingly being viewed as a primary feedstock for renewable fuels and chemicals. The pyrolysis of biomass and its fractionated components, such as lignin, is a promising approach to using this resource. Pyrolysis has been reported as one of the economic ways (i.e., low capital and operating costs) to utilize biomass for biofuels and biobased chemicals.² The products of pyrolysis known as pyrolysis oil however have several challenging properties including poor volatility, high viscosity, corrosiveness and cold flow problems. These problems have limited the practical application of pyrolysis oils. Therefore, bio-oils must be upgraded before use as a replacement for diesel and gasoline fuels. Hydrogenation with hydrotreating catalysts is one of the promising routes to upgrade pyrolysis oils.¹³

Many researchers have examined the hydrogenation of biomass components and pyrolysis oils. For example, the hydrogenation of phenolic pyrolysis oil model compounds to the corresponding aliphatic compounds has been reported recently.^{198, 199} Noble metals such as Ru, Rh, Pd and Pt have been used as catalysts and the conversion for several model compounds such as anisole, 4-ethylphenol,

2-methoxy-4-n-propylphenol and 4-hydroxy-3-methoxyphenyl-acetone to the corresponding aliphatic compounds could be accomplished with yields approaching 100%. A two step hydrogenation process has been reported¹⁰² to upgrade the pyrolysis oils, in the first step, Ru/C was used as catalyst at 125 °C with a H₂ pressure of 10 MPa and in the second step Pt/C was used as catalyst at 250 °C with a H₂ pressure of 10 MPa. By a two step hydrogenation process, the water-soluble fraction of pinewood pyrolysis oil was converted to gasoline like compounds which have a boiling range from 65-175 °C with a carbon yield of 17%.¹⁰² For the hydrogenation of whole pyrolysis oils produced from pinewood,¹⁰² it has been reported that the carbon yield for the gas and coke is 26.5% and 34.6%, respectively. The hydrogenation of whole fast pyrolysis oils produced from beech wood with Ru/C as the catalyst at 350 °C, 20 MPa has also been examined.²⁰⁰ On the basis of ¹H-NMR results, the aliphatic/aromatic proton ratio increased from 6.4:1 to 11.2-16.4:1 after hydrogenation, which suggests the hydrogenation of the benzene ring during the process, however, is not complete. Conversion of carbohydrate model compounds, including sorbitol and furoin,⁵⁶ and sugar solutions prepared by hydrolysis of maple wood²⁰¹ to the C₁-C₁₅ alkanes has also been reported. All these treatments involved hydrogenation process with Pt, Pd or Ru as the catalyst at 120-265 °C with a H₂ pressure of 5.2-6.2 MPa. The carbon yields of conversion of aqueous carbohydrates derived from maple wood into gasoline range products were reported up to 57%.

Our previous work indicated that lignin yields a large amount of water insoluble pyrolysis products-heavy oil (65-85 wt% of pyrolysis products),^{9, 71} whereas tannin and cellulose yield most water soluble pyrolysis products-light oil, which contains large

amount of water (>60 wt%) and water soluble components such as methanol, levoglucosan and catechol et al. For tannin, ~78 wt% of pyrolysis products is a light oil and for cellulose, ~85 wt% of pyrolysis products is a light oil.^{10, 202} Therefore, the bulk of the water insoluble portion of the biomass pyrolysis oil is produced from lignin components. The pyrolysis oils produced from bark and residue contain 60-68 wt% and 55-57 wt %²⁰² heavy oil, respectively. However, this major portion has received much less attention for upgrading than the light oil. The complex high molecular weight aromatic structures of the water insoluble parts make it difficult to upgrade the whole pyrolysis oils by hydrogenation process. Many researchers have reported an incomplete hydrogenation of whole biomass pyrolysis oils.^{102, 200} In this work, a two step hydrogenation of lignin pyrolysis oil was examined and the insoluble heavy oil (weight average molecular weight is 265 g/mol) was converted to the alkanes and aliphatic alcohols which could be used as renewable gasoline. As far as we are aware, this is the first reported effort to upgrade lignin pyrolysis oil to the total aliphatic components by aqueous phase hydrogenation. These results will be of value in the development of complete hydrogenation of whole biomass pyrolysis oils.

10.2 Experimental section

Please see sections 3.1; 3.2.1.2; 3.2.4; 3.3.2-5 and 3.3.7.1-5 of this dissertation for the details.

10.3 Results and Discussion

The two step hydrogenation (HYD) of the heavy oil produced from pyrolysis of

pine wood ethanol organosolv lignin (EOL) at 600 °C for 30 min was examined. Ru/C was used as the catalyst and water was used as the dispersant for the heavy oil and the hydrogenation products. The first hydrogenation step was accomplished at 300 °C with a H₂ pressure of 14 Mpa for 4 h and Ru/C as catalyst. This treatment converts the water insoluble dark brown heavy pyrolysis oil to a transparent product. Further hydrogenation of this product at 250 °C and a H₂ pressure of 14 Mpa with Ru/C as catalyst for 2 h produced the final product. The carbon yields for the first and second step hydrogenation are 35% and 33% (overall molar% of carbon content in the heavy oil) respectively. A summary of experimental procedure was shown in Figure 72.

Figure 73 shows the ¹H-NMR spectrum for the EOL heavy oil, first and second step HYD products and the integration results are shown in Table 43. Compared to the EOL heavy oil and first step HYD product, the aromatic protons are completely eliminated in the second HYD product and 85% of protons belong to the aliphatic protons with no oxygen attached to the α-carbon. It indicates that the second HYD product contains only aliphatic carbons and has relatively low oxygen content, which represents a potential resource for bio-gasoline. Compared to the EOL heavy oil, first step HYD product contains less aromatic protons (See Table 43) but more aliphatic protons, which indicates the hydrogenation of benzene ring also occurred during first HYD process. Table 44 shows the ¹³C-NMR integration results for different functional groups in the EOL heavy oil, first and second step HYD products. The results show that there is no aromatic carbon in the second step HYD product which is consistent with ¹H-NMR result and there are less methoxy groups but much more aliphatic C-O bonds in the second step

HYD product. This is attributed to the hydrogenation of the aromatic ring which converts aromatic C-O bonds to aliphatic C-O bonds. Compared to the EOL heavy oil, there are relatively lower amounts of carbonyl C=O bonds, aromatic C-C bonds and C-H bonds but more aliphatic C-C bonds in the first step HYD product, which is also consistent with ^1H -NMR result and is the evidence that the hydrogenation of carbonyl C=O bonds and benzene ring occurred during the first HYD process.

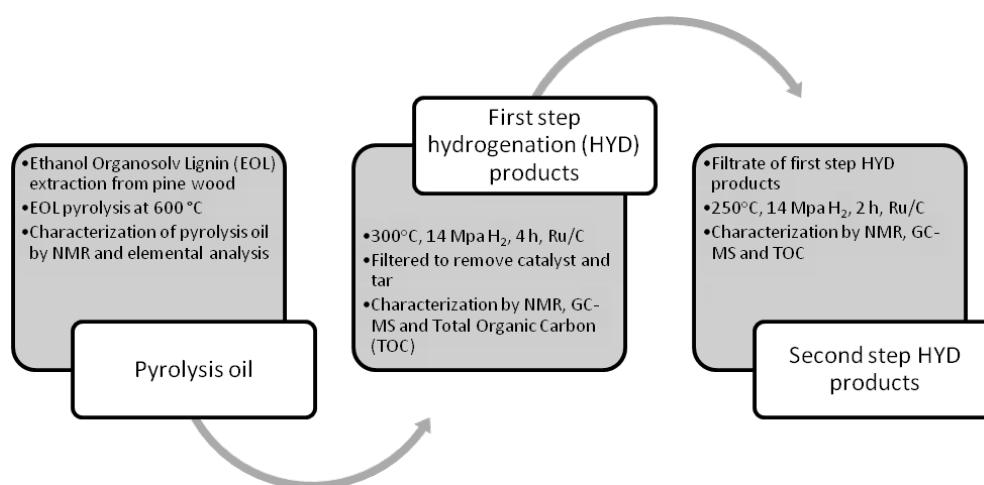


Figure 72. Summary of experimental procedure.

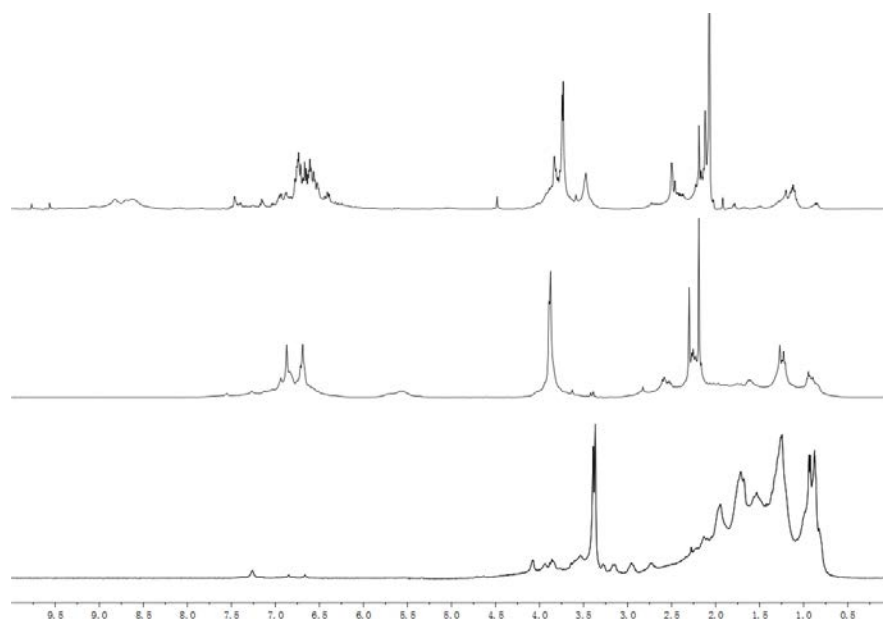


Figure 73. ^1H -NMR spectra for the EOL heavy oil, first and second step hydrogenation products. (from top to bottom)

Table 43. ^1H -NMR chemical shift assignment ranges and functional group contributions for the EOL heavy oil and first and second step hydrogenation products.

Type of protons	Range* (ppm)	EOL heavy oil	first step	second step
$-\underline{\text{C}}\underline{\text{H}}\text{O}, -\text{COO}\underline{\text{H}}$	10-9.6	0 [#]	0	0
$\text{Ar}\underline{\text{H}}, \underline{\text{H}}\text{C}=\text{C}-$	8.2-6.0	31	21	0
$-\underline{\text{C}}\underline{\text{H}}_{\text{n}}-\text{O}-, \underline{\text{C}}\underline{\text{H}}_{\text{n}}-\text{O}-$	6.0-3.0	27	18	15
$-\underline{\text{C}}\underline{\text{H}}_3, -\underline{\text{C}}\underline{\text{H}}_{\text{n}}-$	0.5-3.0	42	61	85

* The assignment ranges are on the basis of literature reports.^{71, 81}

[#] The results are shown as percentage of hydrogen.

Table 44. ^{13}C -NMR chemical shift assignment ranges and functional group contributions for the EOL heavy oil and first and second step hydrogenation products.

Functionality	Range* (ppm)	EOL heavy oil	first step	second step
Carbonyl C=O	215.0-166.5	1 [#]	0	0
Aromatic C-O	166.5-142.0	20	20	0
Aromatic C-C	142.0-125.0	17	13	0
Aromatic C-H	125.0-95.8	40	36	0
Aliphatic C-O	95.8-60.8	1	1	24
Methoxyl	60.8-55.2	10	10	7
Aliphatic C-C	55.2-0.0	11	20	69

* The assignment ranges are on the basis of literature reports.^{9, 90}

[#] The results are shown as percentage of carbon.

To fully characterize the HYD products, DEPT-135 ^{13}C -NMR and HSQC-NMR were used. Figures 74 and 75 show the results of these analyses. Compared to the complexity of the EOL heavy oil, the first step HYD product is relatively easy to identify. On the basis of GC-MS result and HSQC-NMR, the major components in the first step HYD are guaiacol, 4-methylguaiacol and catechol, which indicate that the EOL heavy oil (weight average molecular weight (M_w) is 265 g/mol) has been upgraded to the simple aromatic molecule after first step HYD process. The DEPT-135 and quantitative ^{13}C -NMR also show that after first step HYD process, the carbonyl C=O bonds and the aliphatic C-O bonds in the EOL heavy oil have been reduced consistent with a hydrodeoxygenation (HDO) process. Chen et al.²⁰³ reported that the hydrodeoxygenation

and the cleavage of C-C bond of carboxylic acids to alcohols and alkanes over supported Ru in the aqueous phase are favored at high temperature and with Ru/C as the catalyst, which supports our results. There are also more aliphatic CH₂ peaks (the negative peaks in DEPT 135 spectrum) in the first step HYD product, which is due to the hydrogenation of benzene ring in the EOL heavy oils. Figure 75 shows that all the aliphatic C-O bonds (from 60.8-95.8 ppm) in the second step HYD product contain a tertiary carbon, which is formed from hydrogenation of phenols and represent to the α -carbon in the alcohols. A significant amount of the secondary carbons in the second step HYD products have a chemical shift around 30-40 ppm which represent β -substituted alcohols.

On the basis of our previous work^{10, 202} using HSQC-NMR to analyze various pyrolysis oils, the two peaks around 10-15 ppm belong to the terminal carbon of long aliphatic chains. On the basis of GC-MS results, most peaks in the HSQC-NMR of the second step HYD product could be assigned to cyclohexanol and its derivatives. The carbon yield from first to second step HYD product is very high (~95 wt %), which is similar with literature reports about the hydrogenation of several phenolic pyrolysis oil model compounds.^{198, 199} It is also the evidence that the products of first step HYD process are simple aromatic molecules. Several researchers have reported the tentative reaction pathways of HYD and HDO process of phenolic model compounds.²⁰³⁻²⁰⁷ On the basis of those pathways and our results, the first step HYD process of EOL heavy oil mainly involves the cleavage of ether bonds and methoxyl groups in the heavy oils, which produces simple aromatic molecules, such as guaiacol. The second step HYD process will further upgrade those aromatics to the aliphatic rings, such as cyclohexanol.

The tentative pathways are shown in Figure 76.

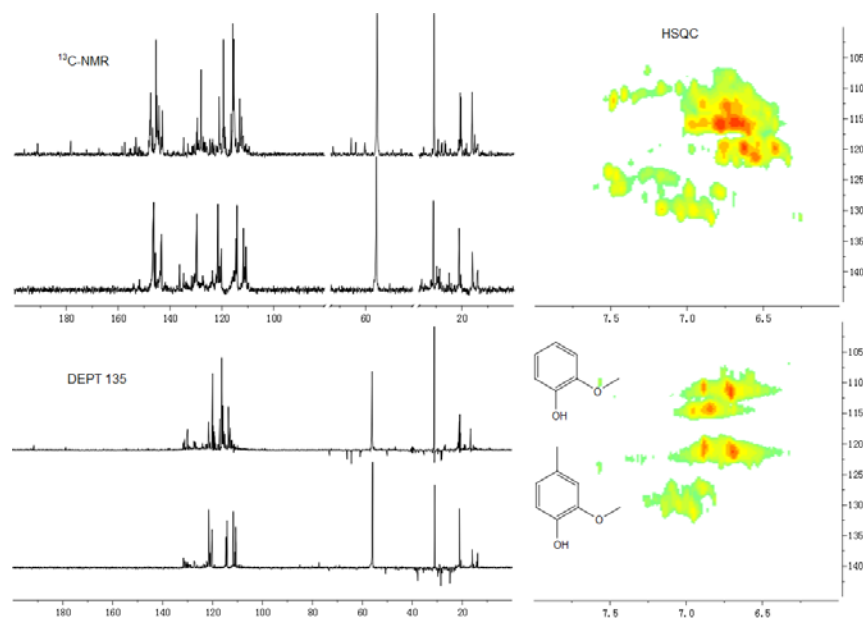


Figure 74. Quantitative ^{13}C -NMR, DEPT-135 and HSQC-NMR spectra for the EOL heavy oil and first step hydrogenation product. (from top to bottom)

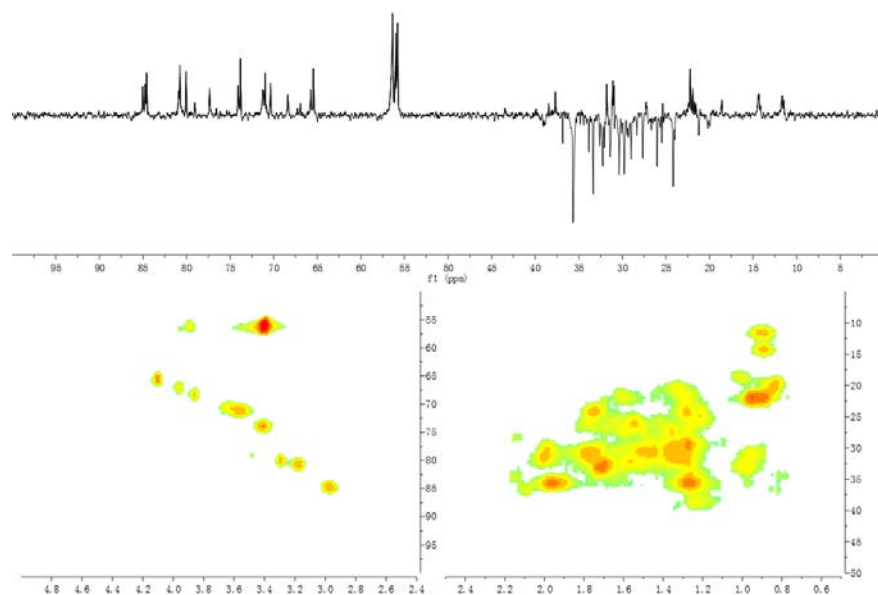


Figure 75. DEPT-135 and HSQC-NMR spectra for the second step hydrogenation product.

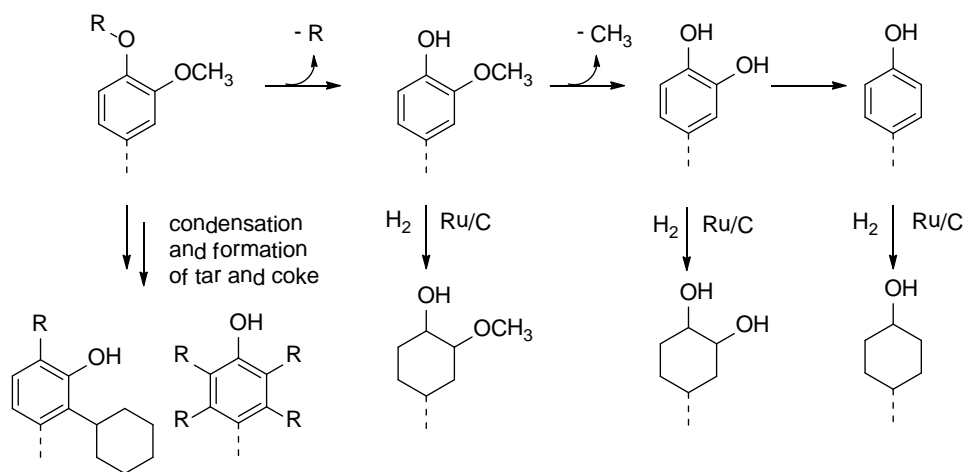


Figure 76. Tentative reaction pathways of HYD and HDO process of EOL heavy oil.²⁰³⁻²⁰⁷

There are some reports that the tar or coke will be formed during the HYD or HDO process of phenolic model compounds^{205, 207} and water soluble pyrolysis oils.^{56, 102} We also find the formation of tar after the first step HYD process. The M_w (462 g/mol) of the tar is almost as twice as EOL heavy oil ($M_w=265$ g/mol). The quantitative ¹³C-NMR (shows in Figure 77) for the tar shows that there are much more condensed aromatic C-C bonds than the EOL heavy oil, which represent condensation reactions during the HYD process. Comparable condensation reactions have been reported during the HYD process of model compounds in the literatures^{205, 207} and the possible pathways are shown in Figure 76. The SEM pictures for the catalysts show that after first step HYD of EOL heavy oil, the catalyst was coated by tar, which may affect the hydrogen transfer and the HYD reactions. The surface of catalyst for the second step HYD was almost intact after the process, which is consistent with the high carbon yield from the first to the second step HYD process. Thermogravimetric analysis (TGA) was also employed to further investigate the spent catalyst after the first step HYD process. The result (see supporting information) indicates a significant weight loss (~40 wt %) from 300-400 °C for the spent

catalyst which is also the evidence the catalyst was coated by tar.

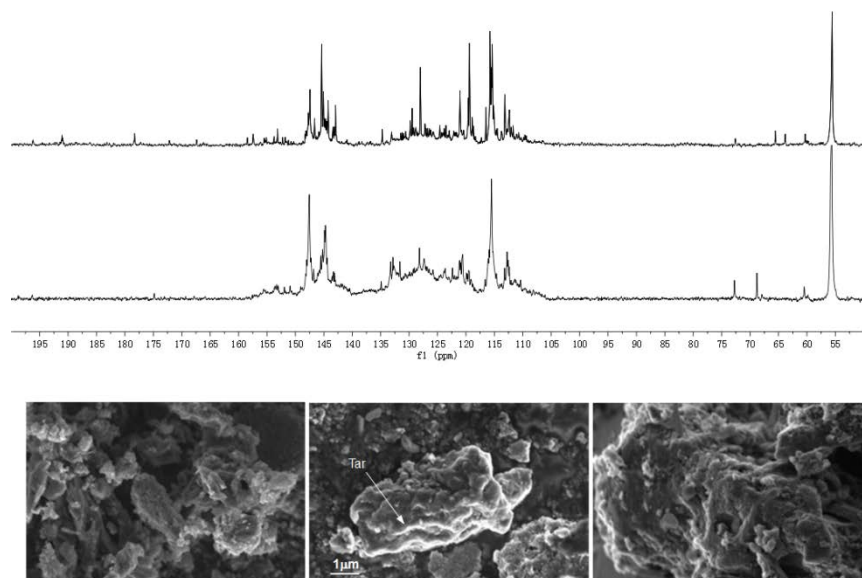


Figure 77. Quantitative ^{13}C -NMR for EOL heavy oil and tar from first step HYD catalyst (from top to bottom), and SEM for the original catalyst, catalyst after first and second step HYD process (from left to right).

10.4 Conclusions

In summary, the two steps HYD processes were examined to upgrade the heavy oil produced from pyrolysis of pine wood EOL. The products of first step HYD are simple aromatic molecules which are produced from the cleavage of ether bonds and methoxy groups in the heavy oils. The further upgrade could convert water insoluble heavy oils ($M_w=265$ g/mol) to the total aliphatic components with 33 molar% carbon yields. As far as we are aware, this is the first study focused at upgrading lignin pyrolysis oil in aqueous phase by hydrogenation. The upgraded pyrolysis oils could be used as green gasoline. The ongoing researches in our group involves reducing tar and coke formation which could increase the yield of first step HYD process or even upgrade the

pyrolysis oils to a renewable gasoline in one step HYD; model compounds study, which could provide kinetics model to improve the HYD conditions. Nevertheless, the concept established in this work opens up a new opportunity for the conversion of lignin pyrolysis oils (which are the major parts of water insoluble product of pyrolysis of whole biomass) to the renewable gasoline.

Chapter 11: OVERALL CONCLUSIONS

The thesis projects accomplished conversions of biomass and biomass components to petrochemicals and total aliphatic gasoline like products. This thesis work includes three major projects. Biomass is very complicated; to understand the thermal decomposition pathways of biomass, the pyrolytic behaviors of various biomass components including lignin and cellulose as well as whole biomass under different temperatures have been investigated in the first project. For the SW kraft lignin studied, 600 °C was the optimized pyrolysis temperature. For the pyrolysis of cellulose, the yields of pyrolysis oil and char decreased but the yield of gas increased when reactor temperatures increased (400-600 °C), which indicated that the point of primary pyrolysis of cellulose and the secondary decomposition of pyrolysis oil is lower than 400 °C. For the pyrolysis of pinewood, the yield of pyrolysis oil only slightly increased (0.85%) when the thermal treatment increased from 500 to 600 °C, in contrast, the yield of gas increased by 2.55%, which indicated that 500 °C is close to the point of primary pyrolysis of pine wood and secondary decomposition of pyrolysis oil.

Due to complexity and limited volatility, the thermal decomposition products from biomass bring insurmountable obstacles to traditional analysis methods such as GC-MS, UV and FT-IR. Therefore, precise characterization of the whole portion of thermal decomposition products has significant impacts on providing insight into the thermal decomposition pathways and evaluating the upgrading processes. Various NMR methods to characterize different functional groups presented in pyrolysis liquid and solid

products by ^1H , ^{13}C , ^{31}P , 2D-HSQC and solid state ^{13}C -NMR have been introduced in the second project. The ^{31}P -NMR results for the lignin light oil showed that it contained nearly 80 w/w% water and another 10 w/w% methanol, catechol and acetic acid. The large amount of water was attributed to dehydration reactions of lignin during pyrolysis. Based on the results of ^{13}C and ^{31}P -NMR for the heavy oil and lignin, the aliphatic OH, carboxyl and methoxyl group in the lignin are the primary target functional groups to decompose during the pyrolysis, the cleavage of ether bond in the lignin is another primary decomposition during the thermal treatment. On the basis of HSQC-NMR analysis for the pyrolysis oils produced from cellulose, levoglucosan was found as the major component and the content increased from 46 to 53% (detected by quantitative ^{13}C -NMR, the results are shown in percentages of total carbon) with the pyrolysis temperature increased from 400 to 600 °C. Furfural (or other compounds containing furan ring) and phenol were also found as the major components in the cellulose pyrolysis oils. The content of 5-hydroxymethyl-furfural (HMF) decreased at higher thermal treatment temperature, which indicated that HMF could be further decomposed at higher temperature. The analysis of HSQC-NMR for the pine wood pyrolysis oils indicated that levoglucosan is also one of the major components presented in the pyrolysis oils and most of aromatic C-H and aliphatic C-H bonds in the pine wood pyrolysis oils were produced from lignin component.

Nevertheless, the major drawback towards commercialization of pyrolysis oils are their challenging properties including poor volatility, high oxygen content, molecular weight, acidity and viscosity, corrosiveness and cold flow problems. In situ upgrading the

properties of pyrolysis oils during thermal conversion process by employing zeolites has been studied in the third project. The influences of $\text{SiO}_2/\text{Al}_2\text{O}_3$ ratio of H-ZSM-5 zeolites on the properties of pyrolysis oils have been investigated. Based on the results of ^{13}C and ^{31}P -NMR for pyrolysis oils, the use of H-ZSM-5 zeolites during pyrolysis process caused the near complete decomposition of aliphatic hydroxyl and carboxyl groups. With exception of carboxylic acid, the H-ZSM-5 zeolite with a relatively higher $\text{SiO}_2/\text{Al}_2\text{O}_3$ was more effective at the elimination of methoxyl groups, ether bonds and aliphatic C-C bonds, and dehydration of aliphatic hydroxyl groups during pyrolysis. However, the H-ZSM-5 zeolite with very large $\text{SiO}_2/\text{Al}_2\text{O}_3$ mole ratio, such as 280, has only limited effects on the properties of upgraded pyrolysis oil. After the use of zeolite, the pyrolysis oils contain some polyaromatic hydrocarbons and the content decreased with the increasing $\text{SiO}_2/\text{Al}_2\text{O}_3$ mole ratio of zeolite. The upgrading effects of various different zeolites have also been examined. FAU and BEA zeolites could significantly improve the cleavage of methoxyl-aromatic and ether bonds in the lignin and yield a pyrolysis oil that has a ‘gasoline’ range molecular weight. The upgraded pyrolysis oil could be used as the precursor of gasoline and possible substitution of petrochemicals. MFI, FER and MOR zeolites could more efficiently decompose the carboxyl groups, which will reduce the acidity of pyrolysis oils and make it more suitable for the usage as biofuel. Further hydrogenation of pyrolysis oils to total aliphatic gasoline like products by heterogeneous catalysis in “green medium” – water have also been studied in the third projects.

The highlights of this thesis work are presented as below:

- ❖ Investigations on pyrolytic behaviors of various biomasses and biomass components at different temperatures. The yields for water insoluble liquid products—heavy oils are from 10-50 wt% and could be used as precursor of bio-fuel and bio-chemical. The water-soluble liquid products—light oils contain >60 wt% of water and other organic products including methanol, catechol and acetic acid etc., which are ready to use bio-chemicals. The solid products have high-energy yield ~50% and HHVs (>31MJ/kg), which are higher than many commercial coals (20-30 MJ/kg) and could be used as bio-coal. The process of producing bio-coal—torrefaction was also accomplished, which could provide another type of bio-energy to reduce the CO₂ emissions.

- ❖ Various innovations of characterization of pyrolysis products have been accomplished, including the first reported efforts to analyze whole portion of pyrolysis oils by HSQC and characterize various solid products by NMR. Several chemical shifts databases for the components presented in the pyrolysis oils were created to facilitate the characterizations by NMR. Four different types of protons, eight types of hydroxyl groups, fifteen different carbons and thirty different C-H bonds in the whole portion of pyrolysis oil could be analyzed by NMR. The first research work on in situ NMR characterization of pyrolysis oil during accelerated aging process has also been investigated.

- ❖ By employing zeolites, one-step thermal conversion of lignin to petrochemicals has been accomplished. The yield of this conversion is ~20 wt% and the top three abundant products are 3-methyl-phenol, catechol and 2, 4-methyl-phenol. This is the first reported efforts to upgrade lignin to the gasoline range low molecular weight (~70-140 g/mol) products in one step. Another breakthrough on hydrogenation of lignin pyrolysis oil, which is the most difficult part to be upgraded, in “Green solvent”—water to produce renewable gasoline has also been examined.

Chapter 12: RECOMMENDATIONS FOR FUTURE WORK

Several other studies might be conducted to further investigate the thermal conversion of biomass and its components to the fuel and chemicals. Some particularly attractive options are as follows:

- ❖ To fully characterize whole biomass pyrolysis products, the other two biomass components—hemicellulose and tannin that is abundant in barks would be necessary to investigate. The NMR chemical shifts databases for the pyrolysis oils produced from these two components should be created to facilitate the assignments in various NMR methods including ^1H , ^{13}C and HSQC-NMR.
- ❖ To provide insight into the upgrading mechanism and evaluate zeolites, more detailed characterizations of zeolites including solid state NMR, XRD, SEM, acid sites measurement and recycle times are recommended.
- ❖ To accomplish one-step conversion of biomass into total aliphatic gasoline like products, pyrolysis of biomass under hydrogen pressure and employing zeolite-supported noble metal catalysts should be examined. Novel catalyst synthesis and quantum chemical simulation of catalytic process would be interesting.

APPENDIX A: TORREFACTION OF LOBLOLLY PINE*

A.1 Introduction

Worldwide energy consumption is predicted to increase by ~50% by 2025.⁵ The carbon dioxide emissions from the consumption of fossil fuels have grown at an average rate of ~2% per year, and the rate continues to increase. Coal is the most carbon-intensive of the fossil fuels and its global share of carbon dioxide emissions, are projected to be almost 46% by 2035.²⁰⁸ Growing concerns about the effects of carbon dioxide emissions from fossil fuels call for sustainable energy sources, such as biomass, because of its carbon neutrality, relative abundance and non-food competition.⁶ Several challenging properties of biomass including low heating value, low energy density, high moisture content, hygroscopic nature, and soot formation during combustion limit its usage as a resource for the bio-energy.²⁰⁹ The charcoal-making process is one of the traditional methods to upgrade the biomass. However, only about 20-55% of the energy in the original raw material is retained in charcoal.²¹⁰ In contrast, a thermal treatment process in an inert atmosphere, known as, torrefaction can address some of the above limitations and provide a relatively higher energy yield.²¹¹

Many researchers have examined the torrefaction of biomass. For example, Pentananunt et al.²¹⁰ found that torrefied wood has significantly less soot generation during combustion and has a relatively faster rate of combustion than the wood. The

* The full data of this research was accepted for publication in Green Chemistry, 2012. It is entitled as "Torrefaction of Loblolly pine". The other author is Arthur J. Ragauskas from the Institute of Paper Science and Technology and School of Chemistry and Biochemistry at Georgia Institute of Technology. Reproduced by permission of The Royal Society of Chemistry. <http://pubs.rsc.org/en/content/articlelanding/2012/gc/c1gc15570a>

weight and energy yields of torrefaction of wood at 250-270 °C for 2-3 hours are 66.7-83.3% and 76.5-89.6%, respectively. Prins et al.^{212, 213} examined the weight loss kinetics and analyzed the products of torrefaction of several bioresources including beech, willow, larch and wheat straw. They proposed torrefaction of wood is a two step reaction, a fast initial step leads to the decomposition of hemicelluloses, and the slower subsequent reaction represents cellulose decomposition. Yan et al.²¹⁴ examined wet torrefaction (hot compressed water, 200-260 °C, ~20 min) and the dry torrefaction (nitrogen, 250-300 °C ~80 min) of Loblolly pine. For the dry torrefaction, the mass yields of solid product were 61-84%, and energy densities increased by 7-21%. They also found that the decomposition of hemicellulose occurs more readily during wet torrefaction than dry torrefaction. Chen et al.¹⁰⁵ torrefied four kinds of biomass, including bamboo, willow, coconut shell and wood (i.e. *Ficusbenjamina* L.). Similarly, with the results proposed by Prins et al.^{212, 213}, they also found that there are two different torrefaction processes, regardless of the biomass resource, involving a light torrefaction, which involved significant decomposition of hemicellulose, at 240 °C. Subsequent severe torrefaction of cellulose occurs at 275 °C. Pimchuai et al.²⁰⁹ examined the torrefaction of rice husks and four other agriculture residues (i.e., sawdust, peanut husks, bagasse, and water hyacinth) at 250-300 °C for 1-2 h. They found that compared to the raw biomass, higher heating values (HHV) were obtained for the torrefied biomass by 7-40%. The hydrophobic properties of torrefied biomass were markedly improved with respect to the starting material which means the torrefied biomass absorbs much less moisture during storage. Chen et al.¹⁰⁴ torrefied some basic biomass constituents, including hemicellulose, cellulose, lignin, xylan, dextran, xylose and glucose at 230, 260 and 290 °C by

thermogravimetry. They indicated that torrefaction at 230 °C has a relatively slight impact on decomposing basic biomass components, 260 °C caused a certain amount of hemicellulose decomposed, and at 290 °C a large amount of decomposition of hemicellulose and cellulose occurred. Brosse et al.¹³⁴ thermally treated beech heartwood (*Fagussylvatica*) at 230 °C for 7h, they indicated that thermally treatment of wood Would degrade the hemicelluloses and cleave the β -aryl-ether linkages in lignin, and condensed aromatic units will be formed by condensation reactions of lignin and cellulose decomposition products. Pastorova et al.²¹⁵ also reported a similar highly condensed aromatic polymer. They examined the structure of char produced by thermal treatment of cellulose at 190-390 °C and concluded that disproportionation occurred above ~310 °C and lead to a highly condensed aromatic polymer.

In summary, although process parameters of biomass torrefaction have been studied the chemistry of torrefaction on wood and other bioresources has received little attention. The goal of this chapter is examine the efforts of torrefaction at different temperatures and times on the chemical structures of torrefied wood derived from Loblolly pine. This was accomplished by using solid-state cross-polarization/magic angle spinning (CP/MAS) ¹³C nuclear magnetic resonance (NMR) spectroscopy and carbohydrate analysis.

A.2 Experimental section

Please see the sections 3.1; 3.2.3.2; 3.3.5; 3.3.6 and 3.3.7.6 of this dissertation for the details.

A.3 Results and Discussion

The mass yields, HHVs, energy densification ratios and energy yields of the torrefied wood samples produced from Loblolly pine wood at 250 and 300 °C are summarized in Table 45. The results indicate that the torrefied wood has a higher HHV than the original wood. Compare to the HHV (20.16 MJ/kg) of dried wood (dried at 75 °C, 48 h), the HHV of torrefied wood increase by 60% after torrefaction at 300 °C for 4 h, which (32.34 MJ/kg) is higher than many commercial coals, such as, anthracite coal (31.84 MJ/kg) and Pittsburgh seam coal (31.75 MJ/kg), and much higher than Converse School — Sub C coal (21.67 MJ/kg), German Braunkohle lignite (25.10 MJ/kg), and Northumberland No.81/2 Sem. Anth. Coal (24.73 MJ/kg).²¹⁶ For the torrefied wood samples produced at 250 °C, with an increase residence time from 0.25 to 8 h, the mass yield and energy yield decreased linearly from 94.97% to 64.36% and 99.79% to 79.12% respectively. In contrast, the HHV increased from 21.22 to 24.78 MJ/kg. The mass yields of torrefied wood samples decreased significantly from 250 to 300 °C as there was less than 50 wt% of biomass after torrefaction at 300 °C, which is similar with the literature reports.^{104, 209, 217} Those dramatic differences between the torrefaction at 250 and 300 °C could be explained by one of the major wood components — cellulose being decomposed near 300 °C.^{104, 183, 209, 212, 213, 217} In contrast with the energy yields of torrefied wood samples produced at 250 °C, the energy yields increased with an increased torrefaction time at 300 °C, which indicate that prolong treatment of wood at 300 °C will produce a material with a much higher energy density. These results indicate that the torrefaction of Loblolly pine wood at 250 °C for 4 h is the optimal condition, which will produce a torrefied wood sample with an HHV of 24.06 MJ/kg and a relatively high energy yield of

81.29%, prolonged treatment only slightly increased the HHV of the torrefied wood.

The carbohydrate profiles of each torrefied wood sample are shown in Table 46. For the torrefied wood samples produced at 250 °C the content of glucose in those samples varied less than 20%. In contrast, the contents of arabinose, galactose, xylose and mannose linearly decreased with an increase in torrefaction time. The contents of arabinose and galactose approached zero and the contents of xylose and mannose decreased by almost 90% after a 4 h torrefaction at 250 °C. Therefore at the optimal conditions, almost all the hemicelluloses will be decomposed, whereas the cellulose remained largely intact. In contrast, the contents of glucose in the torrefied wood samples produced at 300 °C dramatically decreased. Employing a 4 h torrefaction treatment, the contents of all the monosaccharides were nondetect (see Table 46) which indicates that all cellulose and hemicellulose in the wood were decomposed.

Table 45. Influence of the temperatures and residence times on the mass yield, HHV, energy densification ratio and energy yield of the torrefied Loblolly pine wood.

Temperature (°C)	Time (h)	Mass yield ^a (%)	HHV (MJ/kg)	Energy densification ratio ^b	Energy yield ^c (%)
Original pine ^d	-	-	20.16	-	-
250	0.25	94.79	21.22	1.05	99.79
	0.50	86.19	21.87	1.08	93.48
	1.00	80.77	22.18	1.10	88.88
	2.00	75.46	22.61	1.12	84.62
	4.00	68.11	24.06	1.19	81.29
	6.00	66.19	24.40	1.21	80.11
	8.00	64.36	24.78	1.23	79.12
300	0.50	45.74	23.10	1.15	52.41
	1.00	40.36	-	-	-
	2.00	37.61	-	-	-
	4.00	36.65	32.34	1.60	58.79

^aMass yield=mass of dried torrefied wood/mass of dried wood*100%

^b Energy densification ratio=HHV of dried torrefied wood/HHV of dried wood

^c Energy yield=mass yield*energy densification ratio

^dThe original Loblolly pine wood sample was dried at 75 °C for 48 h before the analysis of higher heating value.

Table 46. Influence of the temperatures and residence times on the carbohydrates contents of the torrefied Loblolly pine wood.^a

T (°C)	Time (h)	glucose	arabinose	galactose	xylose	mannose	Klason lignin or char	Sum
Original wood	-	47.89	1.13	2.35	6.20	10.60	28.50 ^b	96.67
250	0.25	46.27	0.66	1.94	4.64	9.19	32.20	94.90
	0.50	48.42	0.28	1.18	2.89	6.55	37.25	96.57
	1.00	49.37	0.16	0.75	2.10	4.64	41.62	98.64
	2.00	47.71	0.00	0.38	1.26	2.83	44.53	96.71
	4.00	44.24	0.00	0.10	0.50	1.15	52.33	98.32
	6.00	43.88	0.00	0.00	0.46	1.00	55.40	100.74
	8.00	38.31	0.00	0.00	0.22	0.49	57.80	96.82
300	0.50	22.34	0.00	0.14	0.49	1.22	73.39	97.58
	4.00	0.00	0.00	0.00	0.00	0.00	99.43	99.43

^a the results were shown as the weight percentage of sample.

^b the content of the acid soluble lignin is less than 0.7% in the original wood, which is not reported in this table.

To fully characterize the chemical structures of the torrefied wood and to understand the chemical changes occurring, CP/MAS ¹³C-NMR was used to analyze the starting and torrefied wood samples as shown in Figures 78 and 79. The NMR chemical

shifts assignments of pine based on literature values are shown in Table 47.^{150, 218-221}

The relative signal intensities of the carbonyl and carboxyl groups slightly increased after torrefaction at 250 °C, which indicates the formation of those functional groups during the torrefaction.¹³⁴ The peak centered at ~148-153 ppm represents aromatic C-O bonds (ether bonds at ~153 ppm and free phenolic hydroxyl groups at ~148 ppm) in lignin, and during torrefaction, this peak shift from ~152 to ~148 ppm, and the intensity of the peak increases with an increased thermal treatment time, which indicates that there are more free phenolic hydroxyl groups after the torrefaction of wood. On the basis of the proposed cleavage pathway of ether bonds (see Figure 80) in lignin during the thermal treatment, the cleavage of ether bonds will produce phenolic hydroxyl groups.^{134, 49} Considering the results of CP/MAS ¹³C-NMR, the increasing intensity of the peak at ~148 ppm indicates that aryl ether bonds in lignin, such as β-O-aryl the linkages, were cleaved during the torrefaction. The signal intensities of aromatic C-C bonds and aromatic C-H bonds in lignin also increased after the torrefaction, which could be attributed to several factors, including the cleavage of lignin ether bonds during the thermal treatment which could re-condense to form aromatic C-C bonds.⁴⁹ The thermal treatment of wood could also converted some carbohydrates to the aromatic C-C and C-H bonds, the proposed possible pathway of this conversion is shown in Figure 80.^{134, 222} The intensity of crystalline C-4 of cellulose at ~89 ppm decreased upon thermal treatment which was in contrast to the intensity of the signal assigned to amorphous C-4 cellulose at ~84 ppm. The latter signal increased with an increasing thermal treatment time from 4-8 h at 250 °C. However, due to unknown effects of the overlapping signals from

hemicellulose and lignin side chains this observation can be attributed, only in part, as indicative of a reduction in the crystallinity of cellulose after the thermal treatment of wood. Ates et al.²²³ used FT-IR to determine the relative crystallinity indexes of the heat-treated (at 130, 180 and 230 °C) Calabrian pine wood and reported a similar result.

An increasing intensity of the methoxyl group signal in lignin appeared after the thermal treatment of wood which an enrichment of this functional group. The intensity of the CH₂ carbons in the aliphatic chain (~32 ppm) is almost intact after the torrefaction, which indicates that the decomposition of aliphatic chain (in fatty acids and tannins) at 250 °C is very limited. The methyl carbons in hemicellulose acetyl groups were no longer present after the torrefaction at 250 °C for 4 h, which is consistent with our previous results.

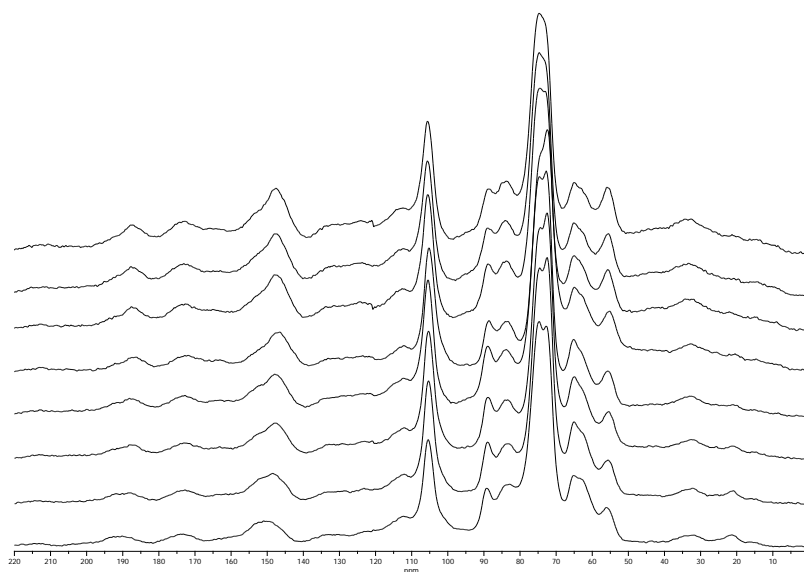


Figure 78. CP/MAS ¹³C-NMR spectra (from bottom to top) of original Loblolly pine wood, torrefied wood samples produced by torrefaction of Loblolly pine wood at 250 °C for 0.25, 0.50, 1.00, 2.00, 4.00, 6.00 and 8.00 hours.

Table 47. NMR chemical shifts assignments of wood.^{150, 218-221}

Functional groups	Chemical shift (ppm)
Carbonyl	220-187
Carboxyl	173
Aromatic C-3 or C-4 in guaiacyl lignin (etherified)	153
Aromatic C-3 or C-4 bond in guaiacyl lignin with free phenolic groups	148
Aromatic C-C bond in lignin	131-137
Aromatic C-H bond in lignin (G6 of lignin)	120
Aromatic C-H bond in lignin (G5 of lignin)	115
Aromatic C-H bond in lignin (G2 of lignin)	112
C-1 of cellulose ^a	105
Crystalline C-4 of cellulose ^{a, b}	89
Amorphous C-4 of cellulose ^{a, b}	84
C-2,C-3,C-5 of cellulose ^{a, b}	75-72
C-6 of cellulose ^{a, b}	65-62
Methoxyl in lignin	56
Methylene carbons CH ₂ in aliphatic chain (fatty acids and tannins) ^b	32
Methyl carbons CH ₃ in hemicellulose acetyl groups ^b	23

^a signals for hemicellulose overlap with those peaks.

^b signals for lignin overlap with those peaks.

The CP/MAS ^{13}C -NMR spectra of torrefied wood samples produced by torrefaction of Loblolly pine wood at 250 and 300 °C are compared in Figure 79. Significant differences of torrefied wood produced at the different temperatures were observed, for the same treatment time ~30 min, the torrefied wood produced at 300 °C shows much higher intensities of carbonyl, carboxyl, aromatic carbons and methoxyl groups than the torrefied wood produced at 250 °C. In contrast, the methyl carbons in hemicellulose acetyl groups were almost completely decomposed. All of those results indicate that the decomposition reactions during the torrefaction were enhanced at higher reactor temperatures.^{104, 183, 209, 212, 213, 217} The spectra shows that, after torrefaction at 300 °C for 4 h, the cellulose and hemicellulose in the wood were completely eliminated, the residue contains a large amount of carbonyl groups, aromatic carbons and methoxyl groups, which represent to the complex condensed aromatics, those aromatics were linked with aliphatic C-O bonds (60-100 ppm) and C-C bonds (10-20 ppm). A similar highly condensed aromatic polymer has been reported by Pastorova et al.²¹⁵ They examined the structure of char produced by thermal treatment of cellulose at 190-390 °C and concluded that disproportionation occurred above ~310 °C and lead to a highly condensed aromatic polymer. On the basis of literature reports,^{58, 117, 118, 134, 222, 224-228} the possible pathway of decomposition of major wood components and the formation of new functional groups and condensed aromatics during the torrefaction shown in Figure 37.

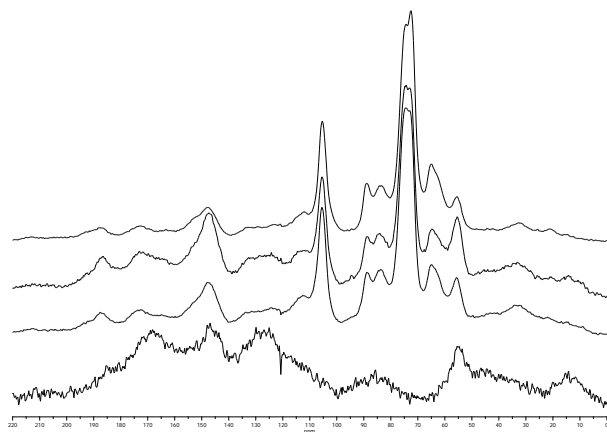


Figure 79. CP/MAS ^{13}C -NMR spectra (from bottom to top) of torrefied Loblolly pine wood samples produced by torrefaction of Loblolly pine wood at 300 °C for 4.00 hours, 250 °C for 4.00 hours, 300 °C for 0.50 hours and 250 °C for 0.50 hours.

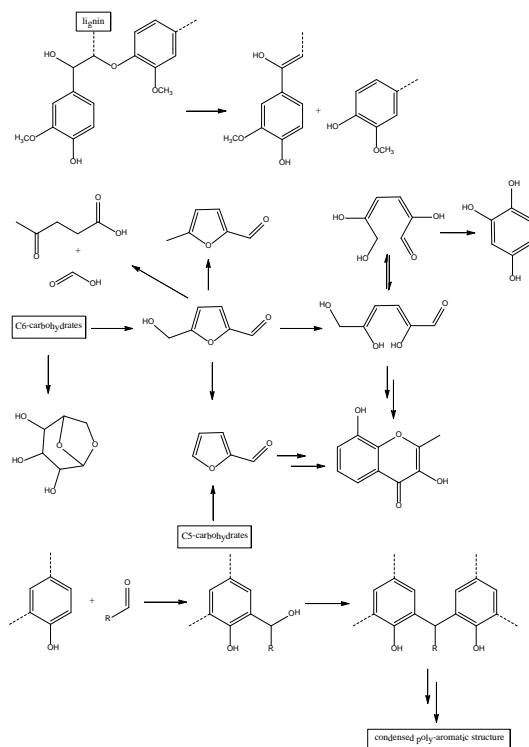


Figure 80. Hypothesized pathways of decomposition of major wood components and the formation of new functional groups and condensed aromatic units during the torrefaction.^{58, 117, 118, 134, 222, 224-228}

A.4 Conclusions

The torrefaction of Loblolly pine wood was accomplished at 250 and 300 °C. The mass yields, HHVs and energy yields of torrefied wood are clearly impacted by the torrefaction temperature and time. Torrefaction at 250 °C for 4 h was found as the optimal condition, which produced a torrefied wood that had a relatively high energy yield of 81.29% and a HHV of 24.06 MJ/kg, which is comparable with several commercial coals. In addition, the carbohydrate analysis and CP/MAS ^{13}C -NMR spectra shows that the hemicellulose in the torrefied wood produced by torrefaction of wood at 250 °C for 4 h was almost completely decomposed, however, the cellulose and lignin were only slightly affected. Torrefaction of Loblolly pine at 300 °C for 4 h completely eliminated all the cellulose and hemicellulose in the original wood and the thermal residue had a complex aromatic structure and a very high HHV (32.34 MJ/kg).

APPENDIX B: COPYRIGHT PERMISSIONS

B.1 Permissions from Energy & Fuels

11/28/12

Rightslink® by Copyright Clearance Center



RightsLink®

Home

Account
Info

Help



ACS Publications
High quality High impact.

Title: NMR Characterization of
Pyrolysis Oils from Kraft Lignin
Author: Haoxi Ben and Arthur J.
Ragauskas
Publication: Energy & Fuels
Publisher: American Chemical Society
Date: May 1, 2011
Copyright © 2011, American Chemical Society

Logged in as:
Haoxi Ben
Account #: 3000589851

LOGOUT

Quick Price Estimate

Permission for this particular request is granted for print and electronic formats, and translations, at no charge. Figures and tables may be modified. Appropriate credit should be given. Please print this page for your records and provide a copy to your publisher. Requests for up to 4 figures require only this record. Five or more figures will generate a printout of additional terms and conditions. Appropriate credit should read: "Reprinted with permission from {COMPLETE REFERENCE CITATION}, Copyright {YEAR} American Chemical Society." Insert appropriate information in place of the capitalized words.

I would like to...

reuse in a Thesis/Dissertation

This service provides permission for reuse only. If you do not have a copy of the article you are using, you may copy and paste the content and reuse according to the terms of your agreement. Please be advised that obtaining the content you license is a separate transaction not involving Rightslink.

Requestor Type

Author (original work)

Portion

Full article

Format

Print and Electronic

Will you be translating?

No

Select your currency

USD - \$

Quick Price

Click Quick Price

QUICK PRICE

CONTINUE

To request permission for a type of use not listed, please contact [the publisher](#) directly.

Copyright © 2012 Copyright Clearance Center, Inc. All Rights Reserved. [Privacy statement](#). Comments? We would like to hear from you. E-mail us at customercare@copyright.com.



RightsLink®

[Home](#)[Account Info](#)[Help](#)ACS Publications
High quality. High impact.

Title: NMR Characterization of
Pyrolysis Oils from Kraft Lignin
Author: Haoxi Ben and Arthur J.
Ragauskas
Publication: Energy & Fuels
Publisher: American Chemical Society
Date: May 1, 2011
Copyright © 2011, American Chemical Society

Logged in as:
Haoxi Ben

[LOGOUT](#)**PERMISSION/LICENSE IS GRANTED FOR YOUR ORDER AT NO CHARGE**

This type of permission/license, instead of the standard Terms & Conditions, is sent to you because no fee is being charged for your order. Please note the following:

- Permission is granted for your request in both print and electronic formats, and translations.
- If figures and/or tables were requested, they may be adapted or used in part.
- Please print this page for your records and send a copy of it to your publisher/graduate school.
- Appropriate credit for the requested material should be given as follows: "Reprinted (adapted) with permission from (COMPLETE REFERENCE CITATION). Copyright (YEAR) American Chemical Society." Insert appropriate information in place of the capitalized words.
- One-time permission is granted only for the use specified in your request. No additional uses are granted (such as derivative works or other editions). For any other uses, please submit a new request.

[BACK](#)[CLOSE WINDOW](#)

Copyright © 2012 Copyright Clearance Center, Inc. All Rights Reserved. [Privacy statement](#).
Comments? We would like to hear from you. E-mail us at customer@copyright.com



RightsLink®

[Home](#)
[Account Info](#)
[Help](#)

ACS Publications
 High quality High impact.

Title: Pyrolysis of Kraft Lignin with Additives
Author: Haoxi Ben and Arthur J. Ragauskas
Publication: Energy & Fuels
Publisher: American Chemical Society
Date: Oct 1, 2011
 Copyright © 2011, American Chemical Society

Logged in as:
 Haoxi Ben
 Account #: 3000589851

[LOGOUT](#)

Quick Price Estimate

Permission for this particular request is granted for print and electronic formats, and translations, at no charge. Figures and tables may be modified. Appropriate credit should be given. Please print this page for your records and provide a copy to your publisher. Requests for up to 4 figures require only this record. Five or more figures will generate a printout of additional terms and conditions. Appropriate credit should read: "Reprinted with permission from {COMPLETE REFERENCE CITATION}, Copyright {YEAR} American Chemical Society," Insert appropriate information in place of the capitalized words.

I would like to...

reuse in a Thesis/Dissertation

Requestor Type

Author (original work)

Portion

Full article

Format

Print and Electronic

Will you be translating?

No

Select your currency

USD - \$

Quick Price

Click Quick Price

This service provides permission for reuse only. If you do not have a copy of the article you are using, you may copy and paste the content and reuse according to the terms of your agreement. Please be advised that obtaining the content you license is a separate transaction not involving Rightslink.

[QUICK PRICE](#)
[CONTINUE](#)

To request permission for a type of use not listed, please contact [the publisher](#) directly.

Copyright © 2012 Copyright Clearance Center, Inc. All Rights Reserved. [Privacy statement](#). Comments? We would like to hear from you. E-mail us at customercare@copyright.com

**RightsLink®**[Home](#)[Account Info](#)[Help](#)**ACS Publications**
High quality. High impact.

Title: Pyrolysis of Kraft Lignin with Additives
Author: Haoxi Ben and Arthur J. Ragauskas
Publication: Energy & Fuels
Publisher: American Chemical Society
Date: Oct 1, 2011
Copyright © 2011, American Chemical Society

Logged in as:
Haoxi Ben[LOGOUT](#)**PERMISSION/LICENSE IS GRANTED FOR YOUR ORDER AT NO CHARGE**

This type of permission/license, instead of the standard Terms & Conditions, is sent to you because no fee is being charged for your order. Please note the following:

- Permission is granted for your request in both print and electronic formats, and translations.
- If figures and/or tables were requested, they may be adapted or used in part.
- Please print this page for your records and send a copy of it to your publisher/graduate school.
- Appropriate credit for the requested material should be given as follows: "Reprinted (adapted) with permission from (COMPLETE REFERENCE CITATION). Copyright (YEAR) American Chemical Society." Insert appropriate information in place of the capitalized words.
- One-time permission is granted only for the use specified in your request. No additional uses are granted (such as derivative works or other editions). For any other uses, please submit a new request.

[BACK](#)[CLOSE WINDOW](#)

Copyright © 2012 Copyright Clearance Center, Inc. All Rights Reserved. [Privacy statement](#).
Comments? We would like to hear from you. E-mail us at customercare@copyright.com



Title: Heteronuclear Single-Quantum Correlation–Nuclear Magnetic Resonance (HSQC–NMR) Fingerprint Analysis of Pyrolysis Oils

Author: Haoxi Ben and Arthur J. Ragauskas

Publication: Energy & Fuels

Publisher: American Chemical Society

Date: Dec 1, 2011

Copyright © 2011, American Chemical Society

Logged in as:

Haoxi Ben

Account #:

3000589851

[LOGOUT](#)

Quick Price Estimate

Permission for this particular request is granted for print and electronic formats, and translations, at no charge. Figures and tables may be modified. Appropriate credit should be given. Please print this page for your records and provide a copy to your publisher. Requests for up to 4 figures require only this record. Five or more figures will generate a printout of additional terms and conditions. Appropriate credit should read: "Reprinted with permission from {COMPLETE REFERENCE CITATION}. Copyright {YEAR} American Chemical Society." Insert appropriate information in place of the capitalized words.

I would like to... ?

reuse in a Thesis/Dissertation

This service provides permission for reuse only. If you do not have a copy of the article you are using, you may copy and paste the content and reuse according to the terms of your agreement. Please be advised that obtaining the content you license is a separate transaction not involving Rightslink.

Requestor Type ?

Author (original work)

Portion ?

Full article

Format ?

Print and Electronic

Will you be translating? ?

No

Select your currency

USD - \$

Quick Price

Click Quick Price

[QUICK PRICE](#)

[CONTINUE](#)

To request permission for a type of use not listed, please contact [the publisher](#) directly.

Copyright © 2012 Copyright Clearance Center, Inc. All Rights Reserved. [Privacy statement](#). Comments? We would like to hear from you. E-mail us at customercare@copyright.com



RightsLink®

[Home](#)[Account Info](#)[Help](#)ACS Publications
High quality. High impact.

Title:

Heteronuclear Single-Quantum
Correlation-Nuclear Magnetic
Resonance (HSQC-NMR)
Fingerprint Analysis of Pyrolysis
Oils

Logged in as:

Haoxi Ben

[LOGOUT](#)

Author:

Haoxi Ben and Arthur J.
Ragauskas

Publication: Energy & Fuels

Publisher: American Chemical Society

Date: Dec 1, 2011

Copyright © 2011, American Chemical Society

PERMISSION/LICENSE IS GRANTED FOR YOUR ORDER AT NO CHARGE

This type of permission/license, instead of the standard Terms & Conditions, is sent to you because no fee is being charged for your order. Please note the following:

- Permission is granted for your request in both print and electronic formats, and translations.
- If figures and/or tables were requested, they may be adapted or used in part.
- Please print this page for your records and send a copy of it to your publisher/graduate school.
- Appropriate credit for the requested material should be given as follows: "Reprinted (adapted) with permission from (COMPLETE REFERENCE CITATION). Copyright (YEAR) American Chemical Society." Insert appropriate information in place of the capitalized words.
- One-time permission is granted only for the use specified in your request. No additional uses are granted (such as derivative works or other editions). For any other uses, please submit a new request.

[BACK](#)[CLOSE WINDOW](#)

Copyright © 2012 Copyright Clearance Center, Inc. All Rights Reserved. [Privacy statement](#).
Comments? We would like to hear from you. E-mail us at customer-care@copyright.com

B.2 Permission from Green Chemistry

11/28/12

Zimbra

Zimbra

hben3@mail.gatech.edu

RE: Permission request to use full article in thesis

From : CONTRACTS-COPYRIGHT (shared) <Contracts-Copyright@rsc.org> Wed, Nov 28, 2012 07:37 AM

Subject : RE: Permission request to use full article in thesis

To : Haoxi 'Ben' <haoxiben@gatech.edu>

Dear Ben

The Royal Society of Chemistry (RSC) hereby grants permission for the use of your paper(s) specified below in the printed and microfilm version of your thesis. You may also make available the PDF version of your paper(s) that the RSC sent to the corresponding author(s) of your paper(s) upon publication of the paper(s) in the following ways: in your thesis via any website that your university may have for the deposition of theses, via your university's Intranet or via your own personal website. We are however unable to grant you permission to include the PDF version of the paper(s) on its own in your institutional repository. The Royal Society of Chemistry is a signatory to the STM Guidelines on Permissions (available on request).

Please note that if the material specified below or any part of it appears with credit or acknowledgement to a third party then you must also secure permission from that third party before reproducing that material.

Please ensure that the thesis states the following:

Reproduced by permission of The Royal Society of Chemistry

and include a link to the paper on the Royal Society of Chemistry's website.

Please ensure that your co-authors are aware that you are including the paper in your thesis.

Regards

Gill Cockhead
Publishing Contracts & Copyright Executive

Gill Cockhead (Mrs), Publishing Contracts & Copyright Executive
Royal Society of Chemistry, Thomas Graham House
Science Park, Milton Road, Cambridge CB4 0WF, UK
Tel +44 (0) 1223 432134, Fax +44 (0) 1223 423623
<http://www.rsc.org>

—Original Message—

<https://mail.gatech.edu/zimbra/h/printmessage?id=95623>

1/3

11/28/12

Zimbra

From: Ben, Haoxi [mailto:haoxiben@gatech.edu]
Sent: 28 November 2012 06:30
To: CONTRACTS-COPYRIGHT (shared)
Cc: customercare@copyright.com
Subject: Permission request to use full article in thesis

Hi,

I am the first author of this publication and I am preparing my PhD dissertation for Georgia Institute of Technology, Atlanta, GA.

I would very much appreciate your permission to use the following material:

Title:

Torrefaction of Loblolly pine

Author:

Haoxi Ben, Arthur J. Ragauskas

Publication:

Green Chemistry

Thank you very much for your help!

Kind regards:

Haoxi Ben

—

Ben, Haoxi
Graduate Student
School of Chemistry and Biochemistry
Institute of Paper Science and Technology Georgia Institute of Technology IPST 450J
Phone, 404-894-9557 Cell Phone, 404-538-1896

DISCLAIMER:

This communication (including any attachments) is intended for the use of the addressee only and may contain confidential, privileged or copyright material. It may not be relied upon or disclosed to any other person without the consent of the RSC. If you have received it in error, please contact us immediately. Any advice given by the RSC has been carefully formulated but is necessarily based on the information available, and the RSC cannot be held responsible for accuracy or completeness. In this respect, the RSC owes

<https://mail.gatech.edu/zimbra/h/printmessage?id=95623>

2/3

11/28/12

Zimbra

no duty of care and shall not be liable for any resulting damage or loss. The RSC acknowledges that a disclaimer cannot restrict liability at law for personal injury or death arising through a finding of negligence. The RSC does not warrant that its emails or attachments are Virus-free: Please rely on your own screening. The Royal Society of Chemistry is a charity, registered in England and Wales, number 207890 - Registered office: Thomas Graham House, Science Park, Milton Road, Cambridge CB4 0WF

<https://mail.gatech.edu/zimbra/h/printmessage?id=95623>

3/3

Acknowledgements to be used by RSC authors

Authors of RSC books and journal articles can reproduce material (for example a figure) from the RSC publication in a non-RSC publication, including theses, without formally requesting permission providing that the correct acknowledgement is given to the RSC publication. This permission extends to reproduction of large portions of text or the whole article or book chapter when being reproduced in a thesis.

The acknowledgement to be used depends on the RSC publication in which the material was published and the form of the acknowledgements is as follows:

- For material being reproduced from an article in *New Journal of Chemistry* the acknowledgement should be in the form:
 - [Original citation] - Reproduced by permission of The Royal Society of Chemistry (RSC) on behalf of the Centre National de la Recherche Scientifique (CNRS) and the RSC
- For material being reproduced from an article *Photochemical & Photobiological Sciences* the acknowledgement should be in the form:
 - [Original citation] - Reproduced by permission of The Royal Society of Chemistry (RSC) on behalf of the European Society for Photobiology, the European Photochemistry Association, and RSC
- For material being reproduced from an article in *Physical Chemistry Chemical Physics* the acknowledgement should be in the form:
 - [Original citation] - Reproduced by permission of the PCCP Owner Societies
- For material reproduced from books and any other journal the acknowledgement should be in the form:
 - [Original citation] - Reproduced by permission of The Royal Society of Chemistry

The acknowledgement should also include a hyperlink to the article on the RSC website.

The form of the acknowledgement is also specified in the RSC agreement/licence signed by the corresponding author.

Except in cases of republication in a thesis, this express permission does not cover the reproduction of large portions of text from the RSC publication or reproduction of the whole article or book chapter.

A publisher of a non-RSC publication can use this document as proof that permission is granted to use the material in the non-RSC publication.

B.3 Permission from RSC Advances

11/28/12

Zimbra

Zimbra

hben3@mail.gatech.edu

RE: Permission request to use full article in thesis

From : CONTRACTS-COPYRIGHT (shared) <Contracts-Copyright@rsc.org> Wed, Nov 28, 2012 07:37 AM

Subject : RE: Permission request to use full article in thesis

To : Haoxi 'Ben' <haoxiben@gatech.edu>

Dear Ben

The Royal Society of Chemistry (RSC) hereby grants permission for the use of your paper(s) specified below in the printed and microfilm version of your thesis. You may also make available the PDF version of your paper(s) that the RSC sent to the corresponding author(s) of your paper(s) upon publication of the paper(s) in the following ways: in your thesis via any website that your university may have for the deposition of theses, via your university's Intranet or via your own personal website. We are however unable to grant you permission to include the PDF version of the paper(s) on its own in your institutional repository. The Royal Society of Chemistry is a signatory to the STM Guidelines on Permissions (available on request).

Please note that if the material specified below or any part of it appears with credit or acknowledgement to a third party then you must also secure permission from that third party before reproducing that material.

Please ensure that the thesis states the following:

Reproduced by permission of The Royal Society of Chemistry

and include a link to the paper on the Royal Society of Chemistry's website.

Please ensure that your co-authors are aware that you are including the paper in your thesis.

Regards

Gill Cockhead
Publishing Contracts & Copyright Executive

Gill Cockhead (Mrs), Publishing Contracts & Copyright Executive
Royal Society of Chemistry, Thomas Graham House
Science Park, Milton Road, Cambridge CB4 0WF, UK
Tel +44 (0) 1223 432134, Fax +44 (0) 1223 423623
<http://www.rsc.org>

<https://mail.gatech.edu/zimbra/h/printmessage?id=95622>

1/3

11/28/12

Zimbra

-----Original Message-----

From: Ben, Haoxi [mailto:haoxiben@gatech.edu]
Sent: 28 November 2012 05:00
To: CONTRACTS-COPYRIGHT (shared)
Cc: customercare@copyright.com
Subject: Permission request to use full article in thesis

Hi,

I am the first author of this publication and I am preparing my PhD dissertation for Georgia Institute of Technology, Atlanta, GA.

I would very much appreciate your permission to use the following material:

Article citation: RSC Adv., 2012, 2 (33), 12892 - 12898

Title: One step thermal conversion of lignin to the gasoline range liquid products by using zeolites as additives

Thank you very much for your help!

Kind regards:

Haoxi Ben

—

Ben, Haoxi
Graduate Student
School of Chemistry and Biochemistry
Institute of Paper Science and Technology Georgia Institute of Technology IPST 450J
Phone, 404-894-9557 Cell Phone, 404-538-1896

DISCLAIMER:

This communication (including any attachments) is intended for the use of the addressee only and may contain confidential, privileged or copyright material. It may not be relied upon or disclosed to any other person without the consent of the RSC. If you have received it in error, please contact us immediately. Any advice given by the RSC has been carefully formulated but is necessarily based on the information available, and the RSC cannot be held responsible for accuracy or completeness. In this respect, the RSC owes no duty of care and shall not be liable for any resulting damage or loss. The RSC acknowledges that a disclaimer cannot restrict liability at law for personal injury or death arising through a finding of negligence. The RSC does not warrant that its emails or attachments are Virus-free: Please rely on your own screening. The Royal Society of Chemistry is a charity, registered in England and Wales, number 207890 - Registered office: Thomas Graham House, Science Park, Milton Road, Cambridge CB4 0WF

Acknowledgements to be used by RSC authors

Authors of RSC books and journal articles can reproduce material (for example a figure) from the RSC publication in a non-RSC publication, including theses, without formally requesting permission providing that the correct acknowledgement is given to the RSC publication. This permission extends to reproduction of large portions of text or the whole article or book chapter when being reproduced in a thesis.

The acknowledgement to be used depends on the RSC publication in which the material was published and the form of the acknowledgements is as follows:

- For material being reproduced from an article in *New Journal of Chemistry* the acknowledgement should be in the form:
 - [Original citation] - Reproduced by permission of The Royal Society of Chemistry (RSC) on behalf of the Centre National de la Recherche Scientifique (CNRS) and the RSC
- For material being reproduced from an article *Photochemical & Photobiological Sciences* the acknowledgement should be in the form:
 - [Original citation] - Reproduced by permission of The Royal Society of Chemistry (RSC) on behalf of the European Society for Photobiology, the European Photochemistry Association, and RSC
- For material being reproduced from an article in *Physical Chemistry Chemical Physics* the acknowledgement should be in the form:
 - [Original citation] - Reproduced by permission of the PCCP Owner Societies
- For material reproduced from books and any other journal the acknowledgement should be in the form:
 - [Original citation] - Reproduced by permission of The Royal Society of Chemistry

The acknowledgement should also include a hyperlink to the article on the RSC website.

The form of the acknowledgement is also specified in the RSC agreement/licence signed by the corresponding author.

Except in cases of republication in a thesis, this express permission does not cover the reproduction of large portions of text from the RSC publication or reproduction of the whole article or book chapter.

A publisher of a non-RSC publication can use this document as proof that permission is granted to use the material in the non-RSC publication.

B.4 Permission from ChemSusChem

Rightslink Printable License

<https://s100.copyright.com/App/PrintableLicenseFrame.jsp?publisherID=...>

JOHN WILEY AND SONS LICENSE TERMS AND CONDITIONS

Nov 04, 2012

This is a License Agreement between Haoxi Ben ("You") and John Wiley and Sons ("John Wiley and Sons") provided by Copyright Clearance Center ("CCC"). The license consists of your order details, the terms and conditions provided by John Wiley and Sons, and the payment terms and conditions.

All payments must be made in full to CCC. For payment instructions, please see information listed at the bottom of this form.

License Number	3022220988034
License date	Nov 04, 2012
Licensed content publisher	John Wiley and Sons
Licensed content publication	ChemSusChem
Book title	
Licensed content author	Haoxi Ben, Arthur J. Ragauskas
Licensed content date	Aug 7, 2012
Start page	1687
End page	1693
Type of use	Dissertation/Thesis
Requestor type	Author of this Wiley article
Format	Print and electronic
Portion	Full article
Will you be translating?	No
Order reference number	
Total	0.00 USD

[Terms and Conditions](#)

TERMS AND CONDITIONS

This copyrighted material is owned by or exclusively licensed to John Wiley & Sons, Inc. or one of its group companies (each a "Wiley Company") or a society for whom a Wiley Company has exclusive publishing rights in relation to a particular journal (collectively "WILEY"). By clicking "accept" in connection with completing this licensing transaction, you agree that the following terms and conditions apply to this transaction (along with the billing and payment terms and conditions established by the Copyright Clearance Center Inc., ("CCC's Billing and Payment terms and conditions"), at the time that you opened your Rightslink account (these are available at any time at <http://myaccount.copyright.com>)

Terms and Conditions

1. The materials you have requested permission to reproduce (the "Materials") are protected by copyright.
2. You are hereby granted a personal, non-exclusive, non-sublicensable, non-transferable, worldwide, limited license to reproduce the Materials for the purpose specified in the licensing process. This license is for a one-time use only with a maximum distribution equal to the number that you identified in the licensing process. Any form of republication granted by this licence must

be completed within two years of the date of the grant of this licence (although copies prepared before may be distributed thereafter). The Materials shall not be used in any other manner or for any other purpose. Permission is granted subject to an appropriate acknowledgement given to the author, title of the material/book/journal and the publisher. You shall also duplicate the copyright notice that appears in the Wiley publication in your use of the Material. Permission is also granted on the understanding that nowhere in the text is a previously published source acknowledged for all or part of this Material. Any third party material is expressly excluded from this permission.

3. With respect to the Materials, all rights are reserved. Except as expressly granted by the terms of the license, no part of the Materials may be copied, modified, adapted (except for minor reformatting required by the new Publication), translated, reproduced, transferred or distributed, in any form or by any means, and no derivative works may be made based on the Materials without the prior permission of the respective copyright owner. You may not alter, remove or suppress in any manner any copyright, trademark or other notices displayed by the Materials. You may not license, rent, sell, loan, lease, pledge, offer as security, transfer or assign the Materials, or any of the rights granted to you hereunder to any other person.

4. The Materials and all of the intellectual property rights therein shall at all times remain the exclusive property of John Wiley & Sons Inc or one of its related companies (WILEY) or their respective licensors, and your interest therein is only that of having possession of and the right to reproduce the Materials pursuant to Section 2 herein during the continuance of this Agreement. You agree that you own no right, title or interest in or to the Materials or any of the intellectual property rights therein. You shall have no rights hereunder other than the license as provided for above in Section 2. No right, license or interest to any trademark, trade name, service mark or other branding ("Marks") of WILEY or its licensors is granted hereunder, and you agree that you shall not assert any such right, license or interest with respect thereto.

5. NEITHER WILEY NOR ITS LICENSORS MAKES ANY WARRANTY OR REPRESENTATION OF ANY KIND TO YOU OR ANY THIRD PARTY, EXPRESS, IMPLIED OR STATUTORY, WITH RESPECT TO THE MATERIALS OR THE ACCURACY OF ANY INFORMATION CONTAINED IN THE MATERIALS, INCLUDING, WITHOUT LIMITATION, ANY IMPLIED WARRANTY OF MERCHANTABILITY, ACCURACY, SATISFACTORY QUALITY, FITNESS FOR A PARTICULAR PURPOSE, USABILITY, INTEGRATION OR NON-INFRINGEMENT AND ALL SUCH WARRANTIES ARE HEREBY EXCLUDED BY WILEY AND ITS LICENSORS AND WAIVED BY YOU.

6. WILEY shall have the right to terminate this Agreement immediately upon breach of this Agreement by you.

7. You shall indemnify, defend and hold harmless WILEY, its Licensors and their respective directors, officers, agents and employees, from and against any actual or threatened claims, demands, causes of action or proceedings arising from any breach of this Agreement by you.

8. IN NO EVENT SHALL WILEY OR ITS LICENSORS BE LIABLE TO YOU OR ANY OTHER PARTY OR ANY OTHER PERSON OR ENTITY FOR ANY SPECIAL, CONSEQUENTIAL, INCIDENTAL, INDIRECT, EXEMPLARY OR PUNITIVE DAMAGES, HOWEVER CAUSED, ARISING OUT OF OR IN CONNECTION WITH THE DOWNLOADING, PROVISIONING, VIEWING OR USE OF THE MATERIALS REGARDLESS OF THE FORM OF ACTION, WHETHER FOR BREACH OF CONTRACT, BREACH OF WARRANTY, TORT, NEGLIGENCE, INFRINGEMENT OR OTHERWISE (INCLUDING, WITHOUT LIMITATION, DAMAGES BASED ON LOSS OF PROFITS, DATA, FILES, USE, BUSINESS OPPORTUNITY OR CLAIMS OF THIRD PARTIES), AND WHETHER OR NOT THE PARTY HAS BEEN ADVISED OF THE POSSIBILITY OF SUCH DAMAGES. THIS LIMITATION SHALL APPLY NOTWITHSTANDING ANY FAILURE OF ESSENTIAL PURPOSE OF ANY LIMITED REMEDY PROVIDED HEREIN.

9. Should any provision of this Agreement be held by a court of competent jurisdiction to be illegal, invalid, or unenforceable, that provision shall be deemed amended to achieve as nearly as possible the same economic effect as the original provision, and the legality, validity and enforceability of the remaining provisions of this Agreement shall not be affected or impaired thereby.

10. The failure of either party to enforce any term or condition of this Agreement shall not constitute a waiver of either party's right to enforce each and every term and condition of this Agreement. No breach under this agreement shall be deemed waived or excused by either party unless such waiver or consent is in writing signed by the party granting such waiver or consent. The waiver by or consent of a party to a breach of any provision of this Agreement shall not

operate or be construed as a waiver of or consent to any other or subsequent breach by such other party.

11. This Agreement may not be assigned (including by operation of law or otherwise) by you without WILEY's prior written consent.

12. Any fee required for this permission shall be non-refundable after thirty (30) days from receipt.

13. These terms and conditions together with CCC's Billing and Payment terms and conditions (which are incorporated herein) form the entire agreement between you and WILEY concerning this licensing transaction and (in the absence of fraud) supersedes all prior agreements and representations of the parties, oral or written. This Agreement may not be amended except in writing signed by both parties. This Agreement shall be binding upon and inure to the benefit of the parties' successors, legal representatives, and authorized assigns.

14. In the event of any conflict between your obligations established by these terms and conditions and those established by CCC's Billing and Payment terms and conditions, these terms and conditions shall prevail.

15. WILEY expressly reserves all rights not specifically granted in the combination of (i) the license details provided by you and accepted in the course of this licensing transaction, (ii) these terms and conditions and (iii) CCC's Billing and Payment terms and conditions.

16. This Agreement will be void if the Type of Use, Format, Circulation, or Requestor Type was misrepresented during the licensing process.

17. This Agreement shall be governed by and construed in accordance with the laws of the State of New York, USA, without regards to such state's conflict of law rules. Any legal action, suit or proceeding arising out of or relating to these Terms and Conditions or the breach thereof shall be instituted in a court of competent jurisdiction in New York County in the State of New York in the United States of America and each party hereby consents and submits to the personal jurisdiction of such court, waives any objection to venue in such court and consents to service of process by registered or certified mail, return receipt requested, at the last known address of such party.

Wiley Open Access Terms and Conditions

All research articles published in Wiley Open Access journals are fully open access: immediately freely available to read, download and share. Articles are published under the terms of the [Creative Commons Attribution Non Commercial License](#), which permits use, distribution and reproduction in any medium, provided the original work is properly cited and is not used for commercial purposes. The license is subject to the Wiley Open Access terms and conditions: Wiley Open Access articles are protected by copyright and are posted to repositories and websites in accordance with the terms of the [Creative Commons Attribution Non Commercial License](#). At the time of deposit, Wiley Open Access articles include all changes made during peer review, copyediting, and publishing. Repositories and websites that host the article are responsible for incorporating any publisher-supplied amendments or retractions issued subsequently. Wiley Open Access articles are also available without charge on Wiley's publishing platform, **Wiley Online Library** or any successor sites.

Use by non-commercial users

For non-commercial and non-promotional purposes individual users may access, download, copy, display and redistribute to colleagues Wiley Open Access articles, as well as adapt, translate, text- and data-mine the content subject to the following conditions:

- The authors' moral rights are not compromised. These rights include the right of "paternity" (also known as "attribution" - the right for the author to be identified as such) and "integrity" (the right for the author not to have the work altered in such a way that the author's reputation or integrity may be impugned).
- Where content in the article is identified as belonging to a third party, it is the obligation of the user to ensure that any reuse complies with the copyright policies of the owner of that

content.

- If article content is copied, downloaded or otherwise reused for non-commercial research and education purposes, a link to the appropriate bibliographic citation (authors, journal, article title, volume, issue, page numbers, DOI and the link to the definitive published version on Wiley Online Library) should be maintained. Copyright notices and disclaimers must not be deleted.
- Any translations, for which a prior translation agreement with Wiley has not been agreed, must prominently display the statement: "This is an unofficial translation of an article that appeared in a Wiley publication. The publisher has not endorsed this translation."

Use by commercial "for-profit" organisations

Use of Wiley Open Access articles for commercial, promotional, or marketing purposes requires further explicit permission from Wiley and will be subject to a fee. Commercial purposes include:

- Copying or downloading of articles, or linking to such articles for further redistribution, sale or licensing;
- Copying, downloading or posting by a site or service that incorporates advertising with such content;
- The inclusion or incorporation of article content in other works or services (other than normal quotations with an appropriate citation) that is then available for sale or licensing, for a fee (for example, a compilation produced for marketing purposes, inclusion in a sales pack)
- Use of article content (other than normal quotations with appropriate citation) by for-profit organisations for promotional purposes
- Linking to article content in e-mails redistributed for promotional, marketing or educational purposes;
- Use for the purposes of monetary reward by means of sale, resale, licence, loan, transfer or other form of commercial exploitation such as marketing products
- Print reprints of Wiley Open Access articles can be purchased from:
corporatesales@wiley.com

Other Terms and Conditions:

BY CLICKING ON THE "I AGREE..." BOX, YOU ACKNOWLEDGE THAT YOU HAVE READ AND FULLY UNDERSTAND EACH OF THE SECTIONS OF AND PROVISIONS SET FORTH IN THIS AGREEMENT AND THAT YOU ARE IN AGREEMENT WITH AND ARE WILLING TO ACCEPT ALL OF YOUR OBLIGATIONS AS SET FORTH IN THIS AGREEMENT.

v1.7

If you would like to pay for this license now, please remit this license along with your payment made payable to "COPYRIGHT CLEARANCE CENTER" otherwise you will be invoiced within 48 hours of the license date. Payment should be in the form of a check or money order referencing your account number and this invoice number RLNK500890257.

Once you receive your invoice for this order, you may pay your invoice by credit card. Please follow instructions provided at that time.

Make Payment To:
Copyright Clearance Center

**Dept 001
P.O. Box 843006
Boston, MA 02284-3006**

For suggestions or comments regarding this order, contact RightsLink Customer Support: customercare@copyright.com or +1-877-622-5543 (toll free in the US) or +1-978-646-2777.

Gratis licenses (referencing \$0 in the Total field) are free. Please retain this printable license for your reference. No payment is required.

B.5 Permission from Fuel

12/8/12

Rightslink Printable License

ELSEVIER LICENSE TERMS AND CONDITIONS

Dec 08, 2012

This is a License Agreement between Haoxi Ben ("You") and Elsevier ("Elsevier") provided by Copyright Clearance Center ("CCC"). The license consists of your order details, the terms and conditions provided by Elsevier, and the payment terms and conditions.

All payments must be made in full to CCC. For payment instructions, please see information listed at the bottom of this form.

Supplier	Elsevier Limited The Boulevard, Langford Lane Kidlington, Oxford, OX5 1GB, UK
Registered Company Number	1982084
Customer name	Haoxi Ben
Customer address	500 10th street NW Atlanta, GA 30318
License number	3038830586482
License date	Nov 30, 2012
Licensed content publisher	Elsevier
Licensed content publication	Fuel
Licensed content title	Production of renewable gasoline from aqueous phase hydrogenation of lignin pyrolysis oil
Licensed content author	Haoxi Ben, Wei Mu, Yulin Deng, Arthur J. Ragauskas
Licensed content date	7 September 2012
Licensed content volume number	
Licensed content issue number	
Number of pages	1
Start Page	
End Page	
Type of Use	reuse in a thesis/dissertation
Portion	full article
Format	both print and electronic
Are you the author of this Elsevier article?	Yes
Will you be translating?	No

https://s100.copyright.com/CustomAdmin/PLF.jsp?IID=2012111_1354291282482

1/5

Order reference number

Title of your thesis/dissertation Thermal conversion of biomass and biomass components to biofuels and biochemicals

Expected completion date Dec 2012

Estimated size (number of pages) 300

Elsevier VAT number GB 494 6272 12

Permissions price 0,00 USD

VAT/Local Sales Tax 0,00 USD / GBP

Total 0,00 USD

Terms and Conditions

INTRODUCTION

1. The publisher for this copyrighted material is Elsevier. By clicking "accept" in connection with completing this licensing transaction, you agree that the following terms and conditions apply to this transaction (along with the Billing and Payment terms and conditions established by Copyright Clearance Center, Inc. ("CCC"), at the time that you opened your Rightslink account and that are available at any time at <http://myaccount.copyright.com>).

GENERAL TERMS

2. Elsevier hereby grants you permission to reproduce the aforementioned material subject to the terms and conditions indicated.

3. Acknowledgement: If any part of the material to be used (for example, figures) has appeared in our publication with credit or acknowledgement to another source, permission must also be sought from that source. If such permission is not obtained then that material may not be included in your publication/copies. Suitable acknowledgement to the source must be made, either as a footnote or in a reference list at the end of your publication, as follows:

"Reprinted from Publication title, Vol /edition number, Author(s), Title of article / title of chapter, Pages No., Copyright (Year), with permission from Elsevier [OR APPLICABLE SOCIETY COPYRIGHT OWNER]." Also Lancet special credit - "Reprinted from The Lancet, Vol. number, Author(s), Title of article, Pages No., Copyright (Year), with permission from Elsevier."

4. Reproduction of this material is confined to the purpose and/or media for which permission is hereby given.

5. Altering/Modifying Material: Not Permitted. However figures and illustrations may be altered/adapted minimally to serve your work. Any other abbreviations, additions, deletions and/or any other alterations shall be made only with prior written authorization of Elsevier Ltd. (Please contact Elsevier at permissions@elsevier.com)

6. If the permission fee for the requested use of our material is waived in this instance, please be advised that your future requests for Elsevier materials may attract a fee.

7. **Reservation of Rights:** Publisher reserves all rights not specifically granted in the combination of (i) the license details provided by you and accepted in the course of this licensing transaction, (ii) these terms and conditions and (iii) CCC's Billing and Payment terms and conditions.

8. **License Contingent Upon Payment:** While you may exercise the rights licensed immediately upon issuance of the license at the end of the licensing process for the transaction, provided that you have disclosed complete and accurate details of your proposed use, no license is finally effective unless and until full payment is received from you (either by publisher or by CCC) as provided in CCC's Billing and Payment terms and conditions. If full payment is not received on a timely basis, then any license preliminarily granted shall be deemed automatically revoked and shall be void as if never granted. Further, in the event that you breach any of these terms and conditions or any of CCC's Billing and Payment terms and conditions, the license is automatically revoked and shall be void as if never granted. Use of materials as described in a revoked license, as well as any use of the materials beyond the scope of an unrevoked license, may constitute copyright infringement and publisher reserves the right to take any and all action to protect its copyright in the materials.

9. **Warranties:** Publisher makes no representations or warranties with respect to the licensed material.

10. **Indemnity:** You hereby indemnify and agree to hold harmless publisher and CCC, and their respective officers, directors, employees and agents, from and against any and all claims arising out of your use of the licensed material other than as specifically authorized pursuant to this license.

11. **No Transfer of License:** This license is personal to you and may not be sublicensed, assigned, or transferred by you to any other person without publisher's written permission.

12. **No Amendment Except in Writing:** This license may not be amended except in a writing signed by both parties (or, in the case of publisher, by CCC on publisher's behalf).

13. **Objection to Contrary Terms:** Publisher hereby objects to any terms contained in any purchase order, acknowledgment, check endorsement or other writing prepared by you, which terms are inconsistent with these terms and conditions or CCC's Billing and Payment terms and conditions. These terms and conditions, together with CCC's Billing and Payment terms and conditions (which are incorporated herein), comprise the entire agreement between you and publisher (and CCC) concerning this licensing transaction. In the event of any conflict between your obligations established by these terms and conditions and those established by CCC's Billing and Payment terms and conditions, these terms and conditions shall control.

14. **Revocation:** Elsevier or Copyright Clearance Center may deny the permissions described in this License at their sole discretion, for any reason or no reason, with a full refund payable to you. Notice of such denial will be made using the contact information provided by you. Failure to receive such notice will not alter or invalidate the denial. In no event will Elsevier or Copyright Clearance Center be responsible or liable for any costs, expenses or damage incurred by you as a result of a denial of your permission request, other than a refund of the amount(s) paid by you to Elsevier and/or Copyright Clearance Center for denied permissions.

LIMITED LICENSE

The following terms and conditions apply only to specific license types:

15. Translation: This permission is granted for non-exclusive world **English** rights only unless your license was granted for translation rights. If you licensed translation rights you may only translate this content into the languages you requested. A professional translator must perform all translations and reproduce the content word for word preserving the integrity of the article. If this license is to re-use 1 or 2 figures then permission is granted for non-exclusive world rights in all languages.

16. Website: The following terms and conditions apply to electronic reserve and author websites:
Electronic reserve: If licensed material is to be posted to website, the web site is to be password-protected and made available only to bona fide students registered on a relevant course if:

This license was made in connection with a course,

This permission is granted for 1 year only. You may obtain a license for future website posting,

All content posted to the web site must maintain the copyright information line on the bottom of each image,

A hyper-text must be included to the Homepage of the journal from which you are licensing at <http://www.sciencedirect.com/science/journal/xxxxx> or the Elsevier homepage for books at <http://www.elsevier.com>, and

Central Storage: This license does not include permission for a scanned version of the material to be stored in a central repository such as that provided by Heron/XanEdu.

17. Author website for journals with the following additional clauses:

All content posted to the web site must maintain the copyright information line on the bottom of each image, and the permission granted is limited to the personal version of your paper. You are not allowed to download and post the published electronic version of your article (whether PDF or HTML, proof or final version), nor may you scan the printed edition to create an electronic version. A hyper-text must be included to the Homepage of the journal from which you are licensing at <http://www.sciencedirect.com/science/journal/xxxxx>. As part of our normal production process, you will receive an e-mail notice when your article appears on Elsevier's online service ScienceDirect (www.sciencedirect.com). That e-mail will include the article's Digital Object Identifier (DOI). This number provides the electronic link to the published article and should be included in the posting of your personal version. We ask that you wait until you receive this e-mail and have the DOI to do any posting.

Central Storage: This license does not include permission for a scanned version of the material to be stored in a central repository such as that provided by Heron/XanEdu.

18. Author website for books with the following additional clauses:

Authors are permitted to place a brief summary of their work online only.

A hyper-text must be included to the Elsevier homepage at <http://www.elsevier.com>. All content posted to the web site must maintain the copyright information line on the bottom of each image. You are not allowed to download and post the published electronic version of your chapter, nor may you scan the printed edition to create an electronic version.

Central Storage: This license does not include permission for a scanned version of the material to be stored in a central repository such as that provided by Heron/XanEdu.

19. **Website** (regular and for author): A hyper-text must be included to the Homepage of the journal from which you are licensing at <http://www.sciencedirect.com/science/journal/xxxxx> or for books to the Elsevier homepage at <http://www.elsevier.com>

20. **Thesis/Dissertation**: If your license is for use in a thesis/dissertation your thesis may be submitted to your institution in either print or electronic form. Should your thesis be published commercially, please reapply for permission. These requirements include permission for the Library and Archives of Canada to supply single copies, on demand, of the complete thesis and include permission for UMI to supply single copies, on demand, of the complete thesis. Should your thesis be published commercially, please reapply for permission.

21. **Other Conditions**: Permission is granted to submit your article in electronic format. This license permits you to post this Elsevier article online if it is embedded within your thesis. You are also permitted to post your Author Accepted Manuscript online however posting of the final published article is prohibited. Please refer to Elsevier's Posting Policy for further information: <http://www.elsevier.com/wps/find/authors.authors/postingpolicy>

v1.6

If you would like to pay for this license now, please remit this license along with your payment made payable to "COPYRIGHT CLEARANCE CENTER" otherwise you will be invoiced within 48 hours of the license date. Payment should be in the form of a check or money order referencing your account number and this invoice number RLNK500908171. Once you receive your invoice for this order, you may pay your invoice by credit card. Please follow instructions provided at that time.

Make Payment To:
Copyright Clearance Center
Dept 001
P.O. Box 843006
Boston, MA 02284-3006

For suggestions or comments regarding this order, contact RightsLink Customer Support: customercare@copyright.com or +1-877-622-5543 (toll free in the US) or +1-978-646-2777.

Gratis licenses (referencing \$0 in the Total field) are free. Please retain this printable license for your reference. No payment is required.

REFERENCES

1. Perlack, R. D. W., L. L.; Turhollow, A. F.; Graham, R. L.; Stokes, B. J.; Erbach, D. C., *Biomass as Feedstock for a bioenergy and bioproducts Industry: the technical feasibility of a billion-ton annual supply* **2005**.
2. Anex, R. P.; Aden, A.; Kazi, F. K.; Fortman, J.; Swanson, R. M.; Wright, M. M.; Satrio, J. A.; Brown, R. C.; Daugaard, D. E.; Platon, A.; Kothandaraman, G.; Hsu, D. D.; Dutta, A., Techno-economic comparison of biomass-to-transportation fuels via pyrolysis, gasification, and biochemical pathways. *Fuel* **2010**, 89, Supplement 1, (0), S29-S35.
3. Czernik, S.; Bridgwater, A. V., Overview of applications of biomass fast pyrolysis oil. *Energy Fuels* **2004**, 18, (2), 590-598.
4. Demirbas, A., Progress and recent trends in biofuels. *Prog. Energy Combust. Sci.* **2007**, 33, (1), 1-18.
5. Ragauskas, A. J.; Williams, C. K.; Davison, B. H.; Britovsek, G.; Cairney, J.; Eckert, C. A.; Frederick, W. J., Jr.; Hallett, J. P.; Leak, D. J.; Liotta, C. L.; Mielenz, J. R.; Murphy, R.; Templer, R.; Tschaplinski, T., The path forward for biofuels and biomaterials. *Science* **2006**, 311, (5760), 484-9.
6. David, K.; Ragauskas, A. J., Switchgrass as an energy crop for biofuel production: A review of its ligno-cellulosic chemical properties. *Energ. Environ. Sci.* **2010**, 3, (9), 1182-1190.
7. Perlack, R. D.; Wright, L. L.; Turhollow, A. F.; Graham, R. L.; Stokes, B. J.; Erbach, D. C., Biomass as feedstock for a bioenergy and bioproducts industry: the technical feasibility of a billion-ton annual supply. *Biomass as Feedstock for a bioenergy and*

bioproducts Industry: the technical feasibility of a billion-ton annual supply **2005**.

8. Mohan, D.; Pittman, C. U.; Steele, P. H., Pyrolysis of wood/biomass for bio-oil: A critical review. *Energy Fuels* **2006**, 20, (3), 848-889.
9. Ben, H.; Ragauskas, A. J., NMR Characterization of pyrolysis oils from kraft lignin. *Energy Fuels* **2011**, 25, (5), 2322-2332.
10. Ben, H.; Ragauskas, A. J., Heteronuclear Single-Quantum Correlation–Nuclear Magnetic Resonance (HSQC–NMR) fingerprint analysis of pyrolysis oils. *Energy Fuels* **2011**, 25, (12), 5791-5801.
11. Ragauskas, A. J.; Nagy, M.; Kim, D. H.; Eckert, C. A.; Hallett, J. P.; Liotta, C. L., From wood to fuels: Integrating biofuels and pulp production. *Industrial Biotechnology* **2006**, 2, (1), 55-65.
12. Huang, F.; Singh, P. M.; Ragauskas, A. J., Characterization of milled wood lignin (MWL) in Loblolly pine stem wood, residue, and bark. *J. Agric. Food. Chem.* **2011**, 59, (24), 12910-12916.
13. Huber, G. W.; Iborra, S.; Corma, A., Synthesis of transportation fuels from biomass: chemistry, catalysts, and engineering. *Chem. Rev.* **2006**, 106, (9), 4044-98.
14. Sannigrahi, P.; Ragauskas, A. J.; Tuskan, G. A., Poplar as a feedstock for biofuels: A review of compositional characteristics. *Biofuels, Bioprod. Biorefin.* **2010**, 4, (2), 209-226.
15. Puri, V. P., Effect of crystallinity and degree of polymerization of cellulose on enzymatic saccharification. *Biotechnol. Bioeng.* **1984**, 26, (10), 1219-1222.
16. Karen Kleman-leyer; Eduardo Agosin; Anthony H. Conner; Kirk, T. K., Changes in molecular size distribution of cellulose during attack by white rot and brown rot fungi.

Appl. Environ. Microbiol. **1992**, 58, (4), 1266-1270.

17. Jahan, M. S.; Mun, S. P., Effect of tree age on the cellulose structure of Nalita wood (*Trema orientalis*). *Wood Science and Technology* **2005**, 39, (5), 367-373.

18. Thygesen, A.; Oddershede, J.; Lilholt, H.; Thomsen, A. B.; Ståhl, K., On the determination of crystallinity and cellulose content in plant fibres. *Cellulose* **2005**, 12, (6), 563-576.

19. Willför, S.; Sundberg, A.; Pranovich, A.; Holmbom, B., Polysaccharides in some industrially important hardwood species. *Wood Science and Technology* **2005**, 39, (8), 601-617.

20. Willför, S.; Sundberg, A.; Hemming, J.; Holmbom, B., Polysaccharides in some industrially important softwood species. *Wood Science and Technology* **2005**, 39, (4), 245-257.

21. Jacobs, A.; Dahlman, O., Characterization of the molar masses of hemicelluloses from wood and pulps employing size exclusion chromatography and matrix-assisted laser desorption ionization time-of-flight mass spectrometry. *Biomacromolecules* **2001**, 2, (3), 894-905.

22. Zakzeski, J.; Bruijninx, P. C. A.; Jongerius, A. L.; Weckhuysen, B. M., Catalytic valorization of lignin for the production of renewable chemicals. *Chem. Rev.* **2010**, 220, 3552–3599.

23. Chakar, F. S.; Ragauskas, A. J., Review of current and future softwood kraft lignin process chemistry. *Industrial Crops and Products* **2004**, 20, (2), 131-141.

24. Caballero, J. A.; Font, R.; Marcilla, A., Study of the primary pyrolysis of Kraft lignin at high heating rates: yields and kinetics. *J. Anal. Appl. Pyrolysis* **1996**, 36, (2), 159-178.

25. Caballero, J. A.; Font, R.; Marcilla, A., Pyrolysis of Kraft lignin: yields and correlations. *J. Anal. Appl. Pyrolysis* **1997**, 39, (2), 161-183.
26. Caballero, J. A.; Font, R.; Marcilla, A.; García, A. N., Flash pyrolysis of Klason lignin in a Pyroprobe 1000. *J. Anal. Appl. Pyrolysis* **1993**, 27, (2), 221-244.
27. Ferdous, D.; Dalai, A. K.; Bej, S. K.; Thring, R. W., Pyrolysis of lignins: experimental and kinetics studies. *Energy Fuels* **2002**, 16, (6), 1405-1412.
28. Ferdous, D.; Dalai, A. K.; Bej, S. K.; Thring, R. W.; Bakhshi, N. N., Production of H₂ and medium Btu gas via pyrolysis of lignins in a fixed-bed reactor. *Fuel Process. Technol.* **2001**, 70, (1), 9-26.
29. Iatridis, B.; Gavalas, G. R., Pyrolysis of a precipitated Kraft lignin. *Industrial & Engineering Chemistry Product Research and Development* **1979**, 18, (2), 127-130.
30. Nunn, T. R.; Howard, J. B.; Longwell, J. P.; Peters, W. A., Product compositions and kinetics in the rapid pyrolysis of milled wood lignin. *Journal Name: Ind. Eng. Chem. Process Des. Dev.; (United States); Journal Volume: 24:3* **1985**, Medium: X; Size: Pages: 844-852.
31. Asmadi, M.; Kawamoto, H.; Saka, S., Gas- and solid/liquid-phase reactions during pyrolysis of softwood and hardwood lignins. *J. Anal. Appl. Pyrolysis* **2011**, 92, (2), 417-425.
32. Chen, H.-W.; Song, Q.-H.; Liao, B.; Guo, Q.-X., Further separation, characterization, and upgrading for upper and bottom layers from phase separation of biomass pyrolysis Oils. *Energy Fuels* **2011**, 25, (10), 4655-4661.
33. Hosoya, T.; Kawamoto, H.; Saka, S., Solid/liquid- and vapor-phase interactions between cellulose- and lignin-derived pyrolysis products. *J. Anal. Appl. Pyrolysis* **2009**,

85, (1–2), 237-246.

34. Hyder, M.; Jönsson, J. Å., Hollow-fiber liquid phase microextraction for lignin pyrolysis acids in aerosol samples and gas chromatography–mass spectrometry analysis.

J. Chromatogr. A **2012**, 1249, (0), 48-53.

35. Jiang, G.; Nowakowski, D. J.; Bridgwater, A. V., Effect of the Temperature on the composition of lignin pyrolysis products. *Energy Fuels* **2010**, 24, (8), 4470-4475.

36. Lou, R.; Wu, S.-b.; Lv, G.-j., Effect of conditions on fast pyrolysis of bamboo lignin. *J. Anal. Appl. Pyrolysis* **2010**, 89, (2), 191-196.

37. Lou, R.; Wu, S.-B.; Lv, G.-J.; Guo, D.-L., Pyrolytic products from rice straw and enzymatic/mild acidolysis lignin. *BioRes.* **2010**, 5, (4), 2184-2194.

38. Mullen, C. A.; Boateng, A. A., Catalytic pyrolysis-GC/MS of lignin from several sources. *Fuel Process. Technol.* **2010**, 91, (11), 1446-1458.

39. Patwardhan, P. R.; Brown, R. C.; Shanks, B. H., Understanding the fast pyrolysis of lignin. *ChemSusChem* **2011**, 4, (11), 1629-1636.

40. yang, Q.; Wu, S.; Lou, R.; Lv, G., Analysis of wheat straw lignin by thermogravimetry and pyrolysis–gas chromatography/mass spectrometry. *J. Anal. Appl. Pyrolysis* **2010**, 87, (1), 65-69.

41. Bocchini, P.; Galletti, G. C.; Camarero, S.; Martinez, A. T., Absolute quantitation of lignin pyrolysis products using an internal standard. *J. Chromatogr. A* **1997**, 773, (1–2), 227-232.

42. Greenwood, P. F.; van Heemst, J. D. H.; Guthrie, E. A.; Hatcher, P. G., Laser micropyrolysis GC–MS of lignin. *J. Anal. Appl. Pyrolysis* **2002**, 62, (2), 365-373.

43. Ingram, L.; Mohan, D.; Bricka, M.; Steele, P.; Strobel, D.; Crocker, D.; Mitchell, B.;

Mohammad, J.; Cantrell, K.; Pittman, C. U., Pyrolysis of wood and bark in an auger reactor: physical properties and chemical analysis of the produced bio-oils. *Energy Fuels* **2007**, 22, (1), 614-625.

44. Jegers, H. E.; Klein, M. T., Primary and secondary lignin pyrolysis reaction pathways. *Industrial & Engineering Chemistry Process Design and Development* **1985**, 24, (1), 173-183.

45. Nowakowski, D. J.; Bridgwater, A. V.; Elliott, D. C.; Meier, D.; de Wild, P., Lignin fast pyrolysis: Results from an international collaboration. *J. Anal. Appl. Pyrolysis* **2010**, 88, (1), 53-72.

46. Scholze, B.; Meier, D., Characterization of the water-insoluble fraction from pyrolysis oil (pyrolytic lignin). Part I. PY–GC/MS, FTIR, and functional groups. *J. Anal. Appl. Pyrolysis* **2001**, 60, (1), 41-54.

47. Saiz-Jimenez, C.; De Leeuw, J. W., Lignin pyrolysis products: Their structures and their significance as biomarkers. *Org. Geochem.* **1986**, 10, (4–6), 869-876.

48. Beis, S. H.; Mukkamala, S.; Hill, N.; Joseph, J.; Baker, C.; Jensen, B.; Stemmler, E. A.; Wheeler, M. C.; Frederick, B. G.; van Heiningen, A.; Berg, A. G.; DeSisto, W. J., Fast pyrolysis of lignins. *BioRes.* **2010**, 5, (3), 1408-1424.

49. Britt, P. F.; Buchanan, A. C.; Cooney, M. J.; Martineau, D. R., Flash vacuum pyrolysis of methoxy-substituted lignin model compounds. *The Journal of Organic Chemistry* **2000**, 65, (5), 1376-1389.

50. Britt, P. F.; Buchanan, A. C.; Malcolm, E. A., Impact of restricted mass transport on pyrolysis pathways for aryl ether containing lignin model compounds. *Energy Fuels* **2000**, 14, (6), 1314-1322.

51. Britt, P. F.; Kidder, M. K.; A. C. Buchanan, I., Oxygen substituent effects in the pyrolysis of phenethyl phenyl ethers. *Energy Fuels* **2007**, 21, (6), 3102-3108.
52. Kawamoto, H.; Nakamura, T.; Saka, S., Pyrolytic cleavage mechanisms of lignin-ether linkages: A study on p-substituted dimers and trimers. *Holzforschung* **2008**, 62, (1), 50-56.
53. Kawamoto, H.; Ryoritani, M.; Saka, S., Different pyrolytic cleavage mechanisms of β -ether bond depending on the side-chain structure of lignin dimers. *J. Anal. Appl. Pyrolysis* **2008**, 81, (1), 88-94.
54. Kawamoto, H.; Saka, S., Role of side-chain hydroxyl groups in pyrolytic reaction of phenolic β -ether type of lignin dimer. *J. Wood Chem. Technol.* **2007**, 27, (2), 113-120.
55. Kawamoto, H.; Horigoshi, S.; Saka, S., Pyrolysis reactions of various lignin model dimers. *J. Wood Sci.* **2007**, 53, (2), 168-174.
56. Huber, G. W.; Chhedha, J. N.; Barrett, C. J.; Dumesic, J. A., Production of liquid alkanes by aqueous-phase processing of biomass-derived carbohydrates. *Science* **2005**, 308, (5727), 1446-1450.
57. Yan, N.; Zhao, C.; Luo, C.; Dyson, P. J.; Liu, H.; Kou, Y., One-step conversion of cellobiose to C₆-alcohols using a ruthenium nanocluster catalyst. *J. Am. Chem. Soc.* **2006**, 128, (27), 8714-8715.
58. Shen, D. K.; Gu, S., The mechanism for thermal decomposition of cellulose and its main products. *Bioresour Technol* **2009**, 100, (24), 6496-6504.
59. Wang, S.; Guo, X.; Wang, K.; Luo, Z., Influence of the interaction of components on the pyrolysis behavior of biomass. *J. Anal. Appl. Pyrolysis* **2011**, 91, (1), 183-189.
60. Alén, R.; Kuoppala, E.; Oesch, P., Formation of the main degradation compound

groups from wood and its components during pyrolysis. *J. Anal. Appl. Pyrolysis* **1996**, 36, (2), 137-148.

61. Christian W. Klampfl; Gerold Breuer; Schwarzing, C. K., B., Investigations on the effect of metal ions on the products obtained from the pyrolysis of cellulose. *Acta Chim. Slov.* **2006**, 53, 437-443.

62. Lu, Q.; Xiong, W. M.; Li, W. Z.; Guo, Q. X.; Zhu, X. F., Catalytic pyrolysis of cellulose with sulfated metal oxides: a promising method for obtaining high yield of light furan compounds. *Bioresour Technol* **2009**, 100, (20), 4871-6.

63. Rutkowski, P.; Kubacki, A., Influence of polystyrene addition to cellulose on chemical structure and properties of bio-oil obtained during pyrolysis. *Energy Convers. Manage.* **2006**, 47, (6), 716-731.

64. Moldoveanu, S. C., Pyrolysis GC/MS, present and future (recent past and present needs). *J. Microcolumn Sep.* **2001**, 13, (3), 102-125.

65. Patwardhan, P. R.; Brown, R. C.; Shanks, B. H., Product distribution from the fast pyrolysis of hemicellulose. *ChemSusChem* **2011**, 4, (5), 636-43.

66. Gao-Jin Lv, S.-B. W., Rui Lou, Characteristics of corn stalk hemicellulose pyrolysis in a tubular reactor. *BioResources* **2010**, 5, (4), 2051-2062.

67. Peng, Y.; Wu, S., The structural and thermal characteristics of wheat straw hemicellulose. *J. Anal. Appl. Pyrolysis* **2010**, 88, (2), 134-139.

68. Shen, D. K.; Gu, S.; Bridgwater, A. V., Study on the pyrolytic behaviour of xylan-based hemicellulose using TG-FTIR and Py-GC-FTIR. *J. Anal. Appl. Pyrolysis* **2010**, 87, (2), 199-206.

69. Scholze, B.; Hanser, C.; Meier, D., Characterization of the water-insoluble fraction

- from fast pyrolysis liquids (pyrolytic lignin): Part II. GPC, carbonyl groups, and ^{13}C -NMR. *J. Anal. Appl. Pyrolysis* **2001**, 58–59, (0), 387-400.
70. Chaala, A.; Ba, T.; Garcia-Perez, M.; Roy, C., Colloidal properties of bio-oils obtained by vacuum pyrolysis of softwood bark: Aging and thermal stability. *Energy Fuels* **2004**, 18, (5), 1535-1542.
71. Kosa, M.; Ben, H.; Theliander, H.; Ragauskas, A. J., Pyrolysis oils from CO_2 precipitated Kraft lignin. *Green Chem.* **2011**, 13, (11), 3196-3202.
72. Boucher, M. E.; Chaala, A.; Pakdel, H.; Roy, C., Bio-oils obtained by vacuum pyrolysis of softwood bark as a liquid fuel for gas turbines. Part II: Stability and ageing of bio-oil and its blends with methanol and a pyrolytic aqueous phase. *Biomass Bioenergy* **2000**, 19, 351-361.
73. Huang, Y.; Wei, Z.; Qiu, Z.; Yin, X.; Wu, C., Study on structure and pyrolysis behavior of lignin derived from corncob acid hydrolysis residue. *J. Anal. Appl. Pyrolysis* **2012**, 93, (0), 153-159.
74. Ke, J.; Singh, D.; Yang, X.; Chen, S., Thermal characterization of softwood lignin modification by termite *Coptotermes formosanus* (Shiraki). *Biomass Bioenergy* **2011**, 35, (8), 3617-3626.
75. Liu, Q.; Wang, S.; Zheng, Y.; Luo, Z.; Cen, K., Mechanism study of wood lignin pyrolysis by using TG–FTIR analysis. *J. Anal. Appl. Pyrolysis* **2008**, 82, (1), 170-177.
76. Liu, Q.; Zhong, Z.; Wang, S.; Luo, Z., Interactions of biomass components during pyrolysis: A TG-FTIR study. *J. Anal. Appl. Pyrolysis* **2011**, 90, (2), 213-218.
77. Shen, D. K.; Gu, S.; Luo, K. H.; Wang, S. R.; Fang, M. X., The pyrolytic degradation of wood-derived lignin from pulping process. *Bioresour Technol* **2010**, 101, (15),

6136-46.

78. Wang, S.; Wang, K.; Liu, Q.; Gu, Y.; Luo, Z.; Cen, K.; Fransson, T., Comparison of the pyrolysis behavior of lignins from different tree species. *Biotechnol. Adv.* **2009**, *27*, (5), 562-567.

79. Lievens, C.; Mourant, D.; He, M.; Gunawan, R.; Li, X.; Li, C.-Z., An FT-IR spectroscopic study of carbonyl functionalities in bio-oils. *Fuel* **2011**, *90*, (11), 3417-3423.

80. Pütün, A. E.; Özbay, N.; Apaydin Varol, E.; Uzun, B. B.; Ateş, F., Rapid and slow pyrolysis of pistachio shell: effect of pyrolysis conditions on the product yields and characterization of the liquid product. *International Journal of Energy Research* **2007**, *31*, (5), 506-514.

81. Mullen, C. A.; Strahan, G. D.; Boateng, A. A., Characterization of various fast-pyrolysis bio-oils by NMR spectroscopy. *Energy Fuels* **2009**, *23*, (5), 2707-2718.

82. Luo, Z.; Wang, S.; Guo, X., Selective pyrolysis of Organosolv lignin over zeolites with product analysis by TG-FTIR. *J. Anal. Appl. Pyrolysis* **2012**, *95*, (0), 112-117.

83. Joseph, J.; Baker, C.; Mukkamala, S.; Beis, S. H.; Wheeler, M. C.; DeSisto, W. J.; Jensen, B. L.; Frederick, B. G., Chemical shifts and lifetimes for Nuclear Magnetic Resonance (NMR) analysis of biofuels. *Energy Fuels* **2010**, *24*, (9), 5153-5162.

84. Gellerstedt, G. r.; Li, J.; Eide, I.; Kleinert, M.; Barth, T., Chemical structures present in biofuel obtained from lignin. *Energy Fuels* **2008**, *22*, (6), 4240-4244.

85. DeSisto, W. J.; Hill, N.; Beis, S. H.; Mukkamala, S.; Joseph, J.; Baker, C.; Ong, T.-H.; Stemmler, E. A.; Wheeler, M. C.; Frederick, B. G.; van Heiningen, A., Fast pyrolysis of pine sawdust in a fluidized-bed reactor. *Energy Fuels* **2010**, *24*, (4), 2642-2651.

86. David, K.; Kosa, M.; Williams, A.; Mayor, R.; Realff, M.; Muzzy, J.; Ragauskas, A., ^{31}P -NMR analysis of bio-oils obtained from the pyrolysis of biomass. *Biofuels* **2010**, 1, (6), 839-845.
87. David, K.; Ben, H.; Muzzy, J.; Feik, C.; Iisa, K.; Ragauskas, A., Chemical characterization and water content determination of bio-oils obtained from various biomass species using ^{31}P NMR spectroscopy. *Biofuels* **2012**, 3, (2), 123-128.
88. Ben, H.; Ragauskas, A. J., Torrefaction of Loblolly pine. *Green Chem.* **2012**, 14, (1), 72-76.
89. Ben, H.; Ragauskas, A. J., In Situ NMR characterization of pyrolysis oil during accelerated aging. *ChemSusChem* **2012**, 5, (9), 1687-1693.
90. Ben, H.; Ragauskas, A. J., Pyrolysis of kraft lignin with additives. *Energy Fuels* **2011**, 25, (10), 4662-4668.
91. Oasmaa, A.; Kuoppala, E.; Solantausta, Y., Fast pyrolysis of forestry residue. 2. physicochemical composition of product liquid. *Energy Fuels* **2003**, 17, (2), 433-443.
92. Şensöz, S., Slow pyrolysis of wood barks from *Pinus brutia* Ten. and product compositions. *Bioresour Technol* **2003**, 89, (3), 307-311.
93. Oasmaa, A.; Solantausta, Y.; Arpiainen, V.; Kuoppala, E.; Sipilä, K., Fast pyrolysis bio-oils from wood and agricultural residues. *Energy Fuels* **2010**, 24, (2), 1380-1388.
94. Diebold, J. P.; Czernik, S., Additives to lower and stabilize the viscosity of pyrolysis oils during storage. *Energy Fuels* **1997**, 11, (5), 1081-1091.
95. Fahmi, R.; Bridgwater, A. V.; Donnison, I.; Yates, N.; Jones, J. M., The effect of lignin and inorganic species in biomass on pyrolysis oil yields, quality and stability. *Fuel* **2008**, 87, (7), 1230-1240.

96. Pan, X.; Xie, D.; Yu, R. W.; Lam, D.; Saddler, J. N., Pretreatment of lodgepole pine killed by mountain pine beetle using the ethanol organosolv process fractionation and process optimization. *Ind. Eng. Chem. Res.* **2007**, 46, 2609-2617.
97. Hallac, B. B.; Pu, Y.; Ragauskas, A. J., Chemical transformations of buddleja davidii lignin during ethanol organosolv pretreatment. *Energy Fuels* **2010**, 24, (4), 2723-2732.
98. El Hage, R.; Brosse, N.; Chrusciel, L.; Sanchez, C.; Sannigrahi, P.; Ragauskas, A., Characterization of milled wood lignin and ethanol organosolv lignin from miscanthus. *Polym. Degrad. Stab.* **2009**, 94, (10), 1632-1638.
99. El Hage, R.; Brosse, N.; Sannigrahi, P.; Ragauskas, A., Effects of process severity on the chemical structure of Miscanthus ethanol organosolv lignin. *Polym. Degrad. Stab.* **2010**, 95, (6), 997-1003.
100. Hu, Z.; Sykes, R.; Davis, M. F.; Charles Brummer, E.; Ragauskas, A. J., Chemical profiles of switchgrass. *Bioresour. Technol.* **2010**, 101, (9), 3253-3257.
101. Nagy, M.; Kosa, M.; Theliander, H.; Ragauskas, A. J., Characterization of CO₂ precipitated Kraft lignin to promote its utilization. *Green Chem.* **2010**, 12, (1), 31.
102. Vispute, T. P.; Zhang, H.; Sanna, A.; Xiao, R.; Huber, G. W., Renewable chemical commodity feedstocks from integrated catalytic processing of pyrolysis oils. *Science* **2010**, 330, (6008), 1222-1227.
103. de Wild, P.; Reith, H.; Heeres, E., Biomass pyrolysis for chemicals. *Biofuels* **2011**, 2, (2), 185-208.
104. Chen, W.-H.; Kuo, P.-C., Torrefaction and co-torrefaction characterization of hemicellulose, cellulose and lignin as well as torrefaction of some basic constituents in biomass. *Energy* **2011**, 36, (2), 803-811.

105. Chen, W.-H.; Kuo, P.-C., A study on torrefaction of various biomass materials and its impact on lignocellulosic structure simulated by a thermogravimetry. *Energy* **2010**, 35, (6), 2580-2586.
106. Wroblewski, A. E.; Lensink, C.; Markuszewski, R.; Verkade, J. G., Phosphorus-31 NMR spectroscopic analysis of coal pyrolysis condensates and extracts for heteroatom functionalities possessing labile hydrogen. *Energy Fuels* **1988**, 2, 765-774.
107. Wroblewski, A. E.; Reinartz, K.; Verkade, J. G., Moisture determination of Argonne Premium coal extracts by phosphorus-³¹P NMR spectroscopy. *Energy Fuels* **1991**, 5, 786-791.
108. Pu, Y.; Cao, S.; Ragauskas, A. J., Application of quantitative ³¹P NMR in biomass lignin and biofuel precursors characterization. *Energ. Environ. Sci.* **2011**, 4, (9), 3154-3166.
109. Jiang, Z. H.; Argyropoulos, D. S.; Granata, A., Correlation analysis of ³¹P NMR chemical shifts with substituent effects of phenols. *Magn. Reson. Chem.* **1995**, 33, 375-382.
110. Samuel, R.; Pu, Y.; Raman, B.; Ragauskas, A. J., Structural characterization and comparison of switchgrass ball-milled lignin before and after dilute acid pretreatment. *Appl. Biochem. Biotechnol.* **2009**, 162, (1), 62-74.
111. Berg, A.; Navarrete, P.; Olave, I., A process for obtaining low and medium molecular weight polyphenols and a solid standardized fuel from tree wood or bark. USA patent application 12/151, 283, May 5, 2008, priority Chilean patent application 1266, May 4, 2007.

- 112.Salanti, A.; Zoia, L.; Orlandi, M.; Zanini, F.; Elegir, G., Structural characterization and antioxidant activity evaluation of lignins from rice husk. *J. Agric. Food Chem.* **2010**, 58, (18), 10049-55.
- 113.Zhang, L.; Gellerstedt, G., Quantitative 2D HSQC NMR determination of polymer structures by selecting suitable internal standard references. *Magn Reson Chem* **2007**, 45, (1), 37-45.
- 114.Qu, C.; Kishimoto, T.; Kishino, M.; Hamada, M.; Nakajima, N., Heteronuclear single-quantum coherence nuclear magnetic resonance (HSQC NMR) characterization of acetylated fir (*Abies sachalinensis* MAST) wood regenerated from ionic liquid. *J. Agric. Food Chem.* **2011**, 59, (10), 5382-9.
- 115.Coughlin, R. W.; Davoudzadeh, F., Coliquefaction of lignin and bituminous coal. *Fuel* **1986**, 65, 95-106.
- 116.Watanabe, T.; Kawamoto, H.; Saka, S., Radical chain reactions in pyrolytic cleavage of the ether linkages of lignin model dimers and a trimer. *Holzforschung* **2009**, 63, (4), 424-430.
- 117.Kallury, R. K. M. R.; Ambidge, C.; Tidwell, T. T.; Boocock, D. G. B.; Agblevor, F. A.; Stewart, D. J., Rapid hydrothermolysis of cellulose and related carbohydrates. *Carbohydr. Res.* **1986**, 158, 253-261.
- 118.Luijkx, G. C. A.; Rantwijk, F. v.; Bekkum, H. v., Hydrothermal formation of 1,2,4-benzenetriol from Shydroxymethyl-2-furaldehyde and D-fructose. *Carbohydr. Res.* **1993**, 242, 131-139.
- 119.Pakdel, H.; Amen-Chen, C.; Roy, C., Phenolic compounds from vacuum pyrolysis of wood wastes. *Can. J. Chem. Eng.* **1997**, 75, 121-126.

120. Czernik, S.; Johnson, D. K.; Black, S., Stability of wood fast pyrolysis oil. *Biomass Bioenergy* **1994**, 7, (1–6), 187-192.
121. Chaala, A.; Ba, T.; Garcia-Perez, M.; Roy, C., Colloidal properties of bio-oils obtained by vacuum pyrolysis of softwood bark: Aging and thermal stability. *Energy Fuels* **2004**, 18, 1535-1542.
122. Naske, C. D.; Polk, P.; Wynne, P. Z.; Speed, J.; Holmes, W. E.; Walters, K. B., Postcondensation filtration of pine and cottonwood pyrolysis oil and impacts on accelerated aging reactions. *Energy Fuels* **2012**, 26, (2), 1284-1297.
123. Nolte, M. W.; Liberatore, M. W., Real-time viscosity measurements during the accelerated aging of biomass pyrolysis oil. *Energy Fuels* **2011**, 25, (7), 3314-3317.
124. Oasmaa, A.; Kuoppala, E., Fast pyrolysis of forestry residue. 3. storage stability of liquid fuel. *Energy Fuels* **2003**, 17, (4), 1075-1084.
125. Ortega, J. V.; Renehan, A. M.; Liberatore, M. W.; Herring, A. M., Physical and chemical characteristics of aging pyrolysis oils produced from hardwood and softwood feedstocks. *J. Anal. Appl. Pyrolysis* **2011**, 91, (1), 190-198.
126. Oasmaa, A.; Kuoppala, E.; Elliott, D. C., Development of the basis for an analytical protocol for feeds and products of bio-oil hydrotreatment. *Energy Fuels* **2012**, 26, (4), 2454-2460.
127. Fratini, E.; Bonini, M.; Oasmaa, A.; Solantausta, Y.; Teixeira, J.; Baglioni, P., SANS analysis of the microstructural evolution during the aging of pyrolysis oils from biomass. *Langmuir* **2006**, 22, 306-312.
128. Garcia-Perez, M.; Chaala, A.; Pakdel, H.; Kretschmer, D.; Roy, C., Characterization of bio-oils in chemical families. *Biomass Bioenergy* **2007**, 31, (4),

222-242.

129. Christensen, E. D.; Chupka, G. M.; Luecke, J.; Smurthwaite, T.; Alleman, T. L.; Lisa, K.; Franz, J. A.; Elliott, D. C.; McCormick, R. L., Analysis of oxygenated compounds in hydrotreated biomass fast pyrolysis oil distillate fractions. *Energy Fuels* **2011**, 25, (11), 5462-5471.

130. Sannigrahi, P.; Kim, D. H.; Jung, S.; Ragauskas, A., Pseudo-lignin and pretreatment chemistry. *Energ. Environ. Sci.* **2011**, 4, (4), 1306-1310.

131. Samuel, R.; Foston, M.; Jaing, N.; Cao, S.; Allison, L.; Studer, M.; Wyman, C.; Ragauskas, A. J., HSQC (heteronuclear single quantum coherence) ^{13}C - ^1H correlation spectra of whole biomass in perdeuterated pyridinium chloride–DMSO system: An effective tool for evaluating pretreatment. *Fuel* **2011**, 90, (9), 2836-2842.

132. Binder, J. B.; Gray, M. J.; White, J. F.; Zhang, Z. C.; Holladay, J. E., Reactions of lignin model compounds in ionic liquids. *Biomass Bioenergy* **2009**, 33, (9), 1122-1130.

133. Nakamura, T.; Kawamoto, H.; Saka, S., Condensation reactions of some lignin related compounds at relatively low pyrolysis temperature. *J. Wood Chem. Technol.* **2007**, 27, (2), 121-133.

134. Brosse, N.; El Hage, R.; Chaouch, M.; Pétrissans, M.; Dumarçay, S.; Gérardin, P., Investigation of the chemical modifications of beech wood lignin during heat treatment. *Polym. Degrad. Stab.* **2010**, 95, (9), 1721-1726.

135. Calvo-Flores, F. G.; Dobado, J. A., Lignin as renewable raw material. *ChemSusChem* **2010**, 3, (11), 1227-35.

136. Zhao, Y.; Deng, L.; Liao, B.; Fu, Y.; Guo, Q.-X., Aromatics production via catalytic pyrolysis of pyrolytic lignins from bio-oil. *Energy Fuels* **2010**, 24, (10),

5735-5740.

137. French, R.; Czernik, S., Catalytic pyrolysis of biomass for biofuels production. *Fuel Process. Technol.* **2010**, 91, (1), 25-32.

138. Jackson, M. A.; Compton, D. L.; Boateng, A. A., Screening heterogeneous catalysts for the pyrolysis of lignin. *J. Anal. Appl. Pyrolysis* **2009**, 85, (1-2), 226-230.

139. Aho, A.; Kumar, N.; Eranen, K.; Salmi, T.; Hupa, M.; Murzin, D., Catalytic pyrolysis of woody biomass in a fluidized bed reactor: Influence of the zeolite structure. *Fuel* **2008**, 87, (12), 2493-2501.

140. Zhang, H.; Xiao, R.; Huang, H.; Xiao, G., Comparison of non-catalytic and catalytic fast pyrolysis of corncob in a fluidized bed reactor. *Bioresour. Technol.* **2009**, 100, (3), 1428-1434.

141. Pan, P.; Hu, C.; Yang, W.; Li, Y.; Dong, L.; Zhu, L.; Tong, D.; Qing, R.; Fan, Y., The direct pyrolysis and catalytic pyrolysis of *Nannochloropsis* sp. residue for renewable bio-oils. *Bioresour. Technol.* **2010**, 101, (12), 4593-4599.

142. Uzun, B. B.; Sarioğlu, N., Rapid and catalytic pyrolysis of corn stalks. *Fuel Process. Technol.* **2009**, 90, (5), 705-716.

143. Pattiya, A.; Titiloye, J. O.; Bridgwater, A. V., Evaluation of catalytic pyrolysis of cassava rhizome by principal component analysis. *Fuel* **2010**, 89, (1), 244-253.

144. Pattiya, A.; Titiloye, J.; Bridgwater, A., Fast pyrolysis of cassava rhizome in the presence of catalysts. *J. Anal. Appl. Pyrolysis* **2008**, 81, (1), 72-79.

145. Agblevor, F. A.; Beis, S.; Mante, O.; Abdoulmoumine, N., Fractional catalytic pyrolysis of hybrid poplar wood. *Ind. Eng. Chem. Res.* **2010**, 49, 3533-3538.

146. Williams, P. T.; Nugranad, N., Comparison of products from the pyrolysis and

catalytic pyrolysis of rice husks. *Energy* **2000**, 25, (6), 493-513.

147. Valle, B.; Gayubo, A. G.; Aguayo, A. s. T.; Olazar, M.; Bilbao, J., Selective production of aromatics by crude bio-oil valorization with a nickel-modified HZSM-5 zeolite Catalyst. *Energy Fuels* **2010**, 24, (3), 2060-2070.

148. Atutxa, A.; Aguado, R.; Gayubo, A. G.; Olazar, M.; Bilbao, J., Kinetic description of the catalytic pyrolysis of biomass in a conical spouted bed reactor. *Energy Fuels* **2005**, 19, 765-774.

149. Beis, S. H.; Mukkamala, S.; Hill, N.; Joseph, J.; Baker, C.; Jensen, B.; Stemmler, E. A.; Wheeler, M. C.; Frederick, B. G.; Heiningen, A. v.; Berg, A. G.; DeSisto, W. J., Fast pyrolysis of lignins. *BioResources* **2010**, 5, (3), 1408-1424.

150. David, K.; Pu, Y.; Foston, M.; Muzzy, J.; Ragauskas, A., Cross-Polarization/Magic Angle Spinning (CP/MAS) ^{13}C Nuclear Magnetic Resonance (NMR) analysis of chars from alkaline-treated pyrolyzed softwood. *Energy Fuels* **2009**, 23, 498–501.

151. Ingram, L.; Mohan, D.; Bricka, M.; Steele, P.; Strobel, D.; Crocker, D.; Mitchell, B.; Mohammad, J.; Cantrell, K.; Pittman, C. U., Jr., Pyrolysis of wood and bark in an auger reactor: physical properties and chemical analysis of the produced bio-oils. *Energy Fuels* **2008**, 22, 614–625.

152. Sannigrahi, P.; Ragauskas, A. J.; Miller, S. J., Lignin structural modifications resulting from ethanol organosolv treatment of Loblolly pine. *Energy Fuels* **2010**, 24, 683-689.

153. Zawadzki, M.; Ragauskas, A., N-Hydroxy compounds as new internal standards for the ^{31}P NMR determination of lignin hydroxy functional groups. *Holzforschung* **2001**,

55, 283-285.

154. Froass, P. M.; Ragauskas, A. J.; Jiang, J. e., Nuclear magnetic resonance studies.

4. analysis of residual lignin after kraft pulping. *Ind. Eng. Chem. Res.* **1998**, 37, 3388-3394.

155. Fu, Q.; Argyropoulos, D. S.; Tilotta, D. C.; Lucia, L. A., Products and functional group distributions in pyrolysis oil of chromated copper arsenate (CCA)-treated wood, as elucidated by gas chromatography and a novel ^{31}P NMR-based method. *Ind. Eng. Chem. Res.* **2007**, 46, 5258-5264.

156. Zou, X.; Yao, J.; Yang, X.; Song, W.; Lin, W., Catalytic effects of metal chlorides on the pyrolysis of lignite. *Energy Fuels* **2007**, 21, 619-624.

157. Bru, K.; Blin, J.; Julbe, A.; Volle, G., Pyrolysis of metal impregnated biomass: An innovative catalytic way to produce gas fuel. *J. Anal. Appl. Pyrolysis* **2007**, 78, (2), 291-300.

158. Tomani, P., The lignoboost process. *Cellulose Chem. Technol.* **2010**, 44, (1-3), 53-58.

159. Sazama, P.; Dedecek, J.; Gabova, V.; Wichterlova, B.; Spoto, G.; Bordiga, S., Effect of aluminium distribution in the framework of ZSM-5 on hydrocarbon transformation. Cracking of 1-butene. *J. Catal.* **2008**, 254, (2), 180-189.

160. Huang, J.; Long, W.; Agrawal, P. K.; Jones, C. W., Effects of acidity on the conversion of the model bio-oil ketone cyclopentanone on H-Y zeolites. *J. Phys. Chem. C* **2009**, 113, (38), 16702-16710.

161. Haw, J. F., Zeolite acid strength and reaction mechanisms in catalysis. *PCCP* **2002**, 4, (22), 5431-5441.

162. Mihalcik, D. J.; Mullen, C. A.; Boateng, A. A., Screening acidic zeolites for catalytic fast pyrolysis of biomass and its components. *J. Anal. Appl. Pyrolysis* **2011**, 92, (1), 224-232.
163. Azeez, A. M.; Meier, D.; Odermatt, J.; Willner, T., Effects of zeolites on volatile products of beech wood using analytical pyrolysis. *J. Anal. Appl. Pyrolysis* **2011**, 91, (2), 296-302.
164. Iliopoulou, E. F.; Antonakou, E. V.; Karakoulia, S. A.; Vasalos, I. A.; Lappas, A. A.; Triantafyllidis, K. S., Catalytic conversion of biomass pyrolysis products by mesoporous materials: Effect of steam stability and acidity of Al-MCM-41 catalysts. *Chem. Eng. J.* **2007**, 134, (1-3), 51-57.
165. Fonseca, N.; Lemos, F.; Laforge, S.; Magnoux, P.; Ribeiro, F. R., Influence of acidity on the H-Y zeolite performance in n-decane catalytic cracking: evidence of a series/parallel mechanism. *Reaction Kinetics, Mechanisms and Catalysis* **2010**.
166. Aho, A.; Kumar, N.; Eranen, K.; Salmi, T.; Hupa, M.; Murzin, D., Catalytic pyrolysis of biomass in a fluidized bed reactorinfluence of the acidity of H-Beta Zeolite. *Process Saf. Environ. Prot.* **2007**, 85, (5), 473-480.
167. Ben, H.; Ragauskas, A., One step thermal conversion of lignin to the gasoline range liquid products by using zeolites as additives. *RSC Advances* **2012**, Accepted.
168. Mullen, C. A.; Boateng, A. A.; Mihalcik, D. J.; Goldberg, N. M., Catalytic fast pyrolysis of white oak wood in a bubbling fluidized bed. *Energy Fuels* **2011**, 25, (11), 5444-5451.
169. Fogassy, G.; Thegarid, N.; Schuurman, Y.; Mirodatos, C., From biomass to bio-gasoline by FCC co-processing: effect of feed composition and catalyst structure on

product quality. *Energ. Environ. Sci.* **2011**, 4, (12), 5068.

170. Chantal, P. D.; Kaliaguine, S.; Grandmaison, J. L., Reactions of phenolic compounds over HZSM-5. *Appl. Catal.* **1985**, 18, (1), 133-145.

171. Mihalcik, D. J.; Boateng, A. A.; Mullen, C. A.; Goldberg, N. M., Packed-bed catalytic cracking of oak-derived pyrolytic vapors. *Ind. Eng. Chem. Res.* **2011**, 50, (23), 13304-13312.

172. Mortensen, P. M.; Grunwaldt, J. D.; Jensen, P. A.; Knudsen, K. G.; Jensen, A. D., A review of catalytic upgrading of bio-oil to engine fuels. *Appl. Catal., A-Gen.* **2011**, 407, (1-2), 1-19.

173. Peralta, M. A.; Sooknoi, T.; Danuthai, T.; Resasco, D. E., Deoxygenation of benzaldehyde over CsNaX zeolites. *J. Mol. Catal. A: Chem.* **2009**, 312, (1-2), 78-86.

174. Chiang, H.; Bhan, A., Catalytic consequences of hydroxyl group location on the rate and mechanism of parallel dehydration reactions of ethanol over acidic zeolites. *J. Catal.* **2010**, 271, (2), 251-261.

175. Pereira, C.; Kokotailo, G. T.; Gorte, R. J.; Farneth, W. E., Adsorption and reaction of 2-propen-1-ol in H-ZSM-5. *J. Phys. Chem.* **1990**, 94, (5), 2063-2067.

176. Min, H.-K.; Hong, S. B., Mechanistic investigations of ethylbenzene disproportionation over medium-pore zeolites with different framework topologies. *J. Phys. Chem. C* **2011**, 115, (32), 16124-16133.

177. Collins, S. J.; Omalley, P. J., A Theoretical description for the monomolecular cracking of C-C bonds over acidic zeolites. *J. Catal.* **1995**, 153, (1), 94-99.

178. Jin, T.; Xia, D. H.; Xiang, Y. Z.; Zhou, Y. L., The effect of metal introduced over zsm-5 zeolite for c₉-heavy aromatics hydrodealkylation. *Pet. Sci. Technol.* **2009**, 27, (16),

1821-1835.

179. Holmes, S. M.; Garforth, A.; Maunders, B.; Dwyer, J., A solvent extraction method to study the location and concentration of coke formed on zeolite catalysts. *Appl. Catal., A-Gen.* **1997**, 151, (2), 355-372.

180. Laforge, S., m-Xylene transformation over H-MCM-22 zeolite 1. Mechanisms and location of the reactions. *J. Catal.* **2003**, 220, (1), 92-103.

181. Magnoux, P.; Rabeharitsara, A.; Cerqueira, H. S., Influence of reaction temperature and crystallite size on HBEA zeolite deactivation by coke. *Appl. Catal., A-Gen.* **2006**, 304, 142-151.

182. Magnoux, P.; Cerqueira, H. S.; Guisnet, M., Evolution of coke composition during ageing under nitrogen. *Appl. Catal., A-Gen.* **2002**, 235, (1-2), 93-99.

183. Yang, H.; Yan, R.; Chen, H.; Lee, D.; Zheng, C., Characteristics of hemicellulose, cellulose and lignin pyrolysis. *Fuel* **2007**, 86, (12-13), 1781-1788.

184. Aho, A.; Kumar, N.; Eränen, K.; Salmi, T.; Holmbom, B.; Backman, P.; Hupa, M.; Yu Murzin, D., Catalytic pyrolysis of woody biomass. *Biofuels* **2010**, 1, (2), 261-273.

185. Aho, A.; Kumar, N.; Lashkul, A. V.; Eränen, K.; Ziolk, M.; Decyk, P.; Salmi, T.; Holmbom, B.; Hupa, M.; Murzin, D. Y., Catalytic upgrading of woody biomass derived pyrolysis vapours over iron modified zeolites in a dual-fluidized bed reactor. *Fuel* **2010**, 89, (8), 1992-2000.

186. Aho, A.; Tokarev, A.; Backman, P.; Kumar, N.; Eränen, K.; Hupa, M.; Holmbom, B.; Salmi, T.; Murzin, D. Y., Catalytic pyrolysis of pine biomass over H-Beta zeolite in a dual-fluidized bed reactor: Effect of space velocity on the yield and composition of pyrolysis products. *Top. Catal.* **2011**, 54, (13-15), 941-948.

187. Carlson, T. R.; Cheng, Y.-T.; Jae, J.; Huber, G. W., Production of green aromatics and olefins by catalytic fast pyrolysis of wood sawdust. *Energ. Environ. Sci.* **2011**, 4, (1), 145.
188. Jae, J.; Tompsett, G. A.; Foster, A. J.; Hammond, K. D.; Auerbach, S. M.; Lobo, R. F.; Huber, G. W., Investigation into the shape selectivity of zeolite catalysts for biomass conversion. *J. Catal.* **2011**, 279, (2), 257-268.
189. Carlson, T. R.; Tompsett, G. A.; Conner, W. C.; Huber, G. W., Aromatic production from catalytic fast pyrolysis of biomass-derived feedstocks. *Top. Catal.* **2009**, 52, (3), 241-252.
190. Adjaye, J. D.; Bakhshi, N. N., Production of hydrocarbons by catalytic upgrading of a fast pyrolysis bio-oil. Part II: Comparative catalyst performance and reaction pathways. *Fuel Process. Technol.* **1995**, 45, (3), 185-202.
191. Adjaye, J. D.; Bakhshi, N. N., Production of hydrocarbons by catalytic upgrading of a fast pyrolysis bio-oil. Part I: Conversion over various catalysts. *Fuel Process. Technol.* **1995**, 45, (3), 161-183.
192. Fabbri, D.; Adamiano, A.; Torri, C., GC-MS determination of polycyclic aromatic hydrocarbons evolved from pyrolysis of biomass. *Anal Bioanal Chem* **2010**, 397, (1), 309-17.
193. Qi, W. Y.; Hu, C. W.; Li, G. Y.; Guo, L. H.; Yang, Y.; Luo, J.; Miao, X.; Du, Y., Catalytic pyrolysis of several kinds of bamboos over zeolite NaY. *Green Chem.* **2006**, 8, (2), 183.
194. Misson, M.; Haron, R.; Kamaroddin, M. F.; Amin, N. A., Pretreatment of empty palm fruit bunch for production of chemicals via catalytic pyrolysis. *Bioresour Technol*

2009, 100, (11), 2867-73.

195. Vitolo, S.; Seggiani, M.; Frediani, P.; Ambrosini, G.; Politi, L., Catalytic upgrading of pyrolytic oils to fuel over different zeolites. *Fuel* **1999**, 78, (10), 1147-1159.

196. Stephanidis, S.; Nitsos, C.; Kalogiannis, K.; Iliopoulou, E. F.; Lappas, A. A.; Triantafyllidis, K. S., Catalytic upgrading of lignocellulosic biomass pyrolysis vapours: Effect of hydrothermal pre-treatment of biomass. *Catal. Today* **2011**, 167, (1), 37-45.

197. Oasmaa, A.; Elliott, D. C.; Korhonen, J., Acidity of biomass fast pyrolysis bio-oils. *Energy Fuels* **2010**, 24, (12), 6548-6554.

198. Yan, N.; Yuan, Y.; Dykeman, R.; Kou, Y.; Dyson, P. J., Hydrodeoxygenation of lignin-derived phenols into alkanes by using nanoparticle catalysts combined with Bronsted acidic ionic liquids. *Angew. Chem. Int. Ed. Engl.* **2010**, 49, (32), 5549-53.

199. Zhao, C.; Kou, Y.; Lemonidou, A. A.; Li, X.; Lercher, J. A., Highly selective catalytic conversion of phenolic bio-oil to alkanes. *Angew. Chem. Int. Ed. Engl.* **2009**, 48, (22), 3987-90.

200. Wildschut, J.; Iqbal, M.; Mahfud, F. H.; Cabrera, I. M.; Venderbosch, R. H.; Heeres, H. J., Insights in the hydrotreatment of fast pyrolysis oil using a ruthenium on carbon catalyst. *Energy Environ. Sci.* **2010**, 3, (7), 962.

201. Li, N.; Tompsett, G. A.; Zhang, T.; Shi, J.; Wyman, C. E.; Huber, G. W., Renewable gasoline from aqueous phase hydrodeoxygenation of aqueous sugar solutions prepared by hydrolysis of maple wood. *Green Chem.* **2011**, 13, (1), 91-101.

202. Ben, H.; Pan, S.; Berg, A.; Ragauskas, A. J., HSQC-NMR fingerprint analysis of pyrolysis oils produced from tannin, pine bark and residue. **2012**, will submit.

203. Chen, L.; Zhu, Y.; Zheng, H.; Zhang, C.; Zhang, B.; Li, Y., Aqueous-phase

hydrodeoxygenation of carboxylic acids to alcohols or alkanes over supported Ru catalysts. *J. Mol. Catal. A: Chem.* **2011**, 351, 217-227.

204. Zhao, C.; He, J.; Lemonidou, A. A.; Li, X.; Lercher, J. A., Aqueous-phase hydrodeoxygenation of bio-derived phenols to cycloalkanes. *J. Catal.* **2011**, 280, (1), 8-16.

205. Nimmanwudipong, T.; Runnebaum, R. C.; Block, D. E.; Gates, B. C., Catalytic conversion of guaiacol catalyzed by platinum supported on alumina: Reaction network including hydrodeoxygenation reactions. *Energy Fuels* **2011**, 25, (8), 3417-3427.

206. Bui, V. N.; Laurenti, D.; Delichère, P.; Geantet, C., Hydrodeoxygenation of guaiacol. *Appl. Catal., B* **2011**, 101, (3-4), 246-255.

207. Bui, V. N.; Laurenti, D.; Afanasiev, P.; Geantet, C., Hydrodeoxygenation of guaiacol with CoMo catalysts. Part I: Promoting effect of cobalt on HDO selectivity and activity. *Appl. Catal., B* **2011**, 101, (3-4), 239-245.

208. Energy Information Administration, U. S. International Energy Outlook 2010 <http://www.eia.doe.gov/oiaf/ieo/emissions.html>.

209. Pimchuai, A.; Dutta, A.; Basu, P., Torrefaction of agriculture residue to enhance combustible properties. *Energy Fuels* **2010**, 24, (9), 4638-4645.

210. Pentananunt, R.; Rahman, A. N. M. M.; Bhattacharya, S. C., Upgrading of biomass by means of torrefaction. *Energy* **1990**, 15, (12), 1175-1179.

211. Svoboda, K.; Pohořelý, M.; Hartman, M.; Martinec, J., Pretreatment and feeding of biomass for pressurized entrained flow gasification. *Fuel Process. Technol.* **2009**, 90, (5), 629-635.

212. Prins, M.; Ptasinski, K.; Janssen, F., Torrefaction of wood Part 1. Weight loss

kinetics. *J. Anal. Appl. Pyrolysis* **2006**, 77, (1), 28-34.

213. Prins, M.; Ptasiński, K.; Janssen, F., Torrefaction of wood Part 2. Analysis of products. *J. Anal. Appl. Pyrolysis* **2006**, 77, (1), 35-40.

214. Yan, W.; Acharjee, T. C.; Coronella, C. J.; Vásquez, V. R., Thermal pretreatment of lignocellulosic biomass. *Environmental Progress & Sustainable Energy* **2009**, 28, (3), 435-440.

215. Pastorova, I.; Botto, R. E.; Arisz, P. W.; Boon, J. J., Cellulose char structure: a combined analytical Py-GC-MS, FTIR, and NMR study. *Carbohydr. Res.* **1994**, 262, (27-47).

216. Channiwala, S. A.; Parikh, P. P., A unified correlation for estimating HHV of solid, liquid and gaseous fuels. *Fuel* **2002**, 81, (8), 1051-1063.

217. Deng, J.; Wang, G.-j.; Kuang, J.-h.; Zhang, Y.-l.; Luo, Y.-h., Pretreatment of agricultural residues for co-gasification via torrefaction. *J. Anal. Appl. Pyrolysis* **2009**, 86, (2), 331-337.

218. Holtman, K. M.; Chen, N.; Chappell, M. A.; Kadla, J. F.; Xu, L.; Mao, J., Chemical structure and heterogeneity differences of two lignins from Loblolly pine as investigated by advanced solid-state NMR spectroscopy. *J. Agric. Food. Chem.* **2010**, 58, (18), 9882-9892.

219. Pournou, A., Deterioration Assessment of Waterlogged Archaeological lignocellulosic material via ^{13}C CP/MAS NMR. *Archaeometry* **2007**, 50, (1), 129-141.

220. Love, G. D.; Snape, C. E.; Jarvis, M. C., Comparison of leaf and stem cell-wall components in barley straw by solid-state ^{13}C NMR. *Phytochemistry* **1998**, 49, (5), 1191-1194.

221. Dick-Pérez, M.; Zhang, Y.; Hayes, J.; Salazar, A.; Zabolina, O. A.; Hong, M., Structure and interactions of plant cell-wall polysaccharides by two- and three-dimensional magic-angle-spinning solid-state NMR. *Biochemistry (Mosc)*. **2011**, 50, (6), 989-1000.
222. Zawadzki, J.; Wisniewski, M., ¹³C NMR study of cellulose thermal treatment. *J. Anal. Appl. Pyrolysis* **2002**, 62, 111-121.
223. Ates, S.; Akyildiz, M. H.; Ozdemir, H., Effects of heat treatment on calabrian pine (*Pinus brutia* Ten.) wood. *BioResources* **2009**, 4, (3), 1032-1043.
224. Ahmad, T.; Andersson, R.; Olsson, K.; Theander, O., On the formation of 2,3-dihydroxyacetophenone from pentoses or hexuronic acids. *Carbohydr. Res.* **1993**, 247, 211-215.
225. Jakab, E.; Liu, K.; Meuzelaar, H. L. C., Thermal decomposition of wood and cellulose in the presence of solvent vapors. *Ind. Eng. Chem. Res.* **1997**, 36, 2087-2095.
226. Tao, F.; Song, H.; Chou, L., Catalytic conversion of cellulose to chemicals in ionic liquid. *Carbohydr. Res.* **2011**, 346, (1), 58-63.
227. Tao, F.; Song, H.; Chou, L., Hydrolysis of cellulose by using catalytic amounts of FeCl₂ in ionic liquids. *ChemSusChem* **2010**, 3, (11), 1298-1303.
228. Huang, J.; Liu, C.; Wei, S.; Huang, X.; Li, H., Density functional theory studies on pyrolysis mechanism of β-d-glucopyranose. *Journal of Molecular Structure: Theochem* **2010**, 958, (1-3), 64-70.